การวิเคราะห์และการสร้างแบบจำลองข้อมูลธรณีฟิสิกส์ทางอากาศในบริเวณแนวหินภูเขาไฟเพชรบูรณ์ ทางตอนเหนือของภาคกลางประเทศไทย

นายอารักษ์ แสงสมพงษ์

วิทยานิพนธ์นี้เป็นส่วนหนึ่งของการศึกษาตามหลักสูตรปริญญาวิทยาศาสตรมหาบัณฑิต
สาขาวิชาธรณีวิทยา ภาควิชาธรณีวิทยา
คณะวิทยาศาสตร์ จุฬาลงกรณ์มหาวิทยาลัย
ปีการศึกษา 2554

ANALYSIS AND MODELLING OF AIRBORNE GEOPHYSICAL DATA IN THE PHETCHABUN VOLCANIC BELT, NORTHERN PART OF CENTRAL THAILAND

Mr. Arak Sangsomphong

A Thesis Submitted in Partial Fulfillment of the Requirements

for the Degree of Master of Science Program in Geology

Department of Geology

Faculty of Science

Chulalongkorn University

Academic Year 2011

Thesis Title	ANALYSIS AND MODELLING OF AIRBORNE GEOPHYSICAL DATA IN THE PHETCHABUN VOLCANIC BELT, NORTHERN PART OF CENTRAL THAILAND
By	Mr. Arak Sangsomphong
Field of Study	Geology
Thesis Advisor	Associate Professor Punya Charusiri, Ph. D.
Thesis Co-advisor	Thanop Thitimakorn, Ph. D.

Accepted by the Faculty of Science, Chulalongkorn University in Partial Fulfillment of the Requirements for the Master's Degree

…….. Dean of the Faculty of Science
(Professor Supot Hannongbua, Dr.rer.nat.)

THESIS COMMITTEE

…….. Chairman
(Associate Professor Montri Choowong, Ph. D.)

……. Thesis Advisor
(Associate Professor Punya Charusiri, Ph. D.)

…….. Thesis Co-advisor
(Thanop Thitimakorn, Ph. D.)

…….. Examiner
(Pitsanupong Kanjanapayont, Dr.rer.nat.)

…….. External Examiner
(Dhiti Tulyatid, Ph. D.)

อารักษ์ แสงสมพงษ์ : การวิเคราะห์และการสร้างแบบจำลองข้อมูลธรณีฟิสิกส์ทางอากาศในบริเวณแนวหินภูเขาไฟเพชรบูรณ์ ทางตอนเหนือของภาคกลางประเทศไทย. (ANALYSIS AND MODELLING OF AIRBORNE GEOPHYSICAL DATA IN THE PHETCHABUN VOLCANIC BELT, NORTHERN PART OF CENTRAL THAILAND) อ.ที่ปรึกษาวิทยานิพนธ์หลัก: รศ. ดร. ปัญญา จารุศิริ, อ.ที่ปรึกษาวิทยานิพนธ์ร่วม: ดร. ฐานบ ธิติมากร, 157 หน้า.

ในวิทยานิพนธ์นี้ วิวัฒนาการธรณีแปรสัณฐานของธรณีวิทยาใต้ดินบริเวณแนวหินภูเขาไฟเพชรบูรณ์ที่ถูกปิดทับด้วยตะกอนยุคใหม่ได้นำมาอธิบาย โดยใช้ข้อมูลธรณีฟิสิกส์ทางอากาศที่ปรับปรุงคุณภาพข้อมูลขึ้นใหม่ร่วมกับการศึกษาทางภาคสนาม เช่นเดียวกันกับการศึกษางานก่อนหน้านี้ ทางด้าน ธรณีกาลวิทยา ธรณีเคมี และการสำรวจทางธรณีวิทยา

ในช่วงยุคเพอร์โม-คาร์บอนิเฟอรัส มวลหินอัคนีบาดาลเริ่มต้นของหน่วยแม่เหล็กยาวเรียวพบว่าอาจเกิดอยู่ในภูเขาไฟรูปโค้งบริเวณการมุดตัวลงของแผ่นเปลือกโลกมหาสมุทรนครไทยไปใต้แผ่นเปลือกโลกภาคพื้นทวีปอินโดไชน่าในขอบเขตแม่เหล็กตอนกลาง

ต่อมาในช่วงยุคเพอร์โม-ไทรแอสสิค การปรากฏของหน่วยแม่เหล็กยาวเรียวสะท้อนว่าเกิดการมุดตัวไปทางตะวันออกอีกครั้ง โดยใช้หลักฐานจากการเปลี่ยนรูปร่างแตก-ยืดเป็นหน่วยแม่เหล็กยาวเรียว และเกิดการโค้งงอ ในบริเวณเขตรอยต่อที่ถูกอัดจากการชนกันของแผ่นธรณีนอกเหนือไปจากแหล่งแร่ทองคำแบบอุณหภูมิสูงเกิดขึ้นในช่วงนี้ ยังทำให้เกิดโครงสร้างแบบแรงอัดในทิศทางตะวันออก-ตะวันตก เกิดหน่วยแม่เหล็กวงแหวนบริเวณใจกลางภูเขาไฟรูปโค้งในอดีต และเกิดหน่วยแม่เหล็กแบบกลมจากหินอัคนีบาดาลแสดงลักษณะผลึกเท่ากัน ตามลำดับ

ในทางตรงข้าม แรงแบบดึงออกในทิศทางตะวันออก-ตะวันตก ในช่วงอายุไทรแอสสิค ทำให้เกิดการสะสมตัวของทองคำอุณหภูมิต่ำขึ้นในช่วงนี้ แรงกระทำแบบดึงออกในทิศทางตะวันออก-ตะวันตก ทำให้เกิดการทรุดตัวลงของแนวหินภูเขาไฟเพชรบูรณ์ของขอบเขตแม่เหล็กตะวันออกและเกิดการยกตัวขึ้นในขอบเขตแม่เหล็กย่อยตอนเหนือ2 ของแอ่งตะกอนโคราชช่วงเริ่มแรก หลังจากนั้นได้พบหน่วยแม่เหล็กขนาดเล็กที่แสดงว่าเกิดจากการแทรกดันขึ้นมาของหินอัคนีบาดาลลักษณะผลึกดอกตามแนวรอยเลื่อนที่เกิดการทรุดตัวลง

ภาควิชา ธรณีวิทยา	ลายมือชื่อนิสิต
สาขาวิชา ธรณีวิทยา	ลายมือชื่อ อ.ที่ปรึกษาวิทยานิพนธ์หลัก
ปีการศึกษา 2554	ลายมือชื่อ อ.ที่ปรึกษาวิทยานิพนธ์ร่วม

5172557623 : MAJOR GEOLOGY

KEYWORDS : PHETCHABUN VOLCANIC BELT / RE-PROCESSING AIRBORNE GEOPHYSICAL DATA / MODELLING / TECTONIC SETTING

ARAK SANGSOMPHONG : ANALYSIS AND MODELLING OF AIRBORNE GEOPHYSICAL DATA IN THE PHETCHABUN VOLCANIC BELT, NORTHERN PART OF CENTRAL THAILAND. ADVISOR: ASSOC. PROF. PUNYA CHARUSIRI, Ph. D., CO- ADVISOR: THANOP THITIMAKORN, Ph. D., 157 pp.

In this thesis, new re-processed airborne geophysical data together with relevant current field verification as well as previous geochronological, geochemical and geological investigations lead to the clarification of the complex structures and tectonic evolution in Phetchabun volcanic terrane covered by thick Cenozoic deposits.

During the Permo-Carboniferous period, the original elongate units in central domain corresponding to intrusive igneous bodies may have occurred in Late Carboniferous volcanic arc and association with subduction of the Nakhonthai oceanic plate beneath the Indochina continental plate.

Subsequently, during the Permo-Triassic period, the elongate units reflect the subduction again as evidence by brittle-ductile structure which is deformed in represent of fold and thrust zone in central domain besides the mesothermal gold deposit in this zone. The structural configuration of this stage is characterized by east-west compressional stress. Ring units of Permo-Triassic volcanic arc centers and the presence of circular units representing equigranular intrusive bodies are occurred from the result of eastward subduction.

On the contrary, the east-west extension stress during the Triassic period is inferred to be contemporaneous diachronous with the subsidence in eastern domain of volcanic arc and deposited the epithermal gold which contemporaneous with the uplift of the preliminary Khorat basin in northern 2 sub-domain. Consequently, the spot units representing shallow porphyritic intrusive bodies occurred along the subsidenced fault zone during this stage.

Department :	Geology	Student's Signature	
Field of Study :	Geology	Advisor's Signature	
Academic Year :	2011	Co-Advisor's Signature	

Acknowledgements

Foremost, I would like to thank Department of Mineral Resource (DMR) for provided the airborne geophysical data and allow me to use the geophysical enhance program and encouragement and permission to publish the results in this study. I am greatly indebted to Mr. Aphichat Piyarom (senior geologist of DMR) who takes care and offered the airborne geophysic data until finish the study.

Sincerely, appreciations also extend to Isara mining limited (Explolation Company of Akara mining) for extremely financial support the research during field observation with all facility, epecially the equipments and data of the company. Speial thanks go to Mr. Prakarn Beunkhuntod, Mr. Veerasak Lunwongsa, Miss. Saranya Nuanlaong, Miss. Sasikan Janplook and Miss. Ladda Tangwattananukul for their helpful and constructive comments advices and idea throughout this field study.

CONTENTS

List of Tables

LIST OF FIGURES

CHAPTER I
Introduction

1.1 General statement

The Phetchabun volcanic terrane (Fig.1.1) is located in the central part of the so–called Loei-Petchabun-Nakhon Nayok volcanic belt (Intasopa and Dunn, 1993) extending approximately north-south trending through central Thailand. The tectonic evolution of the central Thailand has been a subject of interest and controversy in recent years. Since nineteenth century, many geoscientists have widely studied geologic evolution of Thailand. Based on Bunopas (1992), Thailand was comprised of a complex assembly of two micro-continents, namely Shan-Thai in the west and Indochina in the east (Fig.1.2), with the north-south trending linear Loei suture as their entity. The suture zones (or tectonic line) in Thailand occurred as branch sutures (Charusiri et al., 2002) which are numbers of sutures zones were highly possible to preserve remnants of the paleotethys (Barr and MacDonald, 1987 and Metcalfe, 1999). The advent of two newly proposed by Charusiri et al. (2002), suggesting smaller tectonic blocks between Shan-Thai and Indochina, namely the paleotethys Nakhonthai oceanic crust in the east and Lampang-Chiang Rai volcanic arc in the west (Fig. 1.2), significantly changed geological components as well as tectonomagnetic and metallogenic models of Thailand and mainland SE Asia. Tectonism may have caused the pair “Benioff” subduction of the paleotethys-one subducted westward beneath Shan-Thai and the other eastward beneath Indochina (Bunopas and Vella, 1983 and 1992) which may have triggered by the development of Lampang-Chiang Rai and Nakhonthai mainly oceanic plates (Charusiri et al., 2002). Magmatism at plate margins and subsequent collision of individual plates may have occurred. It is also considered by those authors that volcanic rocks along the Loei-Phetchabun-Nakhon Nayok volcanic belt which comprise several mineral deposits (e.g. Au-Ag-Fe-Cu-Mo ores) may have formed in several stages from Late Devonian and extending to the Late Cretaceous with features indicating a diverse range of tectonic settings (Intasopa, 1993). The geochronological data are reported by Intasopa (1993), the rocks of the Loei-Phetchabun- Nakhon Nayok Volcanic Belt are Permo-Triassic to Miocene. However, the Loei suture which extends both northward and

southward has been poorly studied and difficult to delineate due to the fact that some parts of the suture (or “tectonic lines”) are underneath by thick regolith and recent sedimentary covers. These tectonic setting interpretations were discussed based on limited geological evidences of few good exposures. Geological belt correlation from the northern Lao PDR to the south along the Loei suture is very difficult due to the limitation of various geological data. This makes the tectonic setting of Loei suture zone become cryptic and require more understanding issue.

New airborne geophysical interpretation, field verification and the previous work were generated represent significant magnetic units, surface and subsurface structures and tectonic model in study region. The result of this study will provide a better understanding of geologic and tectonic evolution within surrounding the Chatree gold deposit and the Khao Phanom Pha gold deposit. This research was also provided an improved exploration model in the region that may ultimately lead to new discoveries of resources.

1.2 Location and geography

The area under investigation, covers about 22,700 sq km, is located in northern part of central Thailand (Fig. 1.1) between latitude 15^0 16’ 00” - 16^0 43’ 00”N and longitude 100^0 10’ 00” -101^0 29’ 00”E or grid UTM WGS 84 from 1689500- 1850100N and 0624700 – 0766200E. The study area is situated most part of 5 provinces (Phitsanulok, Phetchabun, Phichit, Nakhonsawan and Lopburi) which have an elevation of about 100-1500 meters above mean sea level (Fig. 1.3). Geologically, this area is located on the edge of Tertiary Chao Phaya basin that is on the bounder of Petchabun and Pichit Provinces about 280 kilometers north (or 4 hours drive by car) of Bangkok. This study area can be accessed annually and comfortably by three ways. The first is done by using the Highway No.1 from Bangkok passing Pathum Thani, Saraburi, Lopburi and turning right to Highway No. 11 from Amphoe Tak Fa to Amphoe Thap Klo. The other way is traveled by train to Taphan Hin station of Pichit province, or by an airplane to Pitsanolok, then following Highway no. 11.

The general geography of study area is undulating terrain and mountainous area. Geomorphologically, the slope is gently toward to the west and the land surface is

covered by regolith, a layer of loose, heterogeneous material covering solid rock and surrounded by flat area. This area is divided by water drainage between Pichit province in the west and Phetchabun province in the east. Land in study area has an elevation of 5-10 meters higher than the surrounding low lying plain. In the western part of area is dominated mainly by undulating terrain. The central and eastern part displays as low mountain and isolated hill. The average height in the undulating terrain is from 81 to 141 meters above sea level. The highest point in study area is in the northeast of area or edge of Khorat plateau.

The study area is in the tropical zone and climate can be divided into three seasons, i.e. summer, rainy and winter. The summer season commonly ranges from March to April and the highest temperature. Summer season's weather is very hot; especially in April may be 35-40^{o}C in day time. The rainy season usually starts in May to October with dense raining are in August, September and October. As a result of destroyed forest in rainy time with fast and heavy leaching, soil and sand on the surface are eroded rapidly. In November and February, the climate is cool and strong winding which is about 10-15^{o}C of lowest temperature. Most of the lands in this area are used for cultivation. The cultivation crops are mainly maize, graphs, sugar cane, peanut, season fruits etc. Most of crops have been cultivated in the undulating terrain surrounding the mining site.

1.3 Objectives

The study is aimed to analyze and correlates of subsurface geology and structural evolution with using airborne geophysical processing for identifying geologic features and tectonic setting.

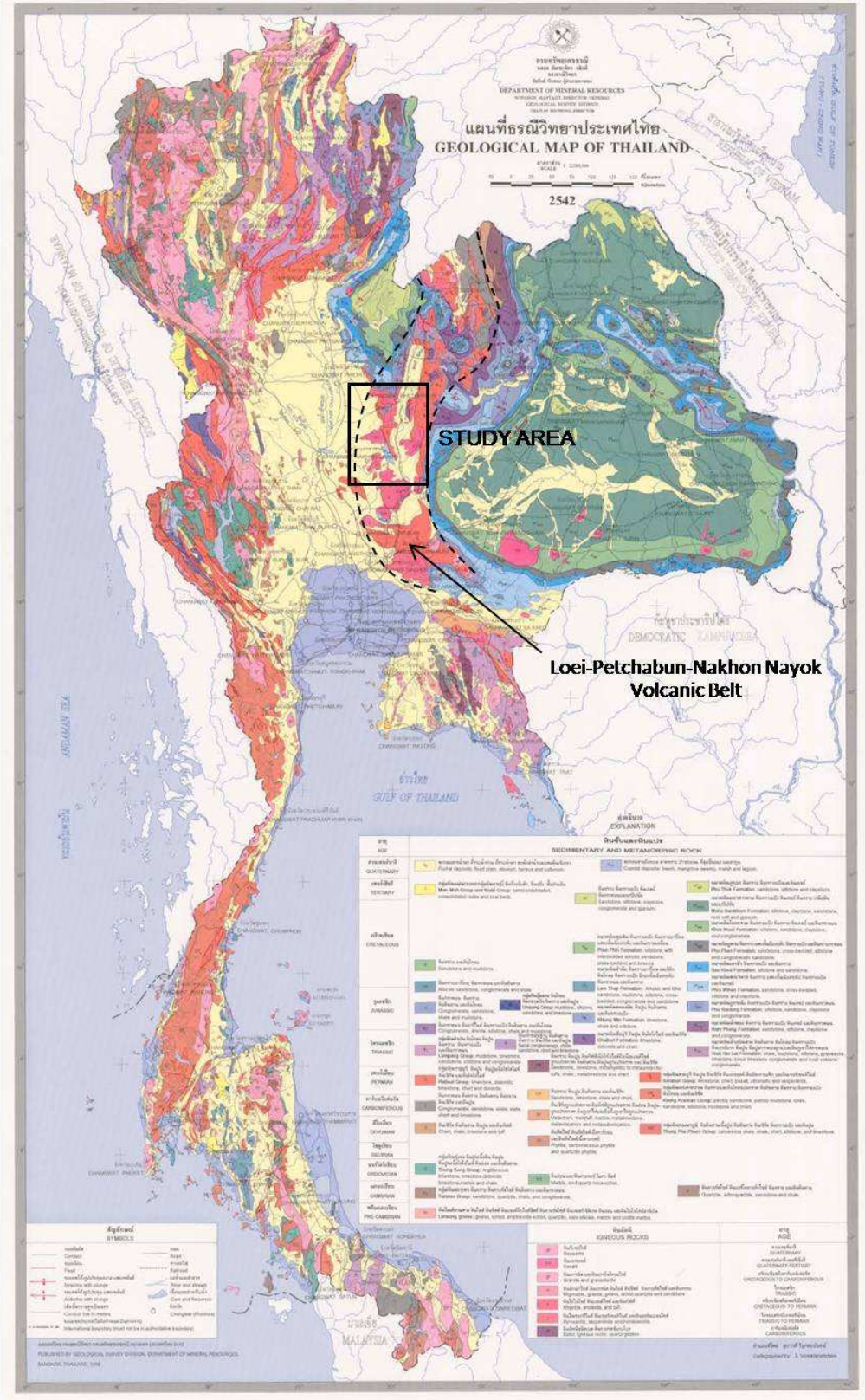

Figure 1.1. Geological map of Thailand (Department of Mineral Resource, 1999) showing the Phetchabun volcanic terrane located within the so–called Loei-Phetcabun-Nakorn Nayok volcanic belt (Intasopa and Dunn, 1993).

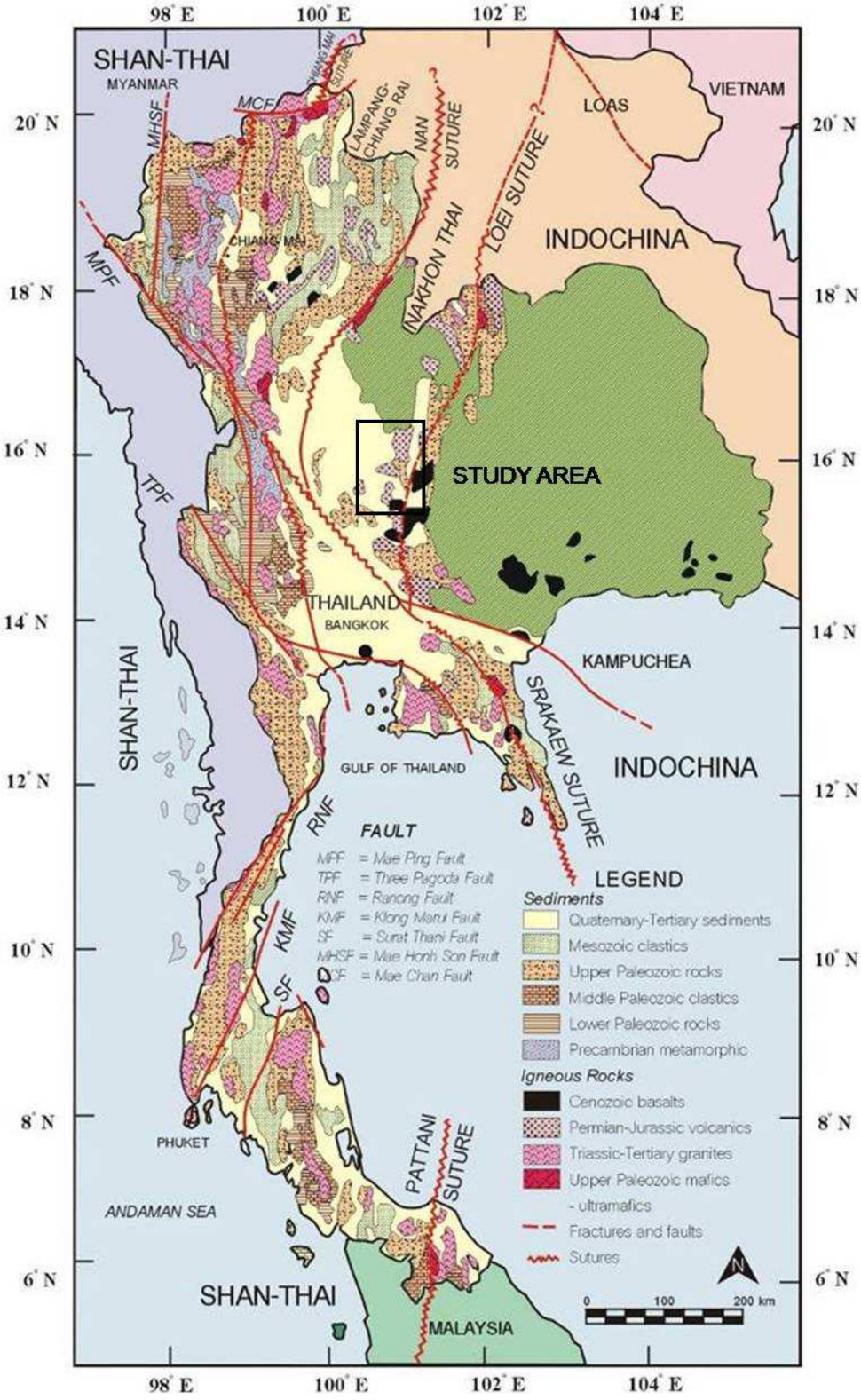

Figure 1.2. The tectonic interpretation map of Thailand based on the result of airborne geophysical and geological data, showing proposed five sutures and two microplates (Nakhon Thai and Lampang-Chiang Rai) between Shan Thai and Indochina terranes (Charusiri et al., 2002).

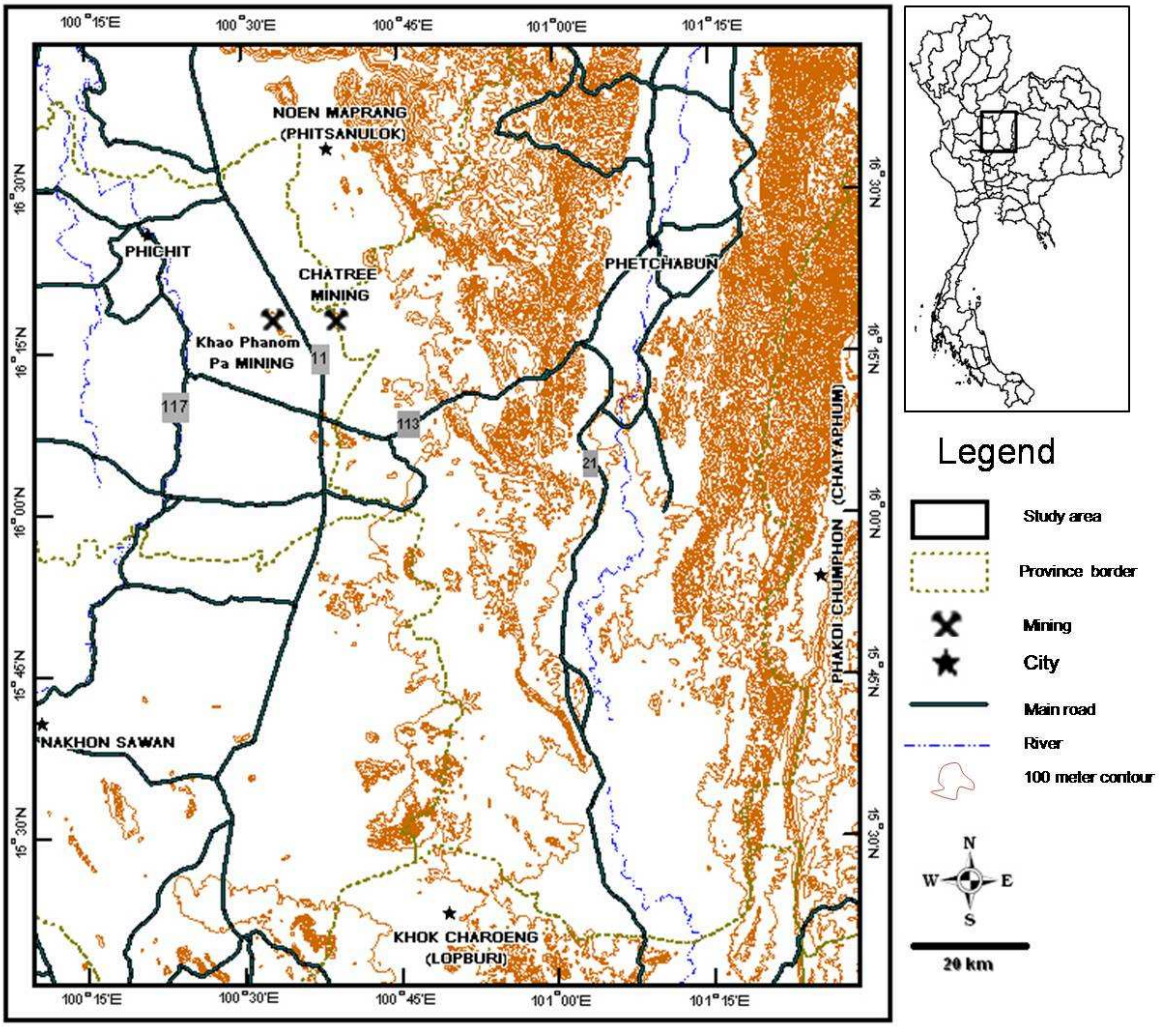

Figure 1.3. Topographic map of Phetchabun volcanic terrane with the inset showing the locating of the study area.

1.4 Thesis Methodology

Objective of this thesis provides base line enhance airborne magnetic data, field work and previous work coverage in the study area. This study area is covered with thick Quaternary transported and in-situ sediments, it is quite essential to comprehend what are the basement rocks by using new enhance airborne magnetic map with verify the magnetic response by using the magnetic susceptibility method and the petrography of rock. Consequently, the project is divided into 6 steps. The proposed research will be involved both detailed field and modern laboratory-based approaches.

1. Documenting the distribution of igneous rocks in the region for lithological, geological, geochemical, petrochemical study and establishment of stratigraphic relations incorporating the data from the previous work.

2. Enhance magnetic data have been created to display more detailed information from the raw data. They are described the enhancement and presentation of airborne geophysical data by using linear and non-linear filtering algorithms that selectively enhanced anomalies due to one group of geological sources relative to anomalies due to other groups of geological sources. Because of the complexity of magnetic pattern especially in the near equator region, such as Thailand, magnetic recognition of a magnetic body is displayed as dipolar pattern in normal induced magnetization generally showing the negative low in the northern side and positive high in the southern side. With this condition, it may bring confusion when interpreting by one who is familiar with magnetic pattern in the near-pole area. In addition to enhance airborne magnetic map, it can be more accurate to identify magnetic body in relation to structural features.

3. Airborne magnetic interpretation is the process by which magnetic field variations are related to litho-stratigraphic and structural features in the ground. In this research, the qualitative interpretation will carry out in conjunction with existing 1:250,000 geological maps and geological information, by constructing airborne magnetic zoning. The zoning is the procedure by which the magnetic domain and units with more or less consistent magnetic characteristics are recognized and delineated. These magnetic characteristics include a large number of parameters which describe not only the intensity and relief of magnetic field but also such textural characteristics as lineament, coherence, symmetry, wavelength and strike length of individual anomalies that make up the magnetic unit. Overall shape and boundary characteristics of the magnetic unit can also provide fruitful information on its geological identification.

4. Field investigation is subsequently taken place to work on magnetic mapping. It also includes and systematically sample collection. About 80 rock samples selected from outcrops in the study area and the rock cutting from Isara mining company by using the rotary ais blast drilling.

5. Magnetic susceptibility with a rock-sampling program was carried out in the area to determine the magnetic susceptibility level for each rock type. Outcrops were chosen measured the magnetic susceptibility in laboratory.

6. Thin section of the rocks for petrographic investigation; most types of rocks were grouped based on their physical appearances before cut of slabs and then make thin sections. Total 27 rocks of petrographic study were carried out to identify mineral compositions and rocks texture under polarizing microscope.

1.5 Previous works in the study area

Geophysical survey data have been used to study structural geology and tectonic setting covered by thick Quaternary sediments. To study a characteristic of subsurface features, magnetic data are used to interpret geometry of structures and rock units. Gunn (1997a) used magnetic and gravity data to construct a model of rifting related with the tectonic process and summarized magnetic and gravity responses in relation to the tectonic setting locations (Gunn, 1997b). Moreover, Milligan and Gunn (1997) reviewed processing enhanced methods for airborne geophysical data prior interpretation. Naidu and Mathew (1998) used directional filtering and angular spectrum methods of aeromagnetic data to identify faults. Rybokov et al. (2000) observed structural features in subsurface geology by using 3-D forward and inverse magnetic and gravity modelling with updated petrophysical data. Pilkington et al. (2000) used the integration of enhanced magnetic and gravity data to interpret structures and rock domains of a basin by applying reduction to the pole.

The geology, mineralization, alteration and geochemistry in Chatree gold deposit has been studied intensively by several geoscientists (Diemar, 2000; Marhotorn, 2002; Deesawat, 2002; Kromkhun et al., 2005; Crossing, 2004; Corbett, 2004; Cumming et al., 2004; Sangsiri and Pisutha-Arnond, 2008, Nakchaiya et al., 2008; Marhotorn et al., 2008; Tangwattananukul et al., 2008). It is widely accepted that in the Loei-Pechabun-Nakorn Nayok volcanic belt contain more intrusive rocks than volcanic rocks exposed in Loei subprovince, ie., diorite at Amphoe Ban Na, Nakhon Nayok (Sitthihawon and Tiyapairach, 1982), porphyritic quartz-monzoite, monzonite, diorite and granodiorite in Phu Lon area, Amphoe Sankho, Changwat Nongkhai (Sitthithaworn, 1989), diorite and granodiorite at Amphoe Khok Samrong and Tambon Khok Krathiem, Chagwat Lopburi, diorite and granodiorite at Amohoe Pak Chong, Changwat Nakhorn Ratchasima, and granodiorite of Changwat Phetchabun. These intrusive rocks are commonly associated

with andesite, rhyolite and andesitic tuff, and generally produce skarn deposits of iron and copper (usually malachite and chalcopyrite). In some relatively well studies areas, such as the Phu Lon, significance amounts of native gold, electrum, silver and molybdenite in which magmatite and chalcopyrite have been reported to relative intrusion which show indication of skarn and porphyry copper deposit (Sithithaworn et al., 1992). In the Chatree region, there are 4 stratigraphic units, including unit 1: fiamme breccia (and andesitic volcaniclastic facies, unit 2: epiclastic and fine volcaniclastic sedimentary facies and rhyolite breccia facies, unit 3: polymict and monomict andesite breccia facies and unit 4: polymict and monomictic andesitic breccia and coherent facies (Cumming et al., 2004). Salam et al. (2007) reported geochronology of mineraizaton and timing of plutonic and volcanic activities. These will be explained in more detail in the discussion part.

1.6 Significance of the proposed work

The result is expected to bring the following implications:

1. Adding new airborne magnetic interpretation,

2. Understanding of geology and tectonic setting,

3. Understanding of strategy for mineral exploration, and

4. Providing new data or ideas on the tectono-magnetism related to mineral exploration to the central portion of the Loei Suture.

CHAPTER II

Geology

2.1 Tectonic Framework of Thailand

The tectonic evolution of Thailand has been proposed by Bunopas and Vella (1983), then systematically re-constructed by Bunopas and Vella (1992) and subsequently revised by Charusiri et al. (2002). Based on the tectonic evolution syntheses of Bunopas and Vella (1992), Thailand was composed of two main tectonic terranes, the Shan-Thai in the west, and the Indochina in the east. Their amalgamation line is situated along the Nan Suture. The Shan-Thai block occupied eastern Myanmar, western Thailand, Laos, Cambodia and some parts of Vietnam. In Thailand, the Shan-Thai terrane comprised basement of granitoids and high-grade metamorphic rocks which were believed to be of Precambrian age (DMR, 1999). The basement was overlain by sedimentary and metamorphic sequences of Palaeozoic, Mesozoic and Cenozoic ages. While the Indochina terrene comprised Permian platform-carbonate and deep-water clastic rocks is covered by the Mesozoic sequence of the Khorat Group, without any exposed Precambrian rocks. Bunopas and Vella (1992) stated that Shan-Thai and Indochina blocks were amalgamated along a moderately high angle, westward-dipping Benioff zone, to form the so-called Nan Suture, before the end of the Triassic. There were two fold-belts, originating from mid-Paleozoic to Triassic sedimentary basins, located between the Shan-Thai and Indochina. They were the Sukhothai Fold-Belt and the Loie Fold-Belt, along the eastern side of the Shan-Thai block and the western side of the Indochina block, respectively. Bunopas and Vella (1992) divided the tectonic evolution in Thailand into four episodes: Archaeotectonic, Palaeotectonic, Mesotectonic and Neotectonic.

Charusiri et al. (2002) proposed more recent information, particularly geochronology, petrology, and presented the latest synthesis of Thai tectonic evolution. They sub-divided two new small geological terranes, named as the Lampang – Ching Rai block and the Nakhon Thai block in the former Sukhothai fold-belt and Loei fold-belt, respectively. These new geological blocks were related to major terranes, Shan-Thai and Indochina, which were initially associated with the Gondwana supercontinent. Two

major tectonic terranes of the Shan-Thai and Indochina were amalgamated in the Late Triassic. Four main tectonic stages are recognized herein on tectonostratigraphic and geochronological grounds, viz. Archaeotectonic, Paleotectonic, Mesotectinic and Neuvotectonic (Fig.2.1).

In the archaeotectonic stage, the Shan-Thai and Indochina microcontinents constituted detached, probably Precambrian, high-grade metamorphic, cratonic fragments of the Gondwana and Pan-Cathaysia supercontinents, respectively. The paleotectonic stage commenced with a major marine transgression (Paleotethys) over both Shan-Thai and Indochina extending from the Cambrian to the Permain. Following oceanic subduction during the Middle Paleozoic, two newly proposed, smaller tectonic blocks intervened between Shan-Thai and Indochina, namely the paleotethyan "Nakhonthai" ocean floor to the east and the "Lampang-Chiang Rai" oceanic plate to the west (Fig. 2.1). Rapid drifting of Shan-Thai to lower latitudes from its parent landmass is recorded by Permo-Carboniferous, glacio-marine diamictes. A transition to warmer environment recorded for Shan-Thai, and all terranes were close to the paleo-equator, as shown by carbonate platform facies along the continental margin during the Late Permian. The arc-type sedimentation took place during Triassic over almost all terranes. The advent of the mesotectonic stage is marked by the collision of all terranes, termination of Paleotethys, development of the major NE- and NW-trending strike-slip faults, and the emplacement of the voluminous Eastern (I-type granitoids with Cu-Fe-Pb-Zn-Au deposits) and Central (S-type dominated, Sn-W-Nb-Ta-REE deposits) Granite Belts. Paleomagnetic relationships demonstrate that Shan-Thai was very close to Indochina at low latitudes in the northern hemisphere during the very Late Paleozoic. All terranes attained the mid-latitudes of the northern hemisphere and came to a halt during very Late Triassic to Early Jurassic times. Thrusting of Shan-Thai over Lampang-Chiang Rai, eastern Lampang-Chiang Rai over Nakhon Thai, eastern Nakhonthai block over western Indochina in eastern Thailand, and partly Shan-Thai over Indochina, triggering the Mesotethyan incursion to the west, may have generated Jurassic-Cretaceous, continental sedimentation over much of Lampang-Chiang Rai, Nakhon Thai, western and southwestern Indochina, respectively. The end of the Mesotectonic stage (Early Tertiary) is marked by the termination of Mesotethyan transgression in the Shan-

Thai/Western Burma collision, causing the generation of the Western (richly-mineralized S-and I-type) Granite Belt. The collision of India with Asia during the Early Eocene marked the beginning of the neuvotectonic stage, which in turn caused the regional uplift of the Mesozoic Khorat and affiliated basins and the generation of the Phu Phan Anticline and Nakhon Thai Synclinorium. The Neuvotectonic stage is marked by the reverse motion on the major strike-slip faults and the occurrence of mantle-derived gem-bearing basalts in Middle to Late Miocene. This Late Cenozoic eruption may have been linked to the late regional uplift and vigorous denudation, generating major, Sn-, Au-, and gem-placer deposits of the country.

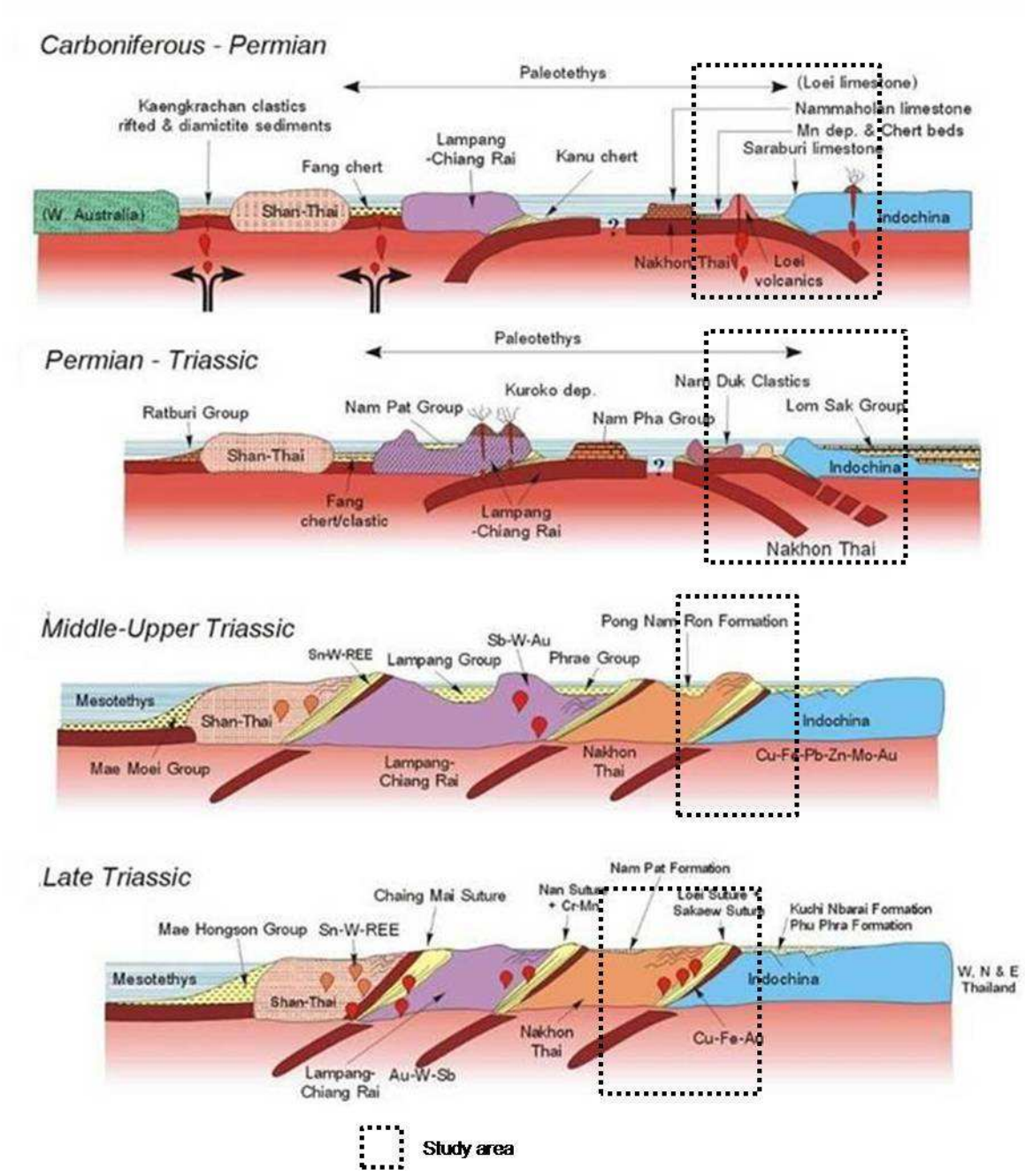

Figure 2.1. Tectonic model of Thailand during Carboniferous to Trassic Period showing distribution and interaction of tectonic plates (Charusiri et al., 2002).

2.2 Igneous Rocks of Thailand

Intrusive and extrusive igneous rocks are widespread in Thailand, except for the northeastern part of the country (Khorat Plateau). It is evident that metallic and non metallic ores, especially those of hydrothermal origin, including tin, tungsten, copper, iron ,gold ,columbite-tantalite, feldspar, fluorite, lithium-bearing minerals, and rare eart-

bearing minerals (monazite and xenotime) are closely related to some types of granitoid in space and time (Charusiri et al., 1993). A better understanding of the evolution and distribution of granites would be of benefit to mineral exploration in Thailand.

2.2.1 Intrusive Rocks

The granites of the Thailand crop out as the north-south trending elongated zone more than 2500 km long and 600 km wide extending throughout the Southeast Asian region (Charusiri et al., 1993). The regional extension of these belts is to Malaysia, Singapore, Indonesia in the south and the southern Yunan in the north. It is well documented that granite belt is one of the world (Charusiri, 1989). The exploited tin minerals from this region comprise three-quarters of the total world tin production (Nakapadungrat, 1982). From 1983 till the present, 40% of primary tin ores has ores been recovered in this region. These granites can be grouped into three sub-parallel magmatic belts or provinces (Fig. 2.2) based on their field occurrence, petrography and chemical characteristics.

Eastern Granitoid Belt

This belt of mainland SE Asia extends from Billiton Island in the south, Indonesia, eastern Peninsular Malaysia, eastern Thailand through the edge of Khaorat plateau in the central and ends at Laos and southern Yunan in the north. Generally this granitic belt is emplaced in Upper Paleozoic sedimentary and volcanic clastic sequences. Granitic activeity was companied by volcanism which persisted from Carboniferous to the Late Triassic. The larger body of granitoid rocks is the Tak Batolith in Tak province, north Thailand which has been systematically studied by Teggin (1975), Smaller plutons are located in the areas of Phrae-Nan, Lampang, Loei, Chantaburi and Narathiwat province.

This terrain is characterized by high level epizonal, felsic to mafic plutonic rock with diorite, granodiorite and granite predominant rock types. Subvolcanic and volcanic suites of expanded composition range similar to those of the plutonic rocks are a common association within this terrain. Characteristic petrographies of the granites are coarse to medium-grained, equigranular, phaneritic texture with subordinate porphyritic and foliated textures. Dark colored xenoliths of mafic composition are relatively abundant. Essential minerals in the granites are 2 feldspar (alkaline and plagiocalse), quartz, and hornblende, and biotite. Alkali feldspar is dominantly pink orthoclase.

Plagiocalse is mainly composed of rich calcium but oligoclase to andesine is insignificant. Plagiocalse formed complex zoning being very common. Greenish brown to green hornblende and biotite are major mafic minerals and muscovite is rare. Geochemical studies of Eastern Granitoid Belts (Mahawat, 1982 and Charusiri, 1989) indicated that the granitoids originate from differential crystallization of partial melting from true magma, “sensu stricto”. According to the classification of Chappel and White (1974), this granite type is I-type affinity. The Eastern Granitoid Belt possesses a widest range of SiO_2 content (57.16 to 76.33%). A large quantity of magnetite is also present in the rocks. The granitoids are called magnetite series granitoid, following the classification of Ishihara et al. (1981). Magnetite, zircon, sphene and apatite are common accessory minerals.

Charusiri et al. (1993) sub-divided granitoid of Eastern belt, using petrological and $^{40}Ar/^{39}Ar$ geochronological characteristics, into 4 episodes. It has been found that ages of the granitoids range from 210 to 245 Ma and can be grouped into 4 intervals; viz. 210 Ma, 220-225 Ma, 227-235 Ma, and 240-245 Ma. With integration of geological study in Loei province, it has been interpreted the granitoids of older interval (>240 Ma or Permo-Triassic to earlier Triassic) is likely to be associated with and related temporally and spatially to gold mineralization whereas granitoids of younger interval (220-225 Ma) are responsible for iron, copper, lead and zinc mineralization. The average age of granitoids at Doi Ngom, Phare province is 235 Ma. A granitic trend from Chantaburi province to the Thai-Cambudia border was sated at approximately 210 Ma (Late Triassic), which is younger than that of Tak province.

Central Granitoid Belt

Central Granitoid Belt occupies mainly the north-western part of the country extending from the Thai-Myanmar border in the north to Gulf of Thailand and covers also the eastern part of the Penisular area. The Central Granitoid Belt covers most of Thailand (Charusiri et al., 1993). In most cases, the granites intruded Lower Paleozoic sedimentary sequences and show close association with migmatite and the high grade metamorphic rocks of the region. Lithologically, these granites are coarse to very coarse grained porphyritic with large (up to 6-7 cm long) K-feldsapar, phenocryst and often show preferred orientation in the matrix comprising quartz, K-feldspar, plagioclase and

biotite. Hornblende, sphene, zircon, apatite and ilmenite are common accessory mineral. Primary muscoveite and tourmaline were observed in the Ternary plots, these granites are syenogranite, monzogranite, quartz synenite and quartz monzonite. Within Thailand, this granitoid belt encloses the areas of Chaiangrai, Chiangmai, Lampang, Lumphun in the north; Chonburi, Rayoung in the east; and Suratthani, Nakorn Srithammarat, Songla, Yala in the south. In comparison, the granitoids of the Central Granitic belt is quite different from those of the Eastern Belt in both origin and geological environment. The country rocks intruded by Central Belt graitoids are mainly Late Paleozoic to Early Mesozoic clastic sedimentary rocks without any associated voluminous volcanic or volcano-sedimentary rocks.

More than 90% of granitoid rocks in this belt are largely confined to granite *sensu stricto*, following the classification of Streckeisen (1976). The belt is considered to be characterized by mesozonal, porphyritic, coarse-grained, biotite-rich plutons (Hutchison, 1983; Cobbing et al., 1986; Charusiri, 1989). Mafic minerals such as green hornblende are not common. Muscovite is normally found and increasingly present in the areas adjacent to tin-tungsten deposits. Quartz is found in equal amounts to feldspar. Long laths of megacrystic feldspar are frequently microcline and microcline-perthite. Geochemistry of granitoids in this belt verifies that they originated from the partial melting of pre-existing upper crustal rocks or pelitic sediments. According to the classification of Chappel and White (1974), the granitoids are of S-type affinity, narrow range of SiO_2 content (65.20-77.21%) but contains high to very high alkali elements. In other category, when ilmenites in these granitoids are taken into consideration, the granitoids are classified as ilmenite-series granitoids (Ishihara, 1977). However, geological and petrochemical analyses indicate that I-type granitoids and magnetite-series granitoids are sporadically present as well, however in a much smaller amount in this belt (Charusiri et al., 1993).

$^{40}Ar/^{39}Ar$ dating (Charusiri, 1989) estimates the age of the Central Granitoid Belt as 180-220 Ma. This period is further subdivided into 2 intervals; 200-220 Ma for northern Thailand, and 180-200 Ma for southern Thailand. The ages of mineralization of Major tin-tungsten deposits such as Doi Mok, Chiangrai province, Tung Luang, Lampang province; Tung Po-Tung Kamin, Songkla province and Pinyok, Yala province, etc., are

mainly in the same of granites in the Central Belt. However, some knowm tin-tungsten deposits which carry rare earth elements (Khantaprab et al., 1990) such as Samoeng in Chiangmai province, and Khao Kamoi in Supanburi province have been proven to be 56 Ma (Tertiary) whereas the main phase granitoids in those areas were previously stated to be of 220-240 Ma (Teggin, 1975; Nakapadungrat et al., 1984; Charusiri et al., 1991) concluded from their recalculation of Rb-Sr whole-rock data that most of the granitoids of the Central belts are of S-type affinity on the basis of high initial Sr isotopic constraints.

Western Granitoid Belt

Western Granitoid Belt lies to the west of the Central Granitoid Belt along the Thai-Myanmar border from Mae Lama Stock, adjunct to northern end of the Moei-Uthai Thani fault zone to Phuket Island in the southwest of the Thai Peninsula. In general, the Western Granitoid Belt contains small to moderate batholiths and plutons of mainly restricted compositional range with a minor amount of the expanded type. Most of these granite plutons intruded into Permo-Carboniferous pebbly rocks of Kangkrachan group with a few exceptions, such as the Mae Lama Stock in Mae Hong Son which intruded into Cambrian-Ordovicain and Ordovicain sedimentary rock units. Intrusion of the Western Granitoid Belt into the border zone of the Central Granitoid Belt is not uncommon and the earlier often show less deformed features. Clarke and Beddoe-Stephens (1987) assigned Cretaceous Sn-W asoociated granite in northern Sumatra to the Western Granitoid Belt.

Geological, petrochemical and mineralogical studies on granitoids of ther belt reflect true granite which, again, is similar to those of Central Granitoid Belt. Hornblende is relatively rare whereas brown biotite and muscovite are very common, as well as quartz and microcline. Geochemically, about 98% of the granitoid rocks in this belt are of S-type and ilmenite-series granitoids are present locally, e.g. those in Phuket and Phang Nga areas (Charusiri, 1989) and in Amphoe Muang Prachaub Khirikhan. The Western Granitoid Belt also has a wide range of SiO_2 content (56.01-75.83%) similar to those of the Eastern Granitoid Belt. However, the majority of the granites of Western Granitoid Belt are highly alkali and posses S-type of Ilmenite Series characteristics. The

calc-alkaline variety of the I-type of Magnetite Series granite plutons is present in very small numbers.

Age determination using the $^{40}Ar/^{39}Ar$ method the granitoids from this belt reveals that both I-type and S-type granitoids in the Western Belt is 50-88 Ma (Late Cretaceous to Early Tertiary). These ages of granitoid emplacement can be further subdivided into 2 periods, 65-88 Ma and 50-60 Ma. Associated tin and tungsten deposits together with rare earth elements are inferred to have been related temporally and spatially with S-type granitoid also occur, but in smaller amounts, and are related to tin and tungsten-mieralization in northern and southern Thailand. These granites were reported by Nakapadungrat et al. (1984) to have 130 Ma age using the Rb-Sr whole-rock method.

Earlier works, such as those of Mitchell (1977), Hutchison (1978), Pongsapich et al. (1983), indicated that granites of SE Asia can be divided into 3 major belts on the basis of lithological, geological, and geochronological characteristics. These have been named the Western, Central, and Eastern Belts, Their details have been re-synthesized by many authors later based on new data, i.e. Charusiri et al. (1993).

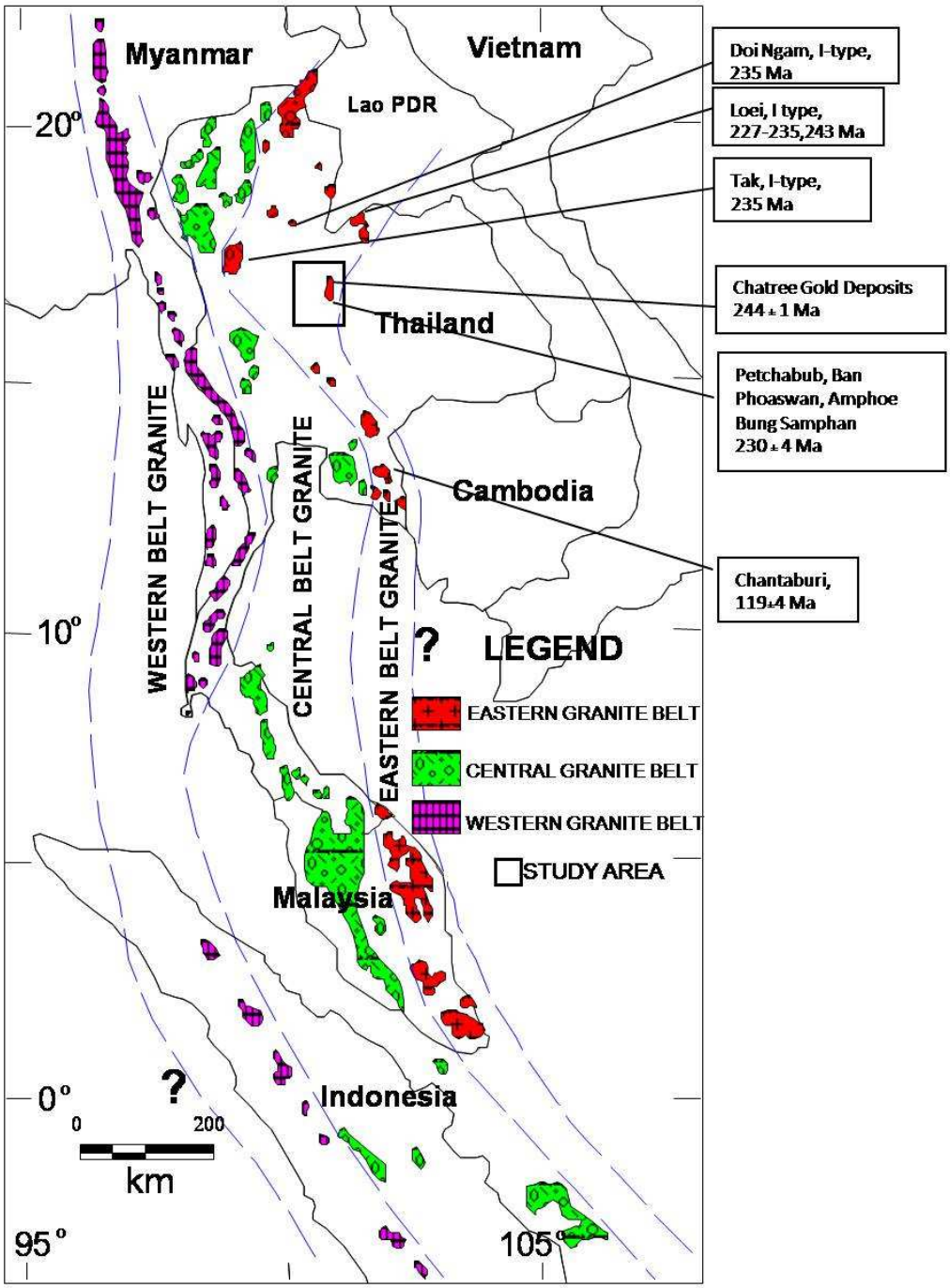

Figure 2.2. Index map of mainland SE Asia showing distribution of granitoids and their ages of Eastern Belt during 220-245 Ma. Numbers in boxes are in million years (Charusiri et al., 1993, Nantasin et al., 2005 and Salam et al., 2008).

Charusiri et al. (1993) sudivided granitoids of these 3 belts into 3 periods (Fig.2.2) by usibg $^{40}Ar/^{39}Ar$ dating data and those previously reported by other methods. They concluded Eastern Granitoid Belt formed in Early to Late Triassic (245-210 Ma), the

Central granitoid belt in Late Triassic to Middle Jurassic (220-180 Ma), and the Western Granitoid belt in Late Cretaceous to Middle Tertiary (80-50 Ma). I- type granitoid rocks are inferred to be related to Cu-Fe-Au-Sb mineralization and are largely limited to Eastern Granitoid belt.

2.2.2 Extrusive Rocks

Volcanic rocks are distributed in most part of Thailand; however, records of volcanic rocks exposed in Southern Thai Peninsular are very few. Based on their tectonic setting, distribution and ages of eruption, these volcanic rocks can be broadly grouped into Ching Mai Volcanic Belt, Ko Chang-Tak-Ching Khong Volcanic Belt, Loei-Prtchanbun-Nakhon Nayok Volcanic Belts and Late Cenozoic Basalts (Jungyusuk and Khositanon, 1992, Phajuy et al., 2004). Charusiri (1989) divided into 4 volcanic belts; Chiang Mai-Chiang Rai (CC), Chiang Khong- Tak (CT), Loei-Petchabun-Nakhon Nayok (LPN) and Volcanic Rock along Nan-Chanthaburi Suture Zone (NCZ) (Fig. 2.3).

Chiang Mai-Chiang Rai (CC) volcanic belt are basics lavas, hyaloclastic and pillow breccias (Panjasawatwong, 1993). Chemical characteristics of the San Kamphang basic volcanic rocks indicate that they are tholeiitic and transitional alkaline in composition. The basic volcanic rock Chiang Rai area may have formed in a subduction environment, but, the rest has erupted in an intraplate environment (Macdonald and Barr, 1978; Barr et al., 1990). Interpretation of the origin of the intraplate basalt is in controversy, whether it be continent affinities (Barr et al., 1990) or oceanic affinities (Panjasawatwong, 1993 and Pansawatwong et at., 1995). The correlation ages of these volcanic rocks have been reported to be Late Carboniferous to Late Permian (Garman Geological Mission or GGM, 1972) and Mid Permian to Permo-Triassic (Chuaviroj et al., 1980; Bunopas, 1981; Bunopas and Vella, 1983; Panjasawatwong, 1993).

Chiang Khong- Tak (CT) volcanic belt is the most abundant volcanic rocks exposed in northern Thailand. The rocks vary in composition from intermediate to acid represented by andesite, rhyolite and pyroclastic rocks. Stratigraphic correlation indicates that the eruption of these volcanic rocks occured in Permo-Triassic period. (Piyasin, 1972, 1975; Bruan and Hahn, 1976 and Charoenpravat, et al., 1987). However,

subordinate volcanic eruptions possibly occurred in Upper Triassic to Lower Jurassic periods.

Loei-Phetchabun-Nakhon Nayok (LPN) Volcanic Belt is the main calc-alkaline rocks in the country which formed as the accurate belt with N-S trending along the western margin of the Khorat Plateau to Sra Kaeo in Eastern Thailand near Cambodia border. Andesite and rhyolite are the predominant rock types with subordinate basaltic variety. Several episodes of volcanic activities occurred in this area which likely started as early as Middle Devonian (Intasopa, 1993). Other volcanic activities occurred during the Permo-Triassic period and ended at Late Tertiary. Rhyolite from the eastern Pakchom district yield a Rb/Sr isochem age of 374±33 Ma with an initial $87_{Sr}/86_{Sr}$ ratio of 0.706 and the spilitic basalt (located 16 km south of Pakchom) gave a Rb/Sr isochem age of 361± 11 Ma with an initial ratio of 0.70455 (Intasopa, 1993). Both ages confirm the ages obtained from the stratigraphic correlation, Upper Middle Devonian in the early phase and Late Devoniam in the later phase (Chairangsee et al., 1990; Jungyusuk and Khositanon, 1992).

Nan Suture (or Nan-Chanthaburi Suture Zone (NCZ)) and the Sukhothai Fold Belt reportred by Singharajwarapan et al. (2000) that reflect the processes associated with the collision between the Shan-Thai and Indochina Terranes in Southeast Asia. The Shan-Thai Terrane rifted from Gondwana in the Early Permian. Preliminary geochemical data from volcanic rocks in the Loei Fold Belt, to the east of the Nan Suture, support subduction-related arc volcanism in that area, but Intasopa and Dunn (1994) showed that these volcanic rocks have diverse tectonic settings of eruption and range in age from Late Devonian to Triassic. The present evidence suggests that most of the volcanic rocks in the Loei volcanic province are older than the Sukhothai Fold Belt and are probably related to an older arc.

Late Cenozoic volcanic rocks are mainly basalts which distribute sporadically in the northern, eastern and central part of Thailand. These basalts can be subdivided into two major groups, the corundum-bearing basalt and the corundum-barren basalts. However, based on geochemistry the basalt can be subdivided categorized into basanitoids and hawaiite basalts (Barr and Macdonald, 1981). The basanitoids comprise nephilinite, basanite, nepheline hawaiite, and mugearite. In contrast, the

hawaiite basalts comprise alkaline olivine basalts, hawaiite and mugearite. It is clearly noted that corundum is commonly associated with basanitoid basalts and not restricted to certain age. Major gemstone variety is sapphire, ruby, topaz, zircon and black spinal. Charusiri et al. (2004) observed at the area of Khao Kradong, Buri Ram Province, NE Thailand, Cenozoic basalt is middle to subalkaline basalt. The rocks are transitional from hawaiite to alkali olivine basalt. In terms of tectonic setting, Khao Kradong volcano is regarded as representative of Cenozoic basalts of continental-rift origin. Sutthirat et al. (2001) reported that an inclusion of corundum (ruby) was found in a clinopyroxene xenocryst in alkali basalt from the late-Cenozoic Chanthaburi-Trat volcanics of eastern Thailand.

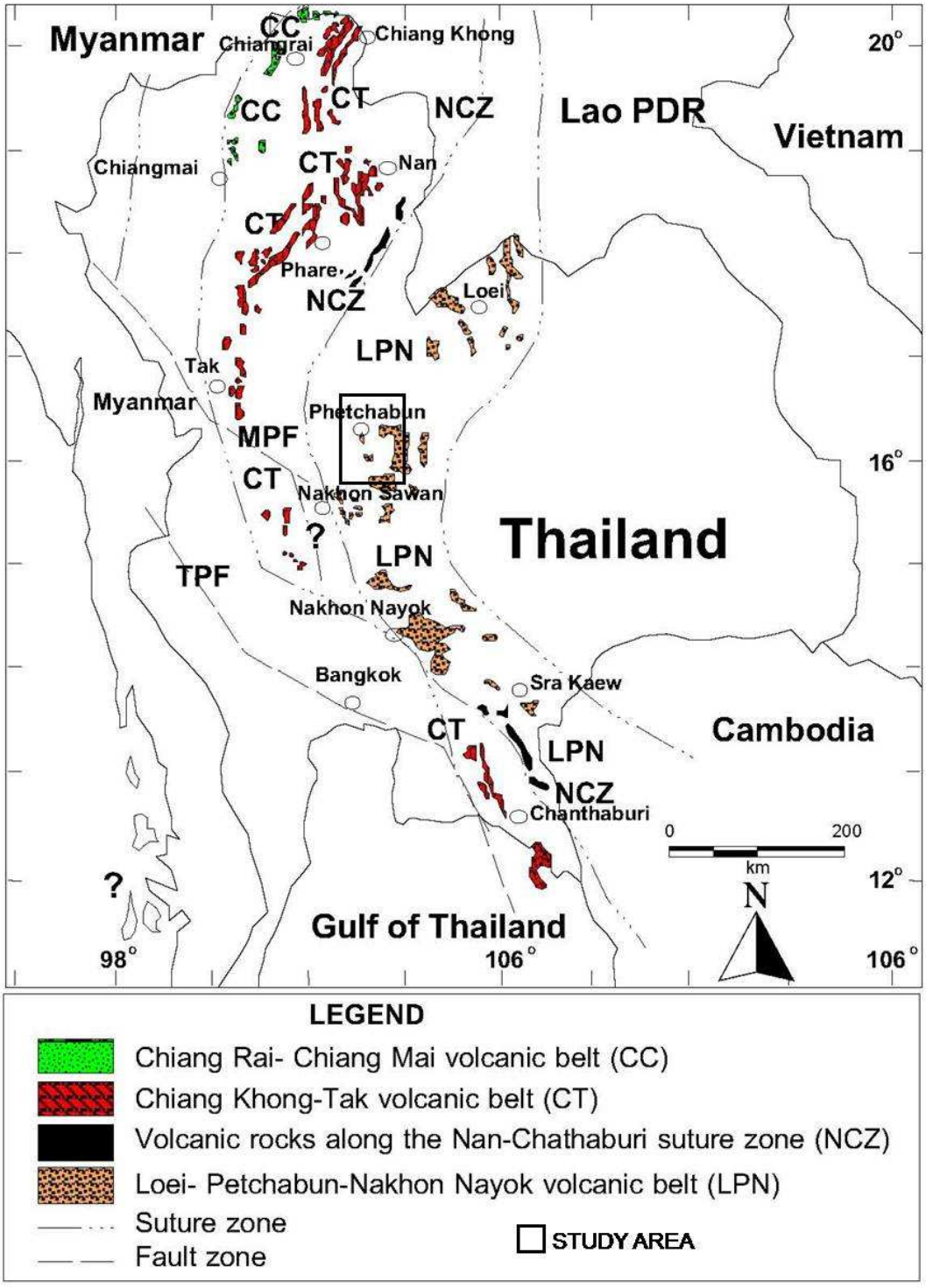

Figure 2.3. Index map of northern half of Thailand showing location of the study area within the Loei - Phetchabun -Nakhon Nayok Volcanic Belt (LPN) as well as the major faults and sutures in Thailand (Intasopa, 1993, Charusiri et al., 2002 and Phajuy et al., 2004).

2.3 Geology of Loei-Petchabun-Nakorn Nayok Volcanic Belt

The Loei-Petchabun-Nakorn Nayok Volcanic Belt (LPN) is consists of a complex terrane extending north-south from Loei province (Fig. 1.1) in the north on the border with Laos then turning northwest-southeast to Phetchabun province and continues to Nakorn Nayok province in the south which is possibly extending well to the east of this point into Cambodia. Age of volcanics and intrusions in the belt is ranging from Caboniferous to Triassic age (Salam et al., 2007). Most volcanics and sediments seem to be Permian on fossil evidence although some intrusions may be as young as Cretaceous. Absolute age dates are very scarce. Volcanics consist largely of andesites, dacites and rhyodacites as ash flow tuffs, flows, and volcaniclastic sediments. The presence of individual volcanic centres in the Loei-Petchabun-Nakorn Nayok Volcanic Belt (LPN) not been demonstrated so far. Intercalated with the volcanics are a series of finer grained volcaniclastic and epiclastic sediments ranging from silty tuffs to carbonaceous and pyritic black shales as well as locally thick limestone and limey sediments (marls). Intrusions are typically dioritic to granodioritic composition although little work has been done on establishing provenance or even the character of the intrusive rocks in the Petchabun-Nakorn Nayok Volcanic Belt (LPN). This may be critical as Chatree and other prospects seem to be associated with large granitoid intrusion centres. No work has been done relating the extrusive volcanics to the intrusions although such a relationship is almost certain and again may be critical for understanding the mineralization. Deformation in the Loei-Petchabun-Nakorn Nayok Volcanic Belt (LPN) around Chatree has not been studied in regional detail.

2.4 Geology of study area

The Phetchabun volcanic terrane is in the Loei-Phetchabun-Nakhon Nayok (LPN) Volcanic Belt which extends from northern Loas through central Thailand and occupies east of Raub Bentong structure in Peninsular Malaysia (Intasopa, 1992). In Thailand, this volcanic belt is dominated by Upper Permian and Triassic parallel zones of island arc felsic to intermediate volcanic and Triassic marine sedimentary rocks which were formed above a subduction zone prior to and during the collision in the Triassic of the Shan-Thai and Southeast Asian continental plates (Bunopas and Vella,

1992). The volcanism is characterized by 3 volcanic successions, specifically Carboniferous basaltic andesite flows; Permo-Triassic andesitic-rhyolitic tuffs, flows and sub-intrusives, which mark the western margin of the Belt; and Neogene basaltic and rhyolitic flows, which are recorded in the southern portion of the Belt possibly representing the reactivation of a zone of crustal weakness (Intasopa, 1992). Permo-Triassic intrusives perceived as cal-alkaline, I-type granites including diorite, quart diorite, granodiorite and quartz monzonite bodies are distributed throughout the Belt (Barr and Macdonald, 1991 and Garwin, 1993). Major structures in the Belt, from north to south comprise the southerly pluging Loei anticlinorium, the north-northwest oriented Chum Phae synclinorium and the west-northwest trending Saraburi anticlinorium (Garwin, 1993). Metal mineralization occurs in the Belt, characterized by base metals (Cu, Pb, Zn), iron ore, barite, manganese, pyrite, silver and gold. The majority of metallogenesis in the Belt is likely related to the Permo-Triassic intrusive magmatic-arc-related rocks and structural preparation provided by anticlinal folds formed during the late Triassic Indosinian Orogeny (Garwin, 1993, Charusiri et al., 1993).

The Phetchabun region is situated within the Loei-Phetchabun volcanic Nakhon Nayok belt, an arcuate belt of calc-alkaline volcanics that extends north-south along the western margin of the Khorat Plateau from Loei Province in the Nakorn Nayok provinve in Thailand. This large belt contains volcanic rocks of felsic to mafic compositions, which deposited during several episodes of volcanic activities extending from Mid-Devonian to Late Tertiary (Jungyusuk and Khositanont, 1992). They sub-divided the belt into six provinces and Phetchabun Province, which is dominated by andesite and basaltic andesite. These volcanics are commonly associated with intrusive bodies of microgabbro, diorite, and granodiorite (Fig. 2.4). Field relationships observed by Jungyusuk (1989) near Chon Daen in Petchabun Province suggest that andesitic lavas flow over and locally crosscut mid Permian Limestones and are overlain by Tertiary sediment. Crossing (2004) considered the Loei-Phetchabun- Nakhon Nayok volcanic belt to be a fossil continental arc developed on the Indo-China Plate during easterly directed subduction. It is situated within the Loei Fold Belt, a Palaeozoic-Mesozoic feature that consists of a series of north-south trending granitoid belts and associated volcanics. The Loei fold belt was formed as a result of subduction between the

Nakornthai and Indo-China Plates (Charusiri et al., 2002), which resulted in the amalgamation or interaction of fossil arcs and microcontinents.

2.4.1 Sediments and sedimentary rocks

The Chon Daen-Thap Klo area is underlain by both sedimentary and igneous rocks ranging in age from Carboniferous to Quaternary (Fig. 2.4). The Carboniferous unit consists mainly of limestone containing crinoids and coral fossils that are Lower to Mid-Carboniferous in age (DMR, 1999). Upper Carboniferous-Permian unit consists of sandstone (in part volcanic derived), shale, conglomerate and chert. Generally, this formation strikes NE-SW and dips SE. The rocks are locally metamorphosed along the contact with granodiorite.

The region of the Chatree deposit can be described following description of the geology of the Chon Daen-Thap Klo District (DMR, 1999). The Chon Daen-Thap Klo area is underlain by both sedimentary and igneous rocks ranging in age from Carboniferous to Quaternary. The Carboniferous unit consists mainly of limestone containing crinoids and coral fossils that are Lower to Mid-Carboniferous in age (DMR, 1999). Upper Carboniferous-Permian unit consists of sandstone (in part volcanic derived), shale, conglomerate and chert. Generally, this formation strikes NE-SW and dips SE. The rocks are locally metamorphosed along the contact with granodiorite.

Fossilifeous limestone is often present at various stratigraphic levels, and varies from thin beds interbedded within the andesite lavas and pyroclastic (e.g. east of Khao Khieo) to very thick and persistent beds of massive limestone dominated by crinoids fossils more distal to the volcanic centres. These limestones are best exposed near Noen Maprang (Crossing, 2004). Based on regional geologic map modified from Chongrakmani and Sattayarak (2004) regional geologic map shown in Figure 2.2, the lithostratigraphy of Saraburi Group and Khorat Group in study area was divided into 9 Formation in ascending order as below:

<u>Dok Du Formation</u>

The rock of this formation is found mostly in the western part of the regional area. The rocks are bedded dark grey limestone with fossil of crinoids stem, fusulinid, bryozoa and brachiopod intercalated bedded chert, yellow with brown sandstone,

metaquartzarenite, black shale and mudstone. The fossil indicate the age of Lower-Middle Carboniferous.

Huai Som Formation

This formation exposes in the west part of the regional area at Khao Noi. The rocks are grayish white tuffaceous sandstone, grayish white sandstone, yellowish brown siltstone, dark grayish white shale and grey mudstone with brachiopod (Brachythyrina sp.) and trilobite that indicate the Upper Carboniferous age.

Pha Nok Khao Formation

The formation consists of well bedded to massive limestones with black chert bed, chert lenses, sandstone, brown shale, siltstone, sandstone and conglomerate. Fossil found in this Formation are fusulinid, gastropod, microfossil, indicate the age of Lower to Middle Permian (Jungyusuk and Jinggit, 1986).

Nam Duk Formation

The formation consists of pelagic shale, clastic turbidites, and thin-bedded allodapic limestone. The facies represents a deep-sea basin depositional environment. This sequence consists of greywacke alternated with shale. In the greywacke all features of the Bouma-cycle can be found, characterizing them as turbidites. This formation also comprises a very thick sequence of clastic rocks, mainly sandstones and shale. Some beds are very rich in fossil and plant remains. In the upper part of this section limestone layers are intercalated generally rich in foraminifers and sometimes contain corals. The fauna are assigned to middle to late Middle Permian age (Helmcke R. and Helmcke D., 1986).

Hua Na Kham Formation

The Formation is mainly grey to black shale interbedded with yellow sandstone, limestone lense, conglomerate, siltstone, and indicate the age of Middle-Upper Permian (Jungyusuk and Jinggit, 1986).

Huai Hin Lat Formation

Rocks in this Formation are dominated by yellowish brown conglomerate, yellowish brown to reddish brown sandstone, reddish brown siltstone, green conglomeratic sandstone showing cross-bedding. Part of these rocks is thermal by

metamorphose to metasandstone (quartzite). This Upper Triassic formation was found in the western part of the regional area (Jungyusuk and Jinggit, 1986).

Nam Phong Formation

This formation exposes in the SE of the regional area. The rocks are sandstone, reddish brown, brown, cross-bedded, conglomerate, pebbles consisting of quartz, chert, red siltstone and sandstone, up to 10 cm in diameter; shale and siltstone, brown, reddish-reddish-brown. This Upper Triassic formation was found in the NE part of the regional area.

Phu Kradung Formation

The rock of this formation is found mostly in the northeast of the regional area. The rocks are shale, brown, reddish-brown, purplished-red, micaceous; siltstone and sandstone, brown, gray, micaceous, small scale cross-bedding with some lime-nodule conglomerate. The age of the rock is lower Jurassic period.

Phra Wihan Formation

The rock is composed of sandstone, white pink, orthoqoartzsitic, cross-bedded, massive, with pebbly layers on the upper bed; some intercalations of reddish brown. The age of the rock is Lower-middle Jurassic period. The rock found in the northeast of the regional geologic map.

Unconsolidated deposit

The Quaternary sediments are the terrace deposit, talus pile and colluvial deposit, composing of gravel, sand, silt and clay. They were found in the western and eastern parts of the regional area.

2.4.2 Igneous rocks

The igneous rocks in this regional area are composing chiefly of felsic to intermediate volcanic rocks, pyroclastic rocks and plutonic rocks.

Volcanic and pyroclastic rocks

The rocks are tuff, lapillistone, agglomerate, volcanic breccia, andesite and basaltic andesite. The unit indicates Permo-Triassic age as they were observed to lie between the Middle-Upper Permian and Upper Triassic unit.

Volcanic rocks with mafic to felsic compositions occur as lava flows, pyroclastic deposits, and dyke and sills. The volcanic rocks predominantly andesite,

andesite tuff, basaltic andesite, andesitic breccia, rhyolite and rhyolitic tuffaceous rocks. Their ages rang from Middle-Upper Permian to Lower Jurassic (Jungyusuk and Khosithanont, 1992). Plutonic rocks are covered by unconsolidated sediments, however, airbone magnetic indicate that dykes and stocks of granodiorite intruded in the area, particularly in the southern part of the Chatree deposit. Stratigraphic relations constrain the age of these plutonic rocks to a minimum Triassic age (DMR,1999). Diemar et al. (1992) have been observed volcanic rocks in this belt which are basaltic andesite and andesite cross cut and flowed over middle Permian limestone and locally overlain by Triassic sedimentary rocks. Crossing (2004) has been interpreted in the Chatree region there are several andesitic volcanic centers and a couple of rhyolitic centres. Proximal to the andesictic volcanic edifices are intercalated lavas, pyroclastics and volcanic clastic sediments displaying significant lateral facies variation and complex interfingering with adjacent volcanic centers. Thick andesite lava flows interdigitate with andesitic auto breccias, and these are interbedded with lithic (lapilli) tuff of andesitic and mixed province, and less volumetrically important crystal and ash fall tuffs. The lithic tuffs are often very large and consistent and extend well beyond the andestite lavas, suggesting they may be large valley filling or submarine mass flows rather than air-fall tuffs. The volcano-sedimentary sequence is mostly gently folded and dips mostly less than 30 and rarely exceeding 45 except near faults. In general the bedding becomes shallower dipping in the eastern half toward the edge of the Khorat plateau. Steeper dips occur in two NE-SW trending structural zones discussed below, especially in the immediate of large faults.

Loei-Petchabun-Nakorn Nayok volcanic belt, an accurate belt of calc-alkaline volcanics that extents north-south along the western of the Khorat Plateau from Loei Province in the north to Nakorn Nayok of Thailand. It is situated within the Loei-Fold Belt, a Paleozoic-Mesozoic feature that consists of a series of north-south trending granitoid belts and associated volcanics. The Loei Fold Belt formed as a result of collision between the Burmalayan and Indo-Sinain Plates, which resulted in the amalgamation of a collection of fossil arcs and micro-continents (Crossing, 2004).

Plutonic rocks

The intrusive rocks can be divided into 3 composition, including diorite, granodiorite and granite. The diorite is the dark grey with porphyritic texture. The pheonocrysts are plagioclase and hornblend with the size of 1 x 1.5 cm. The granodiorite is the dark grey, mainly fine grained with porphyritic texture with 1x 0.5 cm. Phenocryst is hornblende. The granite is white in color. It has a porphyritic texture with phenocryst of plagioclase. Muscovite was observed to be common in this granite. The plutonic rocks are in Triassic age but some may be younger. Become some of them were observed to intrude the Upper Triassic sediment units. The study area is located on boundary between Pichit and Phetchabun provinces, north-central Thailand. The study area lies within Loei-Phetchabun volcanic fold belt (Diemar et al., 2000) which extends from northern Laos through central Thailand and occupies east of Raub Bentong structure in Peninsular Malaysia. In Thailand, the belt is significantly bound by Upper Permian and Triassic parallel zones of ancient island arc that contains felsic to intermediate volcanic and marine sedimentary rocks.

Plutonic rocks are covered by unconsolidated sediments; however, airbone magnetic data indicate that dykes and stocks of granodiorite intruded in the area, particularly in the southern part of the Chatree deposit. Stratigraphic relations constrain the age of these plutonic rocks to a minimum Triassic age (DMR, 1999). Crossing (2004) mapped various intrusive rocks ranging in composition from felsic to mafic inplaced into the sequence as small to medium sized stocks and dykes. Most common are mafic intrusive dominated by diorite but ranging in composition from granodiorite to dolerite, and texturally from fine, even grained to porphyritic. Granitic intrusions occur as several clusters of stocks and dikes, often associated with regional structural trends. Two such clusters occur in the vicinity of Chatree mine where they appear to be spatially associated with intersecting the southeast structural trends. However the largest cluster is arranged along a NE-SW structural trend extending through Ban Khlong Takhian, and most of them are porphyritic texture. Large intrusions of granodioritic and diorite composition also occur to the south and southeast of this area, and some of these are also porphyritic (Crossing, 2004).

2.4.3 Historical Geology

Historical geology in this area begins with Carboniferous rocks that are composed of porcelanite, limestone, conglomerate and sandstone. The limestone contains fossils, such as crinoidstem and corals that indicate shallow marine depositional environment. Until Lower Permian limestone was deposited as thin bed to thick bed. It has abundant fossils which can indicate Lower Permian age. During Lower-Middle Permian, there is deposition of clastic sedimentary rocks, sandstone, conglomerate which is interbedded with thin bedded limestone. Depositional environment of Pemian rocks in this area is shallow marine to land. After that, the younger rocks were deposited but they do not appear in this study area now. Until Upper Permian age igneous rocks occurred in this area which volcanic activity is inferred to Upper Permian to Lower Triassic (Jungyusuk, 1987). From field evidence, it cut Lower Permian limestone and Lower-Middle Permian clastic sedimentary rocks. These igneous rocks are basalt, basaltic andesite, andesite and pyroclastic igneous rocks. They are a cause why country rocks, Lower Permian rock which can be appeared at the same or nearly elevation with younger rocks in other sub areas because they made Lower Permian uplift by their extrusive batholiths. From field evidence, there is limestone, country rocks, found in igneous rocks, Khao Pu Pun. Some younger rocks disappear because of gradation on the earth surface. After this period, there are some intrusive rocks intruded in this area which are diorite and granodiorite. Their age is about Upper Triassic to Lower Jurassic (Jungyusuk, 1987).

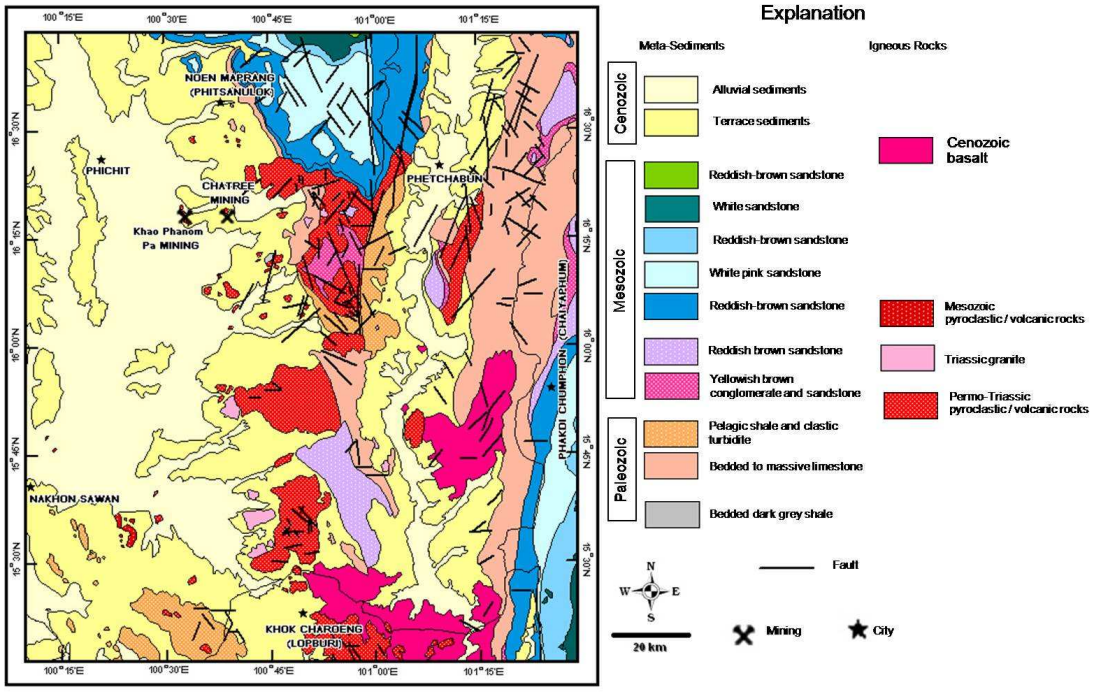

Figure 2.4. Geologic map of the study area (modified from Chonglakmani et al., 2004).

2.5 Mineralization

The Loei-Phetchabun-Nakorn Nayok volcanic belt (LPN) contains a wide variety of metalliferous mineral deposits (gold, copper, silver, lead, zinc, iron, barite, manganese and pyrite) (Fig. 2.5) but Chatree gold mine is the only one currently being exploited. Deposit types include; Porphyry Copper style mineralization and associated Gold-Copper skarns (Jacobson et al., 1969, Vudhichativanich and Sitthihaworn, 1993, Sitthihaworn et al., 1993), epithermal Gold-Silver mineralization (Diemar 1999), base metal-carbonate-gold epithermal veins and quartz-sulfide-gold-copper veins according to the classification of Corbett (2002), as well as Iron±Copper skarns, and deeper level possibly mesothermal quartz-gold veins in Khao Phanom Pa gold mine. Recently, areas of intensely silicified carbonate and siliclastic sediments have been found containing highly anomalous of gold. The relationship of the sediment hosted style of gold mineralization to the other styles of deposit in the belt is unknown. The porphyry deposits and some of the skarns show close relationship to a suite of dioritic to granodioritic intrusions.

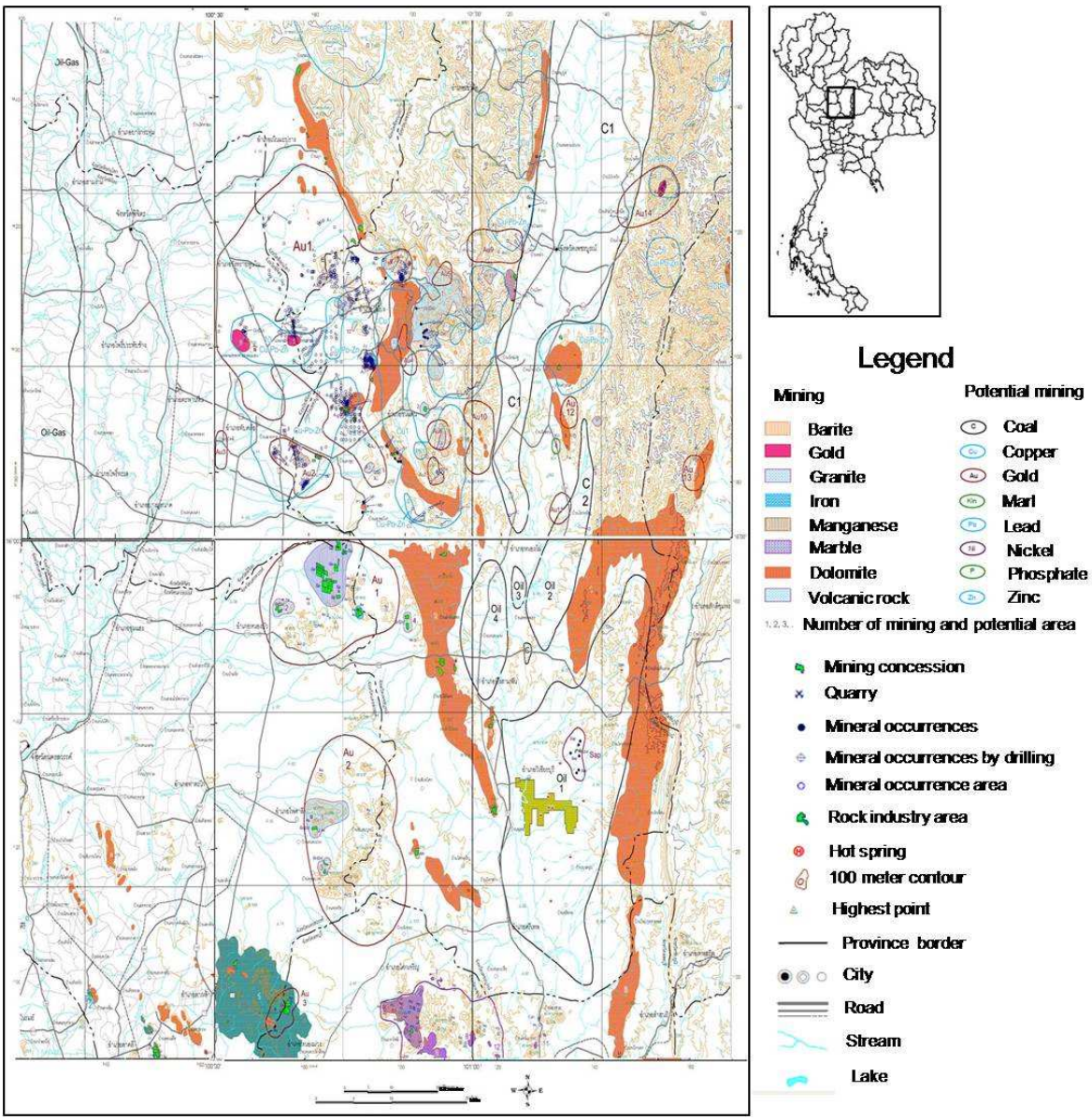

Figure 2.5. The mineral map of study area showing potential mineral occurrence, target and mining in study area (DMR, 2001).

CHAPTER III

Data sets and Methods

The purpose of this chapter is to present a detailed geophysical interpretation of the Phetchabun volcanic terrane by using enhanced airborne geophysical data integrated with field work, previous work and GIS information (MapInfo Professional version 9.0 program). The airborne geophysical and geological data are selectively acquired the Department of Mineral Resources (DMR) of Thailand. The main data set used in this study is comprised of survey B-3, B-4 and C-2 flying to reasonable of north-south across the main geological structure which have 2 km and 5 km line-spacing at 305 above ground level that was used to interpret basement geology (Mineral Resources Development Project, 1987). It is expected that the result of interpretations should help developing and evaluating the structural features in deep part as well as for understanding of regional geology related to tectonic history in the Phetchabun volcanic terrane of study area.

3.1 Previous airborne geophysical data

Regional airborne geophysical data in Thailand has been surveyed in early 1984. Survey methods include magnetic, radiometric and electromagnetic at different line spacing and elevations, depending on the purpose of work. All of the airborne geophysical surveys were performed by the Department of Mineral Resources of Thailand. The geophysical survey B and survey C (Fig. 3.1) were operated with a total of 300,000 line-km, covering an area of 430,000 km^2 by using magnetometer of Geometric G813 proton precession with noise envelope less than 1 nT. The main aim of this survey was for magnetic measurements. This survey was flown at 120 m MTC with 1, 2 and 5 km line spacing in an east-west direction. The difference between Survey B and Survey C indicates the types of aircraft used in the surveys. Survey B was flown by twin engine fixed wing aircraft over low relief terrain while Survey C was helicopter-flown over rugged terrain mostly in the west of the country. Aircraft used on the radiometric surveys were also equipped with magnetometer and VLF-EM sensors.

3.2 Airborne magnetic data acquisition

Most of this section is referred from Kenting International Earth Science (1987). Airborne magnetic measurements collected using a proton precession magnetometer model G-803 manufactured by Geometrics of California, USA. The console was housed in the equipment rack, and the magnetic sensor was towed in a 2 m bird towed at 10 m below the helicopter. This instrument measures the earth's total magnetic field strength by means of the precession of spinning protons, which have magnetic moment in a hydrocarbon fluid. The spin axes are normally oriented and process about the earth's magnetic field direction. To make a measurement of the earth's magnetic field, a polarizing field at a high angle to the earth is impressed on the nuclei for a short period aligning or polarizing the magnetic moments. When the field is removed the moments process around the direction of the earth' s magnetic field with a frequency that is proportion to the earth's magnetic field strength. This frequency is sensed by the same coil as that used to generate the polarizing field and is of the order of 1,700 Hz in a 40.000nT field. The constant of proportionality is 23.4874nT per Hz (KESIL, 1989). The output of the magnetometer was non-continuous, and the sampling interval was chosen as a multiple of the scan rate of the digital acquisition system. The entire sampling interval was set at 1.0 second combining with the average forward helicopter speed (50 m/sec); the sampling interval along the flight line was approximately 50 meters. The survey navigation was primarily by visual means from 1:50,000 topographic maps. At the field operational base, flight path recovery began with matching at intervals along the fight line and tracking film images to topographic map features. The accuracy of the location of the aircraft is limited by accuracy of topographic maps, camera image scale and aircraft altitude. The navigation position information recorded into the database resulted in each database record having a position LAT/LONG geographic coordinate in the IND74 datum. The processing of the data involved the calculation of UTM coordinates for each point in the database. In addition to the line data obtained from the measurements, map sheet at scale 1:50,000 have been produced from interpolation and gridding of measured data. The total-field magnetic line data were gridded using a minimum curvature routine technique. Then, the contour isopachs of the magnetic total

filed have been created from the gridded magnetic total field. Stacked magnetic profiles were generated from the final digital data for verification of data (Fig.3.2). All productions based on scale 1:50,000 consist of airborne magnetic map are the specification of airborne geophysical datasets used in this study follows;

Survey B-3 and B-4 fixed wing survey (Fig. 3.1)

- Flying height of 400 ft MTC
- Line spacing 2000 m (B-4) and 5000 m (B-3)
- Ground speed 50 m/s
- Sample interval 1.0 s
- Crystal volume 50.341
- Measurements of radioactivity, total magnetic field, VLF and altitude (radar)

Helicopter electromagnetic (HEM) follow-up survey, Phetchabun area

- Aircraft flying height 60 m mean terrain clearance (MTC), EM bird height 30 m, magnetic bird height 50 m
- Flight line spacing 400 m (E-W orientation), tie line spacing 5000 m (N-S orientation)
- Ground speed 32 m/s
- Sampling interval EM 0.25 s, magnetic 1.0 s
- Measurements of EM response at three frequencies, 736 Hz (coaxial), 912 Hz and 4200 Hz (coplanar), total magnetic field and altitude (radar)

Survey C-2 (Fig. 3.1)

Survey B and C were for the same purpose that is to provide radiometric coverage, with simultaneous ancillary recordings by magnetometer. Survey line direction and spacing were specified mainly on the basis of geology. Since the principle strike direction of the geological formations in most of the country is north-south to northwest-southeast, and east-west survey direction was maintained throughout. The line spacing depends on the complexity of the geology and the need for detailed information. Five-kilometer spacing was considered adequate for the generally flat-lying

formations of the Khorat Plateau. Along the west of Khorat Plateau and Upper Chao Phraya, the spacing was decreased to 1 km or 2 km.

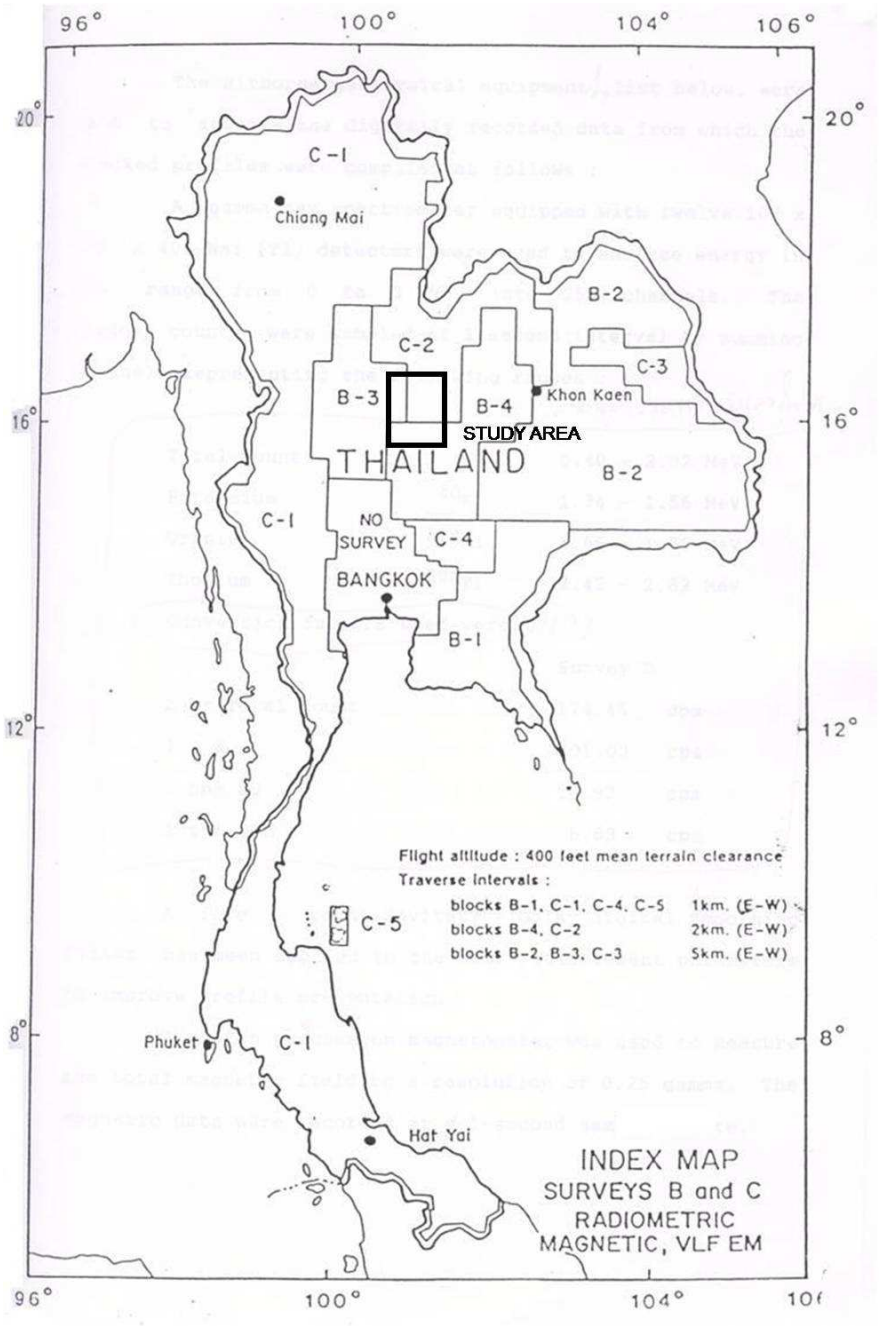

Figure 3.1. Index map of Thailand showing airborne survey B-3, B-4 and C-2 in study area with survey line spacing of 5 km for block B-3 area, 2 km for block B-4 area and block C-2 area. The survey was followed the east-west direction with 50 m data sampling interval. (Kenting Earth Science International, Ltd., 1989).

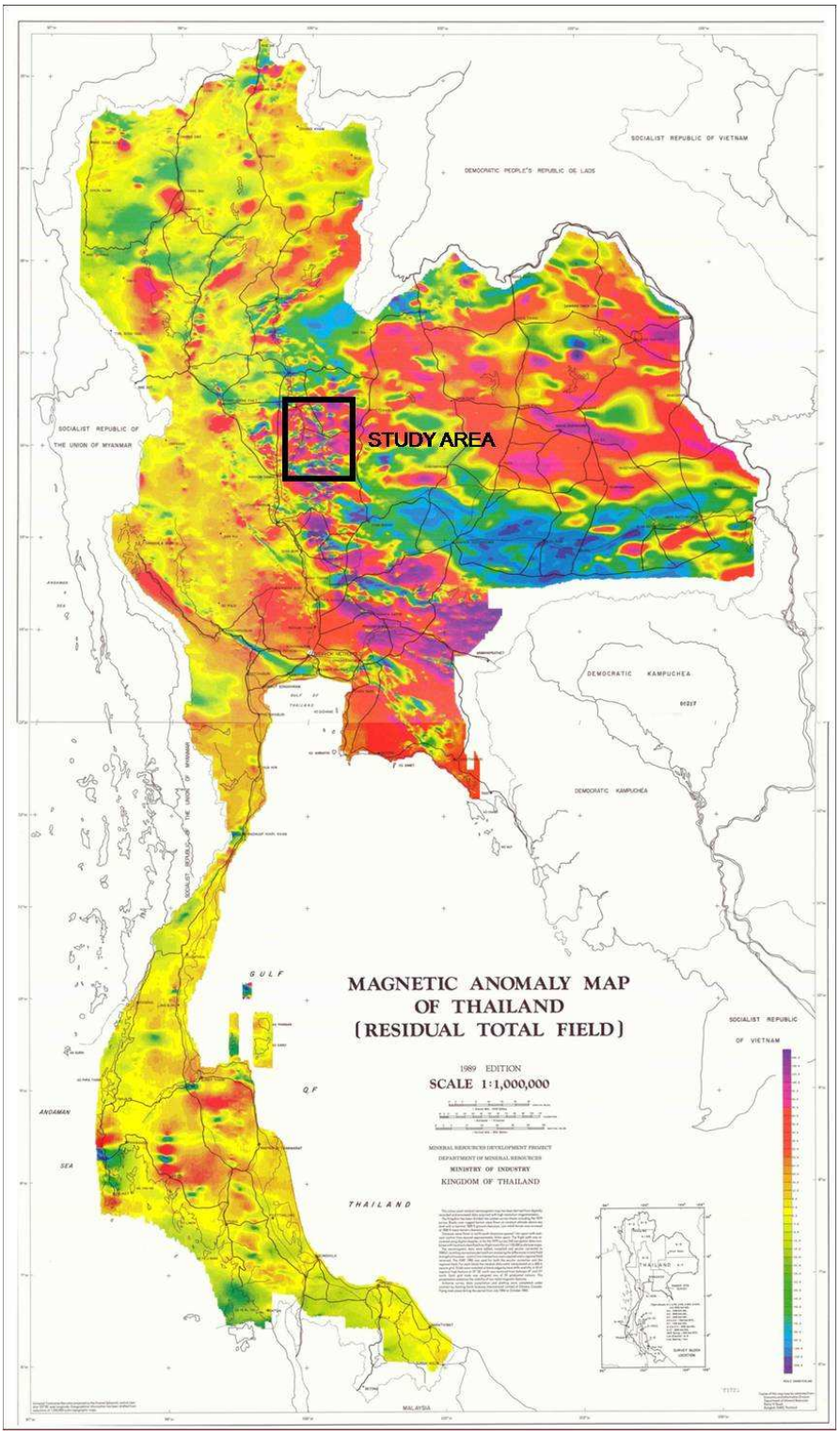

Figure 3.2. Residual magnetic map of Thailand (Kenting Earth Science International, Ltd., 1989) showing the magnetic anomalies responded to the almost north-south trending Phetchabun volcanic belt in the central part of the country.

3.3 Other data sets

3.3.1 Geological map

Geological mapping in the Phetchabun area was compiled from the 1: 100,000 scale geology map from Chonglakmani et al. (2004), and at 1:250,000 scale from Geological Compilation and Edition Section, Mineral Resource Development Project (MRDP, 1984). Geological outlines were digitized and attributed to the Arcview GIS format, in such a way that they could be overlaid on the geophysical map. The image products on the PC computer screen can assist lithological identification and correlation with mapped structures.

3.3.2 Elevation data

An elevation image was used the digital contour topography Mineral Resource Development Project from Mineral Resource Development Project (MRDP). Elevation data images were useful for correlating topography with magnetic features, and mineral occurrences, which assisted interpretation.

3.3.3 Mineral occurrences

Digital mineral occurrence data were selected from the database of the Economic Division from the Department of Mineral Resource (DMR) over the Phetchabun area for prominent minerals such as gold, lead, copper, barite, manganese and iron.

3.3.4 Magnetic susceptibility data

The aim of magnetic interpretation is to elicited geological information from magnetic survey results. Magnetic survey map contrasting magnetization between rocks containing different concentrations of magnetic minerals. There is a need for magnetic petrophysical studies of rocks to constrain the interpretation of magnetic survey results and for fundamental research in magnetic petrology to improve understanding of the geological factors that create, alter and destroy magnetic minerals in rocks. A crucial limitation of 2D magnetic models is controlled by the information on magnetic properties. Understanding of factors that determine magnetization intensities for the geological units within the survey area is essential for resolving geological ambiguity in order to produce a reliable interpretation of subsurface geology. In this study, the rock samples from the field representing all rocks types of the area were selected to measure magnetic

susceptibilities. The magnetic susceptibility data are used to compare with the geology and the modeling.

3.4 Airborne magnetic methods

The interpretation of magnetic anomalies over these geological regions is expedited by the development of special techniques and variation in crustal magnetic susceptibility allows the interpretation of observed magnetic anomalies. However, this is often complicated by the variation of the anomalies with respect to their sources. Many processing methods have been enhanced for improving the magnetic sources, the magnetization of the source material, and the geometry of the bodies. However, all processing methods suffer from the fact that no unique magnetization distribution can be found for a given set of observations. A number of techniques have been successful in predicting source characteristics, using certain assumptions. Enhanced magnetic techniques have been created to display more detailed information from the raw data by several authors. Milligan and Gunn (1997) described the enhancement and presentation of airborne geophysical data by using linear and non-linear filtering algorithms that selectively enhanced anomalies due to one group of geological sources relative to anomalies due to other groups of geological sources. The enhancements of the total magnetic intensity image are including vertical gradient, upward continuation and reduction to the pole. Gunn (1997b) illustrated the detail of quantitative methods for interpreting aeromagnetic data. The depths of magnetic source were determined by using the characteristics of profile data and automatic inversion programs. Furthermore, he described the regional magnetic and gravity response of an extensional sedimentary basin and explained the evolution of 34 extensional sediment basin compared with the characteristic of magnetic and gravity responses in each stage. Many enhancement techniques, such as reduction to the pole, vertical derivative, analytic signal, upward continuation, automatic gain control, and directional cosine filter were applied in this study. Each technique helps to display the edges of magnetized bodies and lateral contrasts in magnetization, which are mainly caused by lithological and structural changes in the buried basement. The image maps of the source edges are initially used

to group trends that have similar orientation. Interpretation of areas that have comparable anomaly amplitudes, and patterns, then domain boundaries and regions can be drawn. The boundaries are mapped more accurately using the source edge maps by placing margins at the position of source edges coinciding with major amplitude changes. The enhancement methods are described below.

3.4.1 Data enhancement methods

Since the aim of map processing is principally to aid the interpretation of the field data, we are at liberty to use any type of process which meets this criterion; mathematical rigor in the perfect separation of wave numbers is not a pre-requisite. However, it should clear that only those derived (enhanced) maps to which some physical meaning can be ascribed are useful in practice.

3.4.1.1 Colour Raster

Perhaps more popular in recent years is the colour raster map which, in effect, simulates the hand colouring of intervals between contour lines with a range of colours from the natural spectrum: red (high) through orange, yellow, green and blue (low). For each grid value, an appropriate colour shade is chosen (most probably again after some judicious contrast stretching across the available colour range) depending on its magnetic value, and plotted on the computer colour screen (Fig. 3.3) or on a paper map using an appropriate colour table. Colour raster maps look attractive to the eye, catching the attention of many new potential data users and reveal at once the difference between 'highs' and 'lows' which may not be immediately obvious on a contour map (Colin R., 2005). However, they do tend psychologically to emphasise long wavelength and high amplitude magnetic features which may not be the most closely related to the near-surface geology.

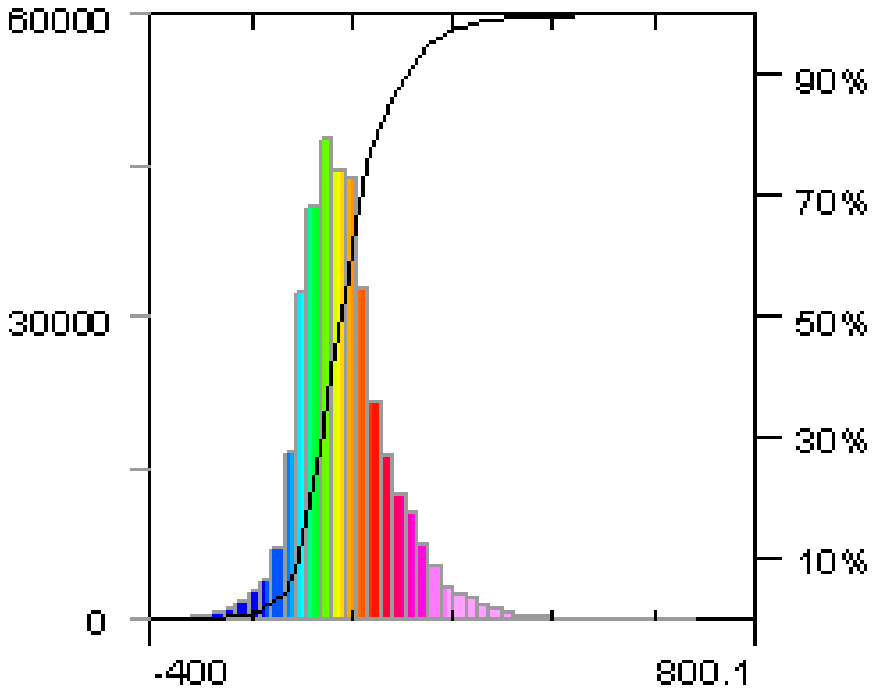

Figure 3.3. An example for grid histogram of reduction to the pole field data in this study.

3.4.1.2 Reduction to the pole (RTP)

Shapes of any magnetic anomaly depend on the inclination and declination angles of the main magnetic field of the Earth relative to the magnetization of the source (Fig. 3.4 B). The same magnetic body will produce a different anomaly depending on where it happens to be in the Earth's field (Fig. 3.4 B and C). In the case of an area has inclined Earth magnetic field (low inclination), the significant anomalies are shown by a couple of high and low magnetic intensities forming a dipole. In contrast, in the area of vertical Earth magnetic field, the magnetic anomalies are only shown by the high magnetic amplitude of the vertical bodies (Fig 3.4 C). Reduction to the pole (RTP) is the process of converting the magnetic field from magnetic latitude where the Earth's field is inclined, to the field at magnetic pole, where the inducing field is transformed to vertical. The RTP filter reconstructs the magnetic field of a data set as if it were at the pole. This

means that the data can be 35 viewed in map assuming a vertical magnetic inclination and a declination of zero (Milligan and Gunn, 1997). As a result, RTP greatly simplifies the interpretation of magnetic data. In this way, the interpretation of the data is made easier than what the raw data maps. The high magnetic boundaries are more accurately positive, because the vertical bodies will produce induced magnetic anomalies that are centered on the body and are symmetrical. However, reduction to pole has a problem where the survey area is setting at very low magnetic latitude (shallow inclination). Since, the study area has the inclination about 18.1 degrees, the reduction to the pole may be affected by the data processing. This problem and the solution for keeping this effect can be used analytic signal method to check this problem (Neawsuparp, et al., 2005).

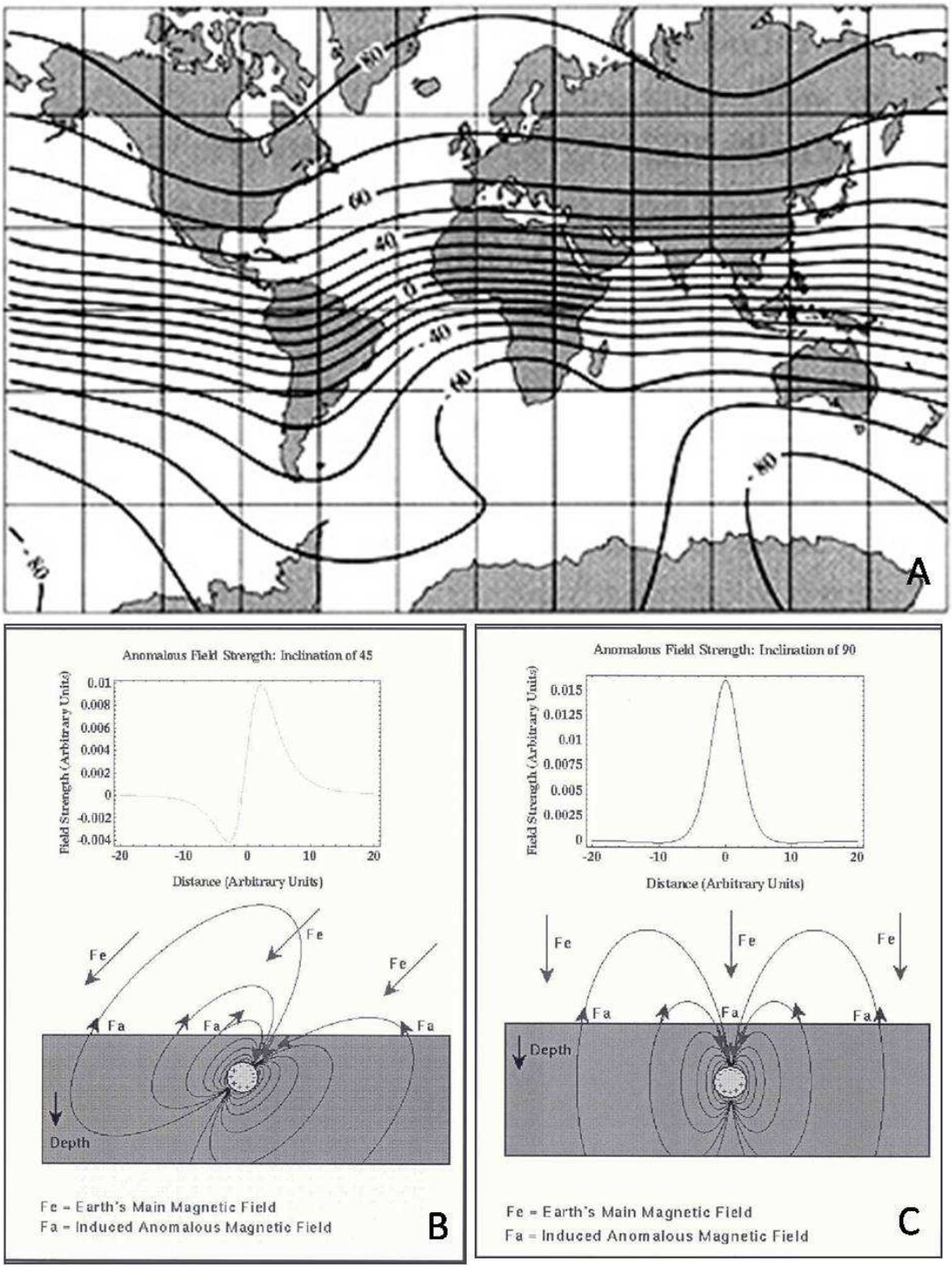

Figure 3.4 (A) magnetic inclination of the world show 10-25° inclination in Thailand (B) the example effect of magnetic anomaly over magnetic body with locate on 45° magnetic inclination (C) symmetry between magnetic anomaly and magnetic body with locate on 90° magnetic inclination (Gunn et al., 1997).

3.4.1.3 Analytic signal

Analytic signal of magnetic anomaly is a combination of the vertical and horizontal magnetic derivative (Roest et al., 1992). It has the useful property of being independent of the magnetization direction of the causative body. As in the case of the vertical derivative, the analytic signal exhibits a maximum at the edge of magnetic source body (Fig. 3.5). Theoretically, variation in dip along the edge has no effect on the location of the maximum. Hence, computing the analytic signal and locating its maxima is an efficient way of mapping the top edge of bodies independent of magnetization orientation and dipping contacts. This means that all bodies with the same geometry have the same analytic signal. Furthermore, as the peaks of analytic signal function are symmetrical and occur directly over the edges of wide bodies and directly over the centers of narrow bodies, interpretation of analytic signal maps and images should, in principle, provide simple, easily understood indications of magnetic source geometry. The computing of the analytic signal (Roest et al., 1992) is a function related to magnetic fields by the sum of derivative as follow:

Analytic signal: $|A(x,y)| = \{(\partial m/\partial x)^2 + (\partial m/\partial y)^2 + (\partial m/\partial z)^2\}^{-2}$

where m = magnetic anomaly

Analytic signal maps and images are useful as a check for reduction to the pole, as they are not subject to the instability that occurs in transformations of magnetic fields from low magnetic latitudes (MacLeod et al., 1993). It also defines source position regardless of any remanence in the sources.

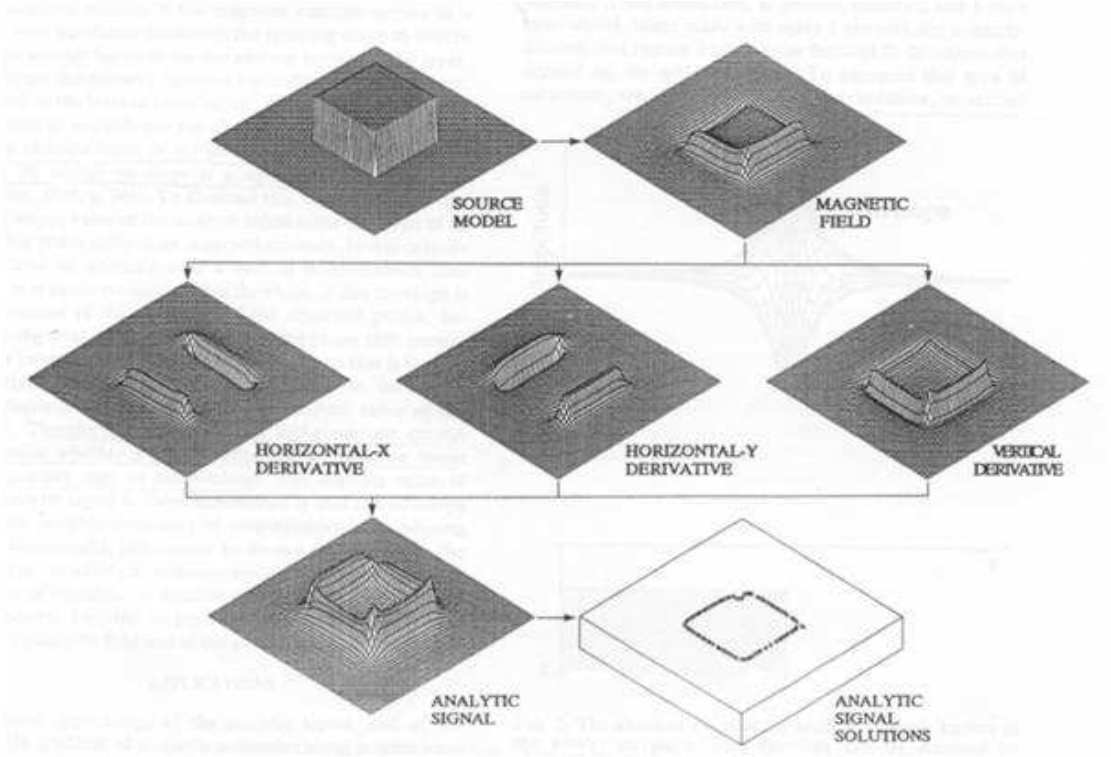

Figure 3.5. Analytic signal method showing peaks anomaly which is symmetrical and occur directly over the edges of wide body and center of narrow body-provide simple and easy interpretation.

3.4.1.4 High pass filtering (HP)

Filtering is a way of separating signals of different wavelength to isolate and hence enhance anomalous features with a certain wavelength (Fig. 3.6). A rule of thumb is that the wavelength of an anomaly divided by three or four is approximately equal to the depth at which the body producing the anomaly is buried. Thus filtering can be used to enhance anomalies produced by features in a given depth range. Traditional filtering can be either low pass (Regional) or high pass (Residual). Thus the technique is sometimes referred to as Regional-Residual Separation. Bandpass filtering isolates wavelengths between user-defined upper and lower cut-off limits. A potential field grid may be considered to represent a series of components of different wavelength and direction (Colin, 2005). The logarithm of the power of the signal at each wavelength can be plotted against wavelength, regardless of direction, to produce a power spectrum

(Fig. 3.6). The power spectrum is often observed to be broken up into a series of straight line segments. Each line segment represents the cumulative response of a discrete ensemble of sources at a given depth. The depth is directly proportional to the slope of the line segment. Filtering such that the power spectrum is a single straight line can thus enhance the effects from sources at any chosen depth at the expense of effects from deeper or shallower sources. It is a data-adaptive process involving spectral shaping. As such, it performs significantly better than arbitrary traditional filtering techniques described above. When magnetic depth slices coincide it is a good indication that the causative bodies are one and the same.

High-pass filter

$L(k) = 0$, for $k < k_0$

$L(k) = 1$, for $k \geq k_0$

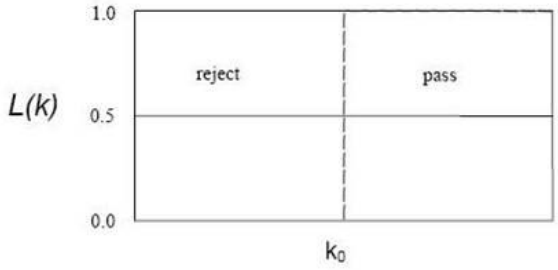

Wavenumber (cycles/ground_unit)

Parameter:

k_0 the cutoff wavenumber in cycles/ground_unit. All wavenumbers below this value are removed.

Ground_unit is the survey ground units used in your grid (eg. metre, feet etc.).

Figure 3.6 High Pass filtering method show cutoff low wave number or long wave length of magnetic signatures (Geosoft Inc., 2005).

3.4.1.5 Upward continuation

Upward continuation is a computation of fields at higher magnetic survey levels. The process has response of L(r) = e-hr (Fig. 3.7). This means that upward continuation

smoothes out high-frequency anomalies. The process can be useful for suppressing high frequency anomalies caused by noise and near surface sources (Fig. 3.8). The practice limits depend on the sample interval and the quality of the data set. A similar effect is achieved using the upward continuation, except that the measurement plane is further from the sources, and fewer side effects are produced (Geosoft Inc., 2005). Upward continued field may reflect the regional field and upward field bring deeper anomalies more focus. A potential field measured on a given observation plane at a constant height can be recalculated as though the observations were made on a different plane, either higher (upward continuation). This is a curve which is zero at zero wave number and increases exponentially at higher wave numbers, thus emphasising the effect of shallow sources and noise. Noise removal is thus an essential first step and continuation depths should not exceed real source depths. Some careful experimentation is usually necessary to obtain acceptable results.

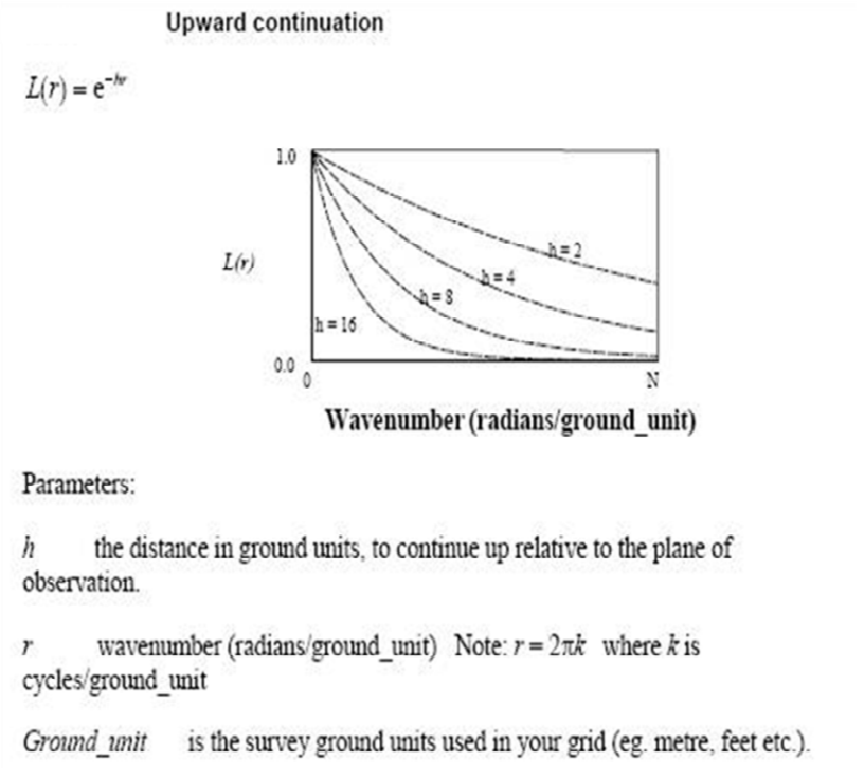

Figure 3.7. Upward continuation formula is used to remove or minimize the effects of shallow sources and noise in grid at higher survey level (Geosoft Lnc., 2005).

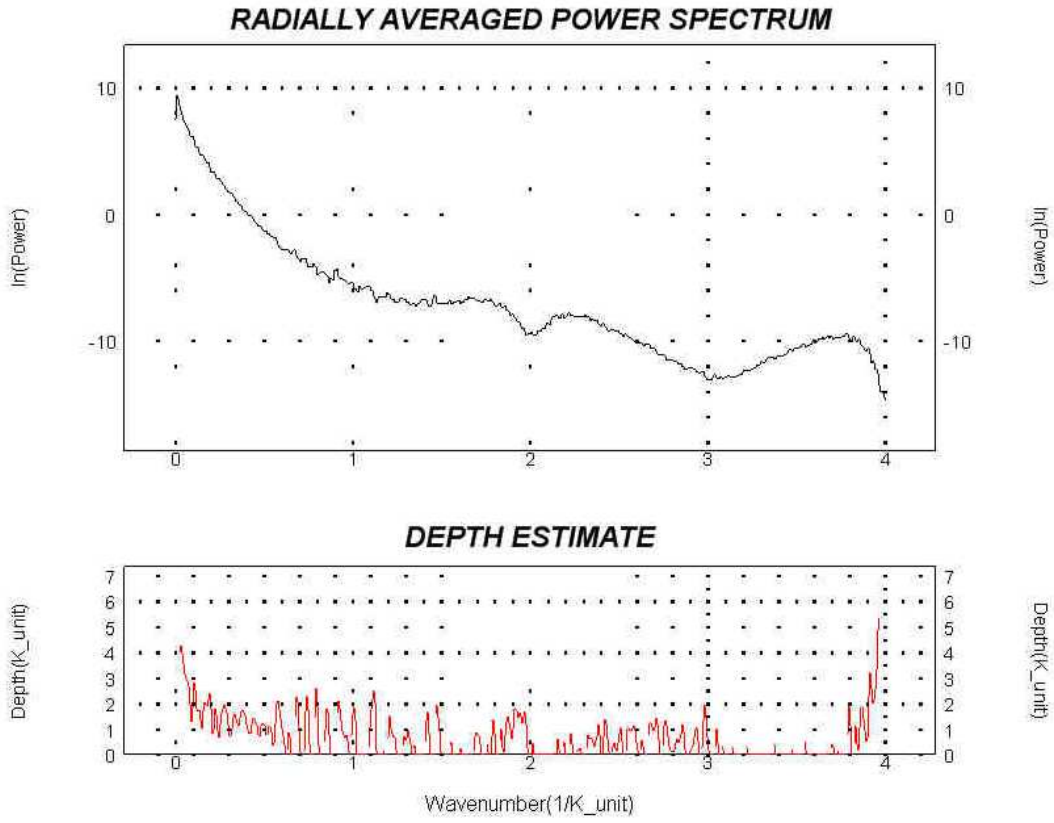

Figure 3.8 Radially averaged power spectrums of magnetic data in this study, show different between low wave number or long wave length and high wave number or low wave length at 1.5 1/K_unit of wave number.

3.4.1.6 Shaded relief (SR)

Shaded relief method can be exploited to give more persuasive visualisations, we would do well to think of capitalising on these advantages. The shaded relief map is perhaps the most widely accepted of these. The human eye can easily be deceived into seeing the magnetic variations as though they were physical topography. Even a simple positive anomaly which appears white (or black) in grey-scale can be made to appear to the eye as a hill by calculating the first horizontal derivative in the direction of a supposed illumination. A positive slope (i.e. a slope facing towards the 'sun' and given a light shade) then appears brighter than a negative slope (i.e. a slope facing away from the 'sun' and shaded dark). Let it be clear from the outset that we are using variations in the intensity of illumination scattered from a white surface to create this effect; shadows are not involved, though some have, confusingly, called their images 'shadowgrams'

(Colin, 2005). This process can easily be carried out on a grid using a small filter operator. The same data seen in Reduction to the pole map is re-displayed in this way in Shaded relief map. Choice of azimuth and elevation of the illumination source can be made to highlight the desired features and suppress others. The software allows the imaginary sun to be moved around the sky interactively and the interpreter can then recognize features that appear only at certain sun-angles that might otherwise be missed.

3.4.1.7 Directional cosine filter

The foregoing filters are completely expressed in their radially averaged representation since they are radially symmetric about the origin of a two-dimensional plot of wavenumbers in the x and y directions. Directional cosine filters are used to selectively remove anomalies or noise (e.g. corrugation) in a certain strike direction and their 2D response has a notch which reduces to zero amplitude at a certain range of wavenumbers and of a certain azimuth (Colin, 2005). A filter with a zero notch in the direction of the flight lines might serve as another way of moving line-related noise such as poor leveling (Fig. 3.9).

$L(\theta) = \left|\cos^n\left(\alpha - \theta + \frac{\pi}{2}\right)\right|$, to reject direction α

$L(\theta) = 1 - \left|\cos^n\left(\alpha - \theta + \frac{\pi}{2}\right)\right|$, to pass direction α

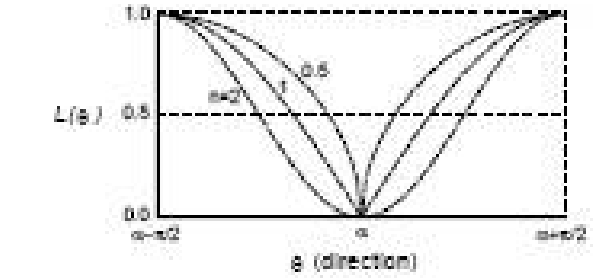

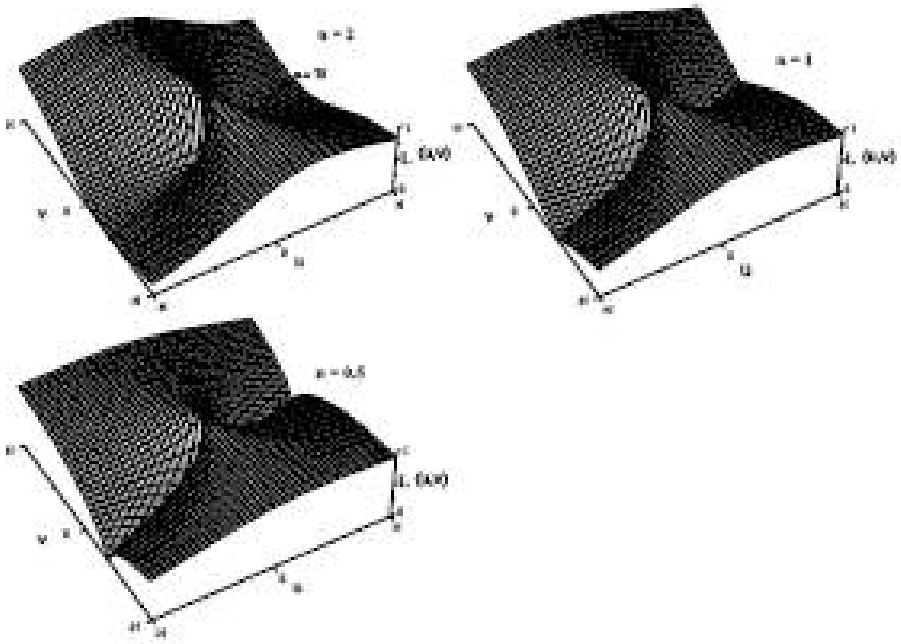

Parameters:

α direction of the filter in degrees (0-360 relative to North).

n the degree of the cosine function. By default, a degree of 2 is used to give a cosine squared function.

0/1 if 1, apply the filter to pass the specified direction; if 0, apply the filter to reject the specified direction. By default, the direction is rejected.

Figure 3.9. Directional cosine filtering method is removed direction feature by setting the degree of cosine function from a grid to good for interpreting structural features (Geosoft Inc., 2005).

3.4.1.8 Grey-scale raster

In this presentation, each cell of the grid is ascribed a grey pixel, the brightness of which depends on the magnetic value at that grid point. The highest values might be white, the lowest black, (or vice versa) with often a total range of 256 grey levels, equivalent to the dynamic range of the 8-bit computer word. To distribute the range of Z values optimally over the available grey levels often requires the use of some type of contrast stretching (see, e.g., Drury, 1987). For example, all the pixels in the image may be divided equally among the available grey levels, defining, then, the boundary between grey levels at an arbitrary set of 'contour' intervals. Subtle variations in grey-tone over long ranges are not detected by the human eye, but local contrasts are easily seen (Colin, 2005). For this reason, short-wavelength anomalies tend to stand out and there is an enhancement of anomalies attributable to near-surface geological features. At certain magnetic inclinations, the negative lobe of an anomaly which flanks a positive (or vice versa) often gives an optical '3D' effect, as through the magnetic anomaly field were an undulating white surface, illuminated from the side of anomalies that appear bright. (It should also be noted that human vision is easily deceived by these effects and the interpreter should take care to make sure that what he thinks he sees is actually what the data is trying to say, particularly since the choice of black or white for the 'high' values is often different for different image makers.)

3.4.2 Interpreting magnetic methods

Several interpretation methods were applied with the final goal of enhancing the signature of fault and rock boundary units. Magnetic data can be displayed as a profile or in a map. The interpretation for the two cases is different One of the most important thing to remember when analyzing magnetic data is that many interpretations may fit the observed data. For this reason it is always helpful to have other data to constrain the interpretation, i.e. geological information. Gunn et al. (1997) mention the interpretation methodology consisted of inspection of computer screen and hardcopy image, maps of the aeromagnetic data, and other relevant data to define:

- Boundaries of magnetic units,
- Structures dislocation or affecting the morphology of magnetic units,
- Depth and attitude of magnetic units,

- Any superposition of magnetic units, lithological units,
- Chemical change
- A structure synthesis relating distribution of inferred lithologies and structure.

The main resulting display data can be providing in form of profiles and contour maps. Profiles are best taken perpendicular to the strike of the anomaly. They can be used to identify zones with magnetic sources, get an indication of dip by comparison with master curves, and get an idea of relative intensities. After removing the regional trend, perform a quantitative interpretation is performed to determine possible depth, shape, size, and magnetization of local anomalies. Contour maps can be used to correlate low/highs magnetization to known geology and can be correlated with lows/highs in gravity map. Furthermore, they used to look for structural features represented in the contours and look for trends and identify area with no known source for magnetic characteristics.

The detail in residual magnetic data, supplemented by the range of enhanced map and image products typically produced to display these data, normally provide an excellent basis for qualitative interpretation in which geological boundaries and lithologies are visually estimated. Interpretation of this type, which in effect, produces outcrop or sub-outcrop maps, are routine for areas where all magnetic units occur at or near the ground surface and when anomalies are relatively discrete. Where magnetic rocks occur at variable depth or beneath substantial nonmagnetic cover, and where it is essential to know the depth to the magnetic sources, quantitative depth determinations are required. In some cases, specific details of geometry and magnetic properties of the magnetic sources are required and complete quantitative interpretation of magnetic anomalies must be undertaken.

3.4.3 Modeling method

Modeling provides a tool for integrating magnetic and other data, such as gravity, seismic, exploration well and surface geology. Using modern software on PC based modeling tool, interpreters can easily test a wide range of geologic models and examine the sensitivity of the magnetic response to the variation in those geologic models. This study uses the Mag2dc 2.10 program (described in the next section) for

determining the geometry of the magnetic sources. The automatic inversion routines produce a geological model, the magnetic affects of which match an observed magnetic data set.

Interpretation forward modeling and inversion foregoing account of magnetic anomaly shapes over common geological bodies is the background knowledge with which an interpreter should be equipped if it is to tackle the interpretation of a magnetic anomaly map. On such a map, usually some anomalies stand out quite clearly from the background (and the 'noise' of lesser anomalies) and may be recognised immediately as suitable cases where the theoretical anomaly of a simple body might be found to approximate closely the observed anomaly. These anomalies should be tackled first; the more difficult cases which remain often pose problems with regard to (1) identification of a sensible background level and (2) separation from adjacent anomalies. These factors test the experience and the perseverance of even the skilled interpreter. The anomaly is best studied, at least in the first instance, in profile form. The profile used may be first extracted from an individual flight line, edited to cover the distance over which the anomaly exceeds, say, 10 or 20% of its peak amplitude. (The flanks are seldom so well defined that a greater distance may be usefully examined without interference from neighbouring anomalies). Alternatively, a profile may be constructed by carefully marking intersections with contour lines along the edge of a piece of paper laid on a contour map or digitally using appropriate software on a grid file. Most often the body is first assumed to be 2D and the selected traverse is more-or-less across strike. (For a truly 2D body, a traverse at any angle other than 90° to strike is simply shortened by multiplying all distances by the cosine of the angle between the traverse and the normal to the body. In many practical cases, since all distances are scaled relative to horizontal profile distances, depth estimates and all horizontal distances made from non-normal traverses may be simply multiplied by such a 'cosine correction' when necessary.) The interpretation then proceeds by examining the profile and deciding (from the foregoing discussion) which type of body is likely to be the source of the anomaly. This decision also requires some geological reasoning; e.g. an anomaly which is nearly circular in plan view is unlikely to be due to a fault. The survey location, forward calculations can

then be made of the anomalies of likely source bodies and compared with the observed profiles (Fig. 3.10 B). A set of such anomalies should be calculated as a starting point for working on any new area. In airborne magnetic surveys, 2D bodies are always crossed by a (considerable) number of flight lines, and the anomaly as represented on each flight line may be interpreted independently from other flight-lines. Similarity between source models on adjacent lines gives added confidence to the robustness of the solution.

3.5 Magnetic susceptibility method

A rock-sampling program was carried out in the area to determine the magnetic susceptibility level for each rock type. Outcrops were chosen from the existing geologic map to ensure that each rock unit was sampled. Each rock sample was cut slab and measured the magnetic susceptibility in laboratory (Fig. 3.10 A).

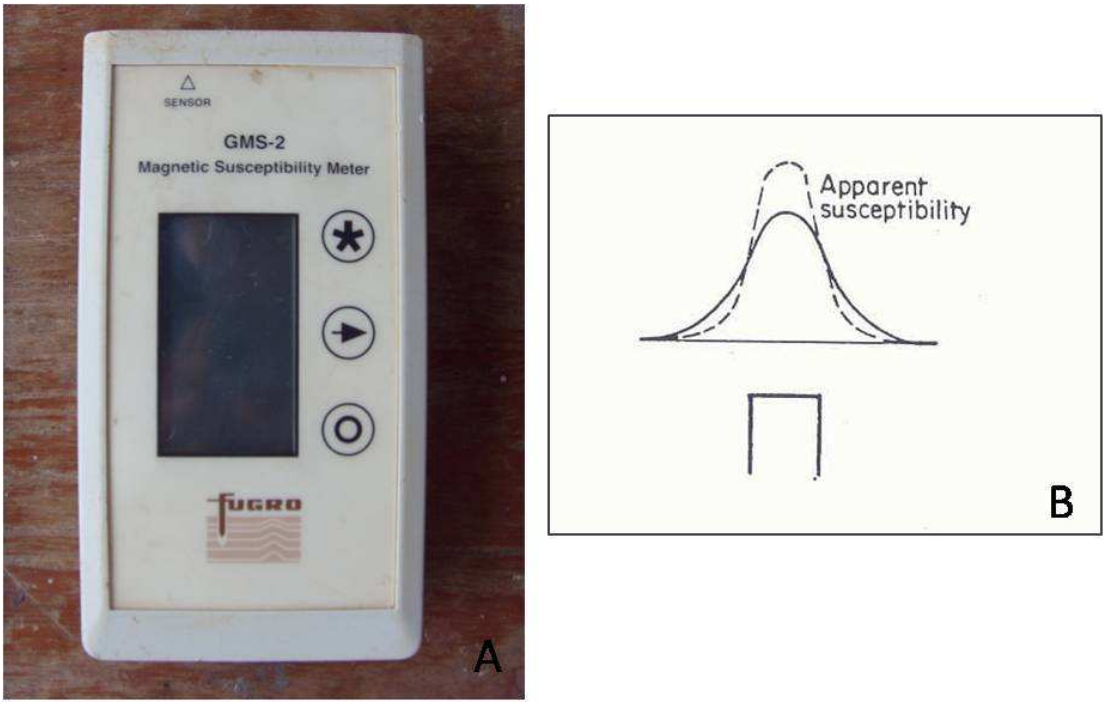

Figure 3.10. (A) Magnetic susceptibility meter from Issara mining Ltd. (B) Magnetic modeling by using magnetic susceptibility method (Gunn et al., 1997).

3.6 Software application

All of the data used in this study are a variety of grid data types and formats that mainly depend on the software employed in the processing. The most efficient system use software packages with compatible data type and grid format, so that conversion between formats is not necessary. The processing methods for this study can be divided to three applications.

3.6.1 Enhancement

A wide range of tools are available for modern PC-base software to enhance the geophysical data to focus on upper crustal structure. Interactive PC-base software provides efficient tools for geophysical dataset by using **Oasis montaj v6.1 program**. Oasis montaj is the software environment that is required to run all Geosoft software applications and tools. Applications are software packages that provide the software capabilities required for a specific earth sciences software application (Mineral Exploration, Oil and Gas Exploration, Earth Sciences and Environmental). The Oasis montaj environment provides direct access to data contained in Oasis databases through a spreadsheet window and an integrated profile display window. The Oasis database is a high-performance database that provides efficient storage and access for very large spatial data sets. The platform enables you to edit maps interactively, apply dynamic linking to maps and track the map creation processes. Visual data links are provided to dynamically connect data in the spreadsheet, profile and map views. Data processing is achieved through the application of Geosoft executable functions (GXs), which can be used to control all aspects of the data processing sequence and environment. DAT Technology (for Accessing Grids and Images) enables the platform to use a variety of grid and image formats in Oasis montaj.

3.6.2 Modeling

Modeling provides a tool for integrating geophysical data with surface geology by using Mag2dc (2.10) software. Using modern PC-based modeling tools, interpreters can easily test a wide range of geologic models and examine the sensitivity of the magnetic response to variation in those models. Mag2dc is written using Borland Delphi, and uses a Talwani type algorithm to calculate the anomaly. The contribution to the anomaly from each of the bodies is stored separately, so that a change to one body

does not require the whole model to be recalculated. There may be up to 50 bodies in the model, each of which may have up to 50 corners. There may be up to 8192 observed magnetic stations. Susceptibilities are measured in c.g.s . or SI units and the anomaly is measured in nT. Distances may be measured in Km or m. As well as forward modelling, Mag2dc allows the use of inversion, wherein mathematical techniques are used to modify the shape (and other attributes) of the model to improve the fit of the calculated curves to the observed data. Whilst being a useful tool, it should be remembered that the blind usage of inversion without reference to the available geological information may result in an incorrect interpretation.

3.6.3 Geographic information system

Geographic information system (GIS) is computer program for managing and integrating spatial data, maps, digital image and geo-reference data in table. For this study, data for GIS conclude geology, topographic and geophysics. Modern GIS computing software and relational data set are provided a unique situation for analysis of geological information by rapid digital integration of multiple data seta as layers in a map. Software for GIS data is used to analyze the data in this study that is MapInfo Professional (9.0). MapInfo Professional software is a comprehensive computer mapping tool that enables you to perform complex geographic analysis such as redistricting, accessing your remote data, dragging and dropping map objects into your applications, creating thematic maps that emphasize patterns in your data, and much more.

All of the research methods in this study are shown in Fig. 3.11.

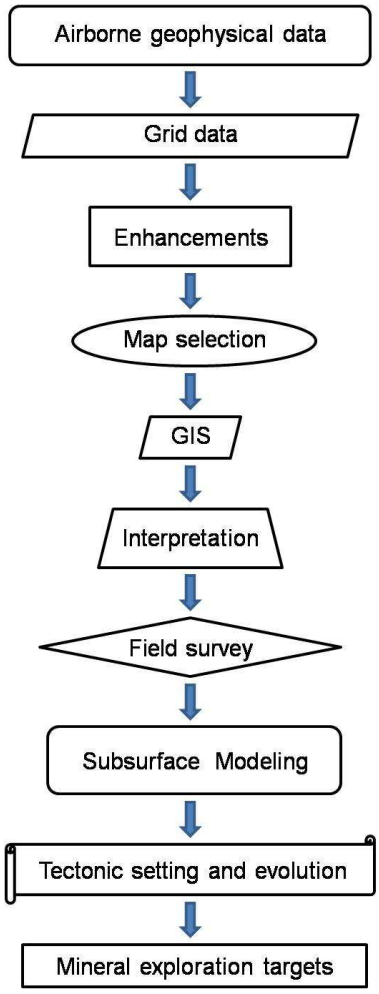

Figure 3.11. Flow chart showing the research methods in this study (Modified from Neawsuparpa et al., 2005).

CHAPTER IV

Result and interpretation

Airborne magnetic data of the study region were reprocessed, enhanced, presented as false-colour composite maps (Figs. 4.1 to 4.5 inserted in pocket), which some of them were accompanied by line contours. Derived magnetic maps were also produced using Fast Fourier Transform (FFT). They are reduction to the pole, residual high pass filtering, upward continuation, shaded relief, and directional cosine filter map, all domains processing of which serve as supplementary data assisting in structural interpretation. Furthermore, the interpretation of these data has been done along with geological information from the field survey at the same scale and data on magnetic susceptibility. Their methodology and results of the interpretation in this research are described below.

4.1 Airborne magnetic result

In this research all airborne magnetic results are displayed as digital image maps. They are residual magnetic intensity map, reduction to the pole map, residual high pass filtering map, upward continuation map, shaded relief map, directional cosine filter map. The magnetic raw data had removed the International Geomagnetic Reference Field (IGRF) from the raw the total magnetic intensity field data by Kenting International Earth Science, Ltd. (1987) to make it easier for interpretation.

The relative residual magnetic map shows magnetic intensity level ranging from -468 to 468 nT and a base level of the map is -12.4 nT. Local variations of field intensity exceed 93 nT in the central part and diminish to less than 72 nT in the eastern parts. The residual magnetic map (Fig. 4.1) exhibits three regional magnetic zones, roughly trending in the north-south direction based on intensity, shape, and pattern contrasting in magnetic responses and features. The most prominent high magnetic intensity is in the central part between Noen Maprang and Khok Chareong sub-province and tends to continue southward to the Lopburi province. Within this zone, there are series of the elongated and relatively higher magnetic intensities trending in the northwest-southeast direction.

The reduction to the pole map (Fig. 4.2) displays similar magnetic features, but more significant, to those of the residual magnetic intensity map. Such enhancements lead to the more outstanding magnetic boundaries. Four magnetic zones as well as geological lithologies and structures shown in the residual magnetic map are quite more distinct in the RTP map. From the east, there exists the low magnetic intensity zone clearly visible on the enhanced map, such as in Phetchabun province. Additionally, the boundary between the central zone and the eastern zone is displayed by the fairly sharp magnetic contrast as clearly observed at Khao Pa Nom Pa gold mine. To the west, the zone is characterized by low magnetic intensity in the southern part as seen in areas around Nakhon Sawan province whereas in the north it is represented by the flat magnetic features with the average diameter of about 20 km at Noen Maprang sub-province. In the eastern zone, central and western the intensities usually range from -349 to 660 nT. In the northern zone, the intensities vary considerably from 20 to 400 nT. Relatively low magnetic intensities from 0 to 50 nT are clearly observed in the central zone from eastern part of Khok Chareong sub-province. The RTP map shows the highest magnetic intensity in the central zone with the average peak to peak at about 446.2 nT. These high anomalies are oriented in the northwest-southeast trend with the total length of about 165 km from Phichit province to Khok Chareong sub-province. The eastern edge of this anomaly is marked by a sharp magnetic gradient in the northwest-southeast trend extending from eastern, western and northern Phichit province to eastern Khok Chareong sub-province. In the western zone, the relatively low magnetic intensity in area especially south of Nakhon Sawan province. It should be emphasized that the boundary contrast within individual zones are quite clear.

Three anomaly patterns are found only in the the study area, such as south of Phetchabun northeast of Chatree mine. Three unit boundaries can be observed from the reduction to the pole map (Fig. 4.15) with the folded structures in central zone. However the folded structure in areas between Phichit and Khao Phanom Pa are less clear, and much obliterated fairly when using upward continuation from the depths of 1000 m (Fig. 4.5). Additionally, the folded structures to the central area are not clear when applying upward continuation from the depths of 1,000 m. However, groups of elongate features in the central part (in Fig 4.15) are changed to the high magnetic intensity from west to

east in the deeper part of 1 km upward continuation, whereas the large circular magnetic body (in Fig. 4.15) in the eastern part remains smaller shape in size at depth of upward continuation 1 km.

The residual high pass filtering map shows high magnetic intensities outside anomalies and low magnetic intensity inside anomalies as ring structure in the eastern and northern domain with regional trend in northwest-southeast. However, the Chatree gold mine is not show low magnetic inside but also show same magnetic intensity as ring anomalies.

Shaded relief map is applied by following reduction to the pole field data which is reveal significant magnetic patterns such as linear structures or lineaments. The zone boundaries are quite clear when using the Shaded relief map (Fig. 4.6) compare to reduction to the pole map.

As shown in directional cosine filtering map (Figs. 4.7, 4.8, 4.9 and 4.10) it is quite clear that linear patterns are more prominent in the central than those in the eastern and western parts, and most of the northwest lineaments are crossed-cut by the northeast lineaments but in the eastern zone the northeast lineaments are crossed-cut by the northwest lineaments. Good examples are between Khao Phanom Pa and Phetchabun province. The difference in lineament patterns is clear for enhanced magnetic zones as displayed by directional cosine filtering. As shown in Fig 4.6, when shaded relief was applied to the reduction to the pole map, it is observed that the enhanced may displays the prominent lineaments close to the northwest-southeast direction. On the other hand, when a pass direction was used for a directional cosine filter in the map (Fig. 4.9), the northwest-southeast lineament (Fig. 4.7) pattern is clearly better observed than those of the other maps. Good examples are at Phetchabun and Khao Phanom Pa areas. The continuous lineaments, about 130 km in length, of this direction seem to cross-cut four regional magnetic zones earlier mentioned. Well-defined examples are Phetchabun to Nakhon Sawan areas.

Additionally, some lineaments in the southwest of Phetchabun show minor displacements, as illustrated in Figs.4.7. The result shown in these maps clearly indicates that the northeast-southwest trending lineaments are cross-cut by the northwest-southeast trending lineaments in the eastern part of the study, such as those

found in Noen Maprang (see Fig.4.6). The upward continuation maps (Fig. 4.5) show the magnetic intensity of high magnetic anomalies in the central part being change to northeast direction.

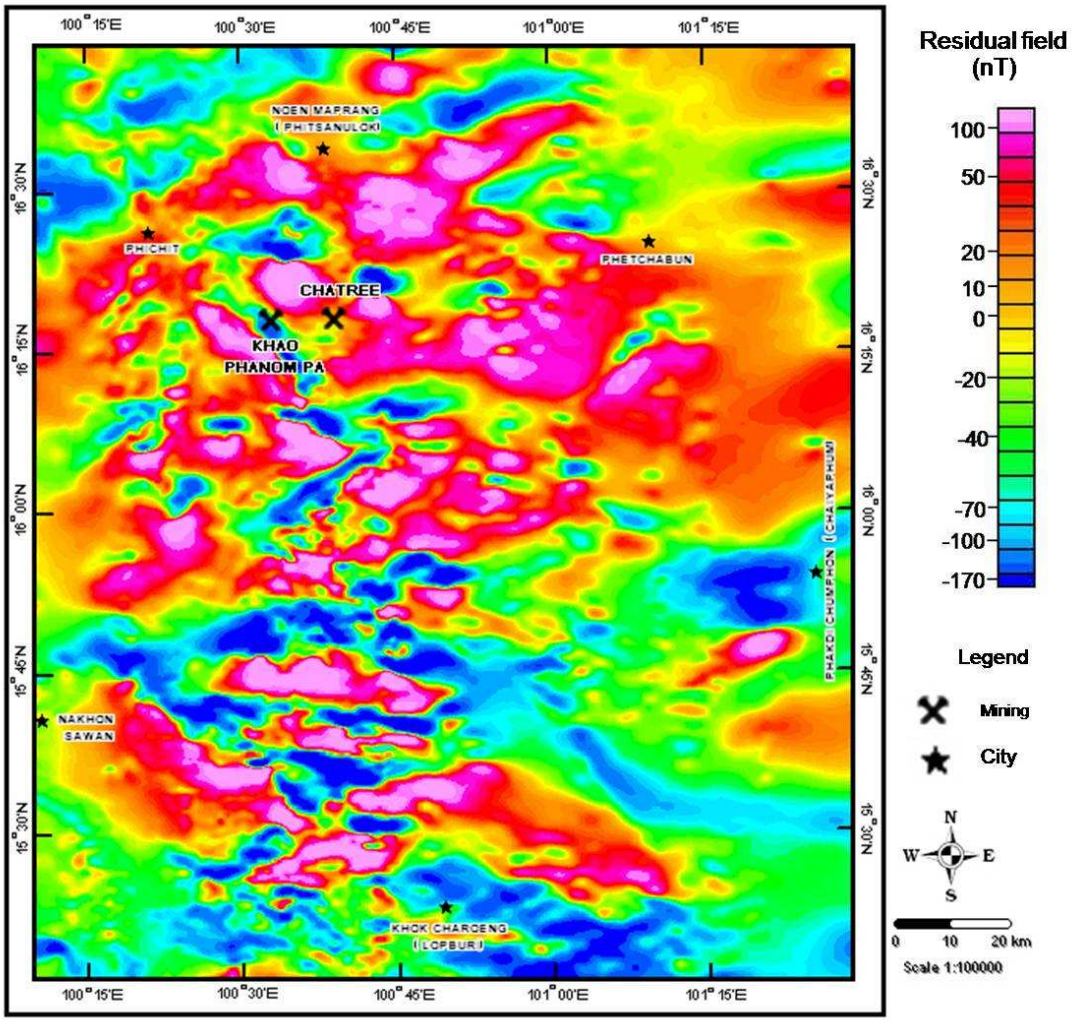

Figure 4.1. Enhanced airborne magnetic map based on residual intensity data with subtracting of International Geomagnetic Reference Field (IGRF) by Kenting International Earth Science, Ltd. (1987) and shows local complex magnetic intensities of the area. The anomalies represent by a pair of high and low magnetic intensities that are depended on magnetic inclination angle of the area.

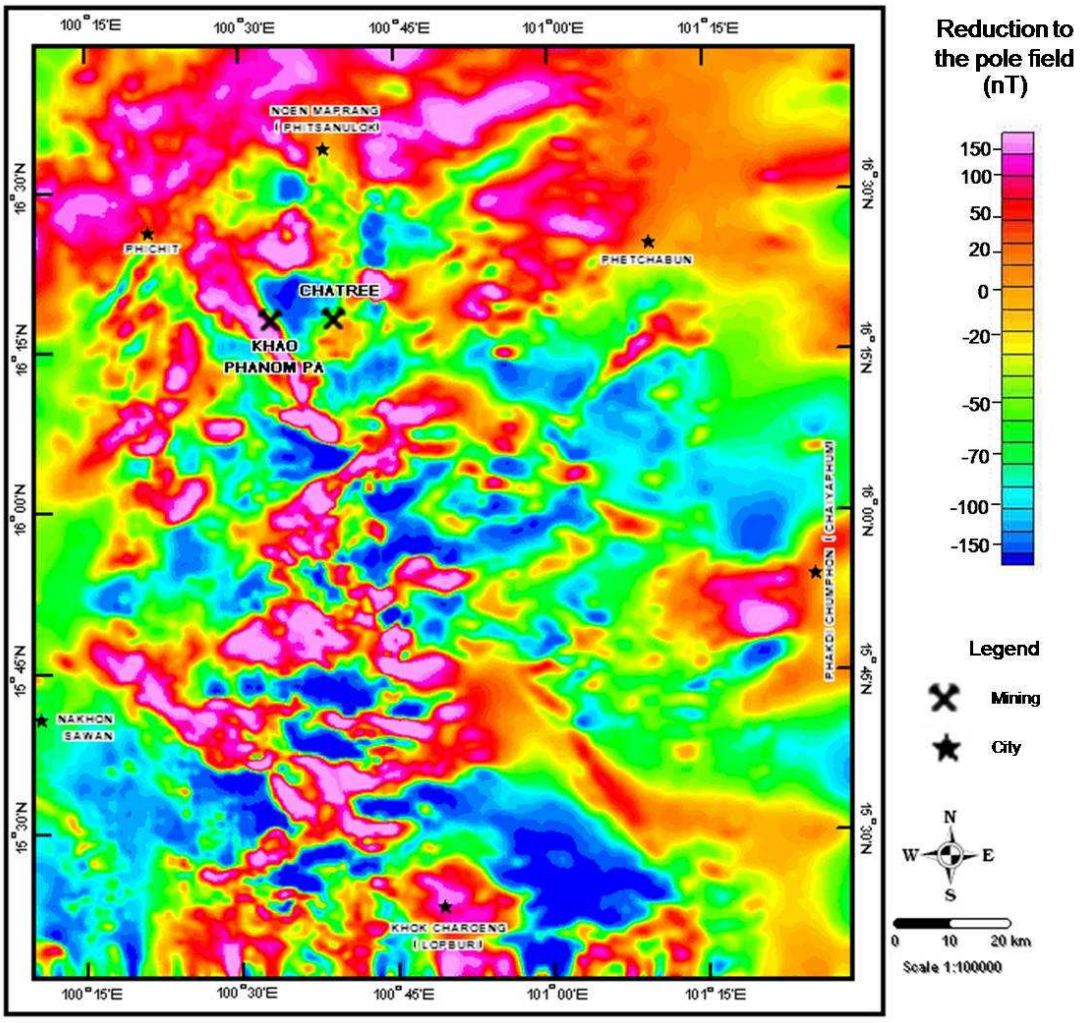

Figure 4.2. Enhanced airborne magnetic map of the Phetchabun volcanic terrane based on reduction to the pole (RTP) data using Inclination 18.1°, declination -0.43° and amplitude 40°. Noted that anomalies are directly induced over magnetic sources.

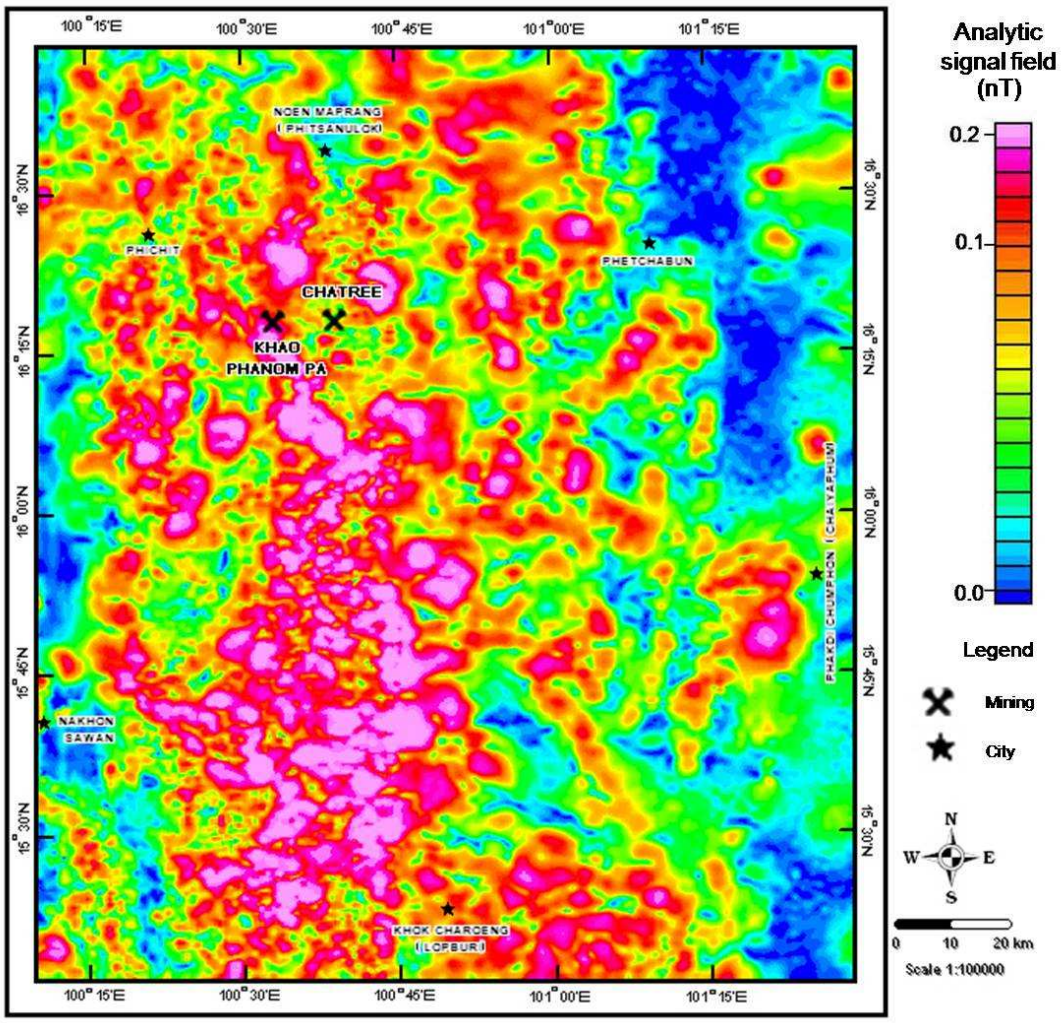

Figure 4.3. Enhanced airborne magnetic map of the Phetchabun volcanic terrane based on analytic signal (ANA) data.

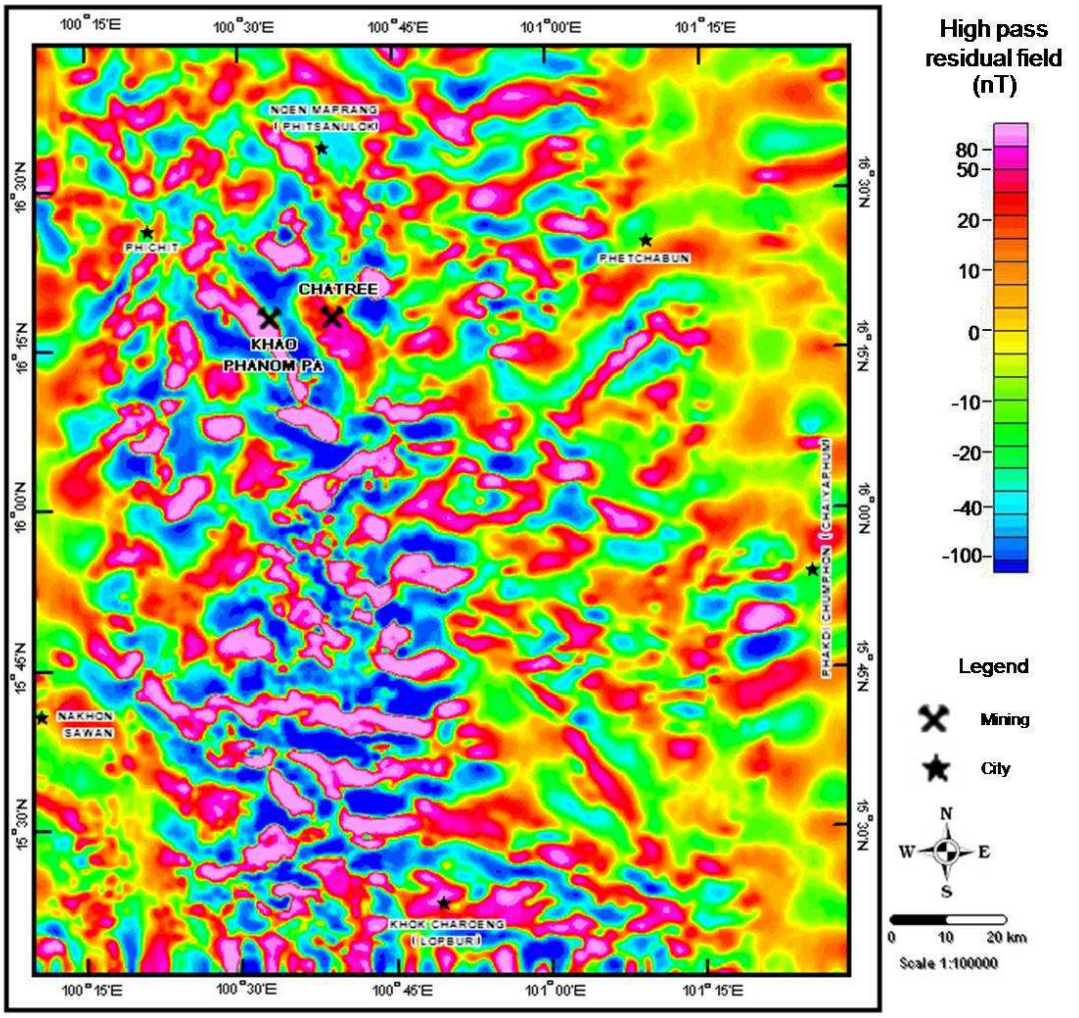

Figure 4.4. Enhanced airborne magnetic map of the Phetchabun volcanic terrane based on high pass residual filtering data by cutoff at 1.5 1/K_unit of wave number for separating long magnetic wavelength form the map.

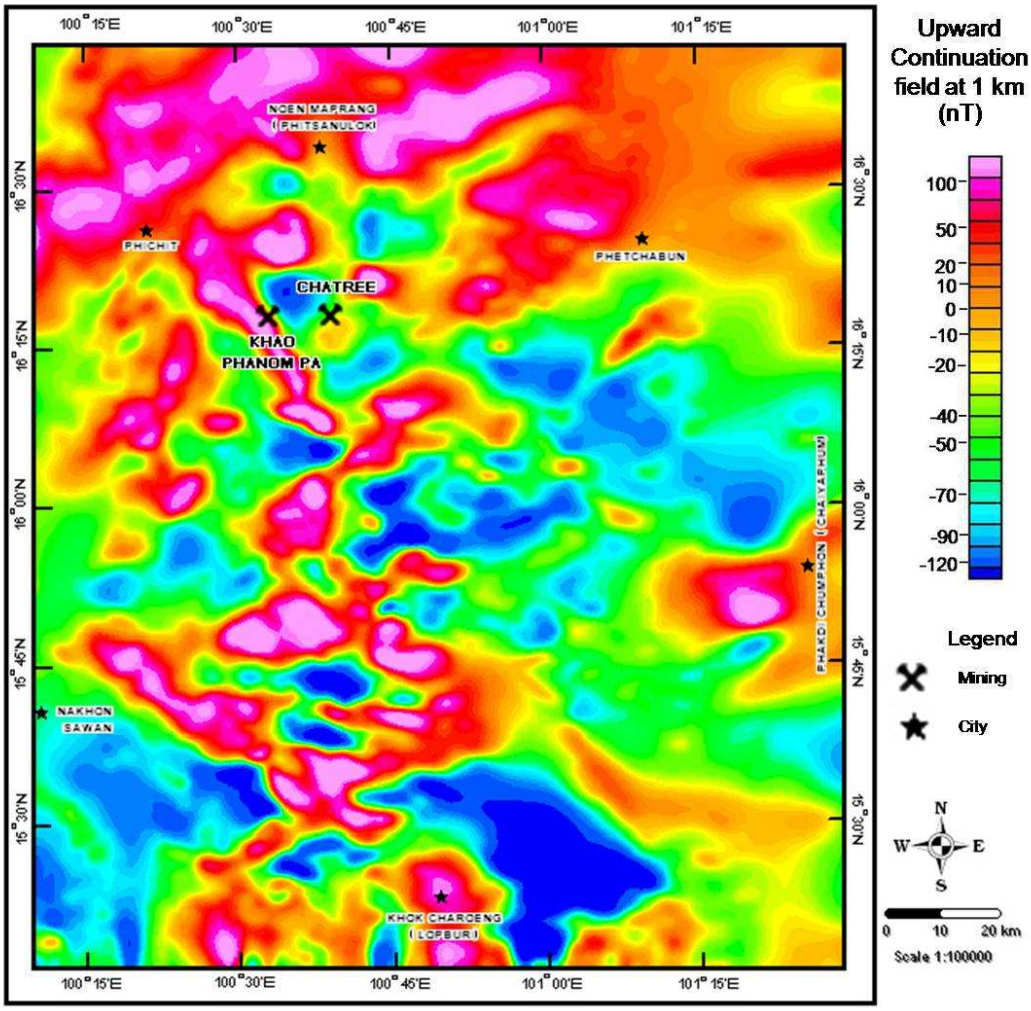

Figure 4.5. Enhanced airborne magnetic map of the Phetchabun volcanic terrane based on upward continuation data of 1 km higher magnetic survey levels useful for visual slope of magnetic intensity to outline geometrical model for source bodies in practice of magnetic dipping.

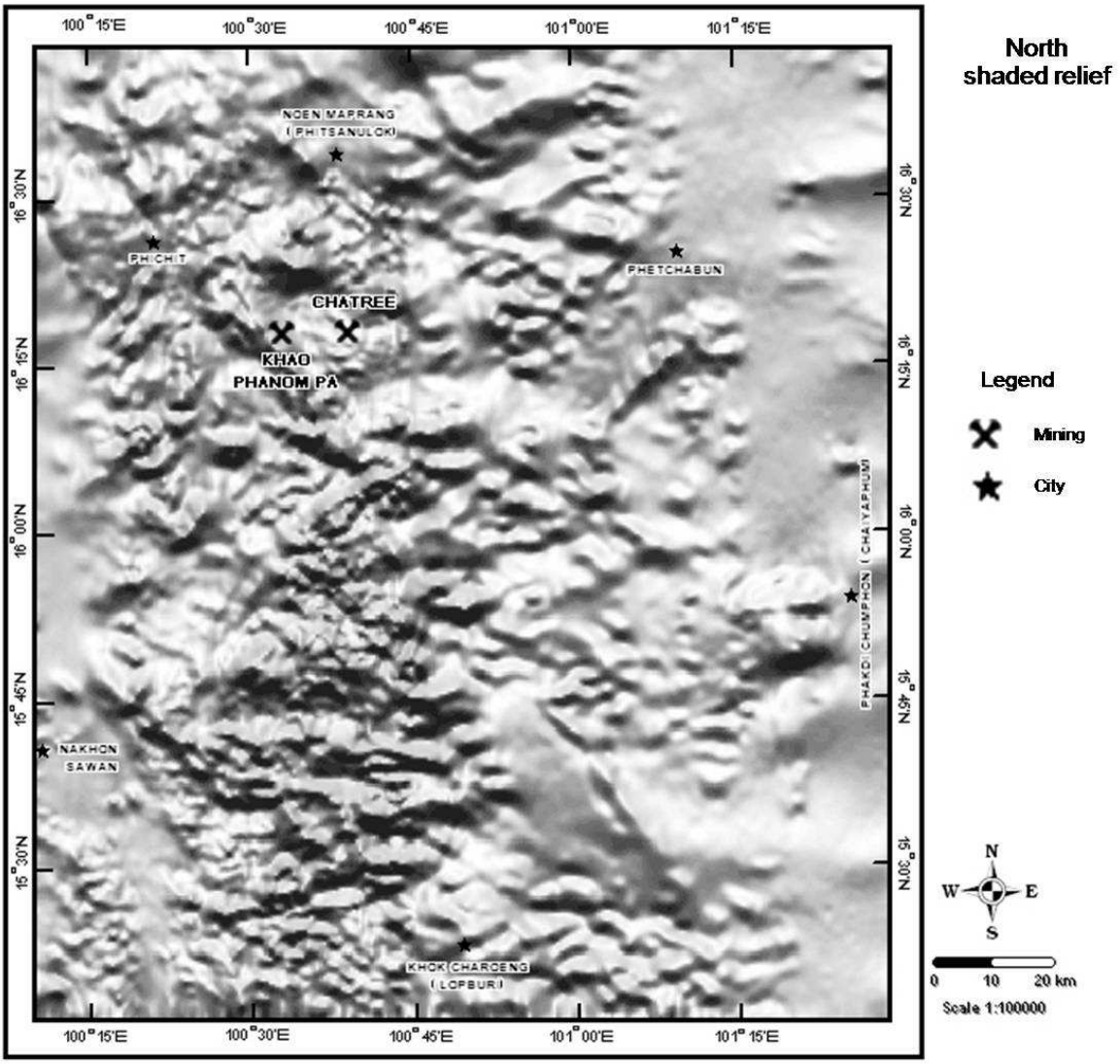

Figure 4.6. Enhanced airborne magnetic map of the Phetchabun volcanic terrane based on shaded relief image by shading from north direction showing linear structures in study area.

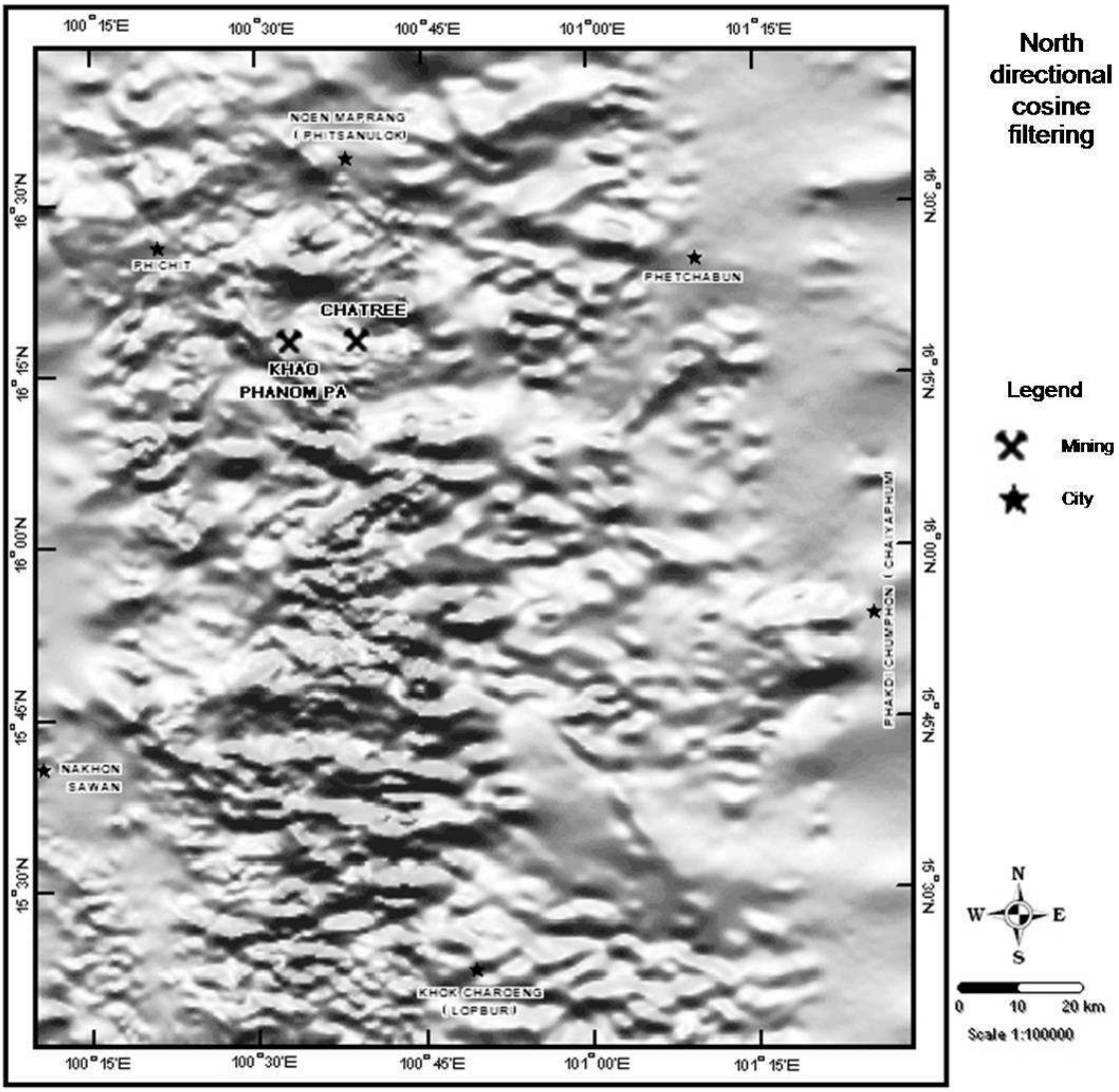

Figure 4.7. Enhanced airborne magnetic map based on directional cosine filtering data by filtering in north direction and show clearly structure of east-west, northwest and northeast lineaments of the Phetchabun volcanic terrane.

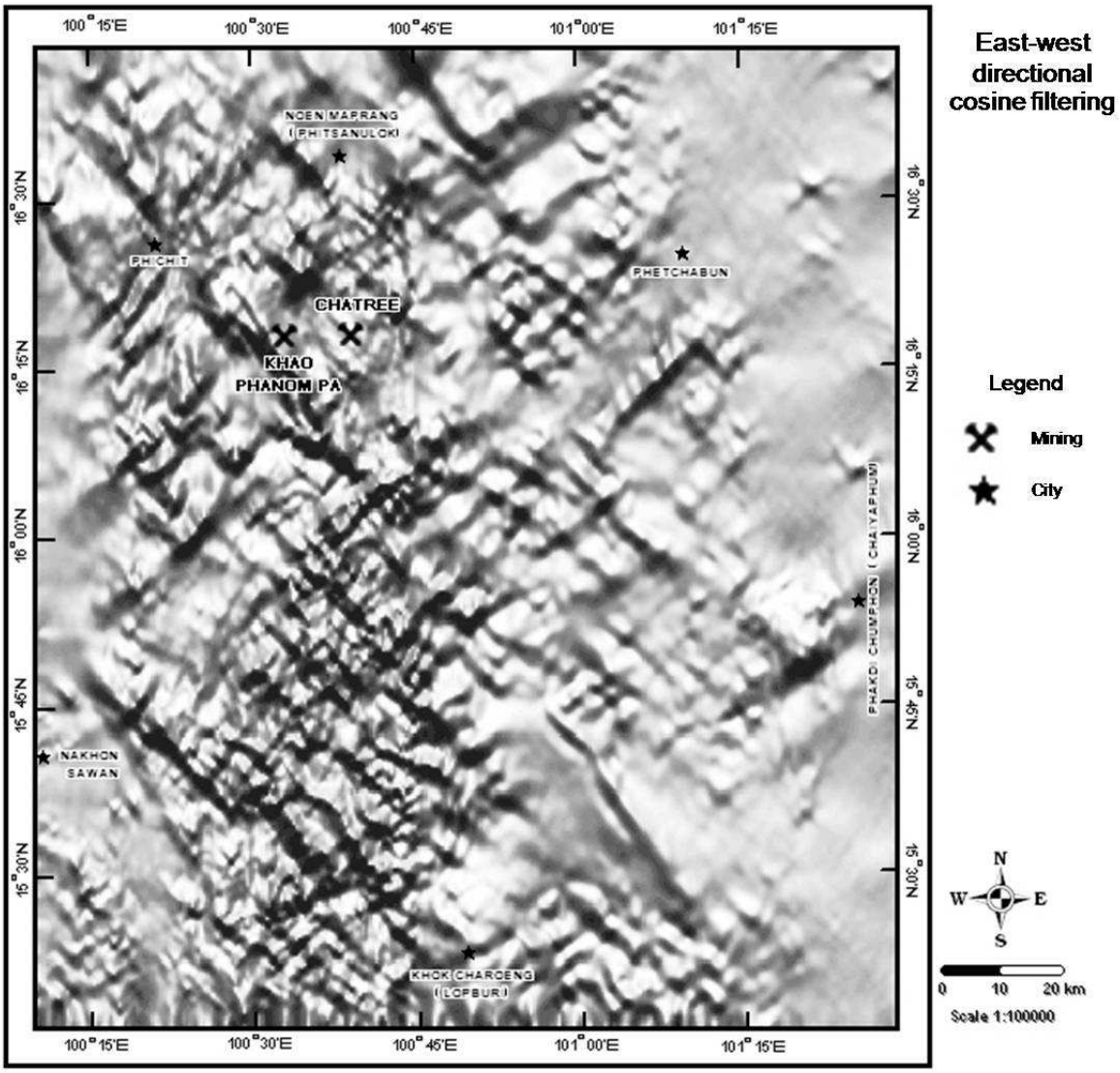

Figure 4.8. Enhanced airborne magnetic map based on directional cosine filtering data by filtering in east-west direction and show clearly structure of north-south, northwest and northeast lineaments of the Phetchabun volcanic terrane.

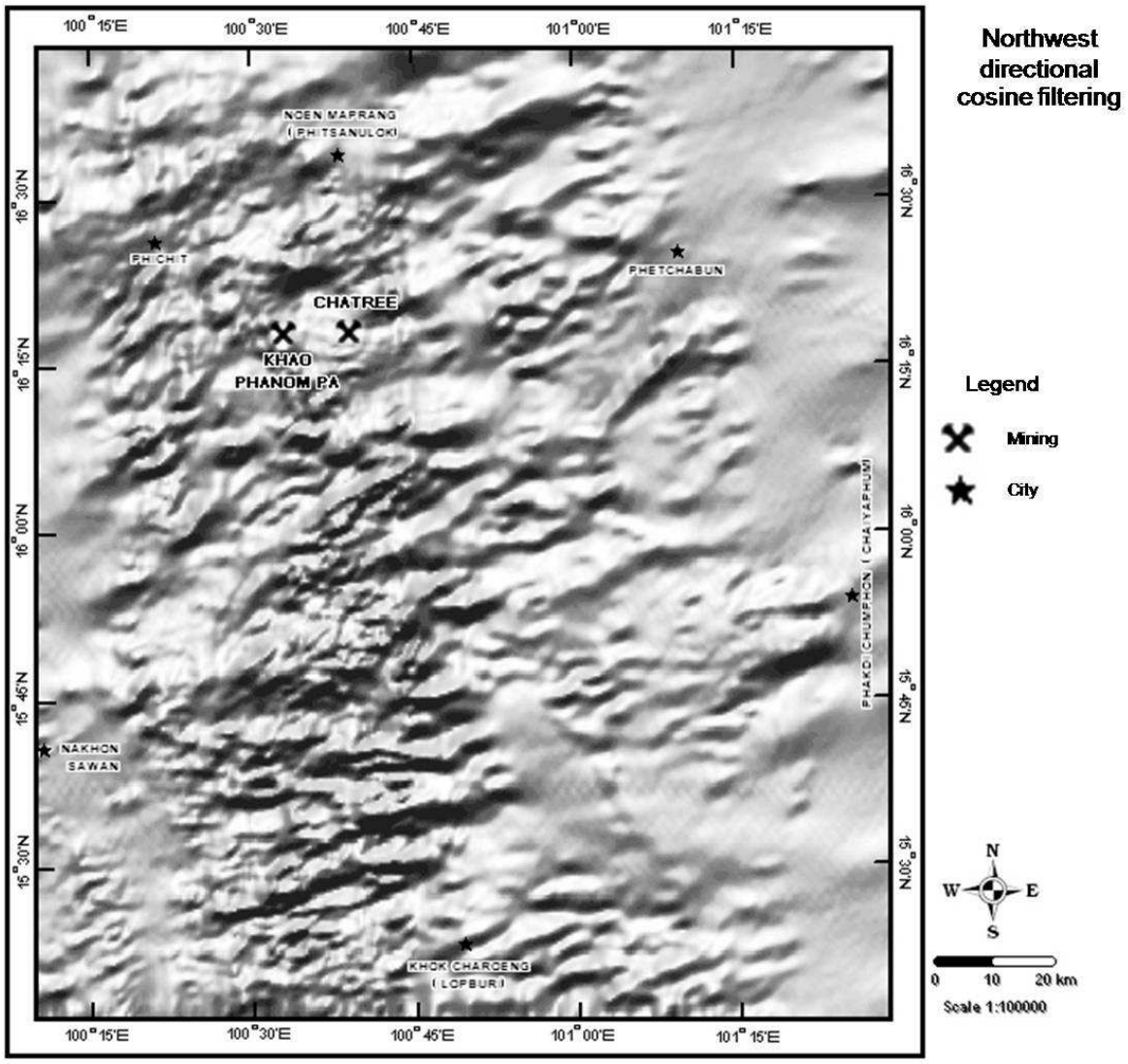

Figure 4.9. Enhanced airborne magnetic map based on directional cosine filtering data by filtering in northwest direction and show clearly structure of north-south, east-west and northeast lineaments of the Phetchabun volcanic terrane.

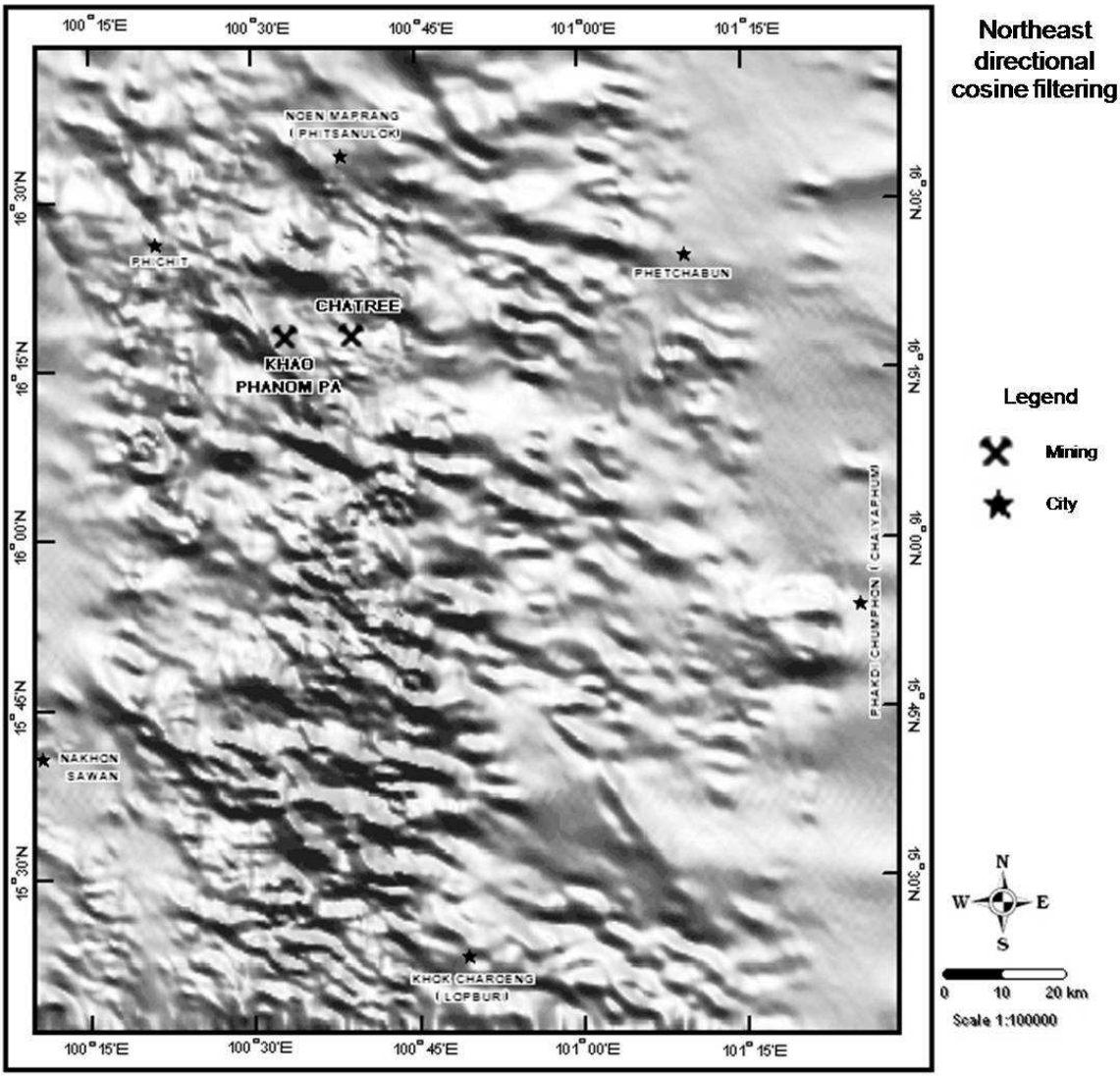

Figure 4.10. Enhanced airborne magnetic map based on directional cosine filtering data by filtering in northeast direction and show well-define structures of north-south, east-west and northeast lineaments in the Phetchabun volcanic terrane.

4.2 Comparison with other results

In order to interpret geophysical data more reliable and more accurately, in this study we integrated the processed aeromagnetic data with the other essential and relevant data.

4.2.1 Magnetic susceptibility result

A rock-sampling program was carried out in the study area to determine the magnetic susceptibility level for individual rock types. Representative outcrop were chosen from the existing geologic map (Chonglakmani et al., 2004) to ensure that almost all rock units were sampled. The locations of rock samples are shown in Fig. 4.11. Magnetic susceptibility was measured for each sample. The detail of sample locations, rock types and magnetic susceptibilities (SI unit) were shown in Tables 4.1, 4.2 and 4.3. Most magnetic susceptibilities in the study area were conformed well with those of the samples reported by Ali et al. (2007) for the rock of the Saruhan, northeast Turkey, Ishihara et al. (2002) for the rocks of Barberton Region, south Africa and Sakiyama, (2005) for rocks of southwest Japan as shown in Table 4.4. Basically, the magnetic susceptibilities of the more mafic rocks higher than the more felsic rocks and the felsic rocks have values higher than the sedimentary rocks. However, the magnetic susceptibility of rock samples depend largely on the magnetite contents in rocks, the samples in this study were mostly collected at the surface outcrops, so magnetite contents in the rock samples may be lost by weathering process.

4.2.2 Geological results

Based on magnetic susceptibility results, high magnetic susceptibility outcrops of igneous and metamorphic rock. But the contact metamorphic rocks and some volcanic rocks found as small outcrop do not show high magnetic anomalies in reduction to the pole map, e.g. southwest of Noen Maprang. Thus, high magnetic anomalies in reduction to the pole map are very likely related to plutonic rocks. However, the geologic map of Permo-Triassic volcanic rocks and Khorat sedimentary rocks in red and blue, respectively in Fig. 2.4 correspond with ring unit as shown in Fig. 4.17. Therefore, the ring units are interpreted as paleo-volcanic center of Permo-Triassic volcanic rocks. The northern domain is largely Khorat sedimentary rocks which are also shown ring structure under Khorat sedimentary rocks. This causes the northern domain having high magnetic intensity and being more attractive in term of regional exploration.

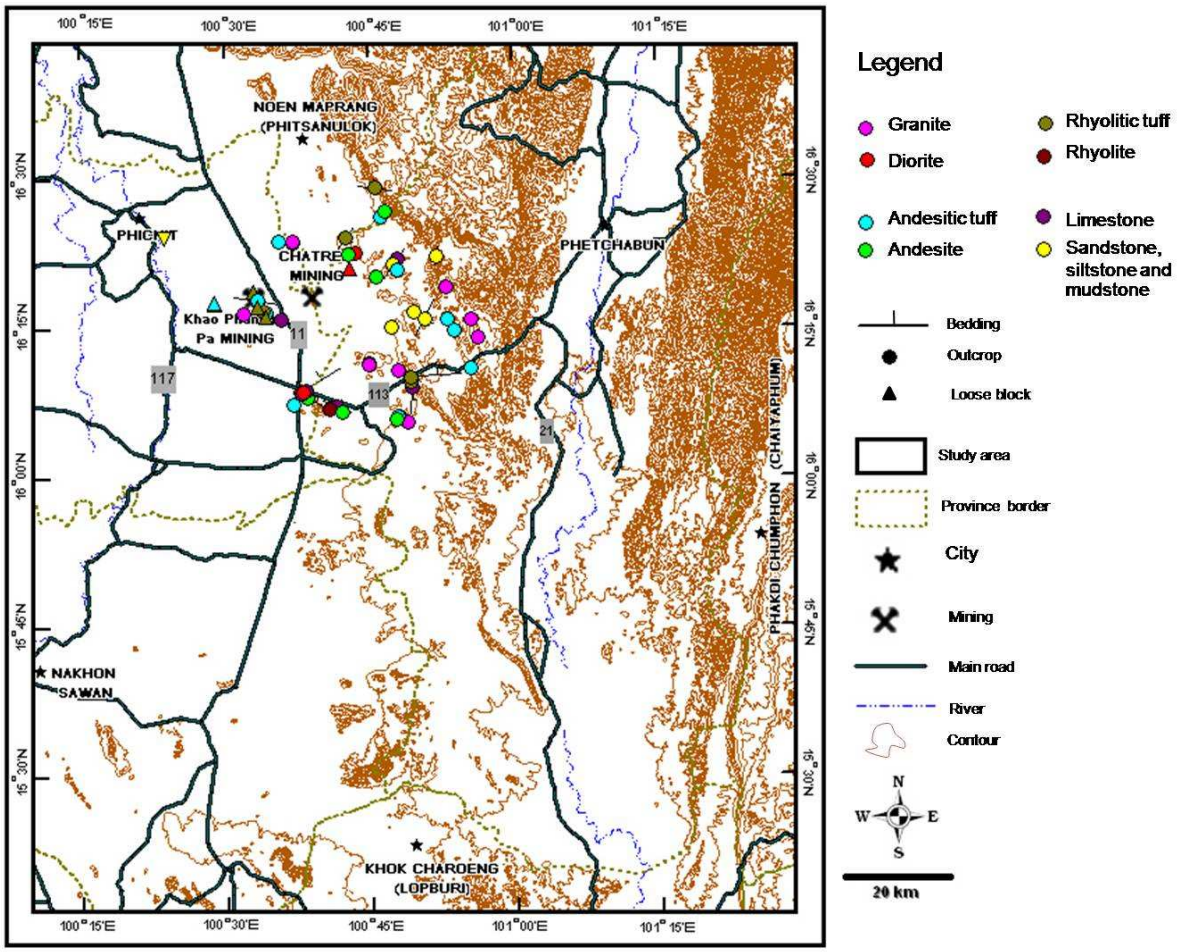

Figure 4.11. Contour map of the Phetchabun volcanic terrane showing locations of rock samples.

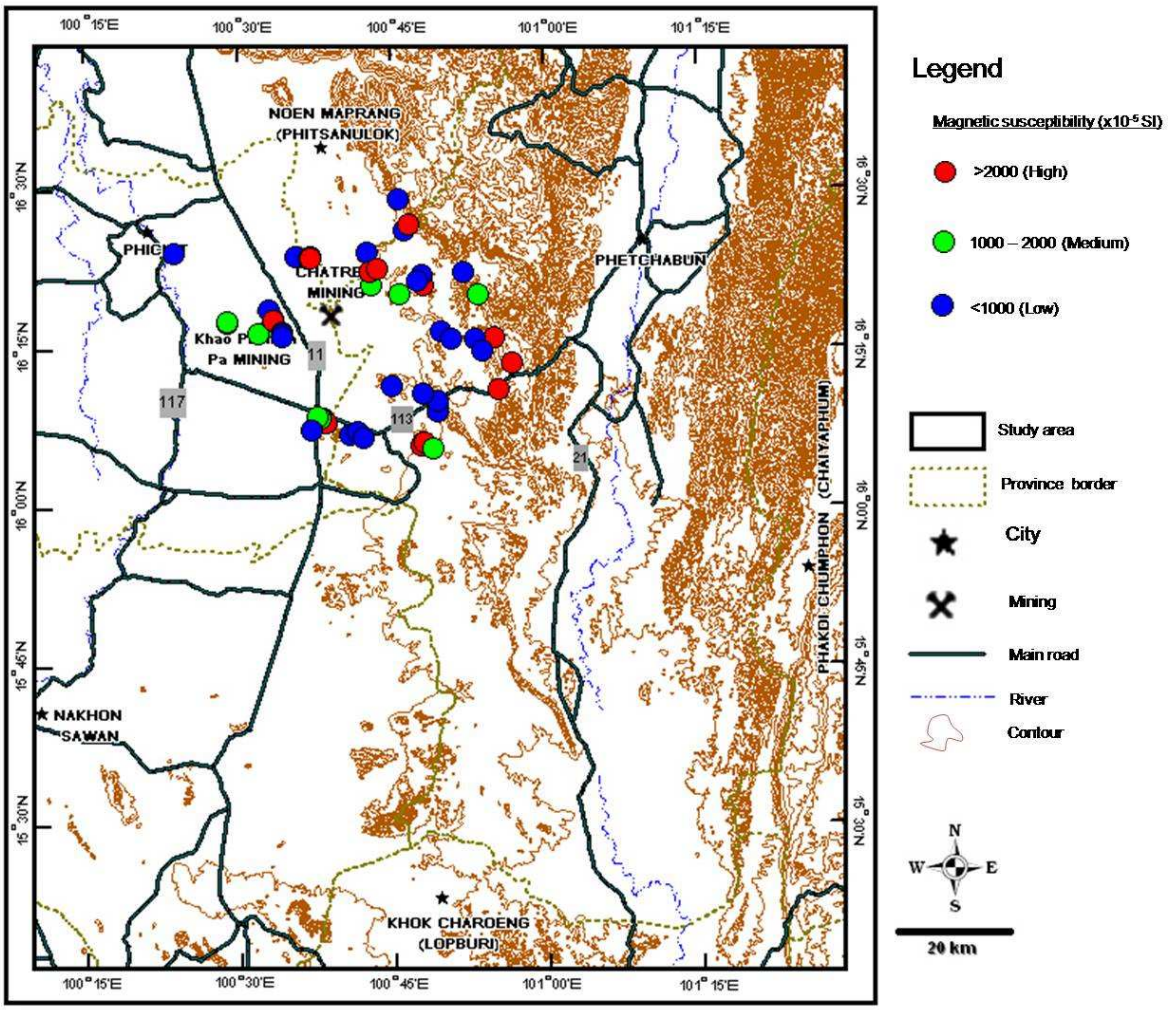

Figure 4.12. Contour map showing locations and results of magnetic susceptibility of rocks in the Phetchabun volcanic terrane.

Table 4.1 Detail of samples collected from the high magnetic anomalies, Chatree regional area Pichit-Phetchabun Provinces.

Easting	Northing	Location	Magnetic domain/ unit	Outcrop Type	Size (m^2)	Rock name	Mag-Susceptibility (10^{-5}SI)
686850	1790950	E	Central/ Elongate	Lower Hill (float)	3x1	Pink granite	118
686850	1790950	E	Central/ Elongate	Lower Hill (float)	3x2	Pink granite	148
686850	1790950	E	Central/ Elongate	Lower Hill (float)	3x3	Pink granite	143
686876	1790523	E	Central/ Elongate	Lower Hill (float)	3x4	Pink granite	116
692318	1789734	F	Central/ Elongate	Quarry (outcrop)		Grano-diorite	31
683271	1808499	I	Eastern/ Circular	Pit (float)	2x1	Micro-diorite	1410
684195	1811389	J	Eastern/ Circular	float	0.3x0.2	Micro-diorite	2935
701776	1806940	H	Eastern/ Circular	Lower Hill (float)	2x1	Grano-diorite	1797
704706	1799687	L	Eastern/ Spot	Lower Hill		Grano-diorite	2693
691000	1797800	K	Eastern/ Spot	Lower Hill (float)	0.2x0.2	Strongly altered diorite	
691000	1797800	K	Eastern/ Spot	Lower Hill (float)	0.2x0.2	Strongly altered diorite	
694162	1780189	G	Central/ Elongate	Lower Hill (float)	1x1.5	Pink granite	1593
707825	1795024	M	Eastern/ Spot	Lower Hill (float)	0.2x0.2	Diorite	3105
674110	1785550	C	Central/ Elongate	Rotary Ais Blast rock cutting (RAB)		Diorite	
674530	1785210	D	Central/ Elongate	RAB		Diorite	
674620	1785460	B	Central/ Elongate	RAB		Grano-diorite	
663680	1799980	A	Central/ Elongate	RAB		Grano-diorite	

Table 4.2 Detail of sample collected from the volcanic rocks

Easting	Northing	Outcrop Type	Size (m^2)	Rock name	Structure	Magnetic susceptibility (10^{-5}SI)
667800	1800000	Top of Hill (outcrop)	3x1	Andesitic tuff		91
667800	1800200	Top of Hill (outcrop)	3x1	Andesitic tuff		42
666000	1801400	Lower Hill (float)	0.2x0.2	Andesitic tuff		1118
665400	1804300	Pit (float)	2x3	Rhyolitic tuff		10
665400	1804300	Lower Hill (float)	0.5x0.5	Rhyolitic tuff		10
670200	1813400	Lower Hill (float)	5x3	Andesitic lapilly-tuff		154
679700	1782600	Quarry (outcrop)		Rhyolite	330/38flow	0
683929	1811020	Top of Hill (float)	1x0.5	Andesite		2466
682500	1814300	Top of Hill (outcrop)		Rhyolitic tuff	55/15bed	0
688900	1818100	Lower Hill (float)	0.3x0.2	Andesite brecia		333
689825	1819158	Lower Hill	0.3x0.3	Andesite		3265
687784	1823462	Top of Hill (outcrop)		Rhyolitic tuff	288/30bed	0
692160	1808453	Lower Hill (float)	0.2x0.2	Andesitic tuff		2007
682004	1782061	Lower Hill (float)	2x1	Andesitic tuff		0
682004	1782061	Lower Hill (float)	2x2	Andesitic tuff		0
694774	1786653	Lower Hill (float)	1x0.5	Rhyolitic tuff		120
694670	1787760	Lower Hill (outcrop)		Rhyolite breccia		0
694681	1788348	Road-cut (outcrop)		Rhyolitic tuff	150/25bed 260/30bed	38
705454	1790533	Road-cut (outcrop)		Andesitic tuff		2423
701420	1799254	Lower Hill(outcrop)		Polymictic tuff		0

Table 4.2 Detail of sample collected from the volcanic rocks (cont.)

Easting	Northing	Outcrop Type	Size (m^2)	Rock name	Structure	Mag-susceptibility (10^{-5}SI)
666253	1802333	Quarry (outcrop)		Andesitic tuff		10
666253	1802333	Quarry (float)	0.5x0.5	Andesitic tuff		2730
666267	1802593	Quarry (outcrop)	>5x5	Andesitic tuff	270/80, 150/75, 345/85 fault	11
666267	1802593	Quarry (outcrop)	>5x5	Andesitic tuff		181
666158	1802619	Quarry (outcrop)	>10x10	Rhyolitic tuff	285/12bed	9
675556	1784593	Quarry (outcrop)	>10x10	Andesite	95/15bed	5283
692599	1781210	Quarry (outcrop)	>5x5	Andesitic tuff		204
692202	1781200	Top of Hill (float)	0.5x0.3	Andesitic tuff		3460
692202	1781200	Lower Hill (float)	0.5x0.4	Rhyoritic tuff		2650
691945	1780654	Top of Hill (float)	0.5x0.3	Andesite		6677
691945	1780654	Top of Hill (float)	0.5x0.3	Andesite		7581
688406	1806602	Lower Hill (float)	2x2	Andesite		1119
688406	1806602	Lower Hill (float)	2x3	Andesite		1926
672836	1783155	Pit		Andesitic tuff		2
667325	1800500	Lower Hill	5x5	Rhyolitic lapilly tuff		0
658300	1801800	Top of Hill	5x5	Andesitic tuff		453
658200	1802000	Top of Hill	5x5	Andesitic tuff		1655
666267	1802593	Quarry (outcrop)	5x5	Andesitic tuff		76

Table 4.3 Detail of sample collected from the sedimentary rocks

Easting	Northing	Outcrop Type	Size (m^2)	Rock name	Structure	Mag-susceptibility (10^{-5}SI)
667800	1799600	Top of Hill (float)	0.2x0.2	Tuffaceous sandstone		15
666000	1801400	Lower Hill (float)	0.2x0.2	Tuffaceous sandstone		452
649000	1814000	Channel (float)	0.2x0.2	Sandstone		0
681000	1783000	Quarry (outcrop)	10x10	Limestone	335/55bed 343/50fault	0
689825	1819158	Lower Hill	10x10	Limestone		0
692025	1810512	Lower Hill	10x10	Limestone		0
691,200	1809285	Quarry (outcrop)	5x5	Siltstone	58/38bed	0
699312	1811008	Quarry (outcrop)	5x5	Siltstone	30/20bed 132/43fault	0
697118	1799394	Road-cut	5x5	Silicified mudstone	40/20bed	0
694774	1786653	Lower Hill	10x10	Limestone	0/25bed	0
675134	1785872	Quarry (outcrop)	5x5	Silicified limestone	58/86, 43/36joint	34
695223	1800515	Quarry (outcrop)	5x5	Siltstone		0
672836	1783155	Lower Hill (float)	0.1x0.1	Silicified Siltstone		0
672836	1783155	Lower Hill (float)	2x2	Limestone		0
670620	1799039	Pit (float)	0.4x0.3	Limestone		0

Table 4.4 Comparison with observed common ranges for magnetic susceptibility of various rock types from previous work.

Rock type	Phetchabun area (10^{-5}SI)	Saruhan, NE Turkey (10^{-5}SI)	Barberton Region, South Africa (10^{-5}SI)	Soust west Japan (10^{-5}SI)
Sedimentary rocks	0-34			
Volcanic clastic rocks	15-452			
Felsic pyroclastic rocks	0-2650			5-300
Intermediate pyroclastic rocks	0-3460			4-2500
Intermediate volcanic rocks	1119-7581			24-3200
Felsic plutonic rocks	31-148	14-255 (calc-alkaline granites)	< 300 (ilmenite-series granitoids)	2-2300
Intermediate plutonic rocks	126-2935		300-3000 (Magnetite series from calc-alkaline suite)	96-9800
Metamorphic rocks	6406-7403			
	References	Ali A. et al., 2007	Ishihara S. et al., 2002	T. Sakiyama, 2005

4.3 Interpretation

From the results of enhanced airborne magnetic maps, I were able to distinguish the magnetic responses due to the difference in magnetic susceptibilities, structures and deformations of the rock units in the area. Characterizing geophysical domains relies heavily on anomaly indicative of the rock units both of local surface and subsurface rocks. However, variable source depths within a domain may also contribute significantly to changes in anomaly shapes and sizes. The interpretation in this study involves of Boundary and Lineaments of Interpretation map by using reduction to the pole, shaded relief, residual high pass and directional cosine filtering of enhanced magnetic map, Sense of movement, Sequence of lithologic units and lineaments and follow by Geophysical modeling. New reduction to the pole map displays four distinct

magnetic domains including northern, eastern, central and western domains (Fig.4.13). Within these domains, three magnetic units of high magnetic anomalies are recognized, namely elongate unit, circular unit, and spot units (Fig.4.15). The reduction to the pole modelings (Figs. 4.46 and 4.47) and upward continuation map (Fig.4.5) show the elongate unit with a northeast dipping. In addition, the residual high pass filtering map also illustrates the ring units with the distinct northwest-southeast regional trend (Fig.4.17). In the central domain, the elongate units display deformation of S fabric foliation trending and the shear planes C in east-west direction which are suggesting northwest-southeast sinistral shear of fault zone (Fig. 4.23), a north-south fold axial plane (Fig. 4.22), east-west trending of sinistral fault about 3-9 km lateral slip (see an example in Fig. 4.24) and northeast-southwest trending of dextral fault about 1-2.7 km lateral slip (see an example in Fig. 4.25). The ring units and the circular units are crosscut by east-west trending sinistral faults and northeast-southwest trending dextral faults. This event considers resulting of compression stress in east-west direction. Based on shaded relief (Fig.4.18) and directional cosine filtering maps (Fig.4.19 and 4.20), northeast-southwest trending sinistral faults about 47 km lateral slip (Fig. 4.26), north-south trending dextral faults about 1-5 km lateral slip (see an example in Fig. 4.27), and northwest-southeast trending faults about 2-10 km lateral slip (see an example in Fig. 4.28) have been encountered result of extension stress in east-west direction. The younger spot units occur along this latest fault segments.

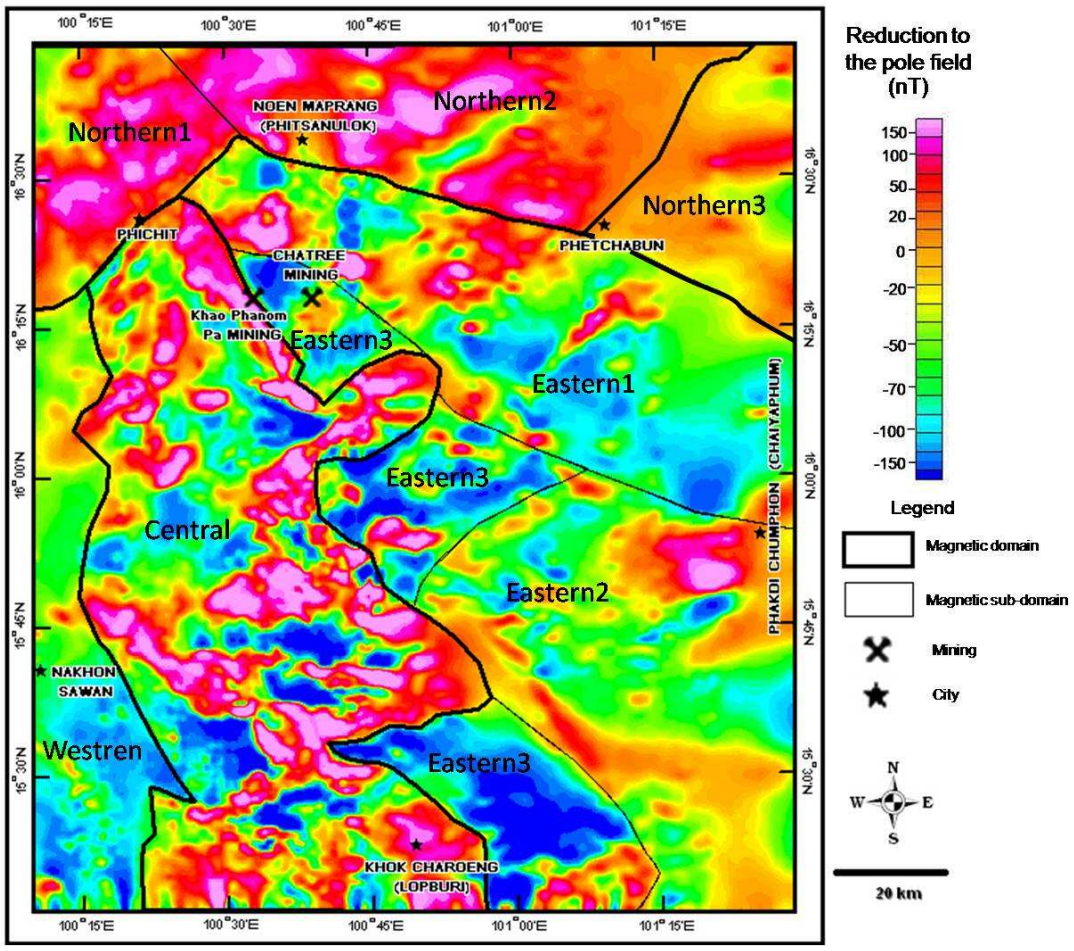

Figure 4.13. Enhanced reduction to the pole map showing clearly defined four magnetic domains of the Phetchabun volcanic terrane, viz. Northern, Eastern, Central and Western domains.

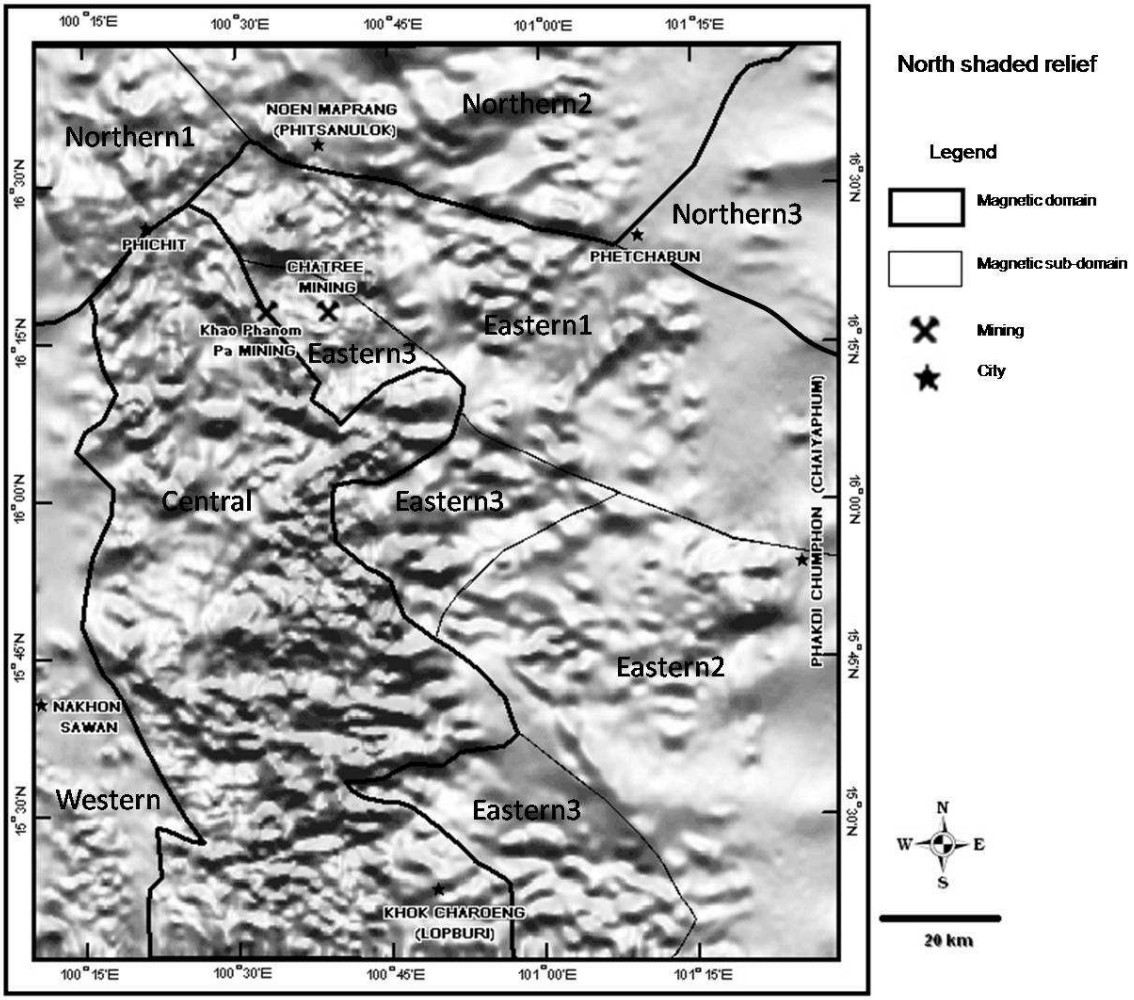

Figure 4.14. Enhanced shaded relief map with the overlain magnetic boundaries (from Fig.4.12) showing good resolution for linear structures of the Phetchabun volcanic terrane. The boundaries are controlled by three main lineaments of northwest-southeast, northeast-southwest and east-west directions.

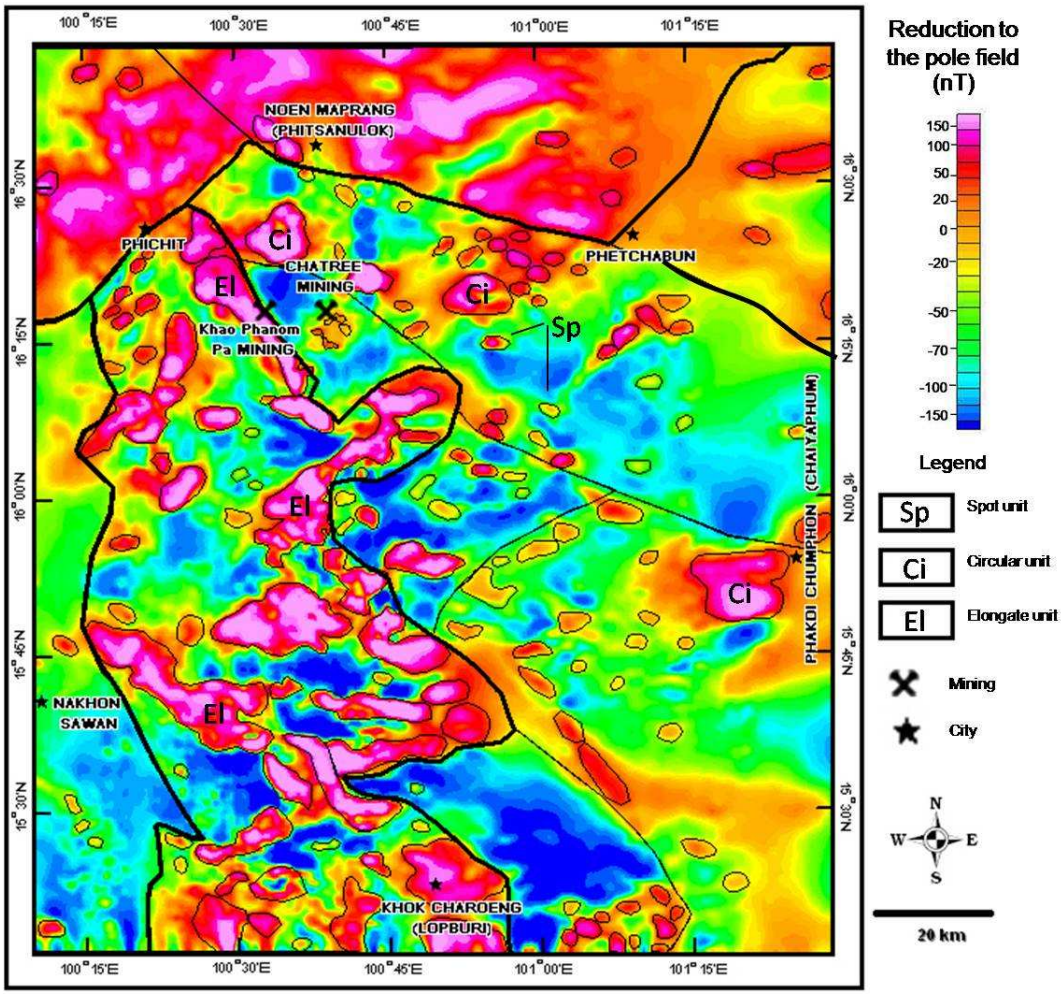

Figure 4.15. Enhanced reduction to the pole map with the overlain magnetic domains (from Fig. 4.12) showing three kinds of high magnetic bodies herein called elongate, circular and spot units within the Phetchabun volcanic terrane.

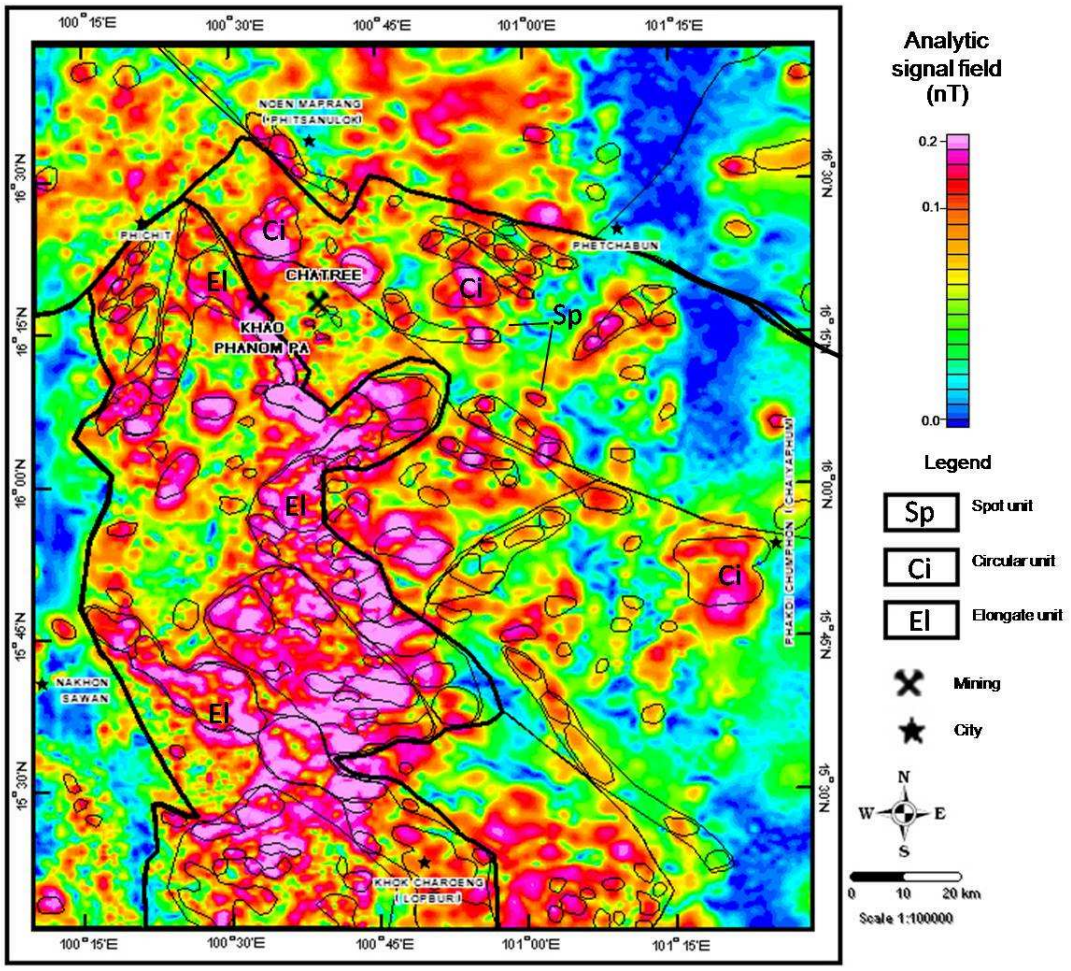

Figure 4.16. Enhanced analytic signal map with the overlain magnetic unit (from Fig. 4.15) showing analytic signal anomalies may does not show good enhance result for the complex structures due to asymmetry of magnetic body same as reported by Gunn (1997). This map uses for locating the high anomalies of circular and spot units which are symmetrical bodies. These anomalies showing similar shape with the reduction to the pole and suggesting less lowest problematic in the data processing of reduction to the pole method at 18.1°, declination -0.43° and amplitude 40° of study area (see appendix I).

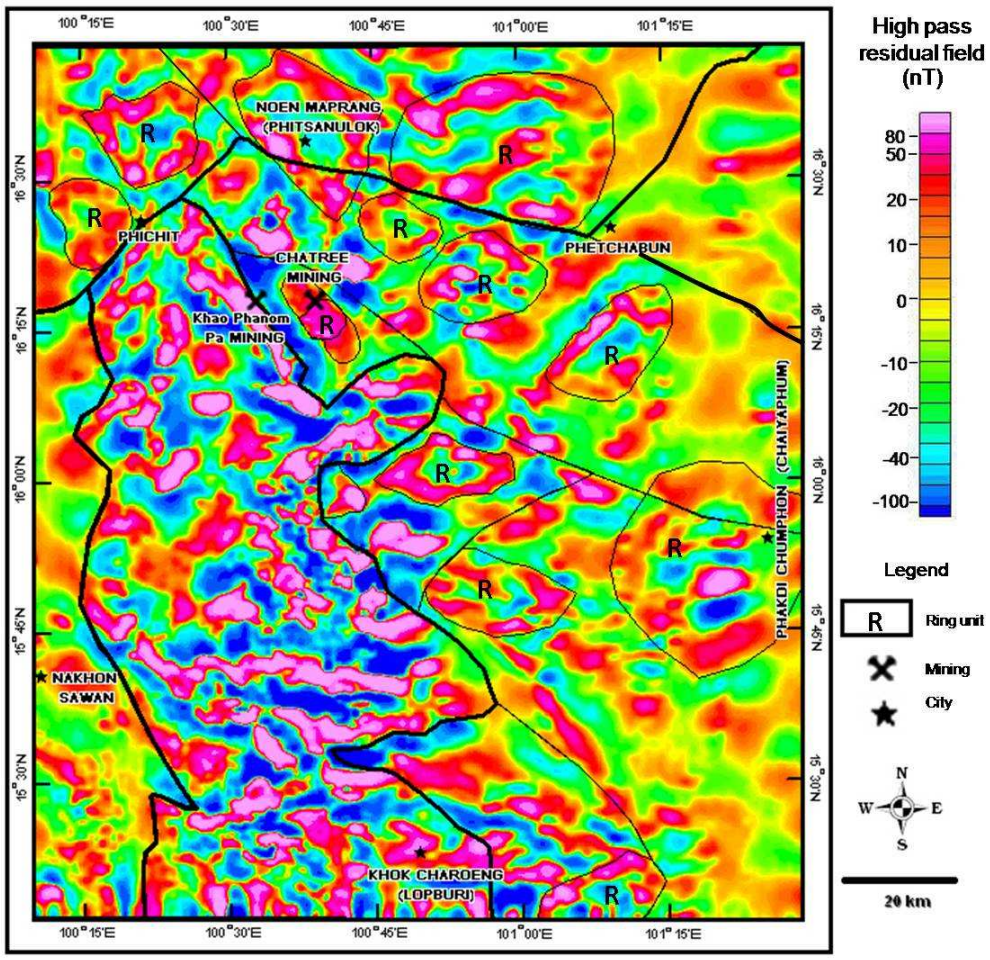

Figure 4.17. Enhanced residual high pass filtering map with the overlain magnetic domains (Fig. 4.13) of the Phetchabun volcanic terrane showing the interpreted ring structures of ring units in the Eastern and Northern domains with the northwest-southeast regional trend.

4.4 Magnetic domains

Based on the results from several enhanced image maps, I created a new interpretation map as shown in Fig. 4.30. With such integration and interpretation, the study area is subdivided into four major magnetic domains on the basis of the magnetic intensities and features, namely northern, eastern, central, and western domains. In general, boundaries of the individual domains coincide with the abrupt changes in average magnetic intensities, anomaly, background variabilities and orientations. Additionally, each domain was further subdivided into sub-domains on the bases of

local magnetization, surface and subsurface geology, lineament patterns, circular and elongate features described in the previous section. The characteristics of individual sub-domains are described by magnetic background and comparing with geological features (see Fig. 4.13 and 2.4).

4.4.1 Northern domain

The northern domain is the geophysical domain clearly trending in the almost northeast-southwest and northwest-southeast direction. The sharp boundary between the northern, eastern, central and western domains is regarded as the northwest-southeast fault with dextral slip and northeast-southeast sinistral faults. This domain is chiefly composed of high magnetic intensities and flat magnetic features possible indicate iron sedimentary formation in the northern domain. The highest magnetic intensity unit in the northern part is indicated by high topography (Fig. 4.29). This topography is shown in the Index map and location of study area (Fig. 1.3). It can subdivide the northern domain into three main sub-domains as northern1, northern 2 and northern 3 sub-domains upon the average magnetization and structural styles and patterns. The northern1 sub-domain is located in the western of the domain between northern Phichit province and western Noen Maprang sub-province. This sub-domain is characterized by less lower magnetization than northern2 corresponding to the Mesozoic non-marine sedimentary rocks and ring unit of volcanic centers. This sub-domain can be distinguished from the northern2 sub-domain by northwest-southeast trending dextral strike-slip faults and northeast-southwest trending sinistral strike-slip faults are observed as an apparent contact of the boundaries between northern2 sub-domain, eastern domain, central domain and western domain. To the eastern boundary of the northern1 sub-domain is connected with the northern2 sub-domain by a series of Mesozoic non-marine sedimentary rocks and ring unit of volcanic centers. The northern2 sub-domain shows the highest magnetic intensities and is located in the central parts of the domain, north of Noen Maprang sub-province. The geological map (Fig. 2.4) indicates the Mesozoic non-marine sedimentary rocks with the residual high pass filtering map show ring unit beneath these sedimentary rocks. These sedimentary rocks account for nearly 90 percent of the northern1 sub-domain, and mostly they align in the

northwest-southeast trend. The northwest-southeast dextral faults are the main controlled structures (herein called Noen Maprang Fault), commonly exceeding 130 km in length. The northwest-southeast dextral faults are characterized by overlapping lineaments and form the 'S' shaped curvy lineaments and ring magnetic body movement with dextral sense in northern domain (Figs. 4.17 and 4.28). Structural geophysical trends of ring unit within the northern2 sub-domain are largely aligned in the northwest-southeast trends. In addition, two northwest trending dextral strike-slip faults are also recognized in the southern part of the northern2 sub-domain. The northern3 sub-domain is located in the western of the domain between western Phichit province and northern Phakdi Chumphon sub-province. This sub-domain is characterized by less lower magnetization than northern2 corresponding to the Mesozoic non-marine sedimentary rocks and Permain marine sedimentary rocks (see geologic map in Fig. 2.4). This sub-domain can be distinguished from the northern2 sub-domain by northeast-southwest trending sinnistral strike-slip faults are observed as an apparent contact of the boundaries between northern2 sub-domain and eastern domain. To the eastern boundary, the northern1 sub-domain is connected with the northern2 sub-domain by a series of Mesozoic non-marine sedimentary rocks.

4.4.2 Western domain

The western domain is largely composed of very low to moderate background of magnetic intensity possible indicate sedimentary rock in the western domain. This domain shows a few of small circular magnetic bodies or spot unit along northwest-southeast dextral faults and lineaments in southern part of domain. This sub-domain is associated with major faults running parallel to a regional structure of northwest-southeast direction. The southern part of this domain is chiefly composed of very low magnetic intensities corresponding to the Permian deep marine carbonates sedimentary rocks of Nam Duk Formation and Mesozoic volcanic rocks as shown in Fig. 2.4.

4.4.3 Central domain

The central domain is composed largely of moderate magnetic intensities of background with elongate shape of high magnetic anomalies possible indicate magmatic arc in the central domain. This domain can be subdivided into elongate unit based upon magnetic shape, magnetic pattern, magnetic intensities and distribution of

high magnetic stocks. The central domain is the long, north-south low to high magnetic zone and corresponds to the intrusive rocks in field survey as large deformed intrusive (deformed pink granite, deformed granodiorite and deformed diorite) with mostly the northwest strike. The deformed pink granite, deformed granodiorite and deformed diorite were obviously affected by tectonic deformation much more intensely than all other rocks in the study area. The deformed intrusive rock was from Late Carboniferous in age as reported by Salam et al. (2007). This domain shows several northwest-southeast, east-west and northeast-southwest trending magnetic linear patterns, interpreted herein to indicate major faults almost parallel to a regional structure. They are the long strike-slip faults with the longest length of about 87 km, identified clearly by the shaded relief map because the extent in high magnetized elongate unit with similarly magnetized intrusive rocks determine from the enhanced airborne magnetic data. To the northern part of this domain, particularly south of Phichit, small circular highs magnetic or spot unit presumably indicate porphyritic intrusion stocks. Embedded into the central domain is in the roughly north-south direction of regional trend, which consists of elongate high magnetic intensity with dominant northwest-southeast trend. This unit is, more or less, equivalent to the felsic-intermediate intrusives of granite, grano-diorite and diorite in composition based on field investigation. This high magnetic unit shows many short to long northwest, east-west and northeast trending lineaments may have a series of folds in north-south and east-west axial plane of elongate unit. The north-south fold can be observed in the road-cut outcrop of Permian bedded clastic rock (Fig.4.39) and geological map of the Chatree district (see appendix VI of James et al., 2007) that are confirm well to the reduction to the pole map. Symmetrical variation of magnetic field intensity show lineament trend as a curved shape interpreted to represent the large folded structure with a long regional wavelength. The regional axial plane is in the north-south and east-west trend. The boundary between the central and eastern

domains is represented by the thrust faults (see discussion part) in the northwest-southeast directions.

4.4.4 Eastern domain

The eastern domain is essentially composed of low to moderate magnetization of magnetic background with ring and circular shape of magnetic anomalies possible indicate magmatic arc in the eastern domain. This domain was subdivided to three sub domains (eastern1, eastern2 and eastern3 sub-domains) based on magnetic intensities and patterns. They are controlled by the northwest-southeast boundary faults. The dominant spot units represented porphyritic intrusive rocks occur along these faults. The previous geochronologies indicate these intrusive rocks are occurred in Early Triassic to Late Triassic time (Salam et al., 2007). The boundary between the eastern and northern domains is indicated by the normal fault in northwest-southeast direction with dextral slip.

The dominant ring magnetic structures observed in the eastern domain are trended in northwest-southeast direction. Based on magnetic susceptibility and distribute of Permo-Triassic volcanic rocks (Fig. 2.4) in study area, found in other countries for ring structure of volcanic center (see in discussion part). The circular magnetic features of ring units were mapped as the paleo-volcanic center of Permo-Triassic volcanic rock. The large circular magnetic anomalies observed in the central part of eastern domain were represented by equigranular intrusive bodies which are show in Figs. 4.31, 4.35 and 4.36. The boundary between eastern and central domains is indicated by the major northwest-southeast thrust fault with dominant the north-trending syncline. A syncline, indicated by high magnetic elongate unit in the central domain with has the length of about 10 km and the axial trace almost in the north-south direction. The predominant small circular feature in central domain with the high magnetic unit of spot unit were occur follow the northwest-southeast and northeast-southeast trending linear structural trend. In the geological map, this sub-domain is mapped as Triassic granite which the previous geochronology of intrusives in the spot unit indicated Early to Late Triassic diorite (Salam et al., 2007). The eastern1 sub-domain is largely filled by massive and interbedded of the Permian carbonate rock (Fig.

2.4). This sub-domain shows the structural trend in the northwest-southeast direction similar to that of the regional mapped unit. The eastern2 sub-domain is in southern part of eastern domain and enclosed between the eastern1 and eastern3 sub-domain. It is shows moderate magnetic intensity higher than eastern1 sub-domain. It is also consist of large circular feature with high magnetic pattern possible intrude cut through the ring unit. This sub-domain is characterized by the northwest-trending major fault and minor northeast-southeast fault. The spot unit found along these faults but less lower magnetic intensity than spot unit in eastern1 sub-domain. The eastern3 sub-domain is located between the western parts of the eastern domain and central domain. It consists of low to very low magnetic background from north to south, respectively. This sub-domain is the straight with major faults in the northwest-southeast direction, minor of northeast-southwest fault and east-west fault. This sub-domain corresponds with the Permo-Triassic felsic to intermediate volcanic rocks of mainly andesitic composition (Fig. 2.4). There are found ring unit in this sub-domain suggesting volcanic occurring in the eastern3 sub-domain. The small circular features of spot represented porphyritic intrusives are occurred along the boundary faults zone.

4.5 Magnetic structures

Figs. 4.18, 4.19, 4.20 and 4.21 display lineaments of various patterns and styles which have drawn using the image manipulation MapInfo Professional software. The lineaments were delineated by visual interpretation on the enhanced airborne geophysical data. Geologic lineaments were superimposed afterward as a separate layer. Comparison of the magnetic lineaments with the geologic lineaments shows that many of the magnetic anomaly trends coincide very well with geologic contacts or inferred faults. The shade relief map (Fig. 4.6) is characterized by a rather linear pattern of magnetic enhanced field containing the long segments with the predominant northwest-southeast linear trend. This map was donated by the sharp, long, northwest-southeast lineaments conformable with regional structures. This map and the overlain boundaries of magnetic domains (Fig. 4.14) show clear resolution for the linear

structures which are controlled by the main linear structures of northwest-southeast, northeast-southwest and east-west direction. This map can be interpreted the lineaments are in northwest-southeast, northeast-southwest, east-west and north-south direction.

Based on north-directional cosine filtering map, this map provides facilitated lineaments clearly in northwest-southeast, northeast-southwest and east-west direction but without north-south direction which show sequence of lineament clearly based upon low of cross-cutting. As Fig. 4.19 in 1 area, eastern of northwest-southeast lineament more clearly cross-cut northeast-southwest lineament while areas 2 show northeast-southwest cross-cut western of northwest-southeast lineaments. Within area 3 shows east-west lineaments are cross-cut through western of northwest-southeast lineaments. The northwest-directional cosine filtering map provides facilitated lineaments clearly in, northeast-southwest, north-south and east-west direction but without northwest-southeast direction. At Fig. 4.20 in area 1 shows north-south lineament more clearly cross-cut northeast lineaments. Within area 2, northeast-southwest lineaments are cross-cut through east-west lineaments. Thus, enhanced directional cosine filtering map can be determine sequence of lineaments that are western of northwest-southeast lineaments occurred first, second east-west lineaments, third northeast-southwest lineaments, followed by north-south and eastern of northwest-southeast lineaments. On reduction to the pole map, the oldest northwest-south lineaments display the S fabric foliation trending and the shear planes C in east-west direction which are suggesting northwest-southeast sinistral shear of fault zone parallel to the foliation planes along the elongate unit which are indicated brittle-ductile features about 87 km long distance (Fig. 4.23). These northwest-southeast faults are cross-cut by east-west lineaments with sinistral sense of movement indicated by displaced lineaments of northwest-southeast as shown in Fig. 4.24. Moreover, the magnetic lineaments can be inferred as axial

planes of the unmapped folds. Good examples are those in the central domain with north-south trend.

The magnetic data also show fold structures (Fig. 4.22) consisting of north-south trending axial plane similar to landsat image. The northeast-southwest trending of sinistral faults show cross-cut though the northwest-southeast of elongate unit display 1-2.7 km lateral slip and S curve folding between the fault indicated sinistral movement (Fig. 4.25). Based on results of north-south folding, sequence of faulting and deformation zone with trended in north-south direction of central domain are indicated σ1 in an east-west direction and ellipsoid of these events as a result of east-west compression and north-south extension stress with sinistral transpression stress in northnortheast-southsoutheast to identify the result of sinistral east-west faults. The structural pattern of study area supported that the major structures was formed in response to a strong tectonic activity in the region. On the contrary, the northeast-southwest boundary in reduction to the pole map between the northern, central, eastern and western domains shows the N1 sub-domain cross-cut thought Central domain with sinistral movement about 47 km (Fig. 4.26). In the central part of study area northeast-southwest fault also shows sinistral movement and possibly folding with east-west axial plane. As shown in Fig. 4.27 can be see dextral movement of north-south fault about 2 km lateral slip. In Fig. 4.28 can see dextral movement of northwest-southeast fault about 5 km lateral slip. Based on results of east-west fold axial plane and sequence of faulting indicated σ1 in a north-south direction and ellipsoid of these events as a result of east-west extension and north-south compression extension stress with dextral transpression stress in northeasteast-southwestwest to identify the result of dextral north-south faults. On Fig. 4.29, this are reduction to the pole map and the overlain topography which shows example of northern domain can see in high area to be given higher magnetic intensity in the same geophysical characteristic of northern domain. Thus, it can be interpret that low magnetic domain related with low topography. This is good result for

interpreted the vertical movement in other domain by using magnetic intensity (Gunn et al., 1997), stress direction and magnetic dipping direction from upward continuation map as result of reverse fault in central and western domains and result of normal fault in eastern and northern domains as shown in northeast subsurface cross section (Fig.4.29). The Chatree gold mine is in E3 sub-domain that is controlled by northwest-southeast normal fault from result of east-west extension with indicated subsidence in the Chatree gold deposit in Triassic time (base on the age of spot unit). Based on geophysical interpretation map (Fig. 4.30) illustrate sequence of magnetic unit and faults, elongate unit occur first and then deformed by northwest-southeast reverse faults with sinistral slip. Later, the ring units and circular units occur which are cross-cut by east-west normal faults with sinistral slip and northeast-southeast normal faults with dextral slip from result of east-west compression stress event. Finally, area was subject to east-west extension stress event by generated northeast-southeast reverse faults with sinistral slip, north-south normal faults with dextral slip and northwest-southeast normal faults with dextral slip and spot unit occur along the normal faults.

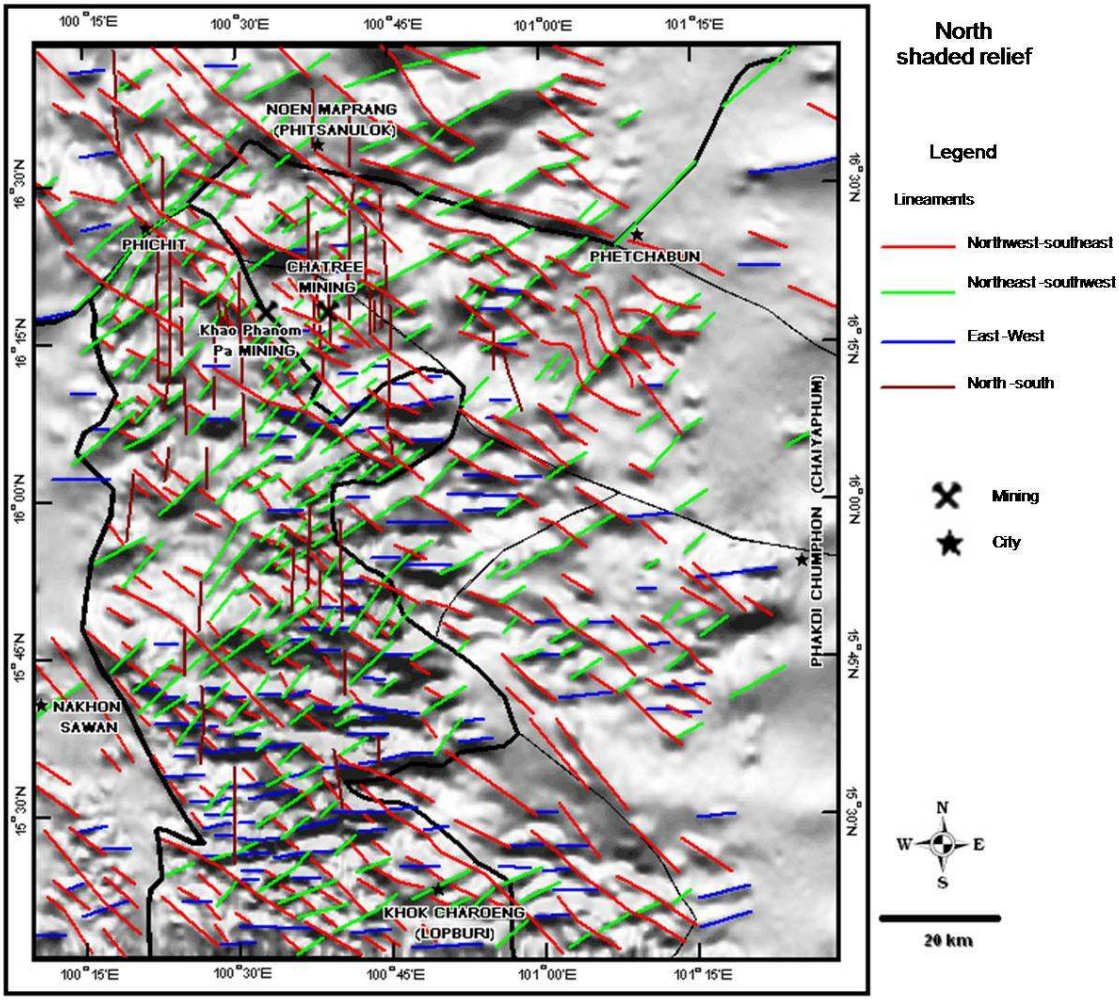

Figure 4.18. Enhanced shaded relief airborne magnetic map with the overlain magnetic domains showing the lineaments in northwest-southeast, northeast-southwest, east-west and north-south directions.

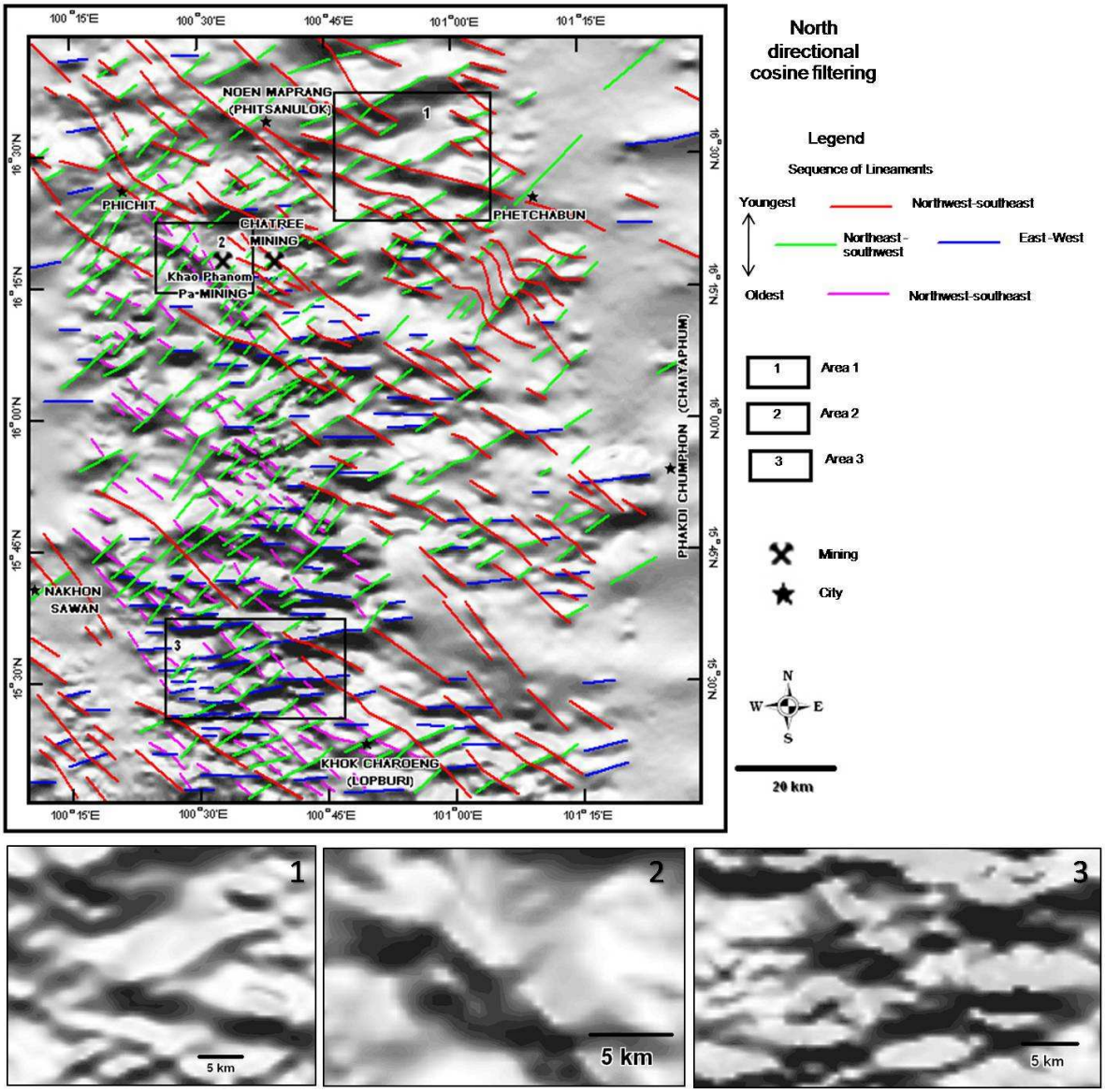

Figure 4.19. Enhanced airborne magnetic map using north-directional cosine filtering method showing lineaments without north-south structure. The northwest-southeast lineaments clearly cross-cut northeast-southwest lineaments in the inserted area 1. In area 2, the northeast-southwest lineaments cross-cut northwest-southeast lineaments. In the area 3, the east-west lineaments cross-cutting the northwest-southeast lineaments.

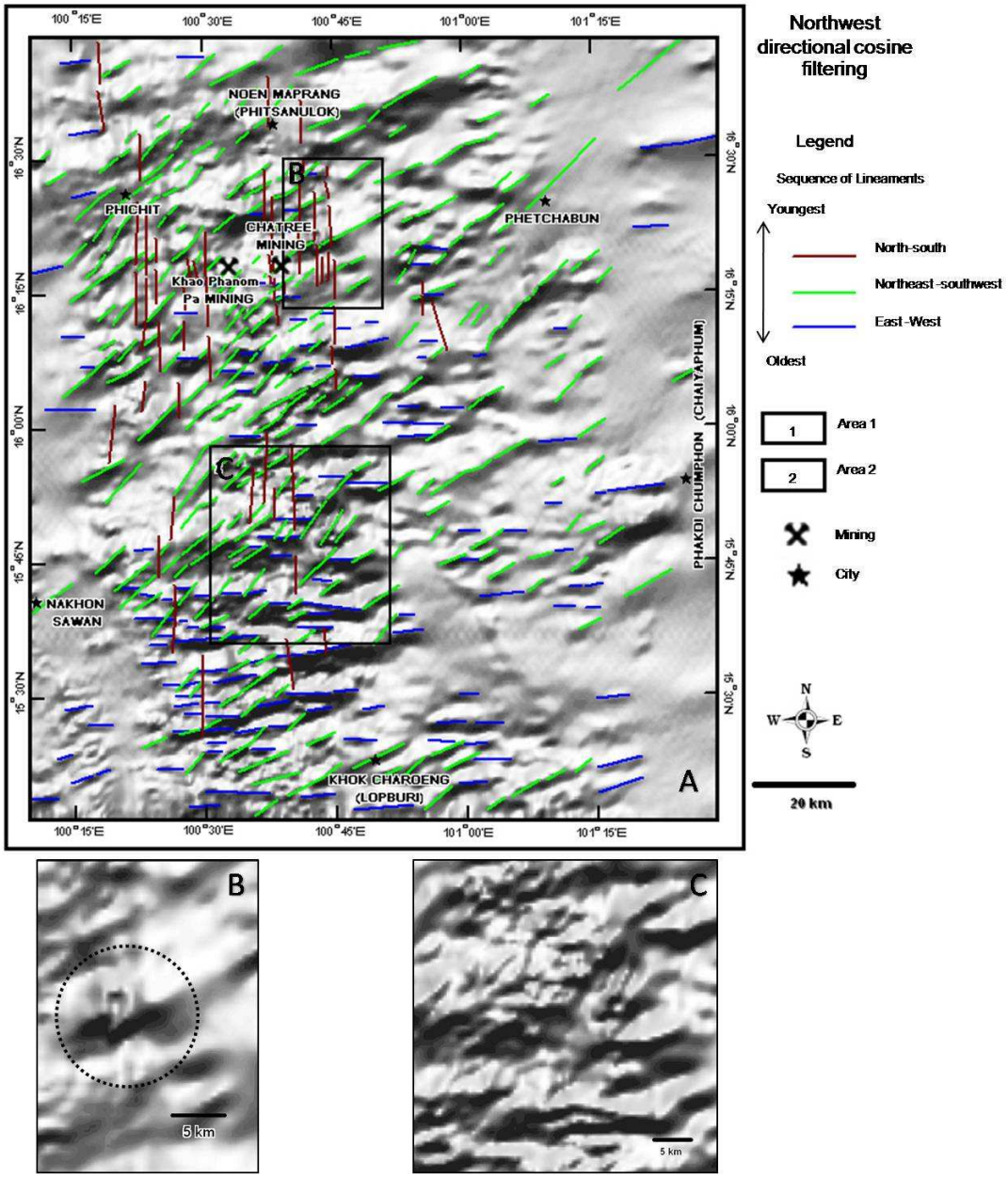

Figure 4.20. (A) Enhanced northwest-directional cosine filtering map showing linear structure with very rare northwest-southeast structure of the Phetchabun volcanic terrane. (B) The north-south lineaments clearly cross-cut the northeast-southwest lineaments (C) The northeast-southwest lineaments cross-cutting the east-west lineaments.

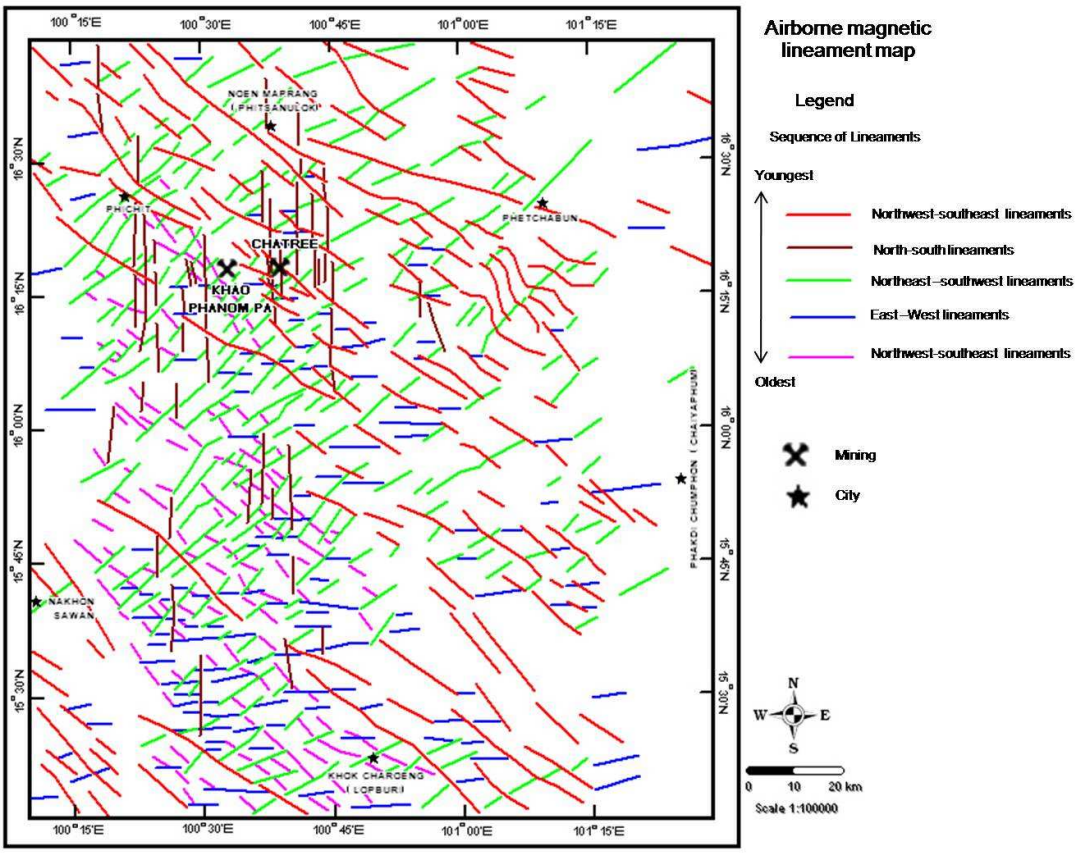

Figure 4.21. A map resulting from the interpretation of airborne geophysical data showing a number of lineament sets in the Phetchabun volcanic terrane.

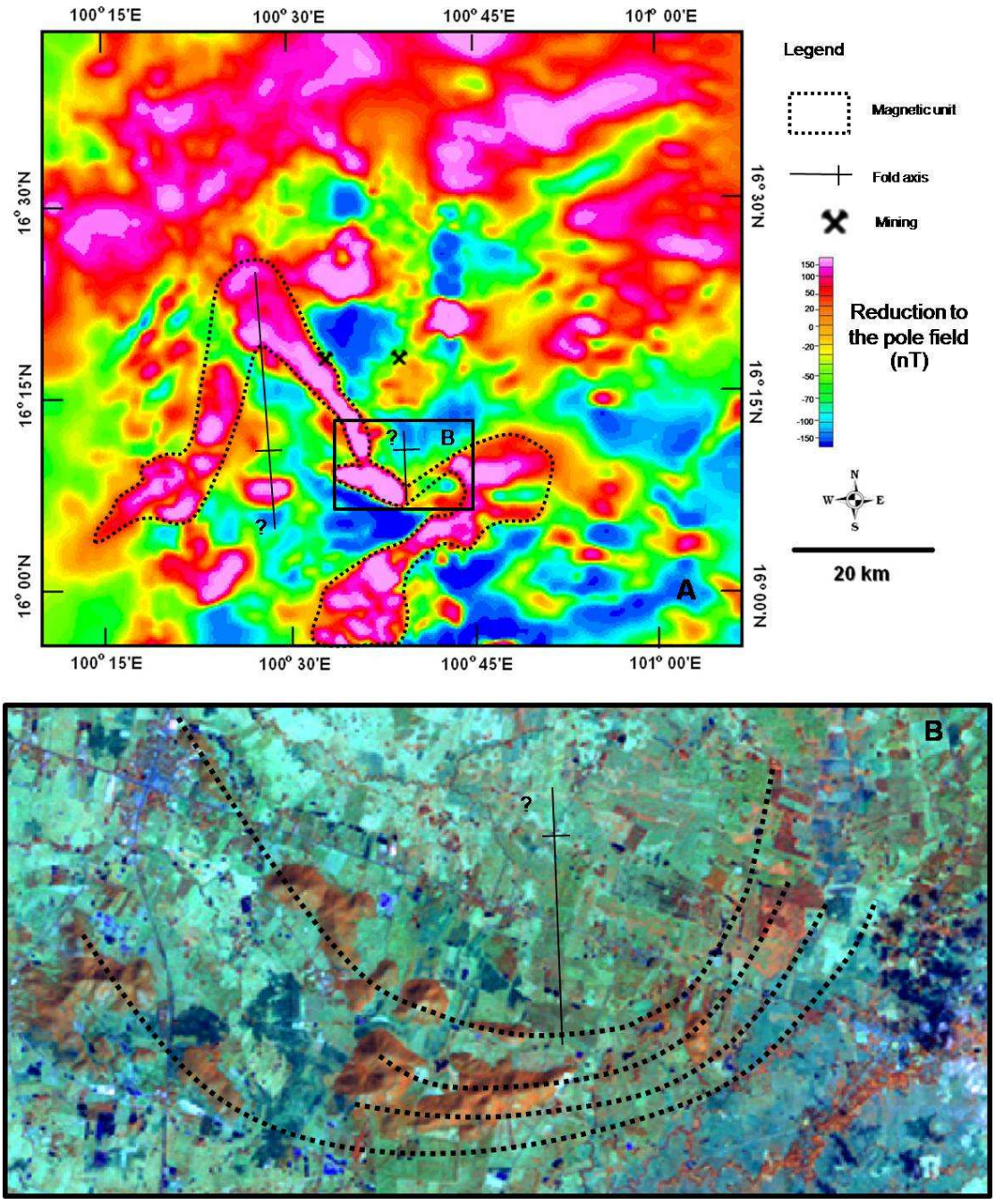

Figure 4.22. (A) Enhanced reduction to the pole map showing the possibly north-south axial plane of folding in elongate unit which indicate east-west compressional stress in the Phetchabun volcanic terrane. (B) Landsat map of area B showing the possibly north-south axial plane of folding which is similar to reduction to the pole map.

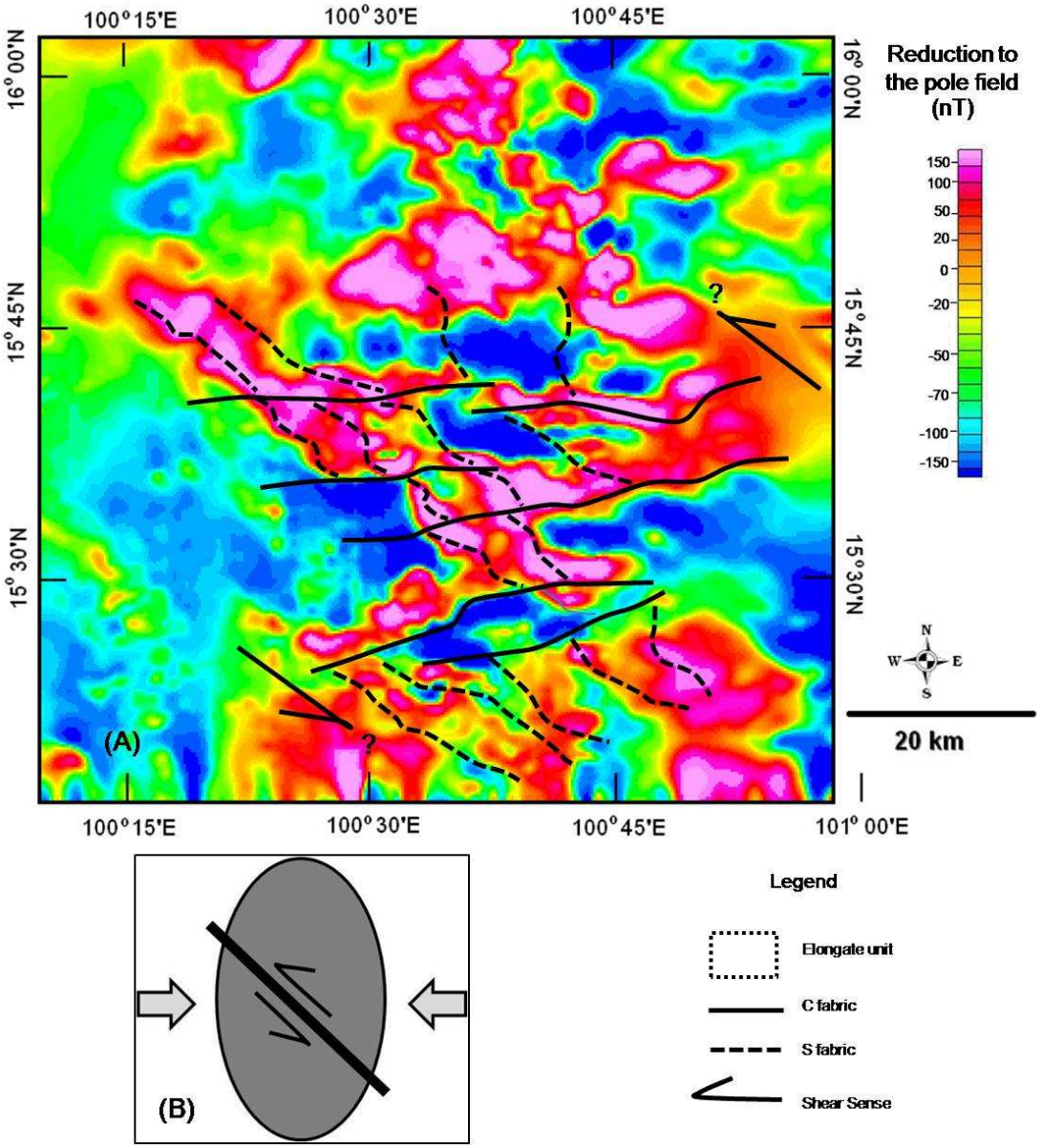

Figure 4.23. (A) Enhanced Reduction to the pole map showing S fabric foliation trending and the shear planes C in east-west direction which are suggesting northwest-southeast sinistral shear of fault zone parallel to the foliation planes along the elongate unit. (B) The ellipsoid with northwest-southeast sinistral fault zone, suggesting the east-west compression stress in the Phetchabun volcanic terrane.

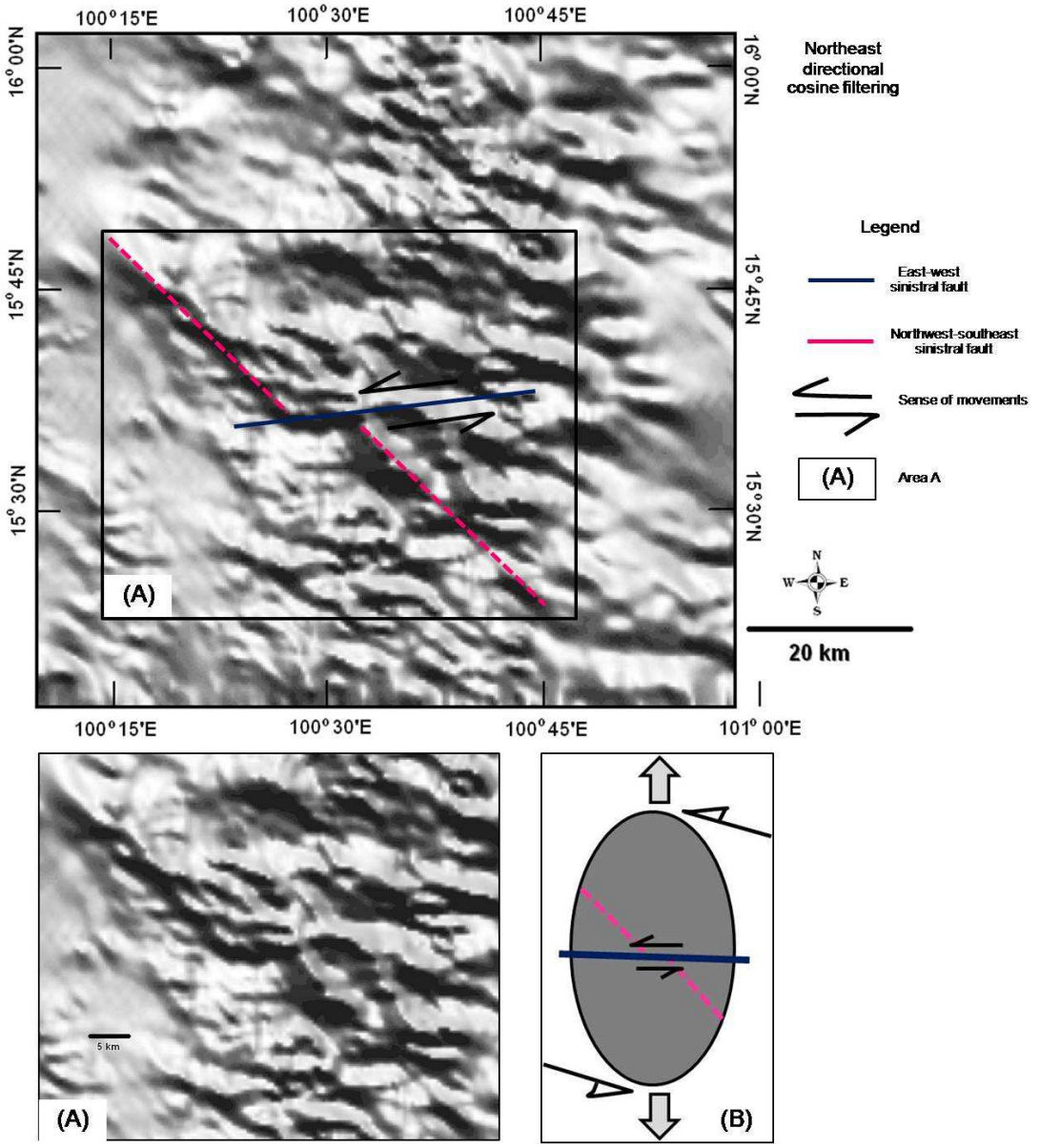

Figure 4.24. Enhanced airborne magnetic map using northeast-directional cosine filtering method showing the east-west sinintral fault with 9 kilometer lateral slip cross-cutting the northwest-southeast fault (or lineament) in an example of area A suggesting the north-south extension stress and northnortheast-southsouthwest sinistral transpression stress in figure B of ellipsoid.

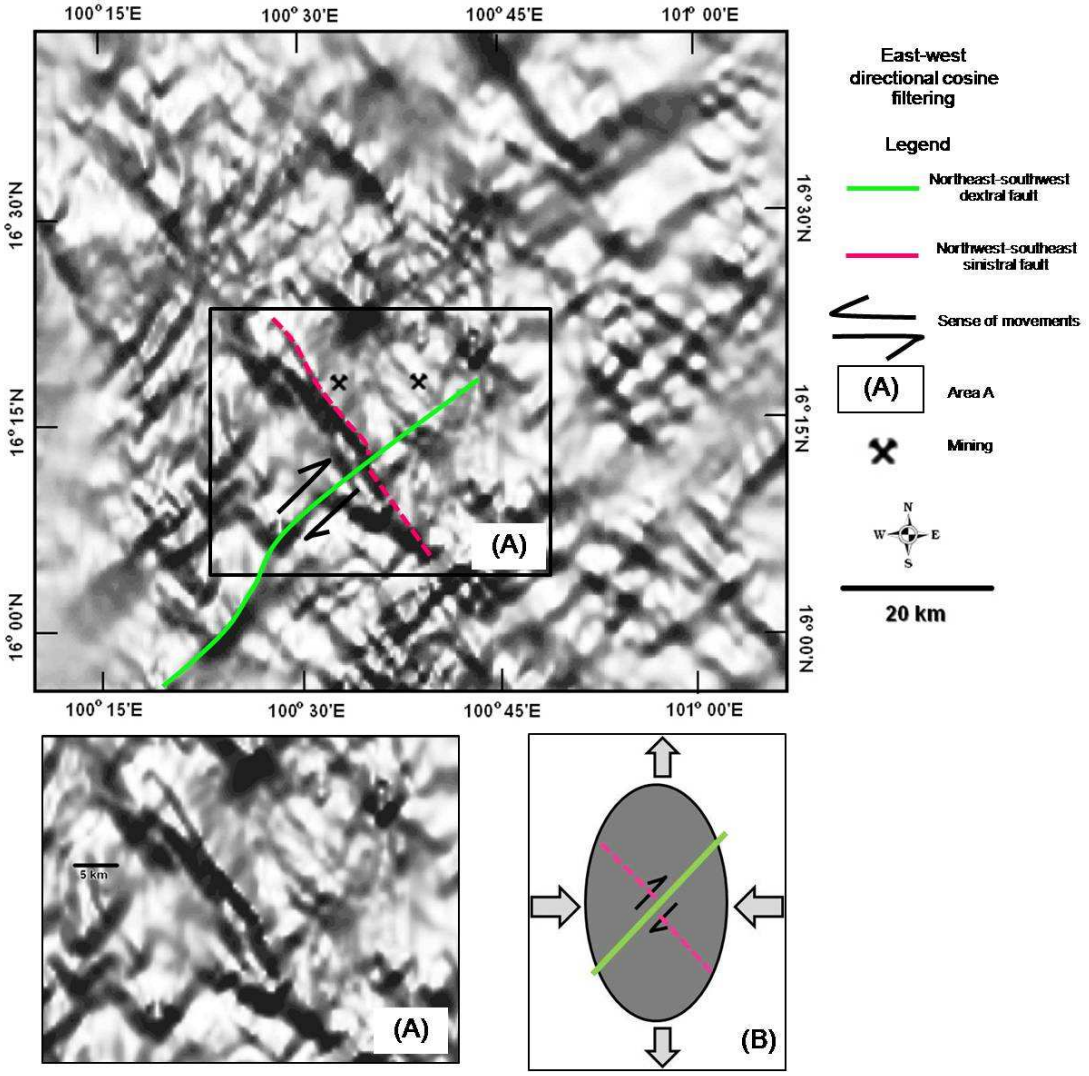

Figure 4.25. Enhanced east-west directional cosine filtering map showing northeast-southeast dextral fault with 2 kilometer lateral slip cross-cut thought northwest-southeast fault in an example of area A that indicate east-west compression and north-south extension strength in figure B of ellipsoid.

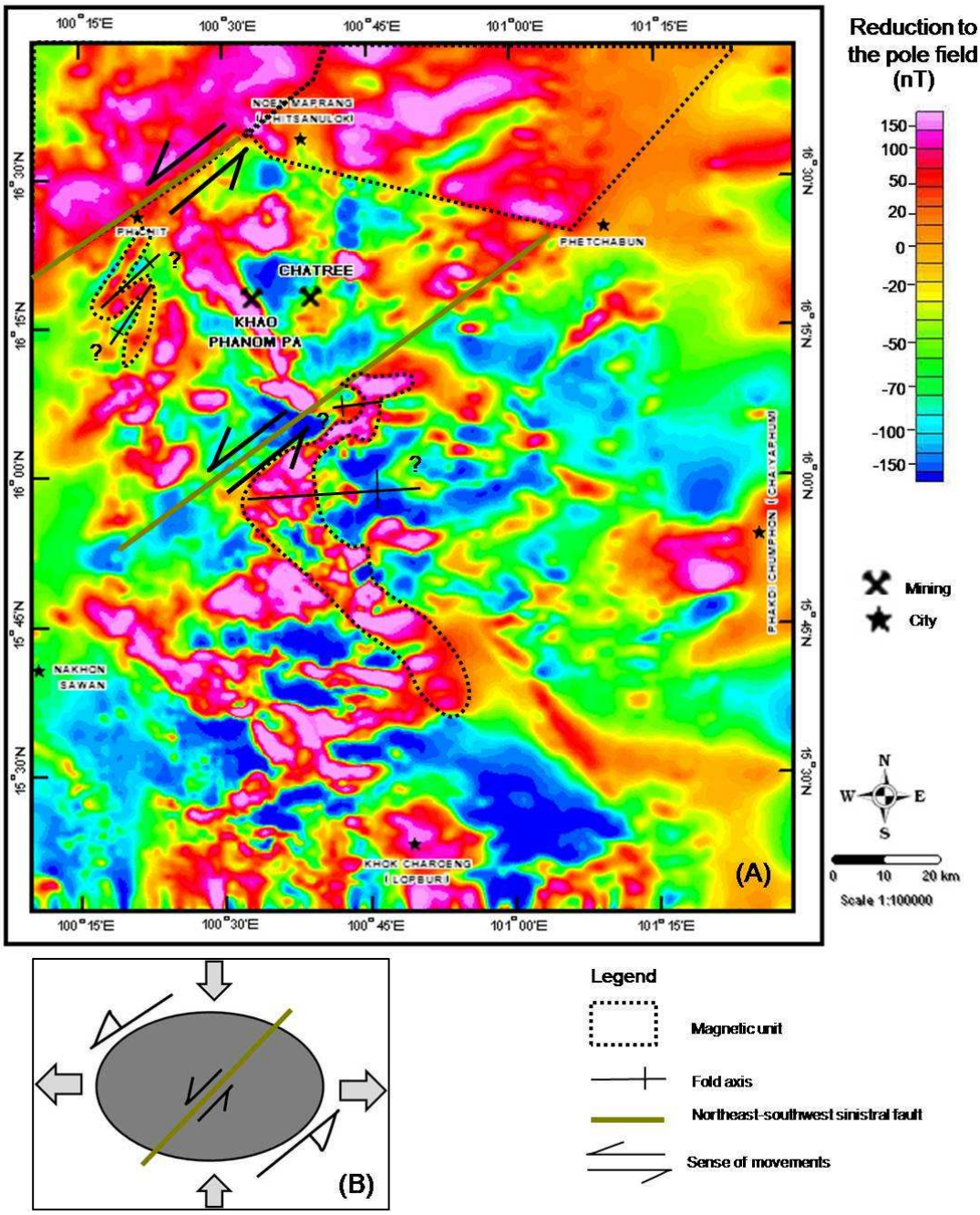

Figure 4.26. Enhanced Reduction to the pole map of the Phetchabun volcanic terrane show east-west axial plane folding in Elongate unit and northeast-southwest sinistral fault with 47 kilometer lateral slip cross-cut thought Flat unit and 9 kilometer lateral slip cross-cut thought Elongate unit that indicate north-south compression strength in figure A of ellipsoid.

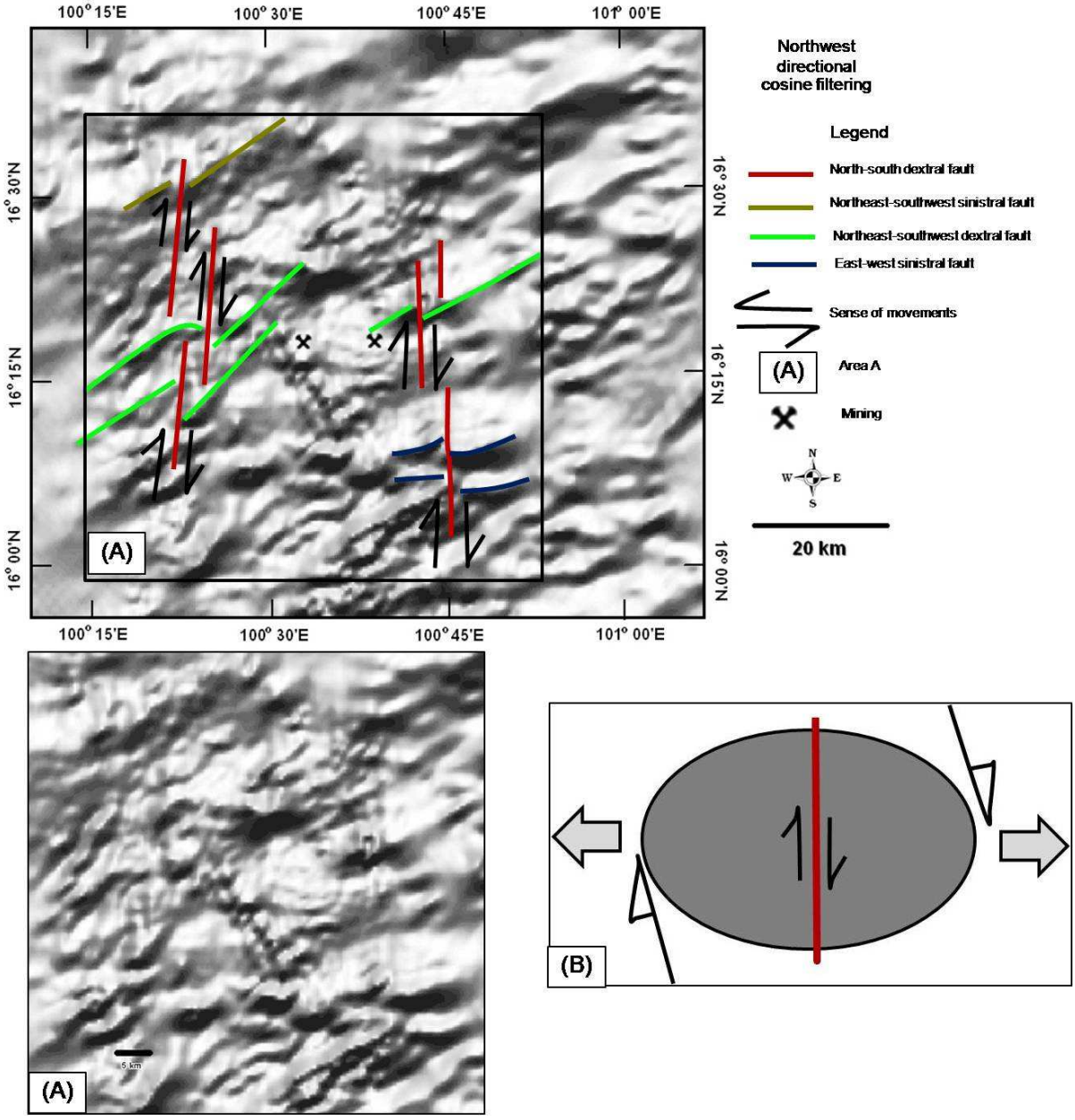

Figure 4.27. Enhanced airborne magnetic map using northwest directional cosine filtering method showing north-south dextral fault in an example of area A with 1-5 kilometer lateral slip cross-cutting through the northeast-southwest and east-west faults due to the east-west extension and northeasteast-southwestwest dextral transpression in figure B of ellipsoid.

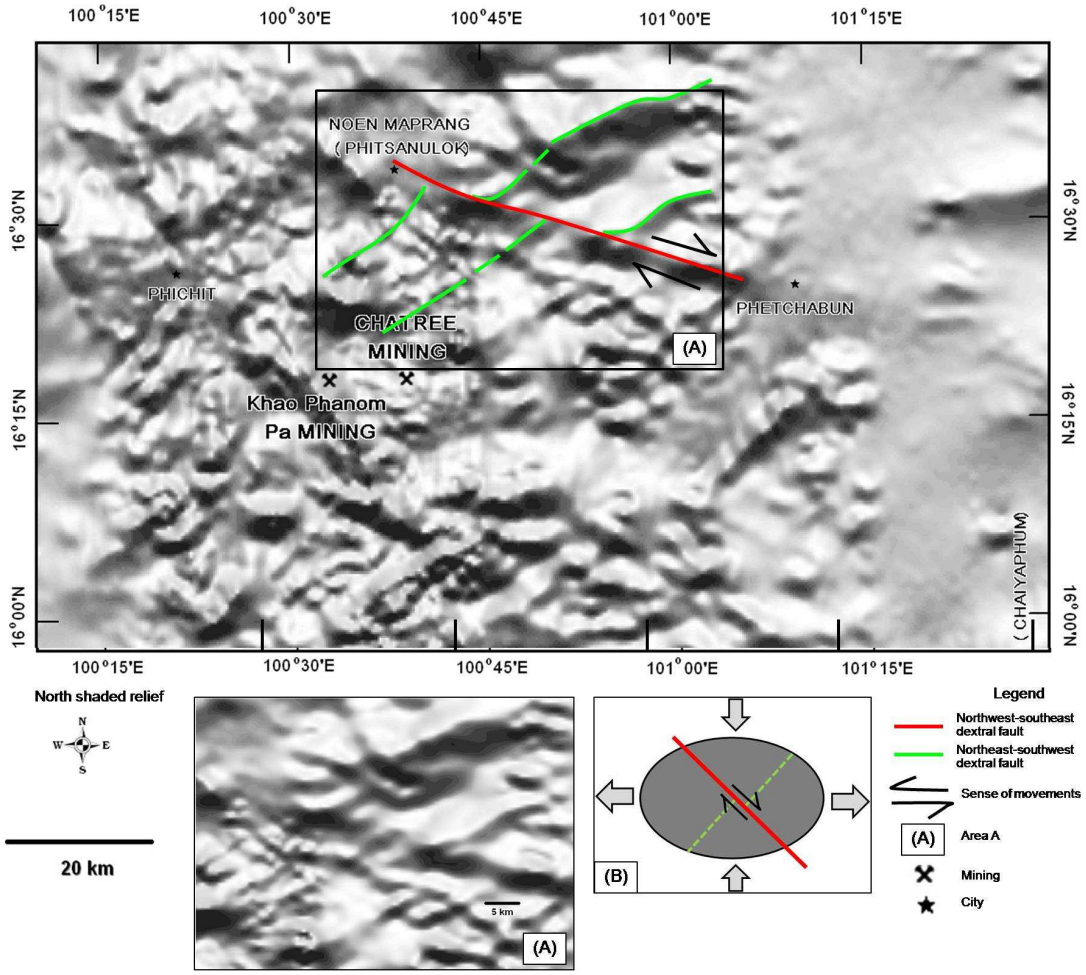

Figure 4.28. Enhanced shaded relief map of the Phetchabun volcanic terrane showing the northwest-southeast dextral fault in an example of area A with 5 kilometer lateral slip cross-cut through northeast-southwest and east-west fault that indicate east-west extension and north-south compression strength in figure B of ellipsoid.

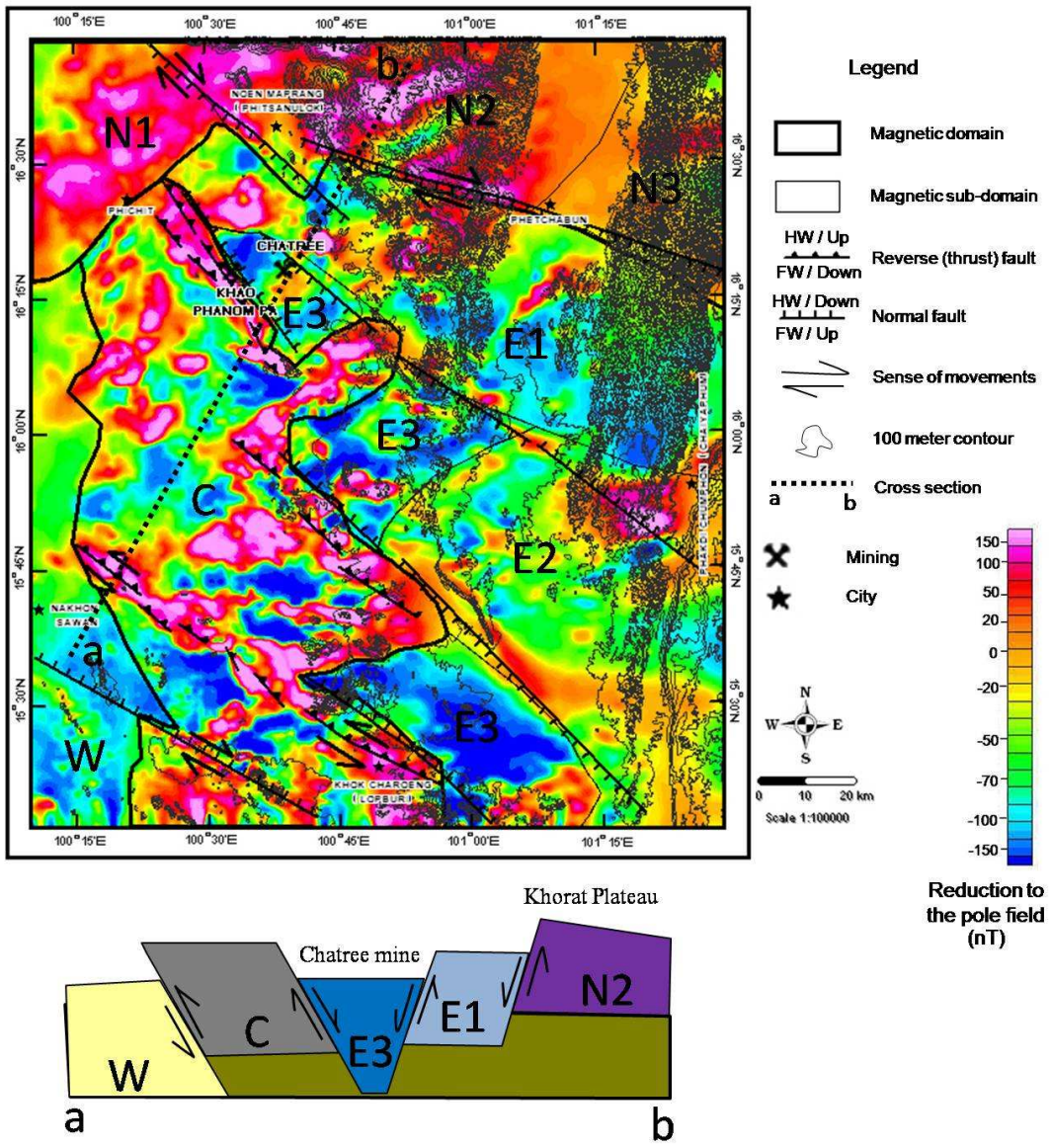

Figure 4.29. Enhanced reduction to the pole map overlain by contour map of the Phetchabun volcanic terrane show in high area to be given higher magnetic in the same geophysical characteristic and low magnetic domain related with low topography indicative of the vertical movement in block diagram of cross section.

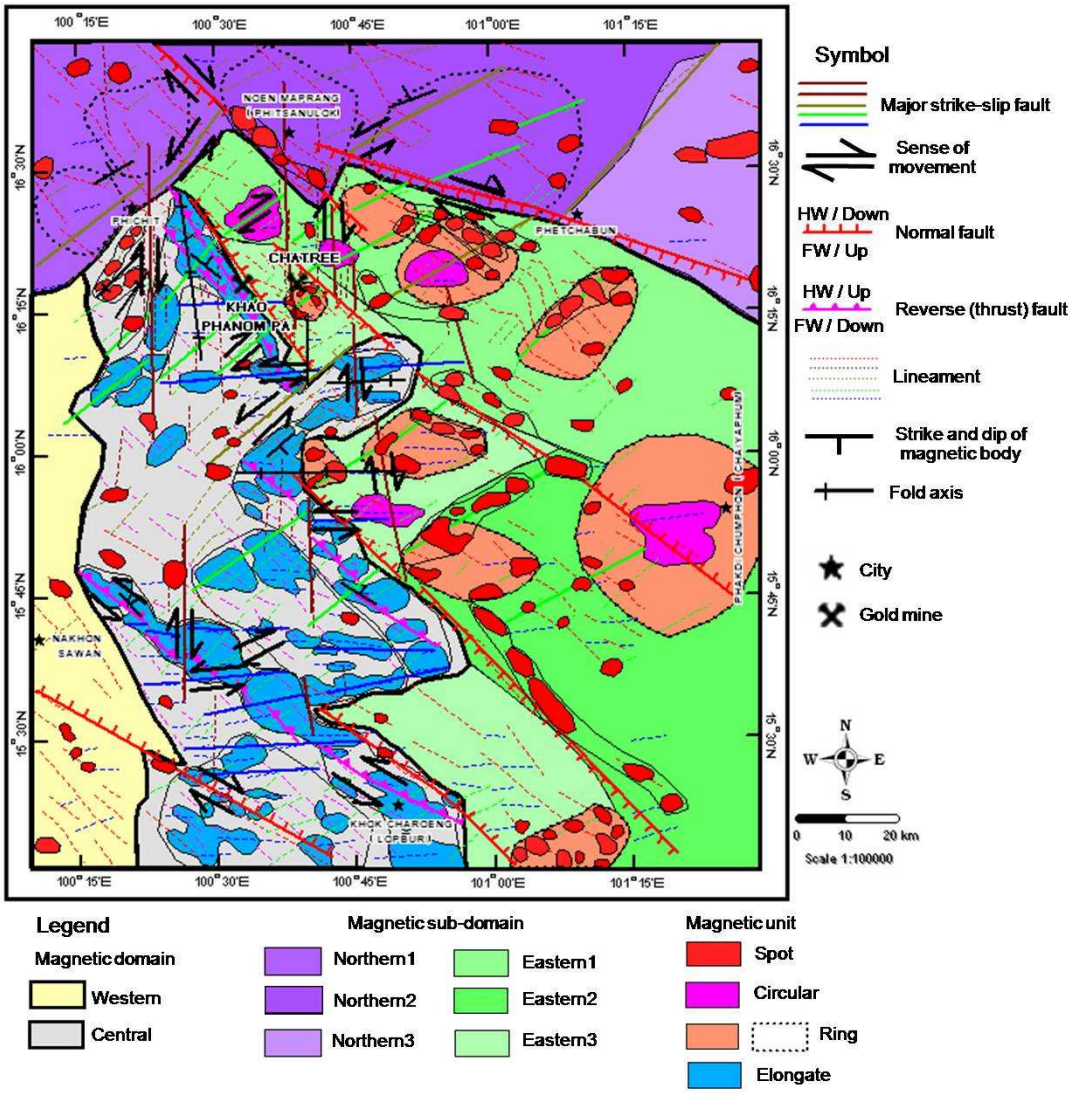

Figure 4.30. Airborne geophysical interpretation map illustrating sequence of magnetic unit and lineaments by result of east-west compression strength generate Elongate unit first, then deformed by northwest-southeast sinistral fault later ring unit and circular unit, east-west sinistral fault and northeast-southwest dextral fault occur, respectively. Subsequencely, the area was subject to east-west extension by generated northeast-southwest sinistral fault, north-south with northwest-southeast dextral fault and spot unit occur, respectively.

4.6 Comparison with field survey

In order to confirm the accuracy of the interpreted maps presented in the previous section, it is important to undertake field investigation in the selected areas where accessibility is not too difficult. Some high magnetic anomalies and structures from 80 locations as shown in Fig.4.11 were selected for more detailed field verification during the summer period of 2009. A, B, C, D, E, F and G (Fig.4.31) are located in the elongate unit of the central domain. It is observed and interpreted that essential rocks of elongate units are deformed intrusive rocks (Figs.4.32, 4.33 and 4.34) which correspond with Permo-Triassic volcanic rocks earlier mapped by Chonglakmani et al. (2004). The area mainly consists of deformed intrusive rocks with sinistral shear (Fig. 4.32) and covered by pyroclastic rock with andesitic composition. Hydrothermal quartz veins and disseminated magnetite are observed in the pyroclastic rock rocks at Khao Phanom Pa. Deformed intrusive rocks show degree of deformation with both brittle fractures and ductile grain (Figs.4.32, 4.33 and 4.34). Deformed granite outcrop with pink color (Fig. 4.32) are found in location E of Fig. 4.31 at lower hill. To the west about 12 km from the pink granite at location C, the rocks are deformed diorite. Under microscope the rock shows deformed characteristic, such as fractures in feldspar grains (Fig.4.33B). Many fractures in diorite are indicated by strong deformation in the rock. From southwest of Khao Phanom Pa from at location A (Fig. 4.34), the rocks is deformed grano-diorite and show deformed characteristic, such as aggregates of quartz, feldspar and plagioclase grains (Fig.4.34B). The elongate units in central domain are interpreted to the deformed intrusive bodies which are indicated degree of deformation as metamorphic cataclasite rock that represent partly of the dismembered or disrupted shear complex. It is considered that this area is a main strong tectonic area by result of subduction along Loei suture zone which is interpreted as represent of fold and thrust zone between collision of 2 plates. Field investigation at H, I and J locations of Fig. 4.31 are in the circular units that are the eastern domain only. Most of the intrusive rocks show medium

grains and equigranular texture with undeformed texture (Fig.4.35 and 4.36). The equigranular intrusive rocks are pyroxene granitoid (Fig. 4.35 C) and hornblende granite (Fig.4.36 C). Moreover, geochemical data from circular unit around location H of hornblende granite reveal that the rocks were originated from the I-type calc-alkalic magma from volcanic arc type setting environment (Kamvong et al., 2006). The association of spot units occurring within the fault zone as recognized by geophysical interpretation map lead to the conclusion these units in this area occurred along the subsidence fault zone. A more detailed field checking area is shown in Fig. 4.31 at location K, L and M. Location M in the eastern1 sub-domain. These locations are displayed by a zone of high spot magnetic anomaly about 5x3 km^2. Field investigation indicates that the main rock type is granodiorite with fine-medium grains and porphyritic texture. Location M and L (Fig.4.37 and 4.38) is situated in the eastern1 sub-domain and is characterized by the spot of moderate magnetic anomaly with the aerial extent of 4x2.5 km^2. The field evidence is supported by the fine grained porphyritic granodiorite with undeform texture. Moreover, geochemical data of the more sub-intrusive rocks reveal that the rocks were originated from the tholeiitic magma from volcanic arc type setting environment (Boonsoong et al., 2011). The geologic map by Chonglakmani et al. (2004) shows mainly covered by the Permo-Triassic volcanic rocks (Fig. 2.4) such as pyroclastic rocks mainly andesitic-rhyolitic composition and andesite flow lava which are show high mag-susceptibility (table 4.2). But volcanic rock is not show high magnetic anomaly in reduction to the pole map. Anyway, the Permo-Triassic volcanic rocks can be found around ring units. Therefore, they can interpret as remnant volcanic center of Permo-Triassic volcanic rocks. Moreover, geochemical data from the andesite flow rocks and pyroclastic rocks around the ring units reveal that the rocks were originated from the calc-alkalic magma from volcanic arc type setting environment (Cumming et al., 2004, Nakchaiya et. al., 2008, Marhotorn et al., 2008, and Boonsoong, et al., 2011). The northern domain is covered by Mesozoic sedimentary rocks which are low-

moderate mag-susceptibility (1-550x10^{-5}SI) base on the work of Bhongsuwan, et al. (2002). In geophysical interpretation based on the residual high pass filtering map show ring units under these sedimentary rocks that cause northern domain is high magnetic intensity in the reduction to the pole map. At location 1 on geophysical interpretation map (Fig. 4.39), we are observed triangular facets (Fig. 4.40) along northwest-southeast at the edge of Khorat Plateau that are indicated normal fault same as show in geophysical interpretation. At location 2 on geophysical interpretation map (Fig. 4.39), we are observed northeast-southwest fault scab (Fig. 4.41) along northeast-southwest mountain similar to the geophysical interpretation. At location 3 on geophysical interpretation map (Fig. 4.39), we are observed northwest-southeast normal fault (Fig. 4.42) cut in the Permian unit same as show in geophysical interpretation. In geophysical interpretation map of field location 2 in Fig. 4.39 shows northwest-southeast dextral with normal fault. In the field survey shows northwest-southeast normal fault (Fig. 4.43) same as show in geophysical interpretation. In geophysical interpretation map of field location 4 in Fig. 4.39 shows folding with north-south axial plane. In the field shows tight fold (Fig. 4.44) in Permian unit probably indicate folding around area. Lateral faults and normal faults are clearly observed that field investigation conforms very well to the interpreted surface and subsurface structures by using airborne geophysical data.

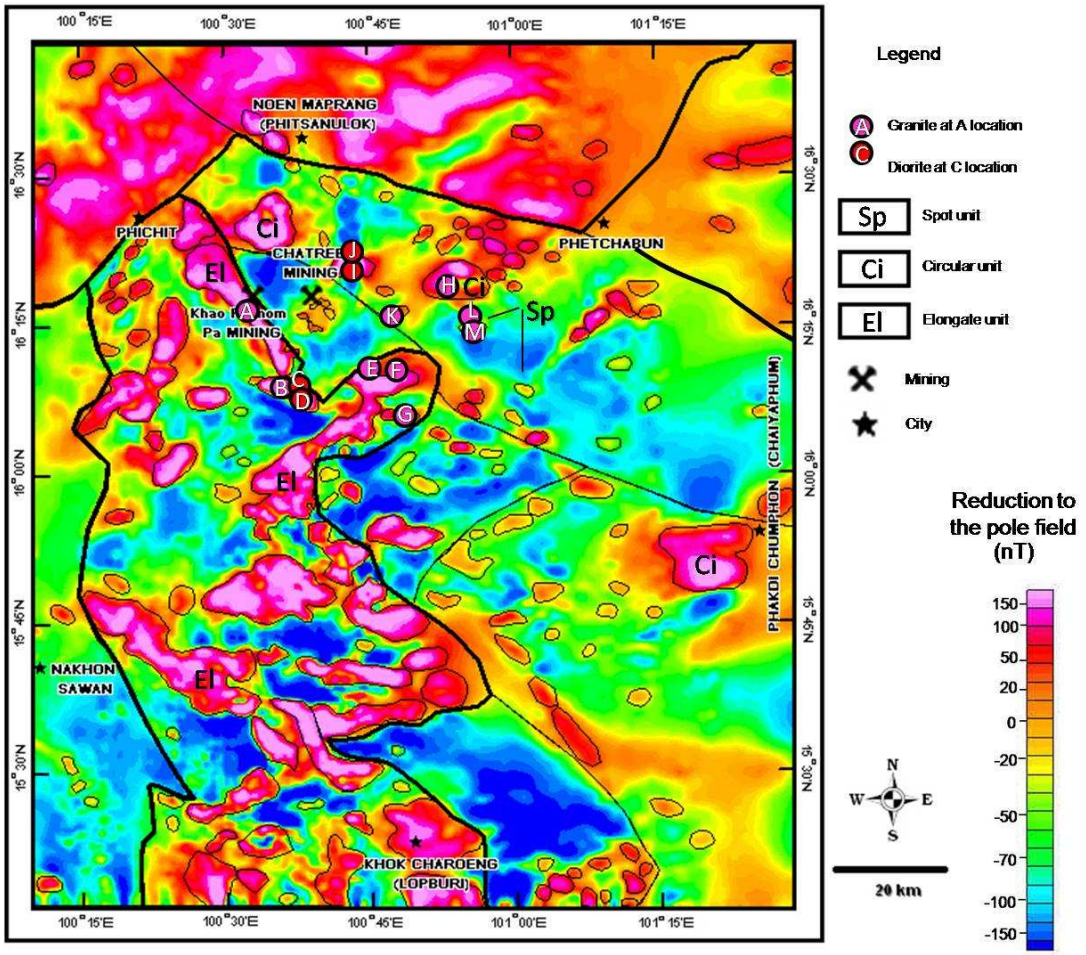

Figure 4.31. Reduction to the pole map showing outcrop location A, B, C, D, E, F and G in Elongate unit consist of deformed granite and diorite, outcrop location H, I and J in Circular unit consist of equigranular granite and diorite with undeform texture and outcrop location K, L and M in Spot unit consist of porphyritic granite with undeform texture.

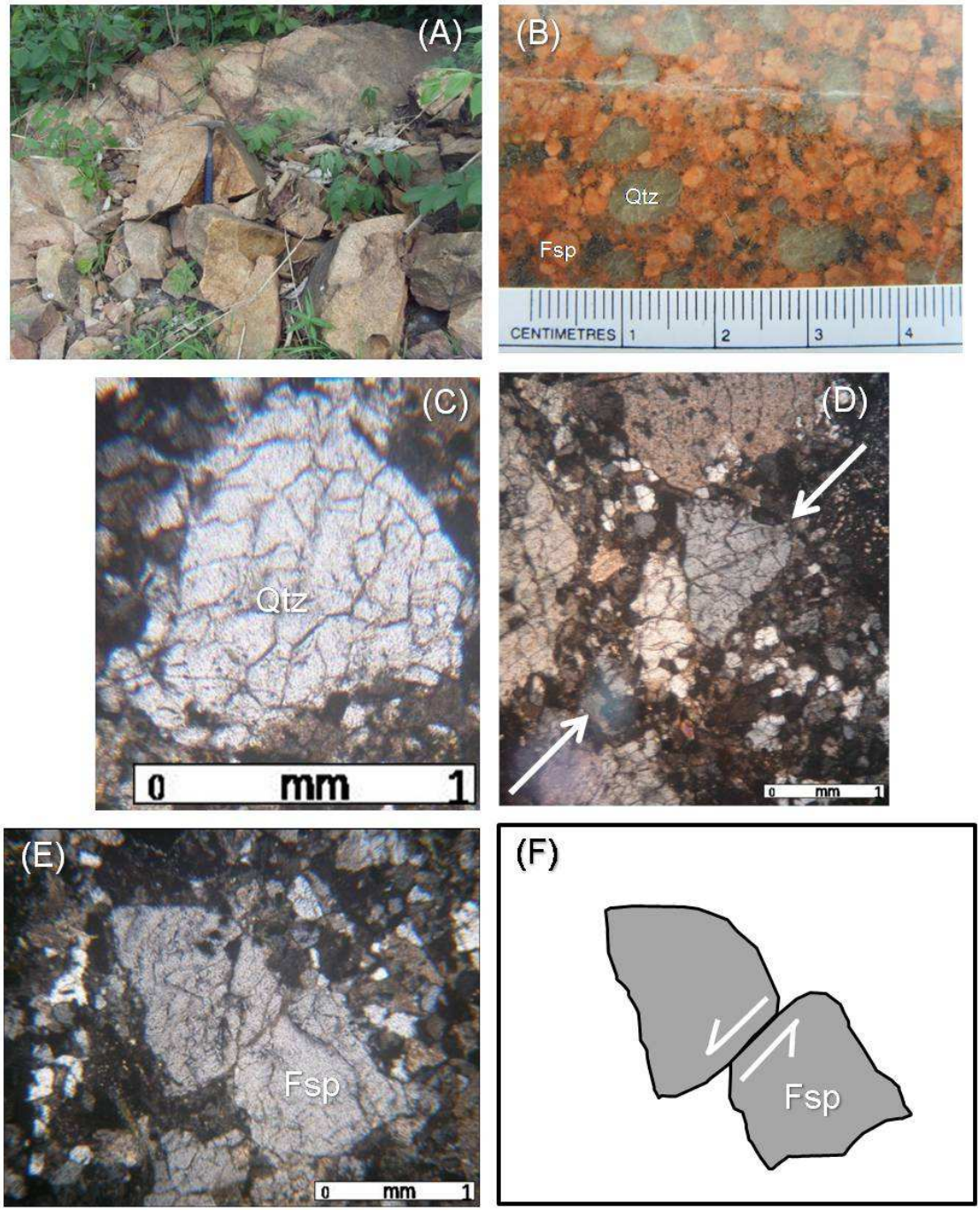

Figure 4.32. (A) Natural exposure of pink granite at location E in Fig. 4.31 is in Elongate unit (B) rock slap showing fractures and rounded shape of quartz grains (C) photomicrographs of quartz grain showing fracture foliation (D) Fine-grained aggregates of quartz+feldspar+biotite along a reactivated joint (E) and (F) Feldspar grain showing sinistral movement. This rock showing cataclasite texture with suggests deformation of intrusive rock in brittle-ductile transition zone.

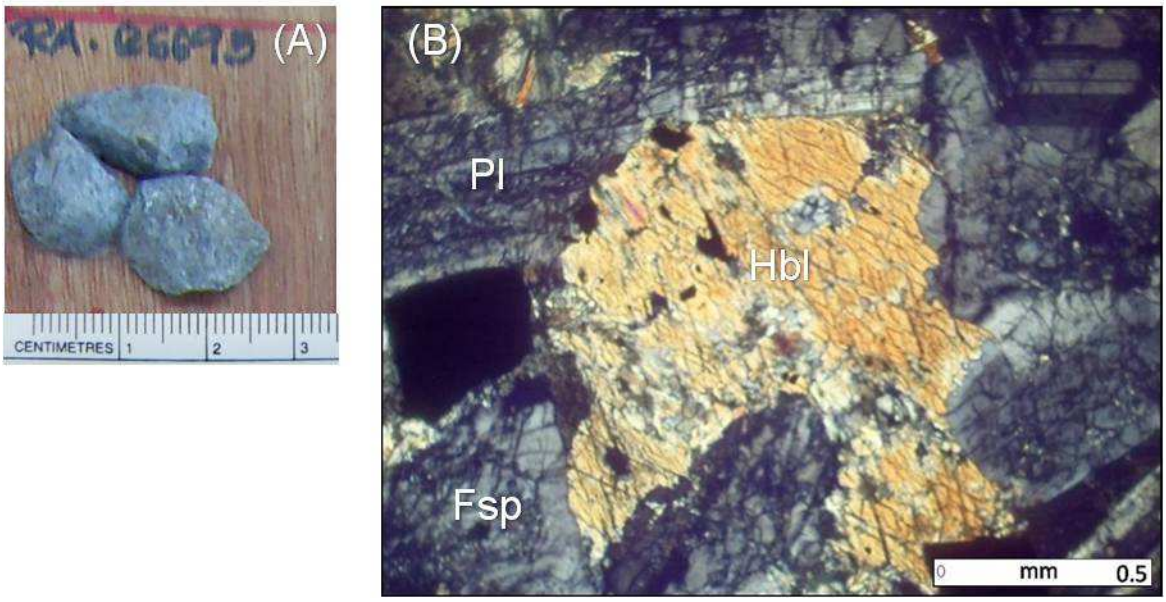

Figure 4.33. (A) Rock cutting from RAB drilling at location C in Fig. 4.31 is in elongate unit (B) photomicrograph of diorite shows fractures of plagioclase and feldspar grains.

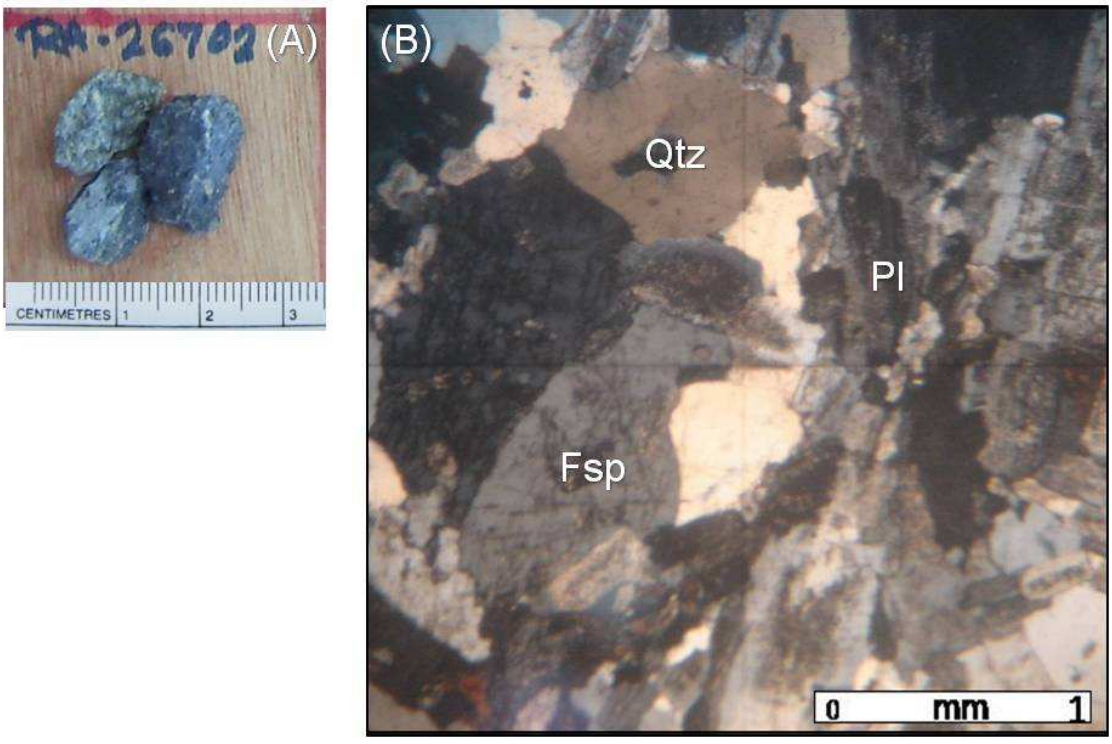

Figure 4.34. (A) Rock cutting from RAB drilling at location A in Fig. 4.31 is in Elongate unit. (B) photomicrograph of granite showing aggregates of quartz + feldspar + plagioclase.

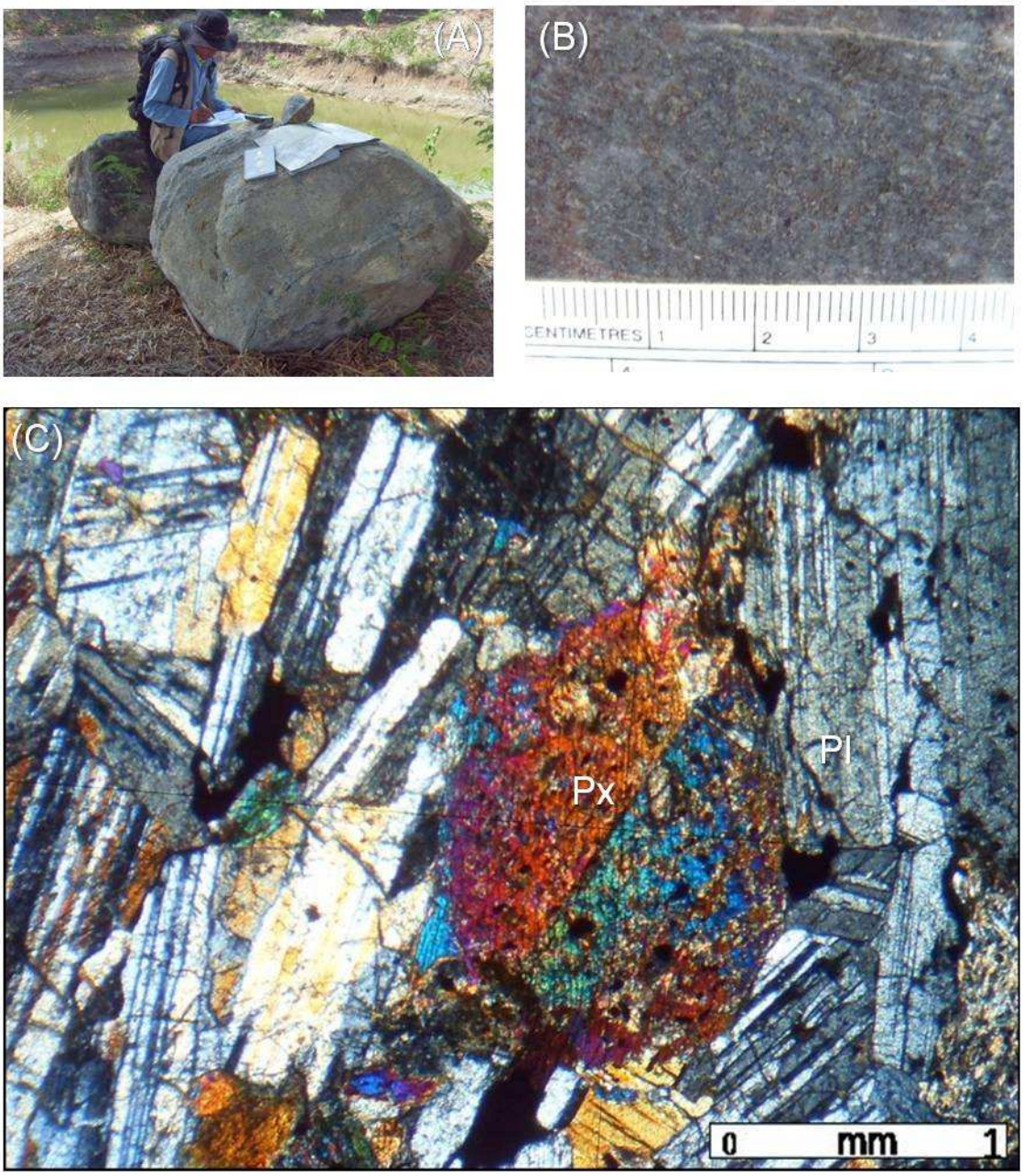

Figure 4.35. (A) Large float blocks close to pit at location I in Fig. 4.31 corresponding to the circular unit (B) rock slap showing medium grain with dark grey color with undeformation texture (C) photomicrograph of diorite showing equigranular and undeformation texture.

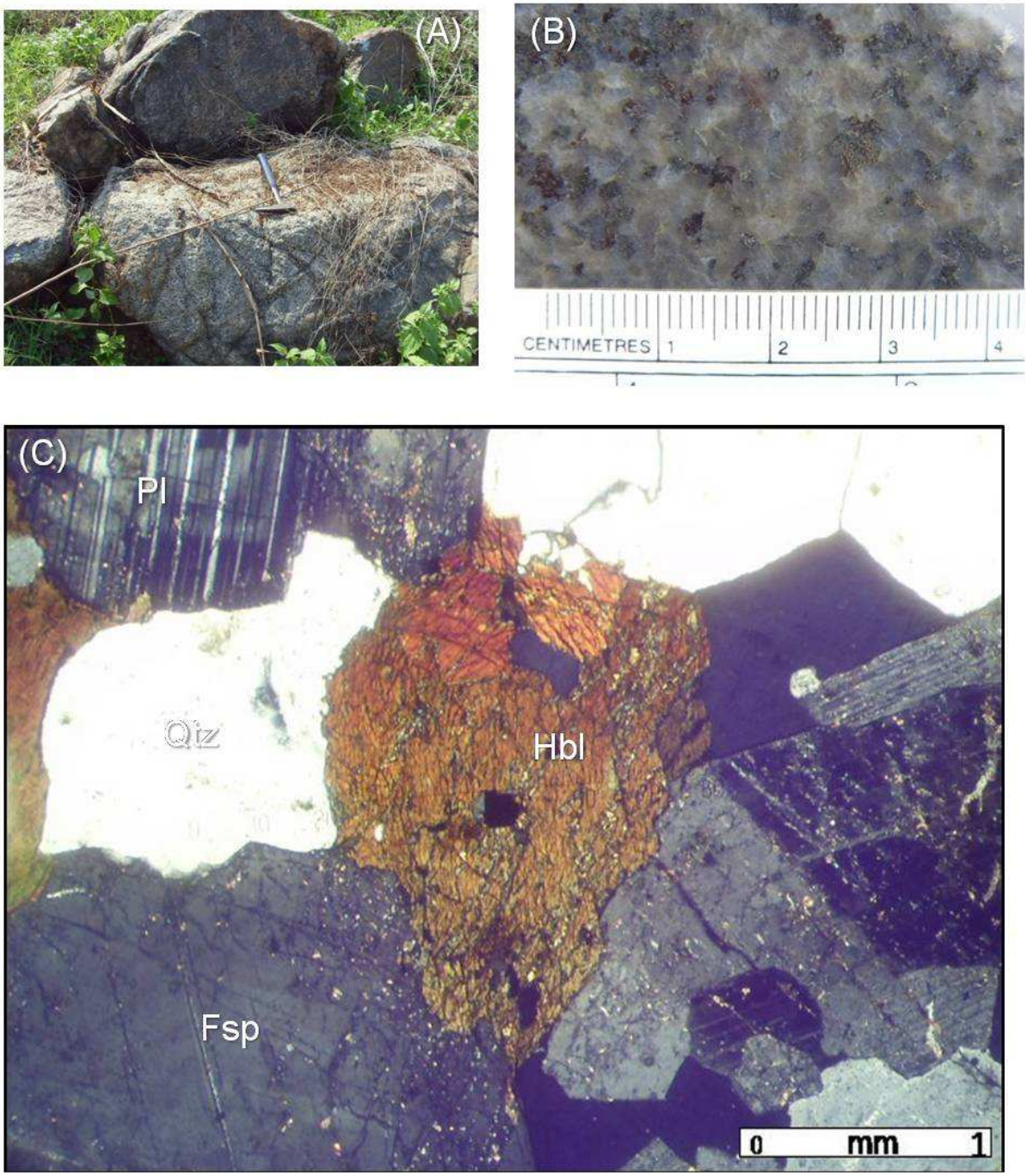

Figure 4.36. (A) Large float blocks lower hill at location H in Fig. 4.31 is in Circular unit (B) rock slap picture shows quartz grains (C) photomicrograph of grano-diorite shows equigranular and undeformation texture.

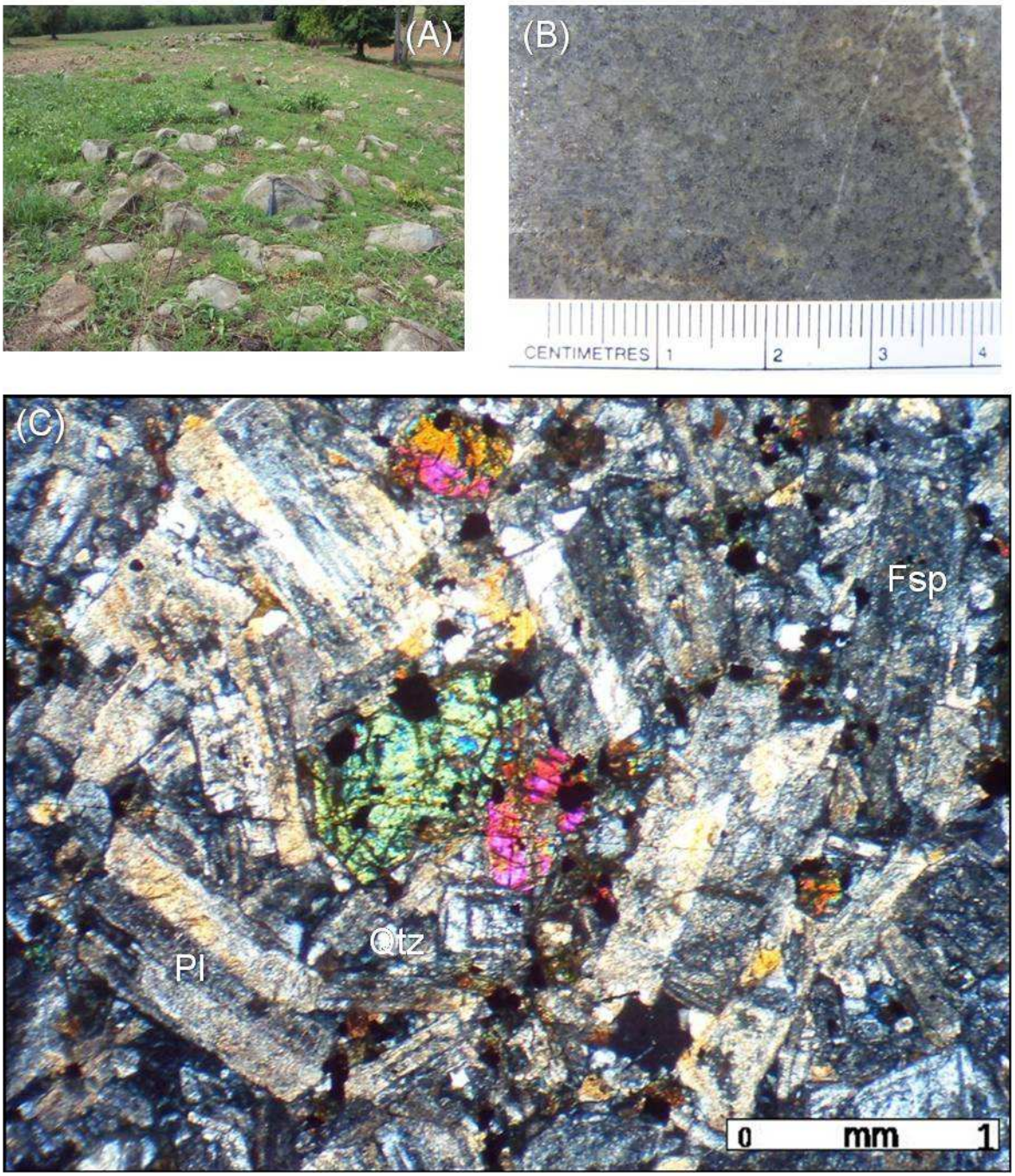

Figure 4.37. (A) Natural exposure at location M in Fig. 4.31 is in Spot unit (B) rock slap picture show fine grain with dark grey color (C) photomicrograph of grano-diorite shows porphyritic and undeformation texture.

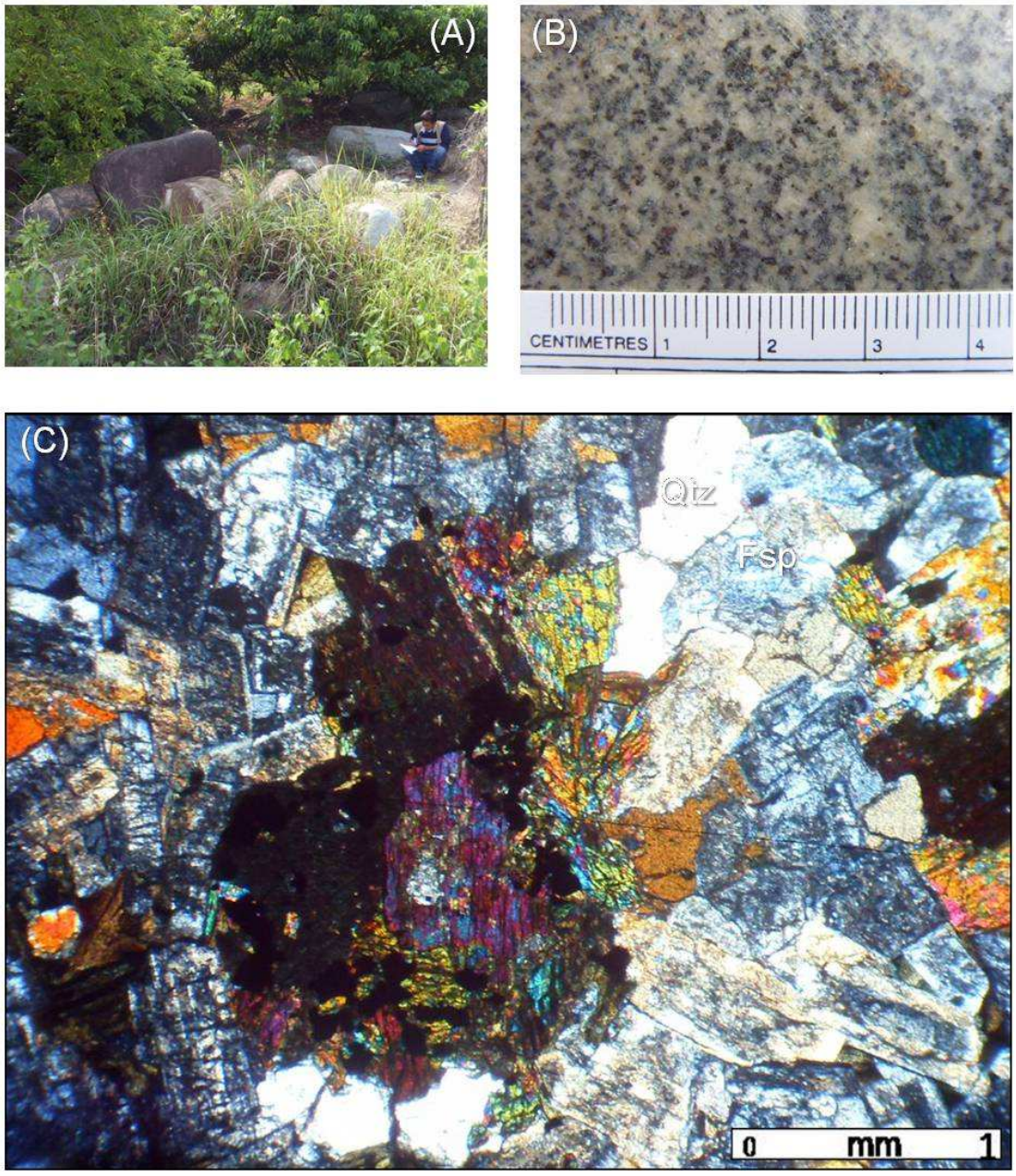

Figure 4.38. (A) Natural exposure at location L in Fig. 4.31 is in Spot unit (B) Rock slap picture showing medium grain with grey color (C) photomicrograph of grano-diorite showing porphyritic and undeformation texture.

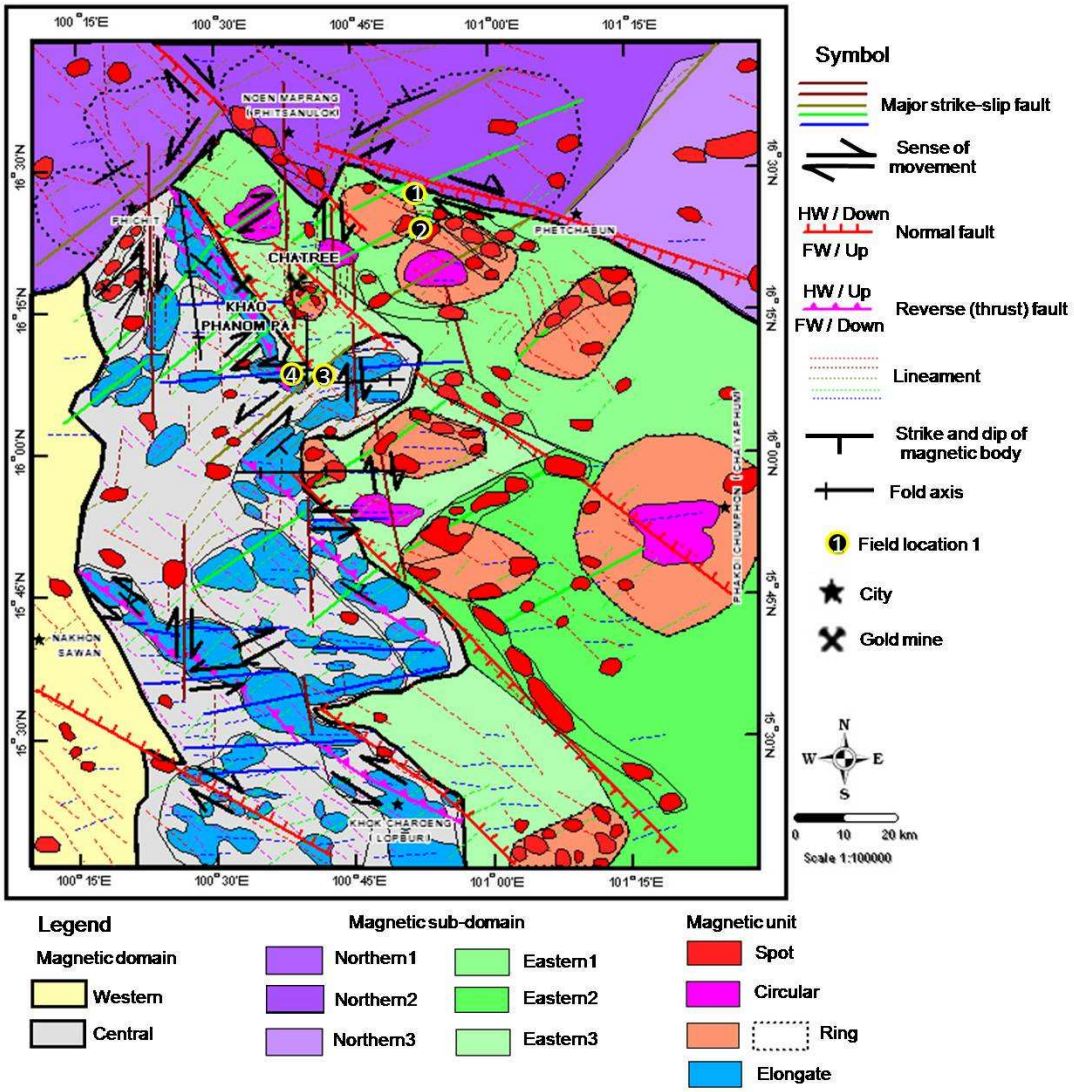

Figure 4.39. Airborne geophysical interpretation map of the Phetchabun volcanic terrane showing field locations 1, 2, 3 and 4, northwest-southeast dextral fault with normal component in red line and the northeast-southwest dextral fault and folds.

Figure 4.40. View of location 1 in Fig. 4.39 showing northwest-southeast dextral strike-slip fault with normal component along the edge of Khorat Plateau. Noted that triangular facets are indicative of normal fault similar to that of the geophysical interpretation.

Figure 4.41. View of location 2 in Fig. 4.39 showing northeast-southwest dextral strike-slip fault. Noted that fault scarp occurring along the northeast-southeast mountain similar to that of the geophysical interpretation.

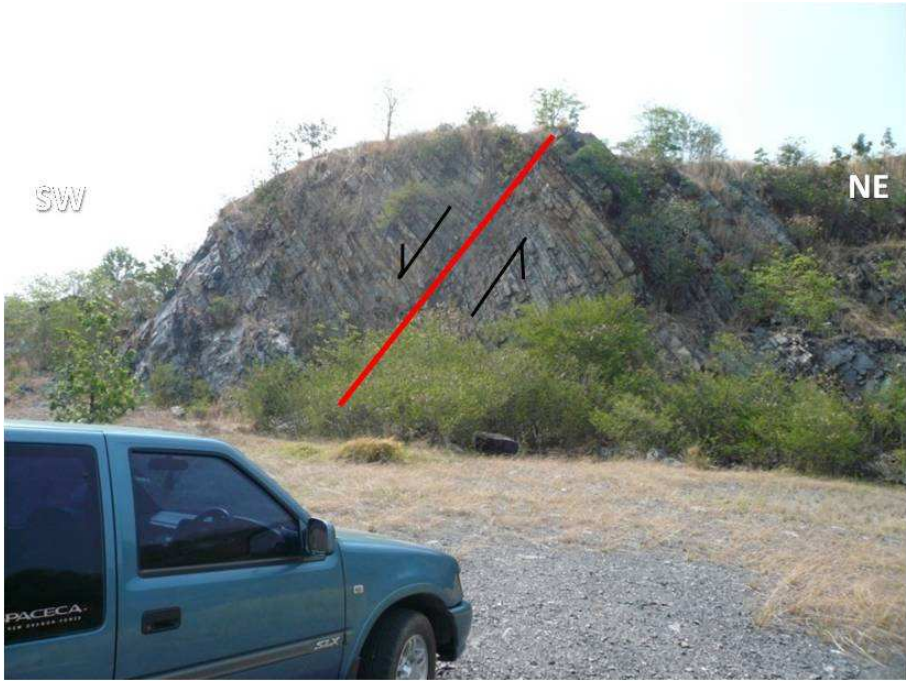

Figure4.42. Abandoned quarry showing the NW-SE trending dextral fault with normal vertical component (location 3 in Fig.4.39) occurring in the Permian well bedded clastic rocks.

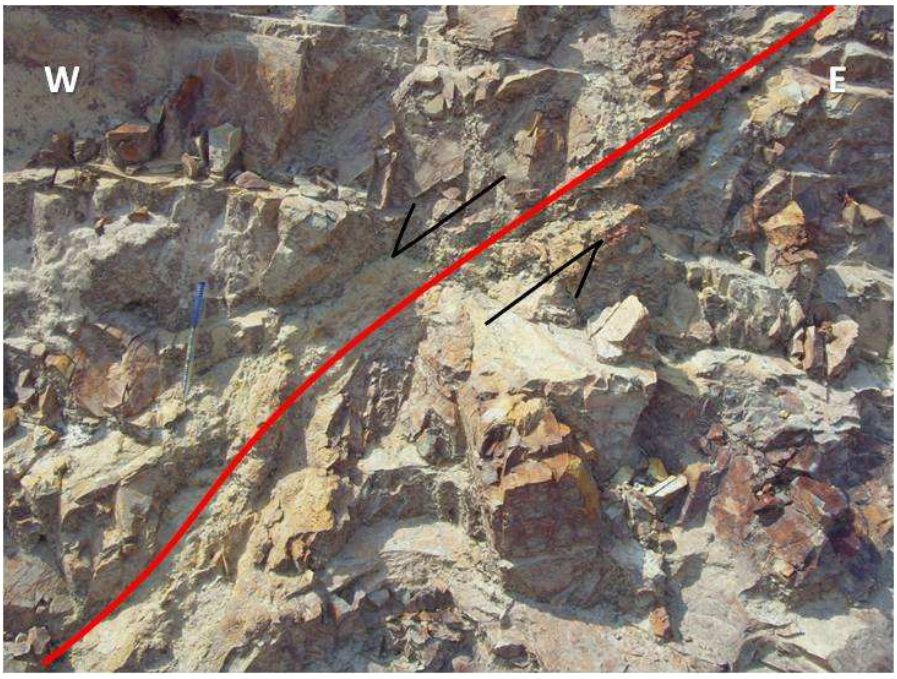

Figure4.43. A quarry front in the field location2 of Fig.4.39 showing the normal fault with the intermediate dipping angle to the west found in Permain bedded mudstone.

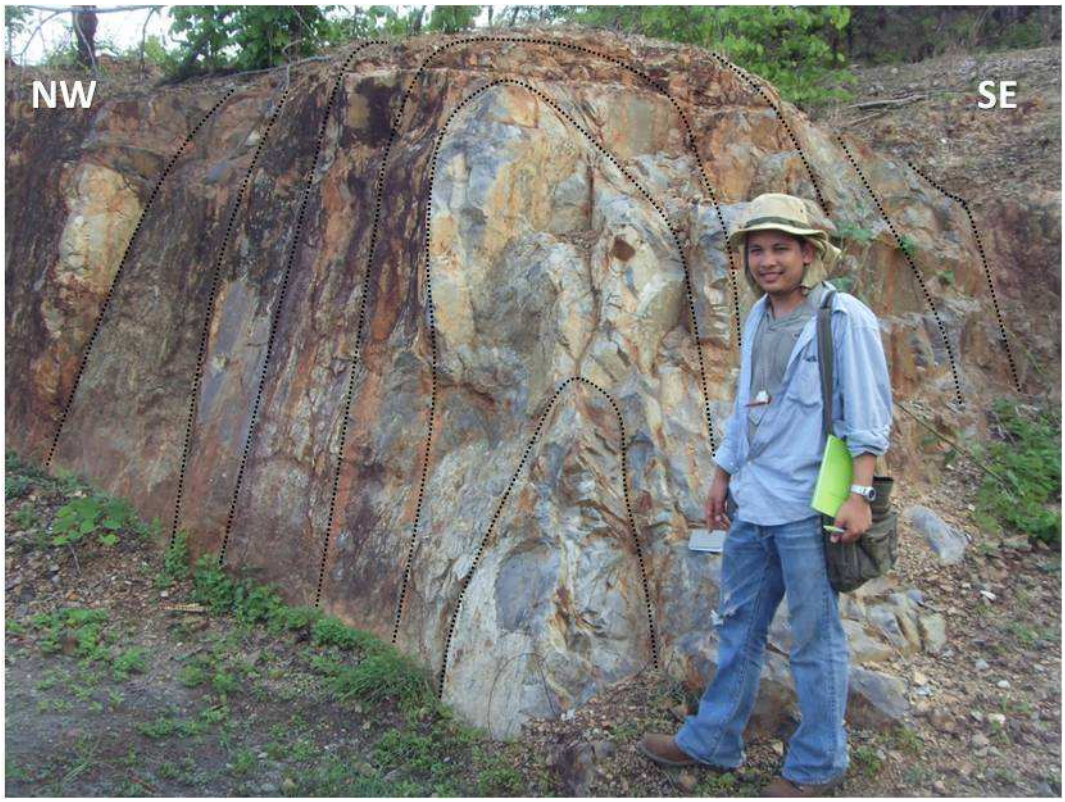

Figure4.44. Road-cut exposure showing Permian bedded clastic rock with tight-folding structure and the north-south trending axial plane corresponding to location 4 in Fig.4.39.

4.7 Magnetic modeling

From the magnetic data interpretation and field observation, geophysical modeling can be constructed by the assistance of the Mag2dc (2.10) software for forward modeling methods. As shown in the previous section, data from the reduction to the pole enhancement seems to give the best result. Therefore, magnetic response profiles of the reduction to the pole were selected for modeling. To simplify the line profile, cross sections were drawn based on latitudes of the Phetchabun volcanic terrane study area (Fig. 4.45). In this study, magnetic modeling is assuming only induce magnetization and using the magnetic susceptibilities measured from the rock samples in the Phetchabun Volcanic area as shown in Tables 4.1, 4.2 and 4.3. The cross-section for modeling is in east-west direction for the main geological structure in the study area in north-south direction. Six cross-sections along line number 1738800N, 1797000N, 1807800N, 646000E, 658000E and 665000E are selected for interpretation (Figs. 4.46,

and 4.47). In the central domain of the study area (in elongate unit), interpreted bodies have magnetic intensity higher than those of the surrounding central domain with elongate shape, suggesting deformed intrusive bodies of granitic to dioritic composition. Very interesting for elongate units, the series of high elongate magnetic bodies are encountered and interpreted to indicate the northeast-dipping faults in the central domain with the largest body. On the surveyed line 1797000N at the 678000E and line 1738800N at the 749000E (ring unit), ring bodies indicate moderate magnetic intensities with circular features of the deep volcanic chamber or center, corresponding to the Permo-Triassic volcanic rocks (andesitic composition) of the eastern and northern domains. Additionally, circular units are corresponded to equigranular intrusive bodies in the eastern domain. These interesting anomalies are interpreted as the circular feature of intrusive bodies in the eastern domain. Magnetic bodies from the potential field source distributions represent deformational dip of elongate units to the eastward, deep magnetic bodies of ring units at more than 4 km with undeformational structure and undeformational structure in circular unit. The most important control on the reliability of magnetic models is information on magnetic properties. Understanding of the factors that determine magnetization of intensities and direction for the geological units is essential for resolving geological ambiguity in order to produce a reliable interpretation of subsurface geology.

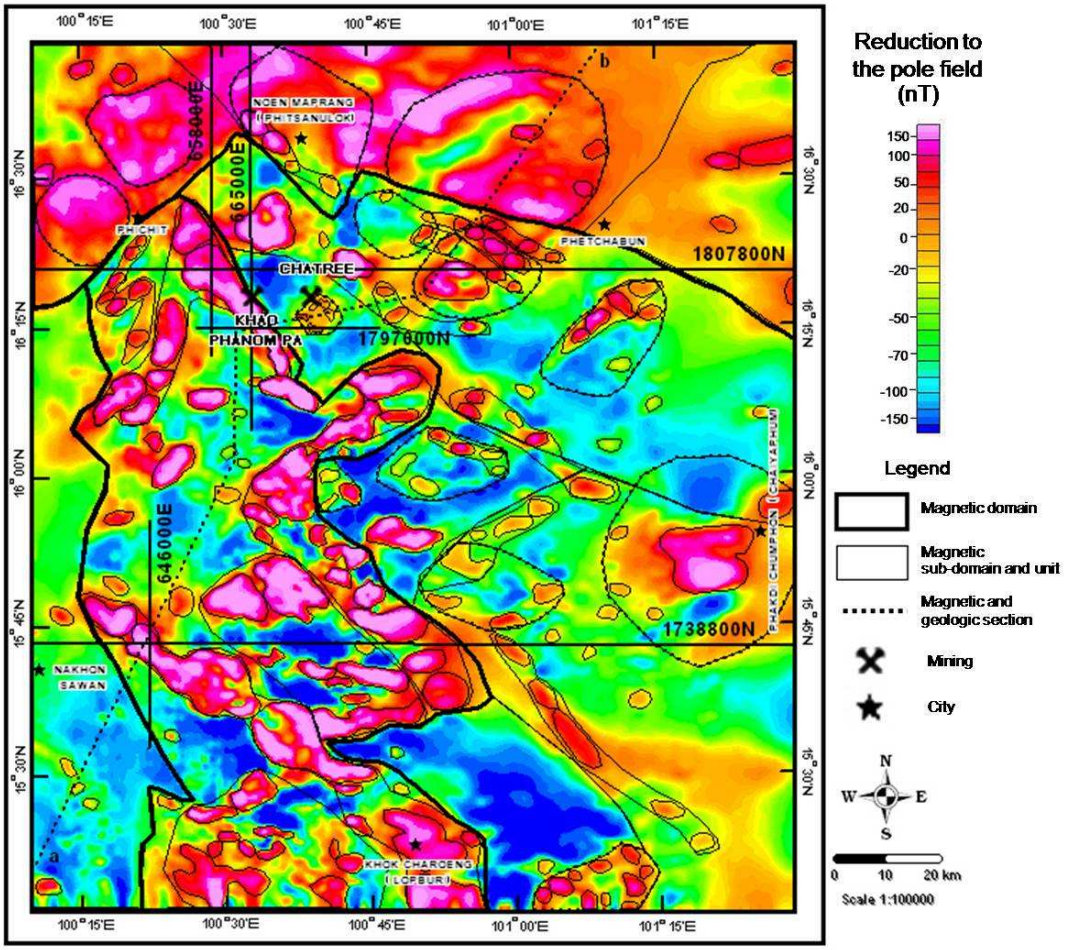

Figure 4.45. The reduction to the pole map of Phetchabun volcanic terrane showing major magnetic domain and locations of airborne magnetic sections 1738800N, 1797000N, 1807800N, 646000E, 658000E and 665000E used for magnetic modeling (see figs. 4.46 and 4.47) and geologic section of (a-b in fig. 4.48).

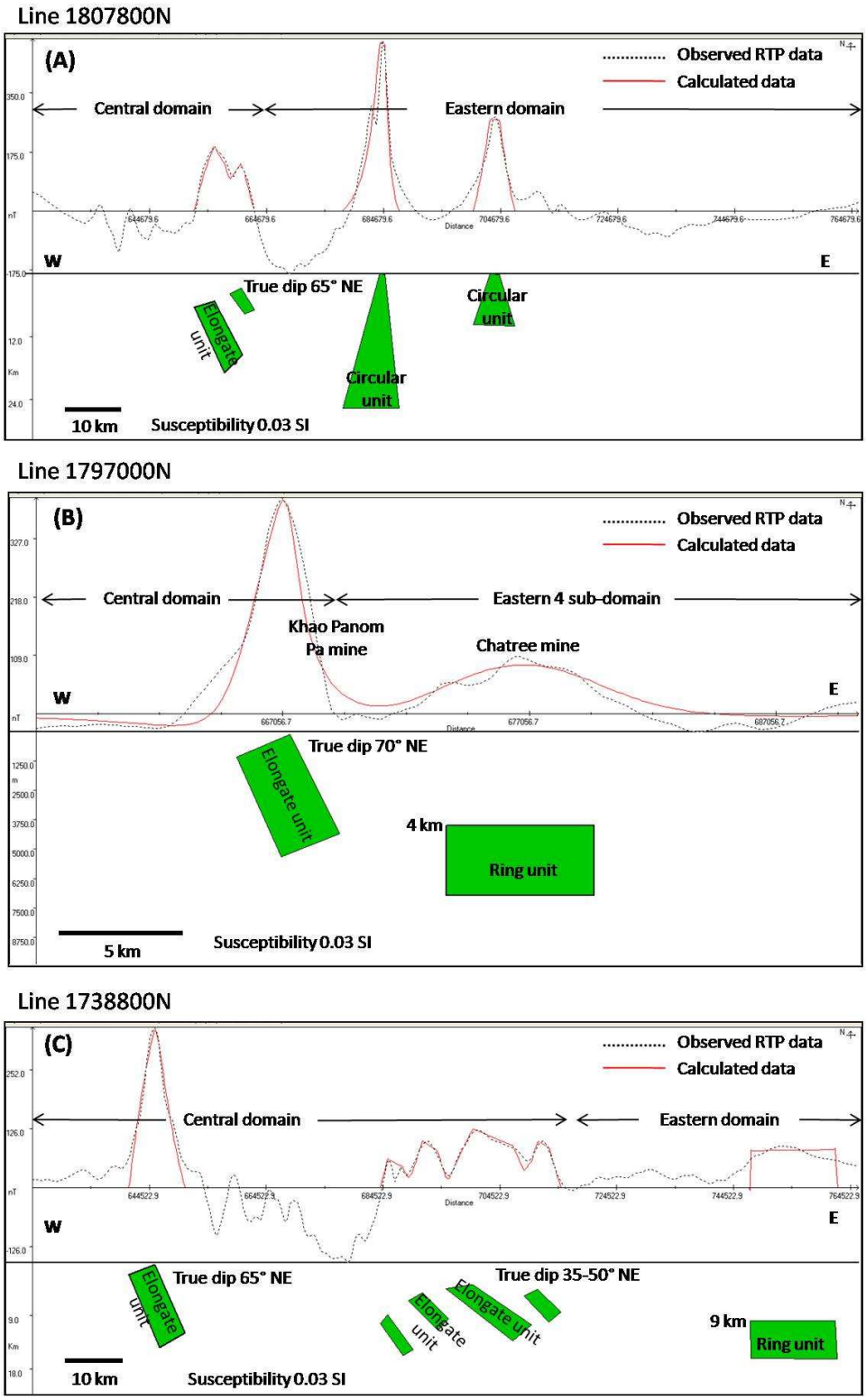

Figure 4.46. Results of airborne magnetic modeling of lines (A) 1807800N, (B) 1797000N and (C) 1738800N (east-west magnetic lines from Fig. 4.45) showing northeast dipping of elongate unit, deep bodies of ring unit and vertical bodies of circular units.

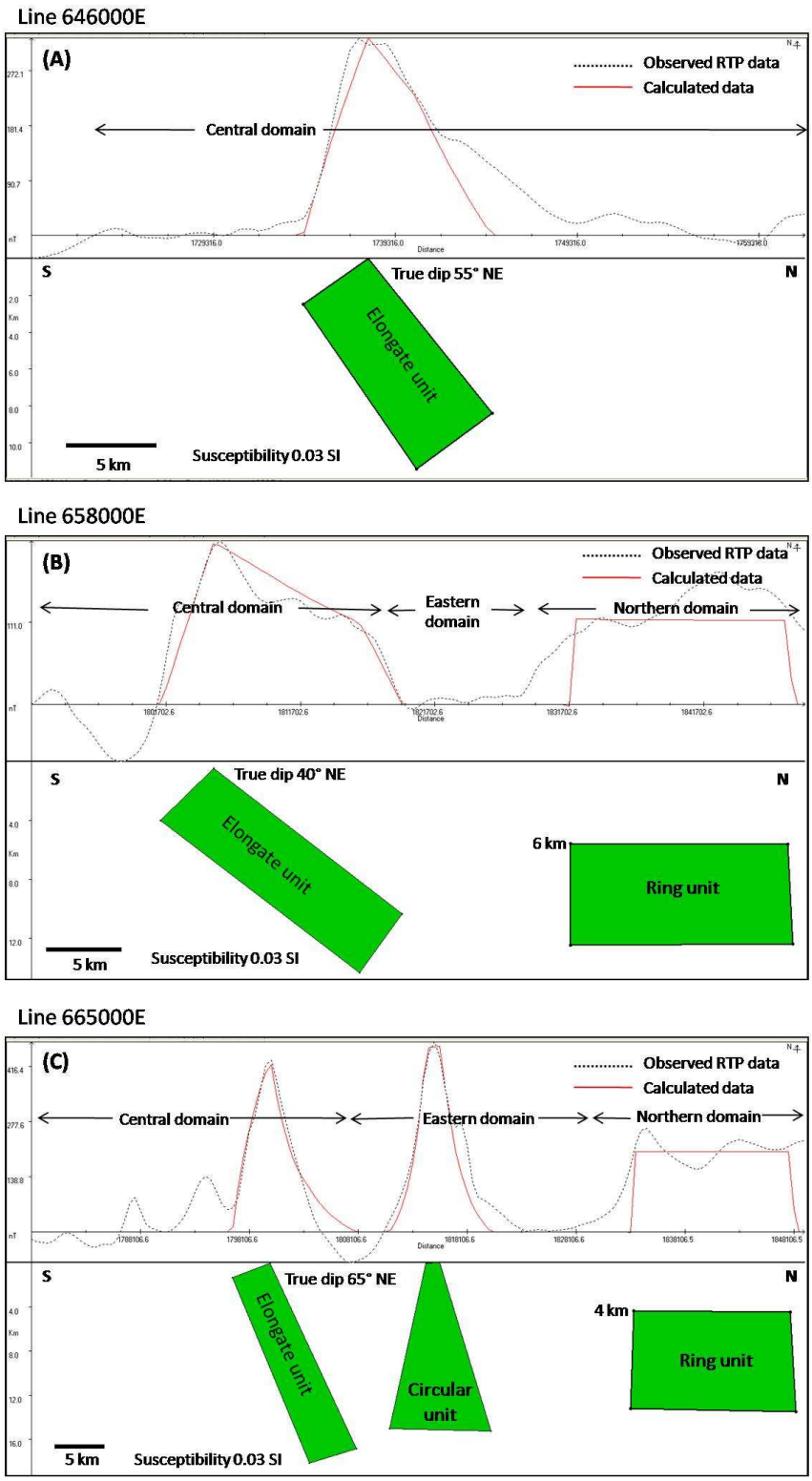

Figure 4.47. Results airborne magnetic modeling of lines (A) 646000E, (B) 658000E and (C) 665000E (north-south magnetic lines from Fig. 4.45) showing northeast dipping of elongate unit, deep bodies of ring unit and vertical bodies of circular units.

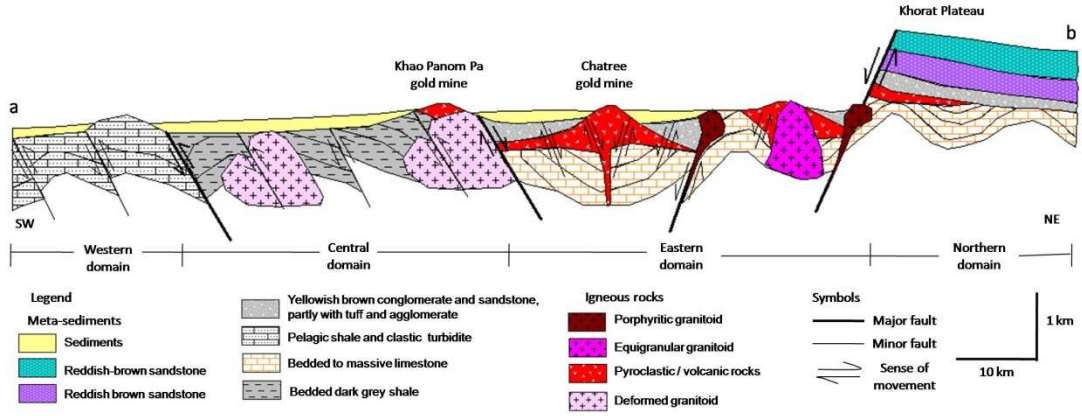

Figure 4.48. Geologic cross-section of Phetchabun volcanic terrane (see a-b line section from Fig. 4.45) using airborne geophysical and geological interpretation.

CHAPTER VI

Discussion

As shown in the earlier chapters, the Phetchabun volcanic terrane sedimentary rocks are generally non-magnetic, whereas igneous rocks rich in iron and magnesium tend to be high magnetic. But volcanic rocks have not shown anomaly out of ring anomalies that is because they do not have enough thickness to induce magnetic field with 2-5 km of airborne grid survey. Therefore, high anomalies on reduction to the pole map are only related to plutonic rocks.

5.1 Interpretation of Individual Anomaly Units.

Based on the results of magnetic units and lineaments in elongate units within the central domain, most of the magnetic anomalies in these areas are observed over poorly exposure of deformed intrusive rocks which are associated with folding and faulting on geophysical interpretation map. The occurrence of deformation structure indicates compressional stress (Fig. 5.1) may have been caused by subduction-related tectonics along the Loei “Suture” or tectonic line (Fig.5.6) which is interpreted by Tulyatid et al. (1999) and Charusiri at al. (2002). A deformed Late Carboniferous ‘Pink’ granitoid (310 ± 8 Ma by Salam et al., 2007) is interpreted in the elongate units as oldest high magnetic anomaly. The central domain is interpreted as fold and thrust zone in tectonic model as boundary between Nakornthai oceanic plate and Indochina Terrane western which is represent of Loei Suture.

Based on the results shown in enhanced maps (Fig.4.13) it is quite likely that the areas with low magnetic signals are widely distributed in the eastern and western parts and usually exhibits magnetic relief of less than -50 nT. These areas correspond to tectonic basins filled by Permian deep bedded carbonate rocks of the Nam Duk Formation (Chutakositkanon et al., 1999) in the western domain whereas Permian shallow bedded-massive carbonate platform of Pha Nok Khao and Hua Na Kham

Formations (Charoentitirat, 2002) may have deposited in back arc environment of the eastern and northern domains (Fig.5.7). These domains are mainly occupied by Permo-Triassic volcanic-pyroclastic rocks (Chonglakmani et al. 2004). These areas are faulted as recognized both in the field and the geophysical interpretation maps (Figs 4.40, 4.41, 4.42 and 4.43).

Ring structures of the Phetchabun volcanic terrane are similar to those described in term of geophysical data as wide spread of volcanic rock with collapse structure in the caldera. Such a ring structure is almost similar to that of the Quaternary lava flows at the Yellowstone National Park in the U.S. which detected by Carol and Lisa (2002) (Fig. 5.2). It is considered explain that the ring structure of collapse caldera can be effected by hydrothermal system which can help to interpret related mineralization for further exploration. Ring units in the Phetchabun volcanic terrane show moderate magnetic intensity with ring pattern anomalies at their volcanic center of Permo-Triassic volcanic rocks (with the age of 250±6 Ma). Such volcanic rocks (Salam et al., 2007; and this study) are similar to those rocks described with Chonglakmani et al. (2004) report these volcanic rocks occurring in Permo-Triassic age stratigraphic evidence as for the Chatree volcanic. Moreover, in terms of petrochemical syntheses, Cumming et al. (2004), Nakchaiya et al. (2008), Marhotorn et al. (2008) and Boonsoong, et al. (2011) also considered that these rocks derived from calc-alkalic magma in the volcanic arc setting environment.

The results of this study can delineate subsurface existence and extent of granitoid intrusions. Large and higher amplitude anomalies (~10 km in diameter) of circular magnetic units in the eastern domain, particularly in the eastern1 sub-domain, supported by exposure of equigranular granitoids. The sequence of geophysical interpretation reveals that the granitoids of the circular unit may have occurred during Permo-Triassic time. These granitoids have been assigned by Kamvong et al. (2006) as

a volcanic arc setting and largely derived from I-type calc alkaline magma of adakitic origin.

The northern domain is covered by thick non-marine sedimentary rocks of the Khorat Group. As reported by Bhongsuwan et al. (2002), these rocks have some magnetization (1-550 SI). The residual high pass filtering map (Figs.4.17) shows the ring anomalies in the northern domain beneath sedimentary rocks of the Khorat Group that cause with is high magnetic intensity. The geophysical interpretation, the northern2 sub-domain shows higher magnetic intensities than northern1 sub-domain. On account of magnetic intensities and topographic reliefs, it is visualized that the rocks in northern2 sub-domain (or preliminary Khorat basin) were tectonically uplift and subsidence of the Permo-Triassic volcanic arc reach in the eastern domain during Triassic extensional stress. Subsequently, deposition of eroded source region of Permo-Triassic volcanic arc may have given rise to the clastic unit of the Huai Hin Lat Formation. Then the preliminary Khorat basin uplift higher than volcanic arc and in turn, sedimentary facies change to the non marine sediments of the Nam Phong Formation with oxidize environment during deposit case of uplifting to appear paleo sea level (Fig. 5.7).

The spots of small circular magnetic features (<5 km in diameter) in most of the Phetchabun volcanic terrane of study area are observed over the exposed porphyritic intrusive stocks, particularly along the subsided fault zone. Salam et al. (2007) has geochronologically reported the granodiorites of the Early to Late Triassic age (244 ±1 Ma and 213 ±10 Ma) whereas Boonsoong et al. (2011) has reported some of these intrusives derive from tholeiitic magma in volcanic arc type setting. These shallow porphyritic intrusive rocks correspond well with several of spot units during east-west extensional stress tectonic event. Both of our and previous geochronogical results are strongly conformable. Therefore these units may have occurred during collapse of arc volcanic structures and uplift of preliminaly Khorat basin.

Moreover, Tangwattananukul et al. (2008) reported that dike rocks in the Chatree mine can be grouped into 2 types: one in the north-south direction and the other in the northeast-southwest direction (see Fig. 5.3). The north-south dike rocks are occurred from tholeiitic and calc-alkaline magma origins for the northeast-southwest dikes and both of them are occurred in volcanic arc type setting. Salam et al. (2007) had reported ages of these dike rocks to be of the Early-Late Triassic (244±7, 238±6 and 221 ±5 Ma). These results confirm very well with that dike rocks occurred during post gold mineralization (Triassic) and correspond with the east-west extensional tectonic event in our geophysical interpretation. These Triassic extensional stress and associated tholeiitic intrusives of spot units and dike rocks may have caused partial melting in Nakornthai oceanic slab which may have subject to westward obduction (upthrusting) from Indochina Terrane or there exists much slower subduction giving rise to crust relax and the extension setting setting developed.

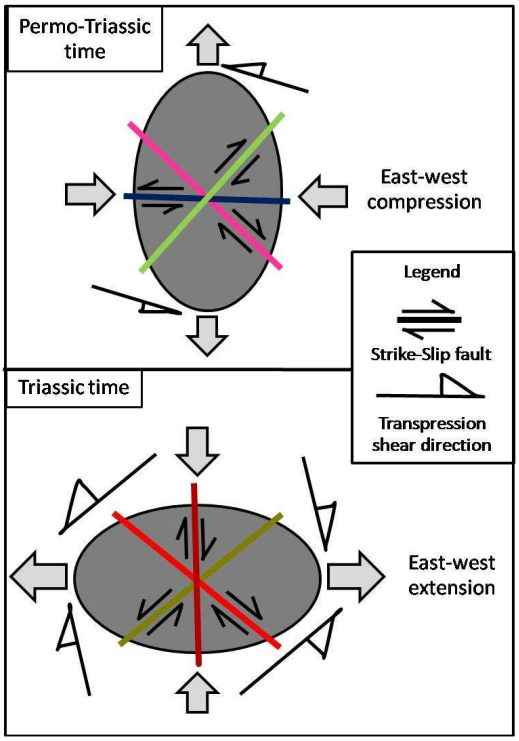

Figure 5.1. Strain ellipsoids showing the east-west compressional stress during the Permo-Triassic time and the east-west extensional stress during the Triassic time.

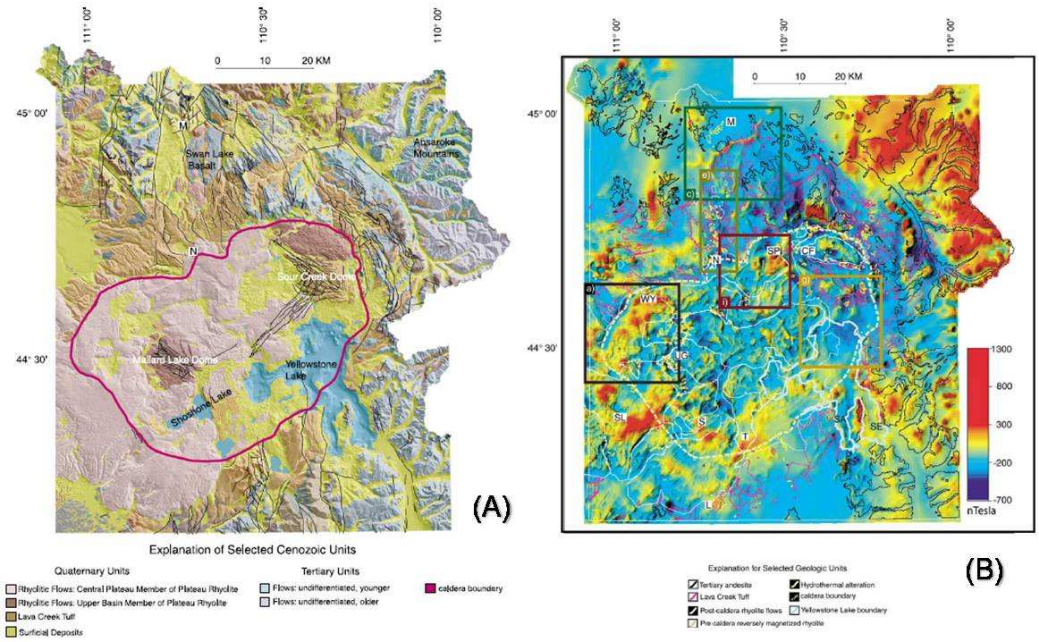

Figure 5.2. (A) Geologic map of Quaternary lava flows at Yellowstone National Park in U.S (Carol and Lisa, 2002) (B) high-resolution of reduction to the pole aeromagnetic data of Quaternary lava flows show ring structure which is related to collapse structure of caldera and effect of hydrothermal system (Carol and Lisa, 2002).

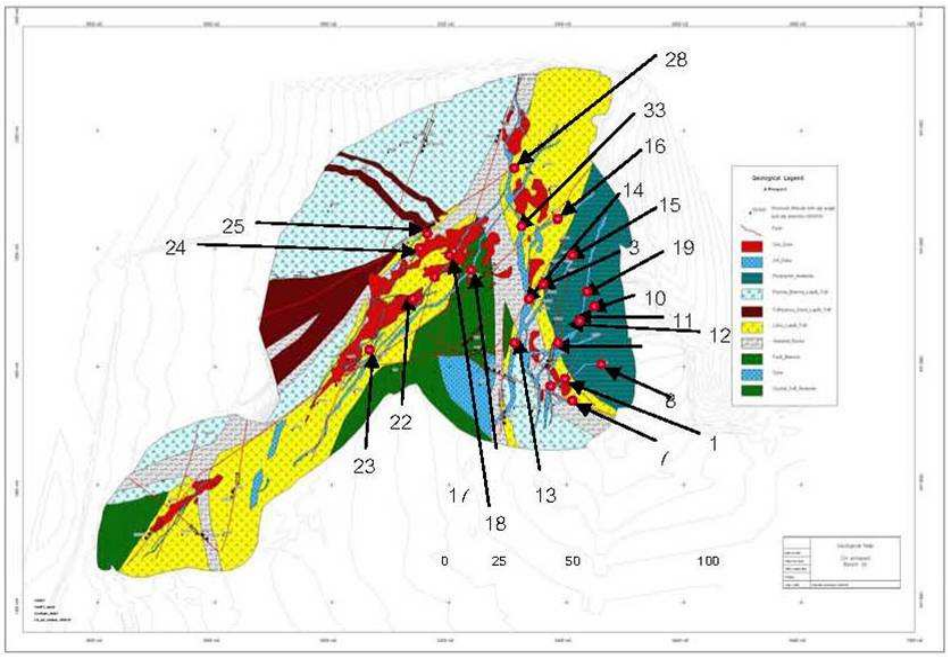

Figure 5.3. Geology of the C-H pit at Akara mine in the Loei-Phechabun Nakorn Nayok volcanic belt Thailand showing dike rocks trend in north-south and northeast-southwest (Tangwattananukul et al., 2008).

5.2 Geophysical structures related tectonic features

Magnetic anomalies display several trends defined by alignment of gradients and shapes of anomalies, and are best illustrated in Figs.4.2 and 4.6. The most essential lineaments are approximately in the northwest-southeast and northeast-southwest directions, followed by the east-west lineament, and the least dominant one is in a north-south direction.

The new processed airborne magnetic data show the long continuity of the northwest-southeast lineaments cross-cutting the high magnetic intensity of elongate amplitude anomalies with the roughly northwest-southeast direction of deformed intrusive bodies in the elongate unit. Based on study of Giulio (2008), the ductile and brittle deformational evolution of the Laxemar-Simpevarp area is interpreted by using magnetic field data. It is suggested that the structural brittle-ductile grains of the intrusive bodies are significantly controlled by large of the east-west trending shear zones which is similar to northwest-southeast shear zone of the elongate unit in Phetchabun volcanic terrane (see Figs. 4.23 and 5.4). Moreover, Sangsomphong et al. (2008) had reported a series of the elongated and relatively higher magnetic intensities trending in the northwest-southeast direction representing Sa Kaeo-Chanthaburi accretionary complex that indicated shear zone along the elongate magnetic feature (see Fig. 5.5). It is also suggested that the elongate shape in airborne magnetic feature similar to structural brittle-ductile of elongate unit in Phetchabun volcanic terrane (see Fig. 4.23). Such deformation structures are interpreted herein to under extensive ductile stress and may have situated deep in the crust. Brittle lineaments representing fault structure may have occurred at the shallower depth in the crust (see also Ramsay, 1980). Therefore, such lineaments are considered to be reverse faults in the central domain. The elongate units corresponding to the northwest-southeast reverse faults with sinistral slip component (Figs. 4.46 and 4.47) have steep dip (~60^{o} degree) in the northeast direction. It is inferred from this investigation that these northwest-southeast trending reverse faults in the central domain represent east-dipping subduction slab along the Loei Suture.

Based on geophysical interpretation, Phetchabun volcanic terrane is controlled by two major east-west paleo-stress patterns – one is the compressional stress during Permo-Triassic period in the western and other is the extensional stress during Triassic period in the eastern of Phetchabun volcanic terrane.

An attempt has been made to correlate the current result with those proposed by Tulyatid et al. (1999), Charusiri et al. (2002), Sangsomphong et al. (2008) and Sangsomphong et al. (2012). As shown in Fig. 4.30 that deformed intrusive bodies in the central domain are interpreted to represent correspond with the part of fold and thrust zone similar to the model of Loei suture (Neawsuparp et al. 2005). The western domain bounded to the west represents an oceanic trench which in turn belongs to the deep-water deposit of clastic rocks of the Nam Duk Formation. These domains have been subject to the east-west compressional stress in the subduction zone between western and central domains.

Three sub-domain of the eastern domain showing contrasting intensities can be related to the topographic relief of the magnetic rocks (as reported theoretically by Gunn et al., 1997). These sub-domains are bounded by normal faults of the northwest-southeast direction and associated with dextral slip movement (or called herein Noen Maprang Fault) from east-west extensional setting. These may have caused subsidence of Permo-Triassic volcanic arc and uplift of northern domain (or herein preliminary Khorat basin).

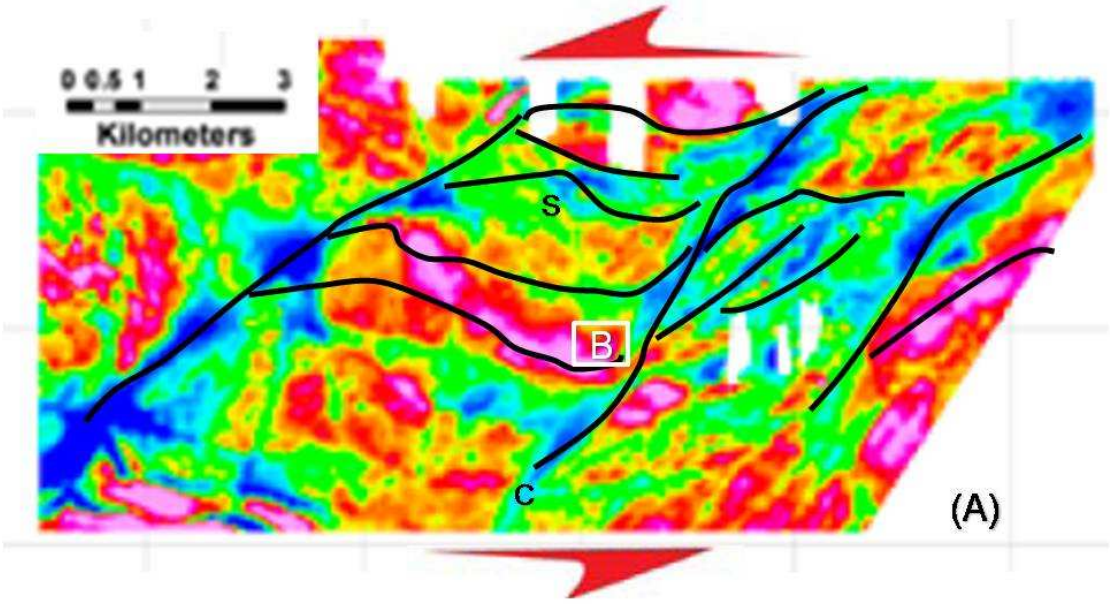

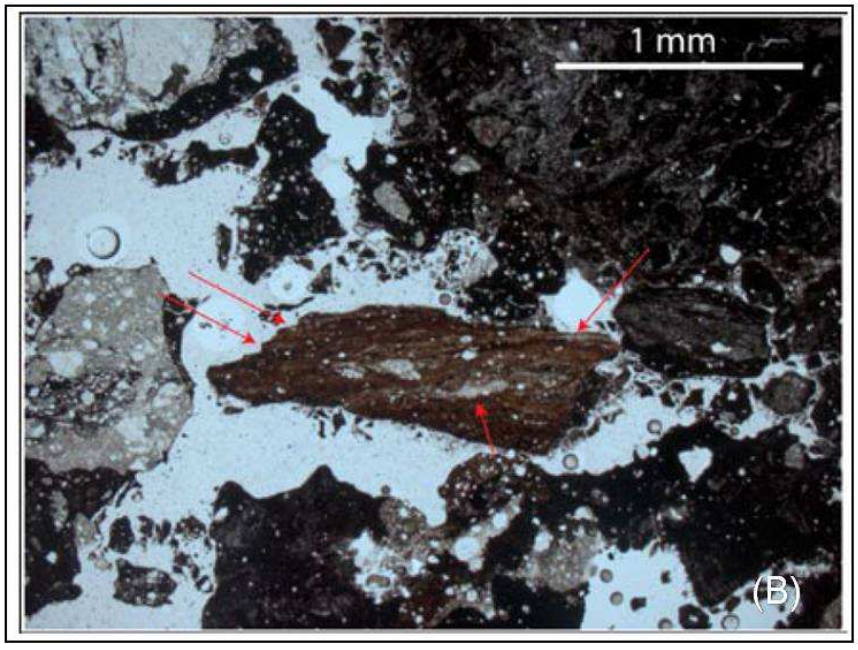

Figure 5.4. (A) Interpreted airborne magnetic results for the Laxemar-Simpevarp regional model showing relationships between the shear planes C and the pre-existing foliation planes S suggesting an overall sinistral sense of shear parallel to the foliation planes (inserted (B) box representing a figure of thin-section shown in (B)). (B) Clast of intrusive foliated cataclasite, red arrows indicate continuous foliation planes that can be followed within the clast. Plagioclase crystals are locally stretched along the foliation (Giulio, 2008).

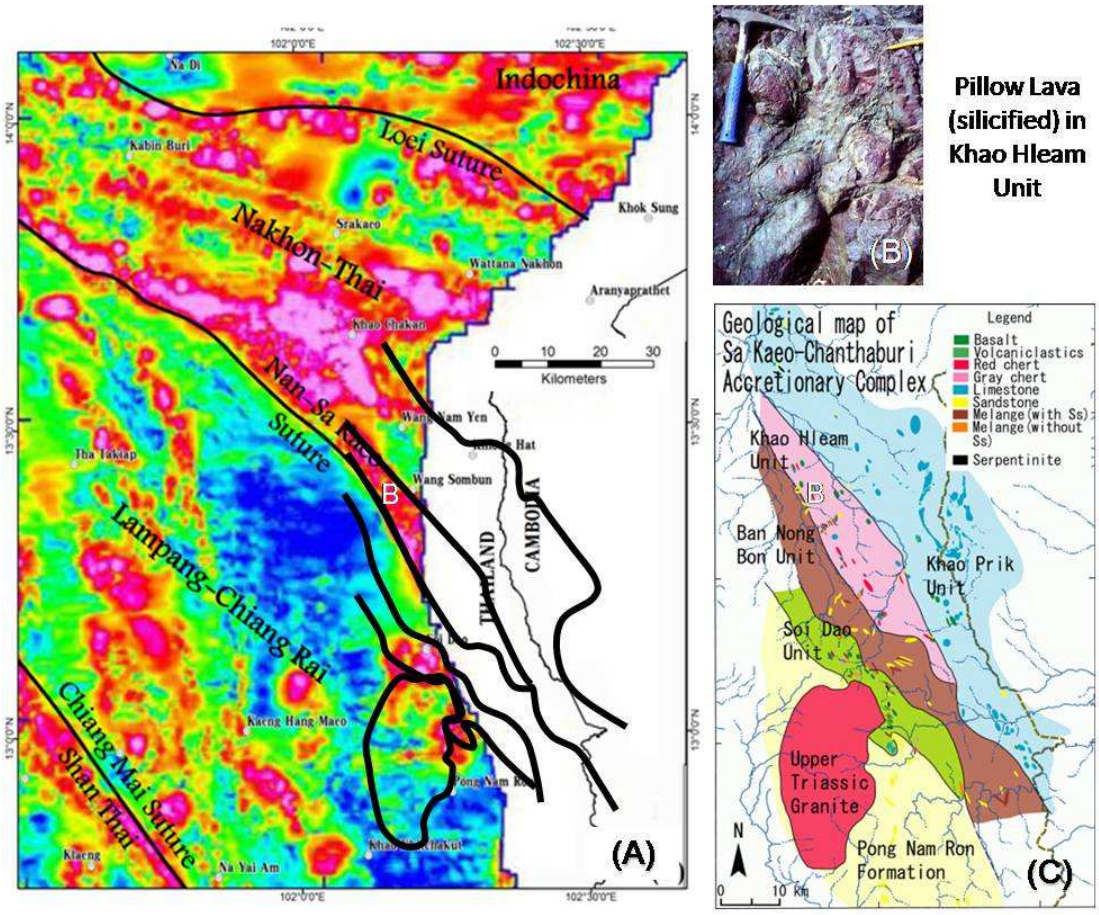

Figure 5.5. (A) A series of the elongated and relatively higher magnetic intensities trending in the northwest-southeast direction representing Sa Kaeo-Chanthaburi accretionary complex which is indicated deformation along the elongate unit (Sangsomphong et al., 2008). (B) and (C) An exposure and a geological map of the Sa Kaeo-Chanthaburi accretionary complex containing Pillow Lava (silicified) in Khao Hleam melange zone, eastern of Thailand (Chutakositkanon et al., 2003).

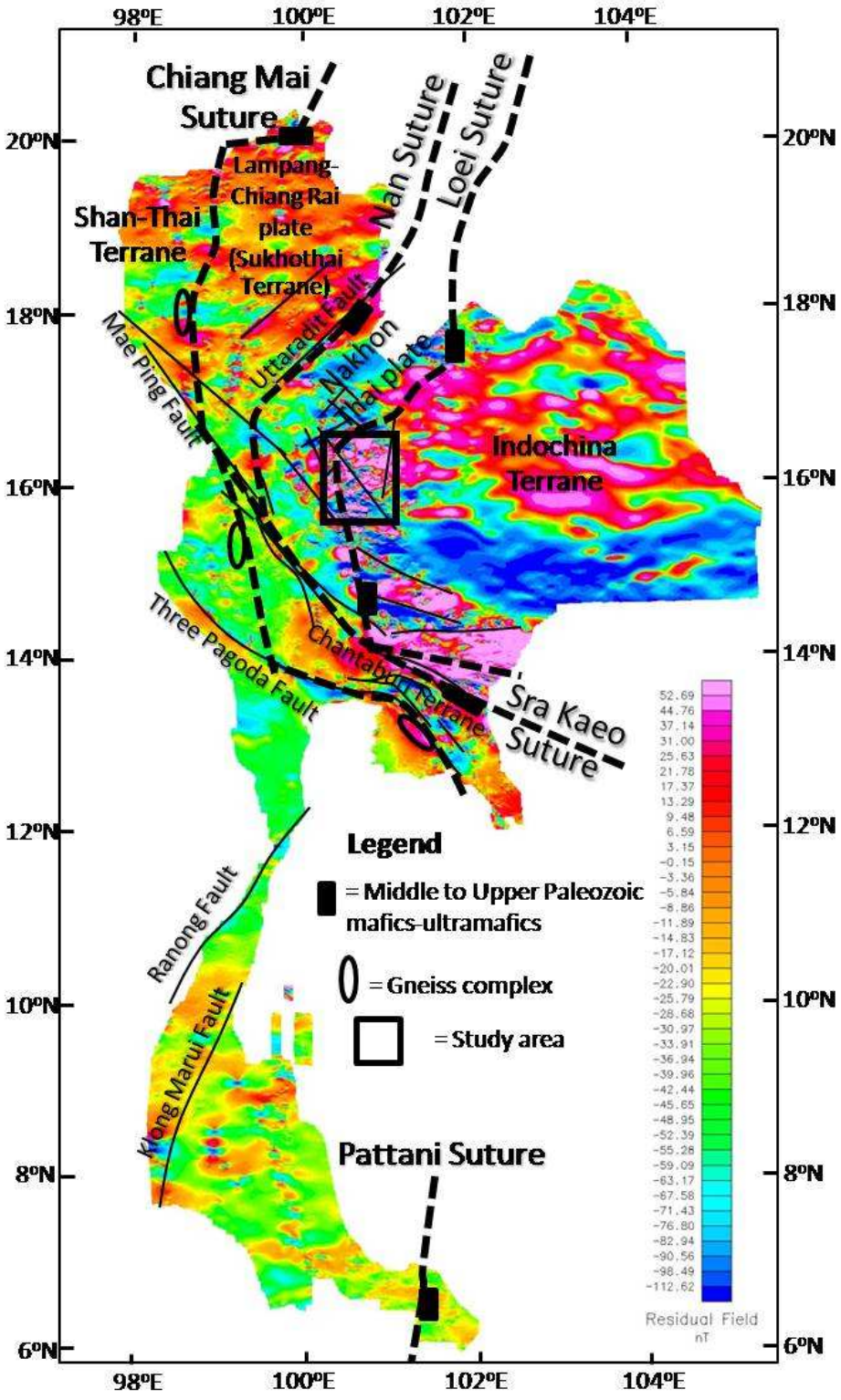

Figure 5.6. Residual magnetic map with the overlain tectonic lines in Thailand (based on data of Tulyatid et al., 1999, Charusiri et al., 2002, Sangsomphong et al., 2008 and Sangsomphong et al., 2012)

5.3 Tectonic evolution using geophysical interpretation

These current interpretations on airborne magnetic data together with field data strongly conform very well with the results on previous petrochemical, geochronological and geological analysis of the Phetchabun volcanic terrane represents volcanic arc setting in response to oceanic plate subduction beneath continental plate (Fig.5.7).

Previous relevant and current results lead to the interpretation that during the Permo-Carboniferous time, the Late Carboniferous intrusive igneous bodies (or the original elongate unit) in the central domain may have occurred as the volcanic arc with eastward subduction of the Nakhonthai oceanic plate beneath the western Indochina continental plate along the Loei Suture line. Then deep carbonate sediments may have filled in the trench zone in the western domain whereas shallow carbonate platform filled in Permian back arc environment or eastern and northern domains.

Subsequently, the eastward subduction has continued in the Permo-Triassic time, the intrusive bodies of elongate units in the central domain were subject to deformation and the elongate unit have been deformed and sheared with dipping to the northeast and ring units of the Permo-Triassic volcanic arc centers have developed in the eastern and northern domains. The circular units of equigranular intrusive bodies have been generated in the eastern domain.

Then during Triassic time, the study area was subject to east-west extensional setting (Fig.5.1) by subsidence of vocanic arc due to westward obduction (upthrusting) of Nakornthai oceanic slab (western domain) from Indochina Terrane or there exists much slower subduction giving rise to crust relax and the extension setting setting developed. Subsequently, or almost contemporaneously, the uplifting of the preliminary Khorat basin with generated shallow porphyritic intrusive bodies of the spot units associated with mineralization develop along the subsided area with structural controls (Fig.5.7).

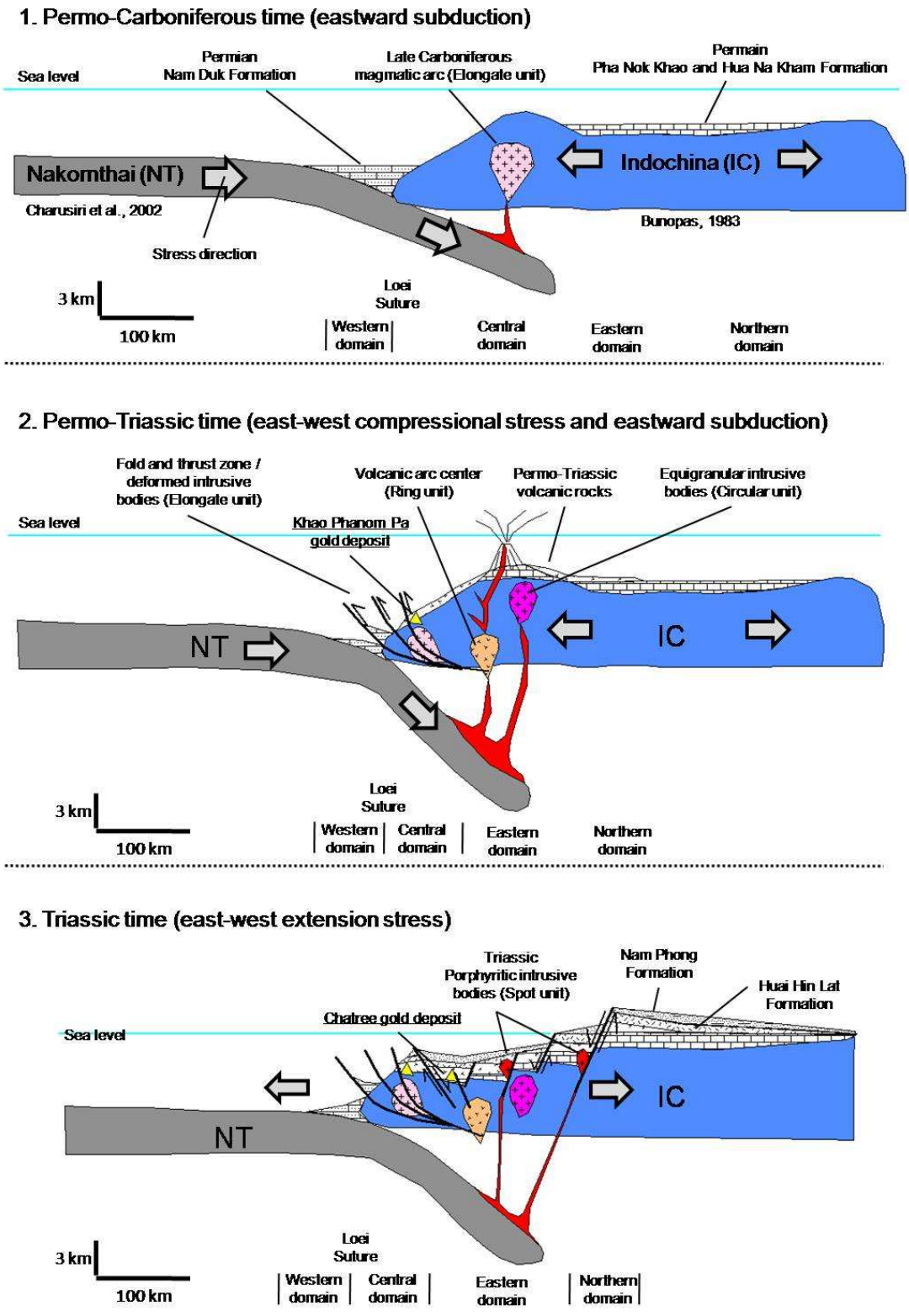

Figure 5.7. New implication 3 stages for tectonic evolution in the Phetchabun volcanic terrane during Carboniferous to Triassic Periods.

5.4 Structures associated with gold deposit

It is inferred that Khao Phanom Pa gold deposit fromed by ore-forming fluids of the gold deposit were derived from magmatic fluids at 350°C to 400ºC and 120 to 460 bars (Khositanont, 2008). This Khao Phanom Pa mesothermal gold veins are found around the center of Khao Phanom Pha in almost the east-west (northeasteast-southwestwest) trending, steep dipping (Visadsri, 2009) (See Fig. 5.8). Based on our geophysical interpretation, the Khao Phanom Pa occurred in the fold and thrust zone of the elongate unit and was cross-cut by major east-west fault through possible volcanic chamber of the Chatree ring unit. This has provided fluids of gold veins developed from the deep Chatree magmatic chamber.

Additionally, Chatree epithermal gold deposit forms within the intersection of the major north-south trending lineament and minor northeast-southwest lineament (see Fig. 5.9) both with sub-vertical dipping. Such structure features may have controlled the Au-Ag epithermal mineralization apart from the stratigraphic control (James et al., 2007). The Triassic east-west extensional tectonic setting in response to crustal relaxation (Charusiri et al., 2003) has caused uplift of the (preliminary) Khorat basin and subsidence of Permo-Triassic volcanic arc along Loei Suture zone. The Chatree epithermal gold deposit can be well-preserved in the northwest-southeast Triassic basin.

5.5 Suggestion for Future Exploration

The current results advocate that the magnetic anomalies and structures can be used for the follow-up detailed exploration. Based on geophysical interpretation, the ring magnetic anomalies interpreted as remnants of volcanic chamber and are possibly source rock of epithermal gold veins. In order to ring target, a litho-geochemical sampling should be done along with the extensive ore assays for gold and silver in such ring anomalous magnetic pattern. As shown in the Fig. 4.17 patterns of ring unit in the

Chatree deposit can be applied as a study for the main target of exploration. The other interesting areas are 1 northwest of Chatree mine, 2 east of Khok Charoeng sub-province in the eastern3 sub-domain, and 3 between east of Chatree mine and Phetchabun province in the eastern1 sub-domain. These targets of epithermal gold deposit along the Loei fold belt possibly have well-preserved in the northwest-southeast Triassic basins. These basins particularly, eastern3 sub-domain (Fig.4.13) on reduction to the pole map showing lower magnetic intensity than Chatree basin to the south which may have deeper basins causing subsidence of volcanic arc. So, the future gold exploration for the epithermal gold may have more expensive cost to drill deeper than Chatree mine and done by underground mining.

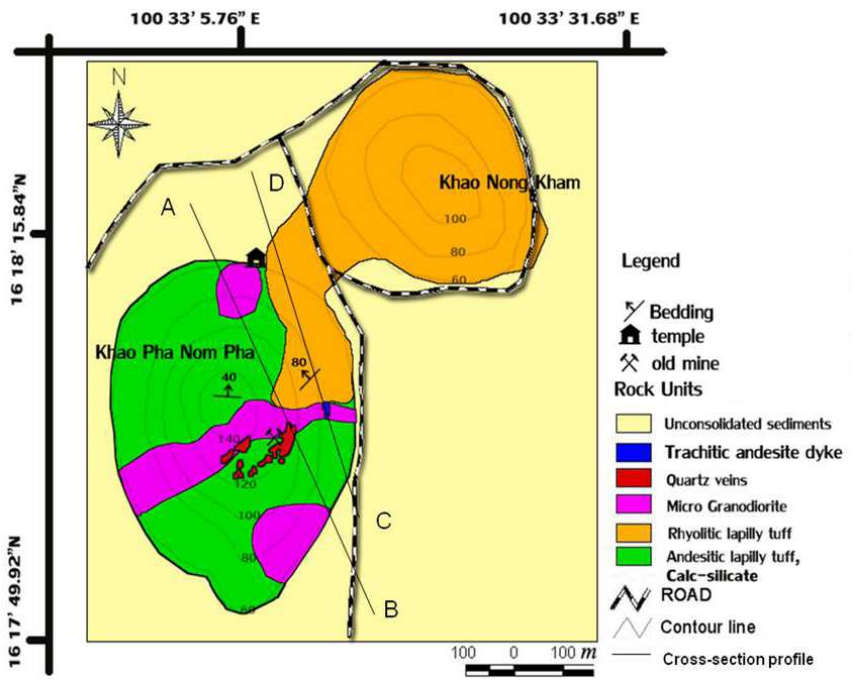

Figure 5.8. Detail geologic map of Khao Phanom Pa gold mine showing quartz gold veins oriented in almost east-west (eastnortheast-westsouthwest) direction (Visadsri, 2009).

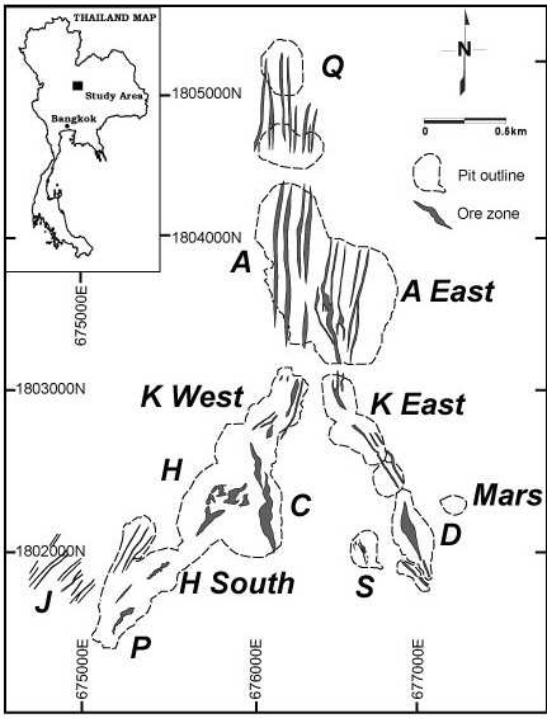

Figure 5.9. Map of Chatree mine showing the position of open cut Pits and prospects gold deposit. The vein zones trend in major north-south and minor northeast-southwest conforming to regional structural trends (James et al., 2007).

CHAPTER VI

Conclusion

1. Based on the geophysical interpretation, the Phetchabun volcanic terrane is divided into four magnetic domains; western, central, eastern and northern domains. The eastern and northern domains are further divided into as eastern1, eastern2, eastern3 northern1, northern2 and northern3 sub-domains. Magnetic anomalies are divided into 4 units based on magnetic feature; elongate, ring, circular and spot units.
2. Based on residual high pass filtering enhancement, Permo-Triassic volcanic centers are represented by ring units in northwest-southeast trend in eastern and northern domains.
3. Phetchabun volcanic terrane can be sub-divided into 3 kinds of intrusive bodies based on geophysical and field data: (1) deformed elongate units of intrusive in central domain, (2) circular units of equigranular intrusive in eastern domain and (3) spot units of porphyritic intrusive dominant along subsidence fault zones.
4. Three stages of tectonic evolution are newly proposed for the Phetchabun Volcanic Belt:

   -Permo-Carboniferous tectonic stage event, the Nakhonthai oceanic plate subject to eastward subduction beneath the Indochina continental plate by generate magmatic bodies of elongate units in volcanic arc which may have formed in Late Carboniferous time. Deep marine deposition of Nam Duk Formation may have taken place in the trench zone and shallow marine carbonate platform of Pha Nok Khao and Hua Na Kham Formations may have been deposited in back-arc basin.

   - Permo-Triassic tectonic stage is represented by the east-west compressive stress, and this may have caused deformation of the elongate unit with northeast dipping and suggesting the eastward subduction of the Nakhonthai oceanic plate beneath the Indochina continental plate. Ring units of paleo-volcanic centers and circular units of equigranular intrusive bodies may have occurred in the volcanic arc of this stage.

- Triassic tectonic stage is dominated by east-west extensional stress which in turn caused uplifting of the preliminary Khorat basin and subsidence of the Phetchabun volcanic arc. The spot units of porphyritic intrusive bodies may have occurred along the depressed basement.

References

Ali, A., Eric, C.F. and Zafer A. 2007. The magnetic susceptibility of granitic rocks as a proxy for geochemical composition: Example from the Saruhan granitoids, NE Turkey. Journal of ScienceDirect Tectonophysics 441: 85–95.

Barr, S. M., Tantisukrit, C., Yaowanoiyothin, W. and Macdonald, A. S. 1990. Petrology and tectonic implications of Upper Paleozoic voleanic rocks of the Chiang Mai Belt, northern Thailand. Journal of Southeast Asian Earth Science 4:37-47.

Bhongsuwan, T. and Ponathong P. 2002. Magnetic Characterization of the Thung-Yai Redbed of Nakhon Si Thammarat Province, Southern Thailand, and Magnetic Relationship with the Khorat Redbed. Journal of ScienceAsia 28: 277-290.

Boonsoong, A., Panjasawatwong, Y. and Metparsopsan, K., 2011. Petrochemistry and tectonic setting of mafic volcanic rocks in the Chon Daen–Wang Pong area, Phetchabun, Thailand. Journal of Island Arc 20: 107–124.

Braun, E. V. and Hahn, L. 1976. Geological map of northern Thailand 1:250,000 Sheet 2 (Chiangrai). Federal Institule of Geosciences and Natural Resource, Thailand. Hanover.

Bunopas, S. 1981. Paleogeographic History of Westory of Western Thailand and Adjacent Parts of Southeast Asia. A Plate Tectonics Interpretation. Geol. Surv. Paper, Department Mineral Resources, Bangkok 5: 810.

Bunopas, S. and Vella, P. 1983. Tectonic and geologic evolution of Thailand. Workshop Stratigraphic Correlation Thailand-Malaysia, Had Yai, Thailand: 307-322

Bunopas, S., and Vella, P. (1992). Geotectonics and geologic evolution of Thailand. National Conference on Geologic Resources of Thailand: Potential for Future Development, Bangkok, Thailand: 209-228.

Carol A.F. and Lisa A. M. 2002. High-resolution aeromagnetic mapping of volcanic terrain, Yellowstone National Park. Journal of Volcanology and Geothermal Research, 115, 207-231.

Chairangsee, C., Ginze, C., Macharoensap, S., Nakornsri, N., Silpalit, M. and Sinpool-Anunt, S. 1990. Geolgical map of Thailand 1:50,000. Exploration for sheet Amphoe

Pak Chom 5345 I Ban Na Kho 5344 I, Ban Huai Khop 5445 III, King Amphoe Nam Som 5444 V., Thailand. Hanover Report: 1-109.

Chappell, B.W. and White, A.J.R. 1974. Two contrasting Granite types. Pacific Geology 8: 173-174.

Chareonpravat, A., Sripongpan, P., Thammadusadee, V. and Wolfrat, R. 1987. Geology of Amphoe Sop Prap and Amphoe Wang Chin, Thailand. Hanover Report (Unpublished Manuscript): 1-52.

Charoentitirat, T. 2002. Permian fusulinodean biostratigraphy and carbonate development in the Indochina Block of Thailand with their paleogeographic implication. Doctoral Thesis, University of Tsukuba, Japan.

Charusiri, P. 1989. Lithophile Metallogenetic Eepochs of Thailand: a Geological and Geochronological investigation. Doctoral dissertation, Department of Geology Queen's University, Kingston, Canada.

Charusiri, P., Arunsrisangchai, W., Nunsamai, S., Deesawat, W., 2003. Knowledge on Gold: Epithermal Au Deposits and their Exploration. Journal of Scientific Research, Chulalongkorn University 1: 2.

Charusiri, P., Pongsapich, P., Daorerk W. and Khantaprab, C. 1991. Granitoid belts in Thailand: New evidence from 40Ar/ 39Ar and K-Ar Geochronology and isotopic investigation. J. Sci. Res. Chulalongkorn University: 1-16.

Charusiri, P., Clark, A.H., Farrar, E., Archibald, D. and Charusiri, B. 1993. Granite belts in Thailand: evidence from the 40Ar/ 39Ar geochronological and geological synthesis. Journal of Southeast Asian Earth Science 8: 127-136.

Charusiri, P., Daorerk, V., Archibald, D., Hisada. K. and Ampaiwan. T. 2002. Geotectonic Evolution of Thailand. A new Synthesis. Journal of the Geological Society of Thailand 1: 1-20.

Charusiri, P., Sutthirat, C., Plathong, C. and Pongsapich. W. 2004. Geology and Petrochemistry of Basaltic Rocks at Khao Kradong, Burirum, NE Thailand. Implications for Rock Wool Potentials and Tectonic Setting. J. Sci. Res. Chula. Univ. (29 May) 2: 83-103.

Chongrakmani, C. and Sattayarak., N. 2004. Geological map of Changwat Phetchabun Thailand 1:250000. Department of Mineral Resources Report, Bangkok, Thailand.

Chuaviroj, S., Chaturongkawanich, S. and Sukawattananan, P. 1980. Geology of geothermal resources of northern Thailand Part I, San Kamphaeng. Department of Mineral Resources Report, Thailand. (Unpublished Manuscript): 20-31.

Chutakositkanon, V., Hisada, K., Charusiri, P. Arai, S. and Charoentitirat, T. 1999. Characteristics of detrital chromian spinels from the Nam Duk Formation: Implication for the occurrence of mysterious ultramafic and volcanic rocks in central Thailand. In C. Khantaprab and others (eds.), Proceedings of the symposium on mineral, energy, and water resources of Thailand: Towards the year 2000, Bangkok, Thailand: 604-606.

Chutakositkanon, V., Hisada, K., Charusiri, P. and Arai S. 2003. Detrital chromian spinels from the Sra Kaeo-Chanthaburi accretionary complex, traces of tectonic evolution of eastern Thailand: In 2003 Japan Earth and Planetary Science Joint Meeting Organization, Chiba, Japan G015-011: 26-29.

Cobbing, E. J., Mallicj, D. I. J., Pitfield. P. E. J. and Teoh, L. H. 1986. The granites of the SE Asian Tin Belt. J. Geol. Soc. London 143: 537-550.

Colin R., 2005. Aeromagnetic anomalies over parts of South Africa, Botswana and Zimbabwe, courtesy of the African Magnetic Mapping Project. Aeromagnetic Surveys, Principles, Practice and Interpretation, published by GEOSOFT.COM: 1-155.

Corbett, G. 2004. Comments on controls to gold mineralization at gold prospects in the vincity of the charee gold mine, Thailand. Australia, Corbett Geological Services Report. (Unpublished Manuscript): 2-23.

Crossing, J. 2004. Geology of the Chatree region Thailand. Compass Geological Australia. Australia. 24 Walpole Street, St James, WA 6102. (Unpublished Manuscript): 3

Deesawat, W. 2002. Preliminary Investigation on Hydrothermal Alteration of the Chatree Gold Deposit, Wangpong Area, Petcgabun. Bechelor's Senior Project. Department of Geology. Faculty of Science. Chulalongkorn University.

Diemar M.G., Diemar V.A. and Udompornwirat S. 2000. The Chatree Epithermal Gold-Silver Deposit, Phichit-Petchabun Provinces, Thailand. In Symposiam on Mineral,

Energy, and Water Resource of Thailand, Bangkok, Thailand (October 28-29, 2000): 423-427

Department of Mineral Resources. 1999. Geology of Thailand, Department of Mineral Resources. Thailand. Thailand. Department of Mineral Resource Report (Unpublished Manuscript).

Garwin, S.L. 1993. The Gold Potential of the Loei-Prachinburi Mineralized Belt, Northeastern Thailand. Newmont (Thailand) Limited. (Unpublished Manuscript): 56-70.

Geosoft Inc. 2005. Montaj MAGMAP Filtering tutorial manual, 2-D frequency domain processing of potential field data extension for Oasis montaj v6.1, www.geosoft.com: 1-66.

German Geological Mission. 1972. Final report of the Geman Geological mission to Thailand 1965-1971. Bundesanstalt fur Bodenforschung. Hanover. (Unpublished Manuscript): 1-94.

Giulio ,V., 2008. Ductile and brittle structural evolution of the Laxemar-Simpevarp area: an independent analysis based on local and regional constraints. Geological Survey report of Norway: 1-87.

Gunn, P.J. 1997a. Quantitative methods for interpreting aeromagnetic data. JGSO Journal of Australian Geology and Geophysics 17 2: 105-114.

Gunn, P.J.,1997b, Regional magnetic and gravity responses of extensional sedimentary, JGSO Journal of Australian Geology and Geophysics 17 2: 115-132.

Gunn, P.J. and Almod, R. 1997. A method for calculating equivalent layers corresponding to large aeromagnetic and radiometric grids. Exploration Geophysics (in press).

Gunn, P.J., Maidment, D. and Milligan, P.R., 1997. Interpreting aeromagnetic data in areas of limited outcrop. AGSO Journal of Australian Geology and Geophysics, 17 2: 175-185.

Hutchison, C. S. 1978. Southeast Asian Tin Granitoids of Contrasting tectonic setting. J. Phys. Earth Tokyo 26: 221-232.

Hutchison, C. S. 1983. Multiple Mesozoic Sn-W-Sb granitoids of Southeast Asia. Circum-Pacific Plutonic Terranes. Geol. Soc. American. Memoir 159: 35-60.

Intasopa, S. and Dunn, T. 1994. Petrology and Syn-Nd isotropic systems of the basalts and rhyolites, Loei, Thailand. Journal of Southeast Earth Sciences 9: 167-180.

Intasopa, S. 1993. Petrology and Geochronology of the Volcanic Rocks of the Central Thailand Volcanic Belt. Doctoral Dissertation, Department of Geology, Faculty of Science, University of New Brunswick.

Ishihara, S. 1981. The granitoid series and mineralization. Econ. Geol., 75th Anniversary Volume: 458-484.

Ishihara, S. 1977. The magnetite-series and ilmenite-series granite rocks. Mining Geol. 27: 293-305.

Ishihara, S., Robb, L.J., Anhaeusser, C.R. and Imai A. 2002. Granitoid Series in Terms of Magnetic Susceptibility: A Case Study from the Barberton Region, South Africa. 2002 International Association for Gondwana Research, Japan 5: 3: 581-589.

Jacobson, H.S., Pierson, C.T., Danusawad, T., Japakasetr, T., Inthaputi, B., Siriratanamongkol, C., Prapassornkul, S. and Pholphan, N. 1969. Mineral Investigations in Northeastern Thailand. Geological Survey Professional. Washington United States Government Printing Office: 618.

James, R. and Cumming, G.V. 2007. Geology and mineralization of the Chatree epithermal Au-Ag deposit, Phetchabun province, central Thailand. GEOTHAI'07 International conference on geology of Thailand: Towards sustainable development and sufficiency economy: 380.

Jungyusuk, N. and Sinsakul, S. 1989. Geology of Ban Na Chaliany, Amphoe Nong Phai and Amphoe Wichianburi. Geological Survey Report 127: 51-60.

Jungyusuk, N. and Khositanont, S. 1992. Volcanic rocks and associated mineralization in Thailand. Conference on Geologic Resources of Thailand. Department of Mineral Resource, Bangkok, Thailand, (1992): 528-532.

Kenting Earth Sciences International Limited KESIL. 1989. Follow-up Survey Report for Airborne Geophysical survey of the Mineral Resources Development Project. Report for Airborne Geophysical survey Thailand. Ottawa, Canada.

Khantaparb and colleagues, 1990. Geological assessment on the potential of rare-earth-bearing mineral resources in Thailand. Bangkok Office of the National Research Council Report (Unpublished Manuscript): 1-71.

Khositanont, S. 2008. Gold and iron-gold minerlization in the Sukhothai and Loei-Phetchabun fold belts. Ph. D. thesis, Department of Geology, Faculty of Science, Chiang Mai University: 146.

Kromkham, K. and Zaw, K. 2005. Geological Setting, Mineralogy and Alteration of the H Zone, the Chatree Deposit, central Thailand, In Proceeding of the International Conference on Geology, Geothecnology and Mineral Resource of Indochailand, Khon Kaen, Thailand, (November 28-30, 2005): 319-323.

Macleod, I.N., Jones, K., and Ting F. D. 1993. 3-D analytic signal in the interpretation of total magnetic field data at low magnetic latitude. Journal of Exploration Geophysics 24: 679-688.

Mahawat, C., 1982. The Petrology and Geochemistry of the Granitic Rocks of the Tak Bathlith, Thailand. Doctoral dissertation. Department of Geology, University of London.

Marhotorn, K., Mizuta, T., Ishiyama, D., Takashima, I., Won-in, K., Nuanlaong, S. and Charusiri, P. 2008. Petrochemistry of Igneous rocks in the Southern Parts of the Chatree Gold Mine, Pichit, and Central Thailand: Implication for Tectonic Setting. Proceedings of the International Symposia on Geoscience Resources and Environments of Asian Terranes (GREAT 2008), 4th IGCP 516,and 5th APSEG. Bangkok, Thailand (November 24-26, 2008): 289-298.

Milligan, P.R. and Gunn, P.J. 1997. Enhancement and presentation of airborne geophysical data. JGSO Journal of Australian Geology and Geophysics 172 : 63-76.

Mitchell, A. H. G. 1977. Tectonic setting for emplacement of SE Asia tin granodiorite. Bull. Geol. Soc. Malaysia Bull. 9: 123-140.

Naidu, P.S., and Mathew, M.P. 1998. Digital analysis of aeromagnetic map: detection of fault. Journal of Applied Geophysics 38:169-179.

Nakapadungrat, S. Beckensale, R. D. and Suensilpong. S. 1984. Geochronology and geology of Thai granites. Proc. Conf. on Application of Geology and National Development. Chulalongkorn University, Bangkok, Thailand (November, 1984): 75-93.

Nakapadungrat, S. 1982. Geochronlogy and Geochemistry of the Thong-Lang Granite Complex, Central Thailand. Doctoral dissertation. Department of Geology, University of London.

Nakchaiya, T., Mitzuta, T., Ishiyama, D., Takashima, I., Won-In, K., Lunwongsa, V. and Charusiri, P. 2008. Stratigraphy and Petrochemistry of Volcanic Rocks in the Chatree Gold Mine, Central Thailand: Implication for Tectonic Setting. Proceedings of the International Symposia on Geoscience Resources and Environments of Asian Terranes (GREAT 2008), 4th IGCP 516 and 5th APSEG. Bangkok, Thailand (November 24-26, 2008): 302-311.

Nantasin, P. 2005. Petrography and geochemistry of intrusive rocks at Ban Pho-Sawan area, Amphoe Bung Samphan, Changwat Phetchabun, In Proceeding of the International Conference on Geology, Geothecnology and Mineral Resource of Indochailand, Khon Kaen, Thailand (November 28-30, 2005): 374-385.

Neawsuparp, K., Charusiri, P. and Meyersb, J., 2005. New Processing of Airborne Magnetic and Electromagnetic Data and Interpretation for Subsurface Structures in the Loei Area, Northeastern Thailand. Journal of ScienceAsia (2005) 31: 283-298.

Panjasawatwong, Y. 1993. Petrology, geochemistry and tectonic implications of igneous rocks in the Nan Suture, Thailand and an H2O on plagioclase-melt equilibria at 5-10 kb pressure. Doctoral dissertation. Department of Geology, University of Tasmania.

Panjasawatwong, Y., Kanpeng, K. and Ruangvatanasirikul, K. 1995. Basalts in Li basin, northern Thailand. In Proceedings of the International Conference on Geology, Geotechnology and Mineral Resources of Indochina, Khon Kaen University, Khon Kaen, Thailand (1995): 225-234.

Phajuy, B., Panjasawatwong, Y. and Osataporn, P. 2004. Preliminary geochemical study of volcanic rocks in the Pang Mayao area, Phrao. Chiang Mai, northern Thailand: tectonic of formation. Journal of Asian Earth Science 24:767-776.

Pilkington, M., Miles, W.F., Ross, G.M., and Roest, W.R. 2000. Potential Field signatures of buried Precambrian basement in the Western Canada Sedimentary Basin. Canadian Journal of Earth Science 37:1453-1471.

Piyasin, S. 1972. Geology of Lampang sheet (NE 41-11), scale 1:250,000, Department of Mineral Resources, Bangkok, Thailand, Report of investigation 14: 1-98.

Piyasin, S. 1975. Gelogy of Changwat Uttaradit (NE 47-11) Qyadrabgkem Scale 1:250,000, Department of Mineral Resources, Bangkok, Thailand. Report of Investigation 16:1-68.

Pongsapich, W., Pisutha-Arnond, V. and Charusiri, P. 1983. Reviews of felsic plutonic rocks of Thailand. Proc. Of the workshop on Stratigraphic Correlation of Thailand and Malasia, Hadyai, Thailand, (September, 1983): 213-232.

Ramsay, J. G. 1980. The crack-seal mechanism of rock deformation. Nature, London 284: 125-139.

Roest. W.R., Verhoef, V., and Pilkington, M. 1992. Magnetic interpretation using the 3-D analytic signal, Journal of Geophysics 57:116-125.

Rybokov, M., Goldshmidt, V., Pleisher, L., and Ben-Gai, V. 2000. 3-D gravity and magnetic interpretation for the Haita Bay area (Israel). Journal of Applied Geophysics 44: 353-367.

Salam A., Zaw, K., Meffre, S., James, R. and Stein, H. 2007. Geological setting, alteration, mineralization and geochronology of Chatree epithermal gold silver deposit, Phetchabun Province, central Thailand. Ores and Orogenesis Symposium at Tucson, Arizona, (24-30 Sep. 2007): 181.

Sakiyama, T. 2005. Magnetic Susceptibility of Igneous rocks from Western Kinki to Eastern Chugoku Districts, Southwest Japan. Jounal of Humans and Nature of Japan 15: 9-28.

Sangsiri, P. and Pisutha-Arnond, V. 2008. Host Rock Alteration at the A Prospect of the Chatree Gold Deposits, Phichit Province, Central Thailand: A Preliminary Re-Evaluation. Proceedings of the International Symposia on Geoscience Resources and Environments of Asian Terranes (GREAT 2008), 4th IGCP 516,and 5th APSEG; Bangkok, Thailand, (November 24-26, 2008): 258-261.

Sangsomphong, A., Tulyatid, D., Thimakorn, T. and Charusiri, P., 2008. Tectonic feature of eastern Thailand using enhanced airborne geophysical data. In Proceeding of the Geosciences, Resources and Environments of Asian Terranes (GREAT2008), Bangkok, Thailand (Extended abstract): 67-70.

Sangsomphong, A., Thimakorn, T. and Charusiri, P., 2012. Analysis and modeling of airborne geophysical data in the Phetchabun volcanic terrane, Northern part of

central Thailand. International Conference on Tectonics of northwestern Indochina (TNI2012), Chiangmai, Thailand (22-24 Feb. 2012) (Extended abstract): 28-29.

Sitthithaworn, E., 1992. Metalllogenic map of Thailand. National conference on Geologic Resource of Thailand. Potential for future Development, Department of Mineral Resources, Bangkok, Thailand (17-24 November, 1992): 1-14.

Sitthithaworn, E. and Tiyapairach, S.1982. Report of magnetic anomaly investigation, Tambon Ban Na, Amphoe Ban Na, Changwat Nakhon Nayok. Ferro-alloy mineral exploration project. Bangkok. Thailand, Department of Mineral Resource. (Unpublished Manuscript)

Sitthithaworn, E., 1989. Gold mineralization at Phu Lan Cu- Fe skarn prospect in northern Thailand. Master's Thesis. Department of Geology, University of Western Ontario.

Sutthirat, C., Saminpanya, S., Droop, G. T. R., Henderson, C. M. B. and Manning, D. A. C. 2001 Clinopyroxene-corundum assemblages from alkali basalt and alluvium, eastern Thailand: constraints on the origin of Thai rubies. Mineralogical Society of Great Britain and Ireland. Mineralogical Magazine (April) 2 65: 277-295.

Tangwattananukul, L., Lunwongsa, W., Mitsuta, T., Ishiyama, H., Takashima I., Won-In, K., and Charusiri, P. 2008. Geology and Petrochemistry of Dike Rocks in the Chatree Gold Mine, Central Thailand: Implication for Tectonic Setting. Proceedings of the International Symposia on Geoscience Resources and Environments of Asian Terranes (GREAT 2008), 4th IGCP 516,and 5th APSEG, Bangkok, Thailand (November 24-26, 2008): 299-301.

Teggin, D. E. 1975. The Granites of Northern Thailand. Doctoral dissertation. Department of Geology, University of Manchester.

Tulyatid, J., and Charusiri, P., 1999. The ancient Tethys in Thailand as indicated by nationwide airborne geophysical data, Proceedings of International Symposium on Shallow Tethys (ST) 5, Chiang Mai, Thailand: 380-388.

Visadsri, P. 2009. Geology and petrography of Khao Pha-Nom-Pa, Wang Saiphun, Phichit, Thailand. B.Sc. senior project, Department of Geology, Faculty of Science, Chulalongkorn University: 181.

Appendices

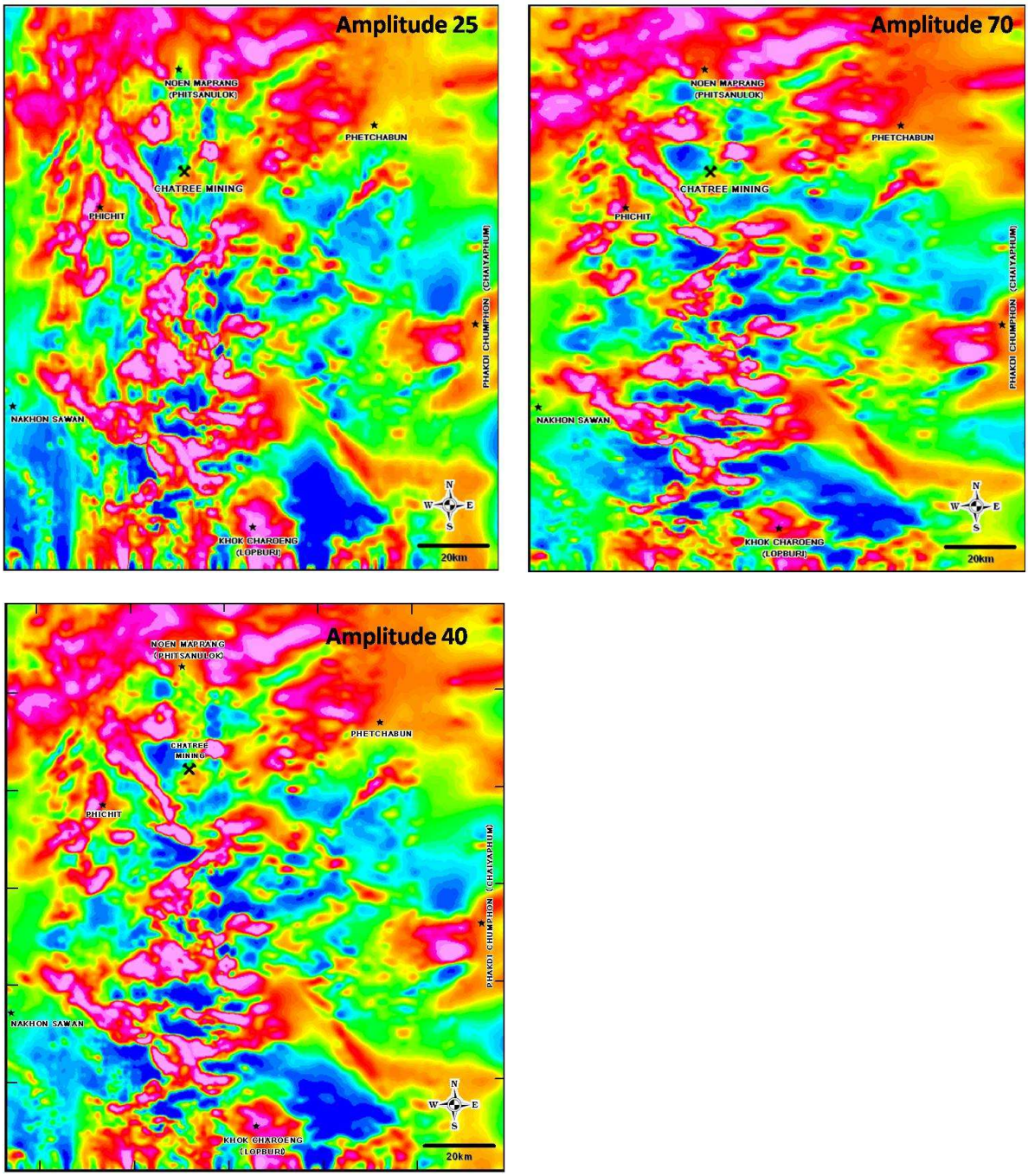

I. Experiment 40 degree amplitude for RTP enhance method can correct of north-south stretching, predominant negative response, east-west stretching problems.

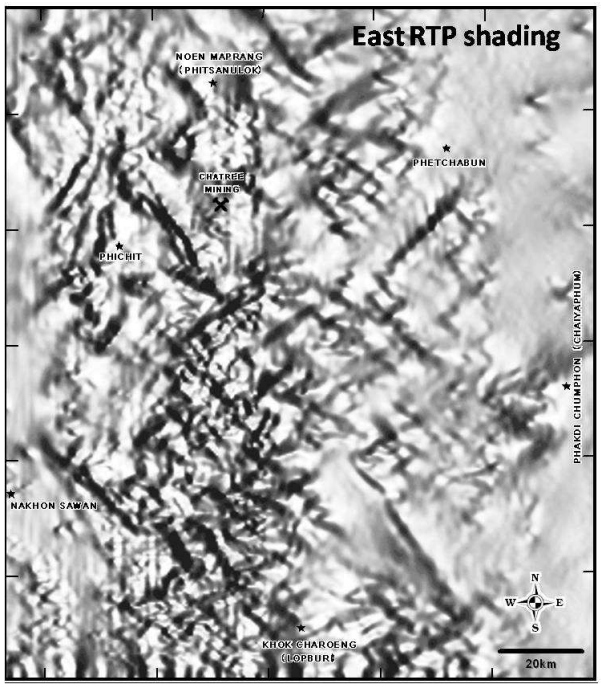

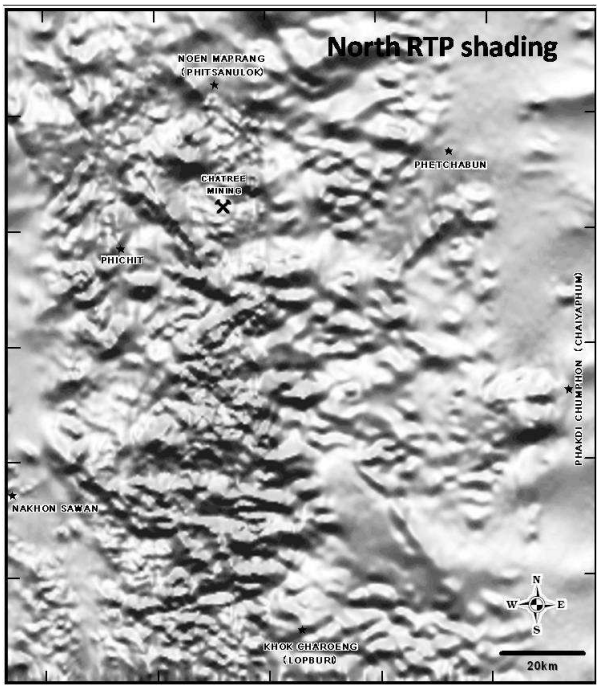

II. North-shaded relief method can correct of predominant north-south stretching problems.

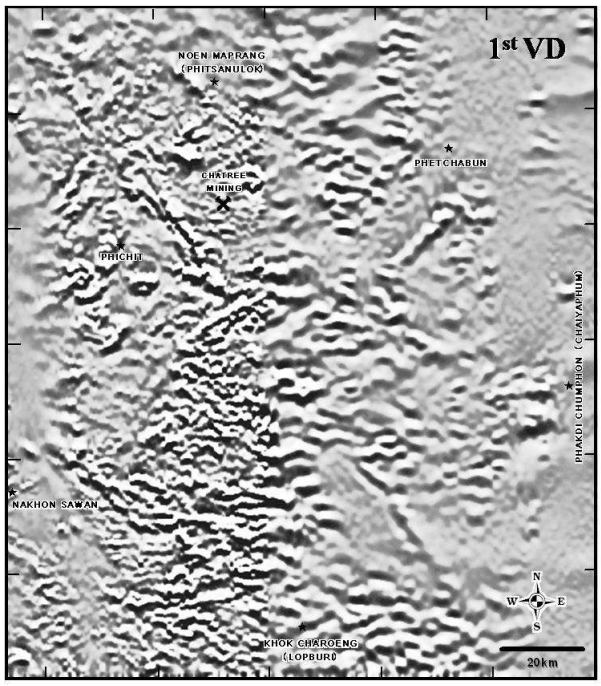

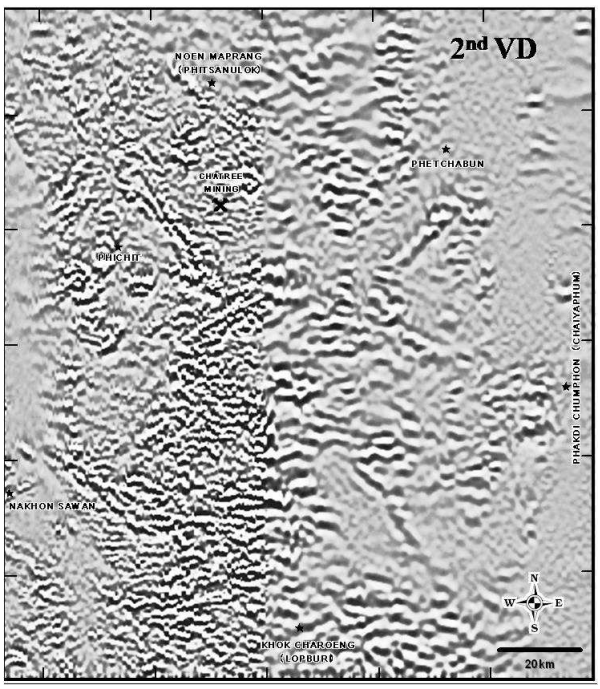

III. 1st vertical derivative and 2nd vertical derivative maps reveal significant magnetic patterns such as linear structures or lineaments with complex structure.

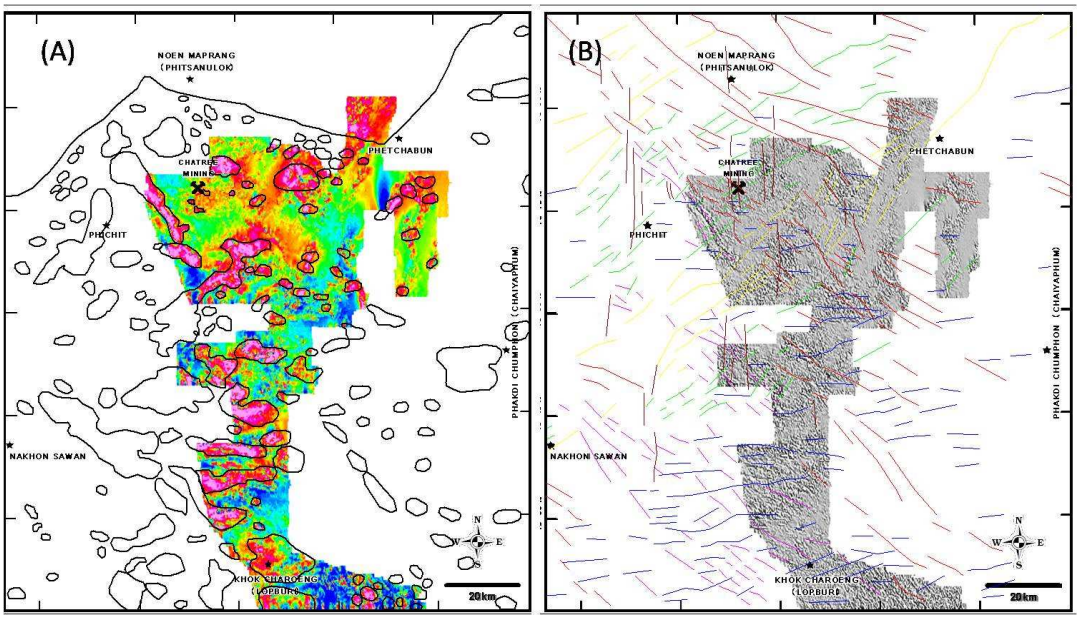

IV. To comparison the geophysical interpretation by using highest resolution airborne magnetic follow-up Survey (HEM) which are 400 km grid spacing fight line, (A) the unit boundary confirm very well with HEM reduction to the pole map (B) and the lineament also confirm very well with HEM 1st vertical derivative map.

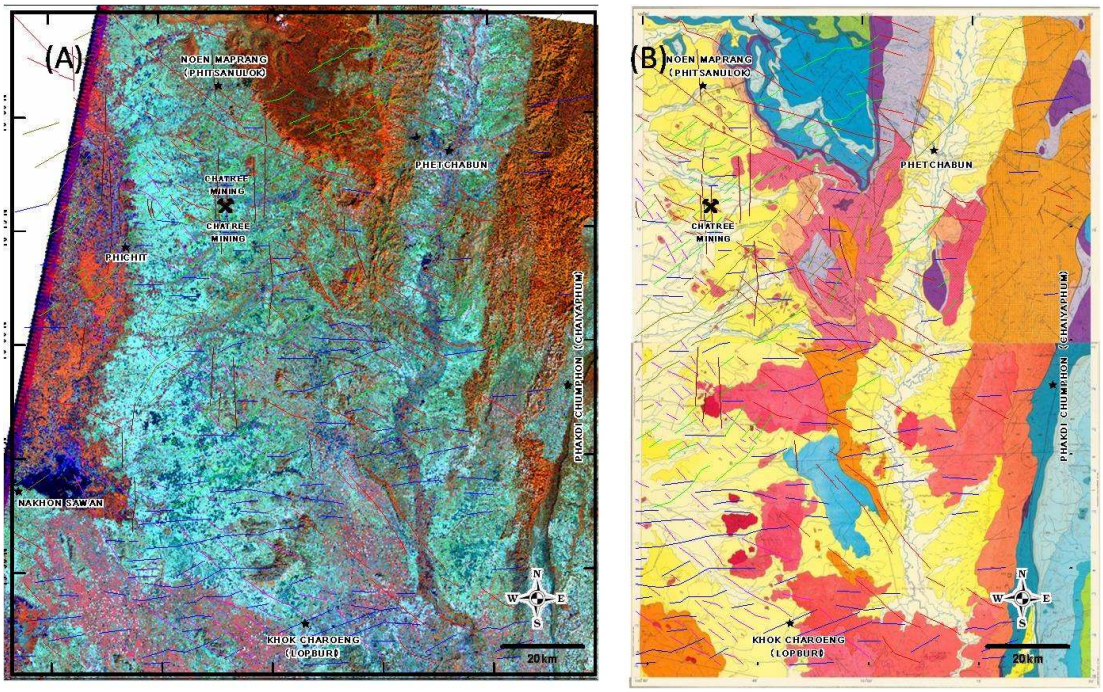

V. To comparison the geophysical responding of lineaments with (A) landsat TM5 in (A) and faults in (B) of geologic map with scale 1:250,000 by DMR (1984), the geophysical lineament confirm very well with both map of structure.

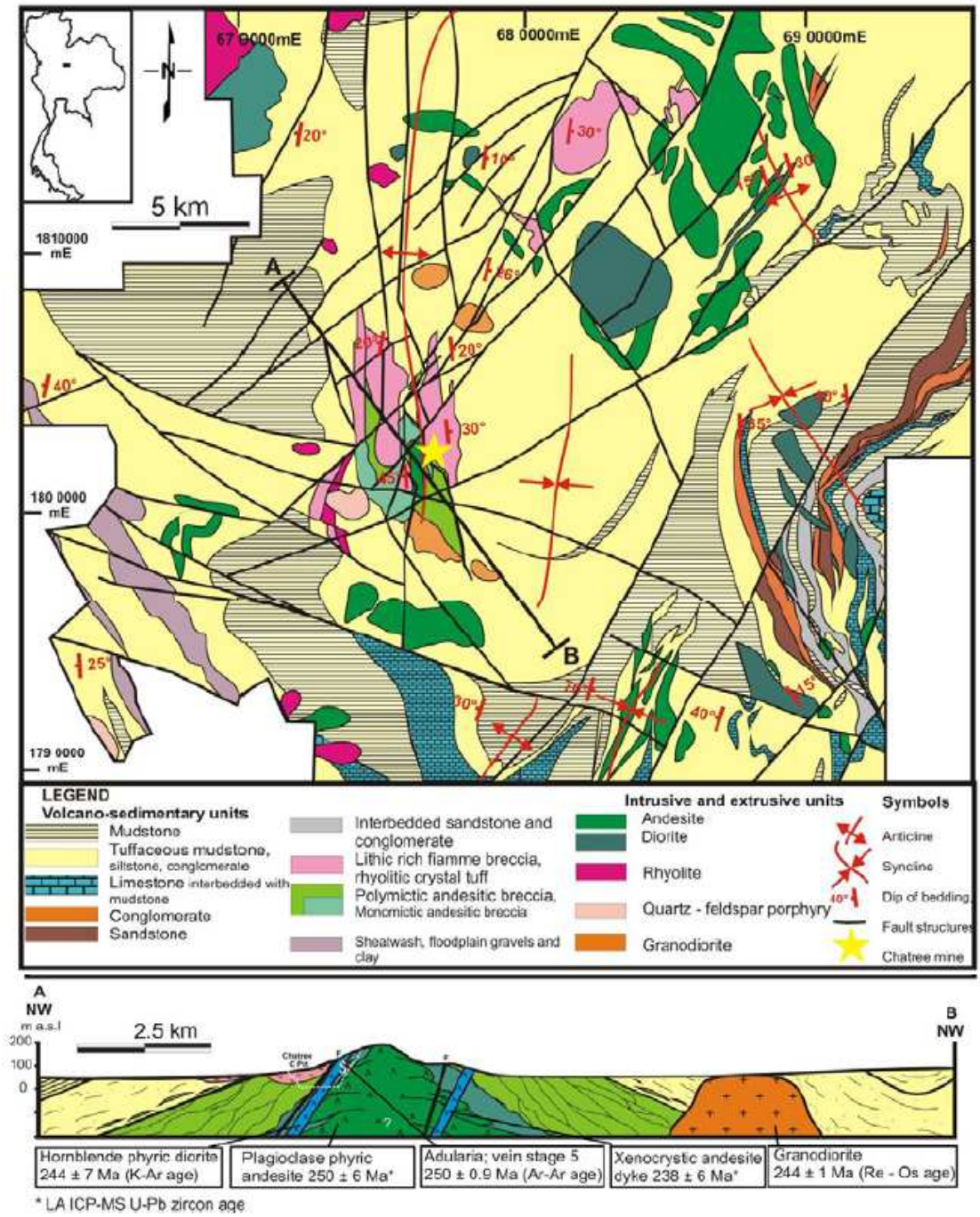

VI. Generalized geology map of the Chatree district (James et al., 2007) showing the location of Chatree (yellow star) which is positioned on a north-south trending axial plane of a gently folded anticline, intersected by NE-SW, N-S, NNW-SSE striking faults.

Biography

Mr. Arak Sangsomphong was born in Chachoengsao province, eastern Thailand on 2nd October 1983. He graduated with a B.Sc. degree in Geology from Chulalongkorn University, Bangkok, in 2005. After his graduation, he has been working works in mud logging service of International logging SA or Weatherford KSP Company. Then, he starts his study as the M.Sc. geology student at Chulalongkorn University, Bangkok, in 2008. The research work has been focused on Airborn geophysical processing and interpretation including field investigation to reconstructs the evolution of structure.

Arak Sangsomphong

Email: rak_geo46@hotmail.com